ROLES AND INTERACTIONS OF ENABLED, DIAPHANOUS AND CAPPING PROTEIN IN REGULATION OF ACTIN STRUCTURES IN *DROSOPHILA* DEVELOPMENT

Stephanie H. Nowotarski

A dissertation submitted to the faculty at the University of North Carolina at Chapel Hill in partial fulfillment of the requirements for the degree of Doctor of Philosophy in the Department of Biology.

Chapel Hill
2014

Approved by:

Mark A. Peifer

Bob Duronio

Steve Rogers

Bob Goldstein

Jim Bear

ABSTRACT

Stephanie H. Nowotarski: Roles and interactions of Enabled, Diaphanous and Capping Protein in regulation of actin structures in *Drosophila* morphogenesis
(Under the direction of Mark Peifer)

Proper regulation of the actin cytoskeleton is integral for development. As a dynamic polymer, actin is highly regulated by a host of binding proteins, which alter the geometry of the polymer network. Specific actin geometries are associated with migration, protrusive behavior, and cell shape changes. Individual cell shape changes are coupled via cell – cell adhesion to affect both wound healing and morphogenesis — the dynamic tissue rearrangements associated with development. Improper actin regulation is associated with cancer and disease.

Here we use *Drosophila* oogenesis and embryonic morphogenesis as models for *in vivo* actin regulation to explore: (1) How the balance between filament elongation and filament capping affects development, finding that the antagonistic relationship between the filament elongator, Enabled, and the filament capper, Capping Protein, is integral for proper oogenesis. (2) How filament elongation factors interact and modulate actin dynamics biochemically, in cell culture and *in vivo*. Here we found Enabled and another elongation factor, Diaphanous, directly interact, resulting in negative regulation of Diaphanous' effect on actin polymerization. (3) Finally I expand on how the relationship between elongation factors works *in vivo*, finding that each elongation factor plays a dominant role in separate tissues in filopodium formation during a dynamic morphogenetic event.

PREFACE

“Man knows that the world is not made on a human scale;

and he wishes that it were.”

Andre Malraux

ACKNOWLEDGEMENTS

There were times I lost sight of the forest of life for the tiny trees. It's easy to get lost and end up walking in unproductive circles in a forest just looking at individual trees with no reference point [1]. Luckily for me there were always people to show me north:

1) My peers, who inside the lab and out kept me on path and kept things more than interesting. Specific thanks to Kaelyn Sumigray, Jess Sawyer, Nathan Harris, and Kelly Alexandre LaFave.

2) Tony Perdue never (admits/aspires) to having the answer but has it just through the virtue of talking and listening. For that I cannot thank him enough.

3) Many thanks to Mark, without whom I would be a much worse writer and scientist and with whom I'm a better citizen.

4) Thanks to my sibling/peers (Melissa, Chris and Ty) who have made science/teaching a family affair and who always *want* to discuss/speculate.

5) The biggest thanks goes to my parents who surely had no clue what to do with three scientists and through experimentation figured it out perfectly.

6) Finally, to Linda, who always seems to understand all the connections and who always reminds me we can do anything. As long as there is a plan.

1. Souman, J. L., Frissen, I., Sreenivasa, M. N., and Ernst, M. O. (2009). Walking straight into circles. Curr Biol *19*, 1538–1542.

TABLE OF CONTENTS

LIST OF TABLES

LIST OF FIGURES

LIST OF ABBREVIATIONS

AJ	Adherens Junction
AS	Amnioserosa
Dia	Diaphanous
Ena	Enabled
FA	Focal Adhesion
LE	Leading Edge

CHAPTER 1: INTRODUCTION

Morphogenesis: Choreography of form and function

The fundamental question of what we are and how we work has more than likely existed from the dawn of humankind, though certainly since the dawn of written record. One of the earliest records in western philosophy regarding the nature of the world around us and ourselves comes from Thales of Miletus in 500BCE, who postulated that the originating principle of nature is water (Russell,1945). While in the intervening years philosophy and science (often hand in hand) put forth many theories describing what we are made of, the first true hint of understanding the physical basis of our form occurred in 1653 — when Robert Hooke looked at a piece of cork with a simple microscope and discovered, and subsequently recorded, the smallest building block of life: the cell (Hooke and Gunther, 1961). Later, in the first half of the 19th century, the discovery that plants and animals are multicellular organisms further rooted our understanding of ourselves and the living world around us (Schleiden, 1838; Schwann, 1847).

In 1876 Oscar Hertwig found that sea urchin fertilization required two cells — the sperm and the egg (Hertwig, 1915) — and subsequent work applied this to mammals (reviewed in Austin, 1961). The current best estimate of number of cells present in the average human adult is 37.2 trillion (Bianconi et al., 2013). From two to tens of trillions of cells,2 development and homeostasis is awe-inspiring and is even more so when its high fidelity is taken into account. Our inherent self-assembly though development, and subsequent ability to repair ourselves, is truly amazing.

While the fidelity of both development and homeostasis is high, things can and do go wrong. In the United States alone this year, one out of every thirty-three children will be born with a major birth defect (CDC), and cancer is projected to take the lives of 585,720 people (ACS). In 2008, over 12,000,000 cancer cases were projected worldwide (ACS). This makes

Cancer the second-most common cause of death in the US, accounting for nearly 1 of every 4 deaths (ACS). Outcome is inversely correlated with tumor metastasis, or tumor cell migration away from the primary tumor site, and an estimated 90% of deaths are associated with metastatic events (ACS; Mehlen & Puisieux, 2006). These numbers underscore the need to understand how proper development and homeostasis work so that we can better comprehend both our own existence and how cellular mechanisms become unregulated or hijacked in the disease state.

In order to ensure proper development, cells need to accomplish many diverse tasks after fertilization: (1) they need to multiply through organized divisions, (2) once divided those cells need to either remain pluripotent stem cells or differentiate into specific cell types such as neurons or osteoclasts, (3) these cells need to be able to change their shape and (4) often migrate to find their proper place in the body plan and (5) these cells also need to adhere to neighboring cells to assemble tissues and organs. The coupling of cell shape change with adhesion to neighbors makes the proper placement of cells and the development of complex tissues possible through large-scale tissue rearrangements known as morphogenesis.

We use the morphogenetic movements in the fruit fly *Drosophila melanogaster* at various life stages as a model to explore the molecular underpinnings of individual cell shape change and ultimately to reveal how individual cell shape changes are coordinated and transduced at the tissue level through cell-cell adhesion. *Drosophila* provides an excellent model for this as its rich research history has provided a full annotated genome and with it, many useful genetic tools to manipulate individual cells and tissues *in vivo* (Beckingham, Armstrong, Texada, Munjaal, & Baker, 2005; del Valle Rodríguez, Didiano, & Desplan, 2012; Elliott & Brand, 2008). Further, advances in fixed and live imaging via modern microscopy (Hensel, Klingauf, & Piehler, 2013; Shaner, Patterson, & Davidson, 2007) have allowed this model system, already amenable to imaging, to yield even more detail. The work below uses both *Drosophila* embryonic and germline morphogenesis to focus on how cell shape change and migration are modulated by the actin cytoskeleton and its regulator

Actin's Rich History: Monomer to Polymer to Monomer…

Our everyday existence relies on our ability to accomplish physical work, and the origin of the cytoskeletal field lies in the question of our daily motion. How do I move? How can I type this chapter? The cytoskeletal protein Actin is involved at the architectural and mechanical level in many ways as I write this. From my gastrulation, to the initial growth of neuronal axons to innervate their muscle targets and their subsequent continual synaptic remodeling, to the contractile motion of muscles themselves, actin is at the foundation of human muscle and neuromechanics (Pollard & Cooper, 2009). In 1887 W.D. Halliburton began with the basic research question of how muscles move in frog legs and subsequently applied this question to mammals. Halliburton noted a factor that caused myosin (a motor protein discovered in 1859) to coagulate in his preparations but unfortunately did not pursue this observation (Halliburton, 1887; Kühne, 1859). Actin lay dormant for years until in the 1940s when Albert Szent-Gyorgyi's lab turned from work on Vitamin C to muscle research. Gyorgyi termed his viscous myosin preparations "activated myosin," and fellow lab member, Brunó Ferenc Straub revealed another protein was the activator of this viscous effect, and thus named this new protein "actin" (Szent-Gyorgyi 1941,1942; Straub 1942; reviewed in Perry, 2003). In the past 70 years the scientific community has uncovered so much more about this small protein that enables our smallest and largest movements.

There are several cytoplasmic actin isoforms in mammals: (1) α-actin, which is associated with contractile structures, (2) γ-actin found in stress fiber filaments and (3) β-actin, located at the edge of cells using the projection of their membranes as a means of mobility and protrusive behavior (Perrin & Ervasti, 2010). In the cell, actin exists in an equilibrium between two states: the monomeric form (globular or G-actin) and as a polymer (filamentous or F-actin; reviewed in Blanchoin, Boujemaa-Paterski, Sykes, & Plastino, 2014). G-actin contains an ATP binding site and can hydrolyze ATP to ADP and a phosphate. ATP binding is integral for incorporation of a monomer into a filament (Pollard & Cooper, 2009). The assembly of G-actin into F-actin occurs in a polar manner,

with monomers added facing the same direction. This produces two distinct filament ends: one where the ATP binding site is facing outward known as the minus (-) or pointed, and the other known as the plus (+) or barbed end, where most new monomers are added (Figure 1.1; the barbed and pointed designations come from the appearance of myosin S1 decorated filaments; Begg, Rodewald, & Rebhun, 1978). In the cellular context, the barbed end generally faces the plasma membrane, while the pointed end is more often oriented towards the cell body (Figure 1.1). The polarization of F-actin is physiologically important, as polymerization is directional and can generate force used by the cell (reviewed in Blanchoin et al., 2014; Pollard & Cooper, 2009). Notably, the weak associations between actin monomers in the polymerized state allow for the filament to readily release and add monomers— making actin a highly dynamic and editable structure within the cell (Alberts et al., 2002-).

Actin can spontaneously polymerize *in vitro* in the presence of ATP along with a concentration of actin monomers above the critical concentration (Cc; Alberts et al., 2002; Carlier & Pantaloni, 1997). Polymerization occurs in 3 distinct phases: nucleation, elongation and steady state. Nucleation of a polymer involves the formation of an 'actin nucleus complex' comprised of three monomers. This is followed by rapid addition of new monomers, and thus, elongation. While monomers can be added to the pointed end of a filament, the addition of monomers to the barbed end is inherently favored by the rates of polymerization, a Cc and hydrolysis (Pollard & Cooper, 2009). To maintain polymerization past the rapid elongation rate, a steady state of monomers must be available. ATP monomers added to the barbed end undergo hydrolysis to ADP-actin, a form favored by ADF/Cofilin, which actively enriches severing activity at the barbed end (Carlier et al., 1997; Maciver & Weeds, 1994). Finally, steady state is reached when rate of assembly at the barbed end and disassembly at the pointed end reach a state of equilibrium with Cc of monomers in solution. Thus, when the association of ATP-GActin exceeds the rate of subunit loss, the filament will grow with a 'cap' of ATP-rich subunits, while when the association of ATP-G actin is lower than the rate of subunit

loss, the filament will shrink (reviewed in Pollard, Blanchoin, & Mullins, 2001). These distinct phases of actin polymerization also occur in cell culture and *in vivo* but in these more complex environments numerous binding partners regulate events.

Actin Binding Proteins: Modifying Actin Geometries

Despite actin's aforementioned self-assembly capabilities, *in vivo* two factors ensure spontaneous polymerization does not occur. First, actin often exists at levels below the Cc (Dominguez & Holmes, 2011; Sept & McCammon, 2001). Second, the ubiquitous actin binding protein, profilin, is highly associated with free monomers (50% of polymerizable actin is thought to be profilin-actin; (Pollard & Borisy, 2003a), and suppresses spontaneous polymerization in the absence of free barbed ends (Pantaloni & Carlier, 1993; Vinson, La Cruz, Higgs, & Pollard, 1998). Profilin plays many roles, as it also catalyzes nucleotide exchange and promotes barbed end addition through its affinity for elongation factors (Hansen & Mullins, 2010a; Romero et al., 2004).

However, profilin is not the only actin-binding partner, nor does it provide the only level of regulation of actin polymerization. Actin's highly conserved structure throughout evolution (Hightower & Meagher, 1986) and its dynamic nature makes it unsurprising that a host of proteins interact with it. Research in the past 70 years has uncovered a host of actin binding proteins (ABPs) that modulate arrangement of F-actin and network dynamics. These fall into several broad categories (reviewed in Pollard & Borisy, 2003a): (1) Severing factors such as ADF/Cofilin depolymerize filaments along the whole length but their preference for ADP-Actin enriches it's activity at the pointed end, allowing for recycling of monomers for reincorporation to the barbed end (Bernstein & Bamburg, 2010); (2) Elongation factors, which act in tandem with the previously mentioned profilin bound actin, promoting more rapid monomer addition to filament barbed ends (Dominguez, 2009); (3) Capping factors halt monomer addition (Menna, Fossati, Scita, & Matteoli, 2011). (4) Branching factors of the Arp 2/3 complex nucleate actin filaments from the sides of existing filaments (Rotty, Wu, & Bear, 2013), while formins can nucleate filaments de novo (Breitsprecher & Goode, 2013) and (5) bundling

factors like fascin bind lateral filaments together (Khurana & George, 2011). While thorough biochemical analysis is beginning to reveal the mechanism of action of each ABP on actin, we still do not fully understand how they work together as a network, driving the assembly and disassembly of different actin structures and thus affecting individual cell morphology and behavior, and ultimately, those of tissues and organisms

Driving Actin: A Decision Between the Brake and Gas

One key dichotomy for an actin filament is the decision to continue elongating or to terminate? At the most binary level, this dichotomy is governed by binding protein occupation status of the filament's barbed end. Here, monomer addition can be promoted by elongation factors associated with the barbed end (see below). Conversely, if a capping protein binds the barbed end, it inhibits monomer addition and thus terminates the filament (Figure 1.2). The subsections below detail current knowledge about elongation factors and Capping Protein.

Capping Protein

Capping Protein (CP) is an obligate heterodimer comprised of an alpha and beta subunit (Casella, Maack, & Lin, 1986). Each subunit is highly evolutionarily conserved in eukaryotes (J A Cooper et al., 1991; Wear, Yamashita, Kim, Maéda, & Cooper, 2003), but in sequence, the two subunits are unlike one another (reviewed in John A Cooper & Sept, 2008) and also do not resemble other filament capping proteins (Maruyama et al., 1990). Vertebrates have two somatically expressed genes encoding two distinct alpha subunits, while a single locus produces two beta isoforms via alternative splicing (Hart, Korshunova, & Cooper, 1997; Hurst, Howes, Coadwell, & Jones, 1998); in contrast, *Drosophila* has one locus for each subunit. *In vitro,* chicken CP binds actin barbed ends with nanomolar efficiency (Schafer, Jennings, & Cooper, 1996). *In vivo,* these properties endow CP with complex effects—e.g., in mammalian cell culture CP has been shown to be integral for cell migration speed (Bear et al., 2002) and in *Drosophila* cell culture loss of CP induces filopodia formation (see below; Rogers, Wiedemann, Stuurman, & Vale,

2003). *In vivo* loss of either subunit increases F-actin levels (Gates et al., 2009; Hopmann & Miller, 2003; Janody & Treisman, 2006). Further CP is required for integrity of the adult retina (Delalle, Pfleger, Buff, Lueras, & Hariharan, 2005), proper formation of the adult bristles (Frank, Hopmann, Lenartowska, & Miller, 2006; Hopmann, Cooper, & Miller, 1996), cortical integrity of nurse cells in the egg chamber and oocyte determination (Chapter 2; Gates et al., 2009).

In both humans and *Drosophila,* CP appears to act as part of a tumor suppressor module. It is a key player in restriction of tissue growth through inhibition of the oncogene Yorkie, which modulates growth via the Hippo pathway in the *Drosophila* wing disc epithelium (Fernández et al., 2011; Sansores-Garcia et al., 2011) and in mammary epithelial cells (Aragona et al., 2013). Further, in the *Drosophila* wing disc, CP prevents JNK-mediated apoptosis or proliferation (Jezowska et al., 2011) and counteracts oncogenic Src (Fernández, Jezowska, & Janody, 2014). Recent research has also revealed that reduced expression of the human alpha1 subunit is correlated with cancer-related death and can increase gastric cancer cell migration and invasion *in vitro,* whereas overexpression has the opposite effect (Lee et al., 2013). In *Drosophila,* the Cpa and Cpb subunits stabilize protein levels of each other, ensuring a balance of functional levels of heterodimer, thus maintaining a normal level of tissue growth (Amândio, Gaspar, Whited, & Janody, 2014).

Elongation Factors

There are two classes of elongation factors, the Diaphanous – related formin family (DRF) and the Ena/VASP family. Diaphanous (Dia) is the single Diaphanous - related formin (DRF) in *Drosophila*. DRFs nucleate and elongate linear actin filaments and play a key role in cytokinesis and filopodia formation across species (Castrillon & Wasserman, 1994; Kovar, Harris, Mahaffy, Higgs, & Pollard, 2006; Schirenbeck, Bretschneider, Arasada, Schleicher, & Faix, 2005; Severson, Baillie, & Bowerman, 2002; Swan et al., 1998). In addition, DRFs stabilize microtubules and cell junctions and can modulate transcription via MAL/SRF activation through G-actin depletion (Faix &

Grosse, 2006; Kobielak, Pasolli, & Fuchs, 2004; Sahai & Marshall, 2002). Dia has a highly conserved domain architecture composed of an N-terminal GTPase Binding Domain (GBD), Dia Interacting Domain (DID), Dimerization Domain (DD), Formin Homology 1 and 2 (FH1 FH2), and a C-terminal Dia Autoinhibitory Domain (DAD) (Breitsprecher & Goode, 2013). Interactions between the DAD and DID domains result in an intramolecular autoinhibition, which is relieved when Rho binds the GBD, activating Dia and recruiting it to the cortex (Alberts, 2001; Gorelik, Yang, Kameswaran, Dominguez, & Svitkina, 2011; Li & Higgs, 2003; T. Otomo, Otomo, Tomchick, Machius, & Rosen, 2005; Rose et al., 2005). Mutant versions of Dia lacking the DAD are constitutively active.

Once Dia is activated, the FH2 domain (Figure 1.1) nucleates actin filaments and is highly processive at the barbed end, blocking filament capping (Higashida et al., 2004; Kovar & Pollard, 2004; Pruyne et al., 2002; Romero et al., 2004; Zigmond et al., 2003). Mammals have 3 DRFs, and in cell culture they have been implicated in directional cell migration, stress fiber assembly, targeted secretion, organelle dynamics, and coordination of microtubules and actin (Faix & Grosse, 2006). *mDia1* mutants present immune system defects (Tanizaki et al., 2010), while *mDia2* knockout mice have multinucleate erythroblasts (Watanabe et al., 2013), and compound mDia1;mDia3 mutants have defects in neuronal migration (Thumkeo et al., 2011). The redundant and overlapping roles of these three DRFs make dissecting their participation in protrusive behavior *in vivo* challenging.

Drosophila Dia is integral for development, as mutants are lethal. First identified through its penetrant and evolutionarily conserved cytokinesis defects (Castrillon & Wasserman, 1994), Dia also helps coordinate actin assembly during the modified form of cytokinesis known as cellullarization (Afshar, Stuart, & Wasserman, 2000). Dia also has a role in coordinating actomyosin contractility and adhesion at AJs (Homem & Peifer, 2008). Further, Dia regulates actin-based protrusive activity in cell culture (Chapter 3; Bilancia et al., 2014; Homem & Peifer, 2009) during morphogenesis in migrating cells

(Chapter 4; Homem & Peifer, 2009), and recent work has shown it plays critical roles in thin cytoneme signaling protrusions in wing discs (Roy, Huang, Liu, & Kornberg, 2014) and in bract cell protrusions (Y. Peng, Han, & Axelrod, 2012). We further explore the role of Dia in protrusive activity in Chapters 3 and 4.

Ena/VASP proteins are also actin elongation factors, and in mammals play essential roles in craniofacial development, endothelial barrier function, and neuronal development (Dent et al., 2007; Furman et al., 2007; Hauser et al., 1999; Kwiatkowski et al., 2007; Lanier et al., 1999). Ena/VASP family members bind and elongate actin barbed ends via a conserved set of domains (Hansen & Mullins, 2010b; Loureiro et al., 2002). The Nterminal Ena/VASP Homology 1 (EVH1) domain helps localize Ena to regions of dynamic actin turnover like focal adhesions, the leading edge of lamellipodia, or filopodia tips, by binding partners carrying the consensus sequence: (D/E) FPPPPX (D/E)(D/E) (FP4; (Carl et al., 1999; Chakraborty et al., 1995; A. A. Fedorov, Fedorov, Gertler, & Almo, 1999; Laurent et al., 1999; Niebuhr et al., 1997). The central proline rich region (PRO) binds proteins with SH3 or WW domains, such as Ena's negative regulator Abelson Kinase (Abl), and also binds profilin to facilitate actin monomer addition to the filament barbed ends (Gertler et al., 1995; Lambrechts et al., 2000; Reinhard et al., 1992). The C-terminal EVH2 domain has three subdomains: G-actin binding (GAB), F-actin binding (FAB) and C-terminal coiled-coil (COCO), the latter of which allows Ena to tetramerize (Bachmann, Fischer, Walter, & Reinhard, 1999; Barzik et al., 2005; Chereau & Dominguez, 2006; Harbeck, Hüttelmaier, Schluter, Jockusch, & Illenberger, 2000; Hüttelmaier et al., 1999; Kuhnel et al., 2004; Walders-Harbeck, Khaitlina, Hinssen, Jockusch, & Illenberger, 2002; Winkelman, Bilancia, Peifer, & Kovar, 2014).

The current mechanism for actin filament elongation in the presence of Ena/VASP family members is that Ena/VASP is targeted via EVH1 binding partners (perhaps in response to tension- see Chapter 5 and Addendum). In the case of targeting Ena/VASP to the leading edge, once there, the localization is strengthened by the FAB, within the

EVH2 domain, binding F-actin. In cells lacking all three mammalian family members the EVH2 domain is sufficient to localize to a broad portion of the lamellipodia while a form of Mena lacking the FAB loses robust localization to the leading edge (Bear et al., 2002). The exact mechanism of Ena/VASP family members' actin polymerization is still under question as individual members display different properties. For example, while human VASP uses profilin-actin to accelerate polymerization via a combination of it's polyproline region and the GAB (both bind profilin; Breitsprecher et al., 2011; Hansen & Mullins, 2010a), *Drosophila* Ena is indifferent to profilin-actin (Winkelman et al., 2014).

Enabled is the single *Drosophila* Ena/VASP family member and mutants in it were initially identified through suppression of Abelson Kinase phenotypes (Gertler, Doctor, & Hoffmann, 1990). Ena has since been found to play important roles in axon guidance. Ena acts downstream of the repulsive guidance factor, Slit, through regulating transduction of its receptor, Robo (Bashaw, Kidd, Murray, Pawson, & Goodman, 2000). *ena* mutants have mild CNS defects and display a bypass phenotype of the intersegmental nerve, in which branching at the appropriate location fails (Gertler et al., 1995; Wills, Bateman, Korey, Comer, & Van Vactor, 1999). In addition to these roles in the nervous system, work from our lab has revealed Ena plays key roles in embryonic epithelial morphogenesis, as well as roles in formation of specialized actin structures in oogenesis (Gates et al., 2009; 2007). Below I describe in detail the integral role of Ena in *Drosophila* oogenesis (Chapter 2), as well as further explore the role of Ena in protrusive activity in cell culture and during embryonic morphogenesis *in vivo* (Chapters 3 and 4).

Actin Geometry: Roles in Form and Function

The ability of the actin cytoskeleton network to be shaped, tuned and modulated by its binding partners allows this shape shifting polymer to be a master of forces and function in the cell, thus contributing to many cellular events. Each of these roles involves a different actin network geometry governed by a different suite of actin regulators. Populations of actin in the cell can be broken into nuclear and cytosolic pools. The cytosolic pool can be further divided into three broad categories: (1) Those that

modulate migratory/protrusive behaviors at the cell membrane/periphery, (2) Those that create internal actin structures or are involved in specialized developmental structures/scaffolding roles (non-migratory but shape changing), and (3) junctional actin at cell adhesions. It is important to note that these are not mutually exclusive, as the plastic network nature of actin can inherently link protrusive actin to junctional actin and junctional/cortex actin to internal scaffolding structures.

The roles of actin in protrusive and adhesive behavior have been heavily studied and elegant work from the Borisy and Svitkina labs has revealed that the geometric form of the actin network along the periphery of a cell is correlated to modes of protrusive behavior (Svitkina & Borisy, 1999; Svitkina et al., 2003) and thus relates to their cellular function. Highly branched networks assembled by activity of the Arp2/3 complex (Svitkina & Borisy, 1999) and high levels of CP are associated with the leading edge of the broad lamellipodium (Iwasa & Mullins, 2007; Wear & Cooper, 2004). Lamellipodia are membrane-encased protrusions that resist deformation and generate forces that advance the cell membrane (Carlier, Le Clainche, Wiesner, & Pantaloni, 2003; Le Clainche & Carlier, 2008; Mitchison & Cramer, 1996; Pollard & Borisy, 2003b; Theriot & Mitchison, 1991). This type of protrusion is correlated with cellular migration and transduces the forces of actin against the protruding membrane, anchored by basal adhesion to the substrata (Giannone et al., 2007). Lamellipodia are remarkably sufficient for migration, as fibroblasts and keratocytes whose lamellipodia that were removed from the cell body can exhibit motion in the absence of the cell body and microtubules (Euteneuer & Schliwa, 1984; Verkhovsky, Svitkina, & Borisy, 1999). While sufficient for migration in this context, there are conditions in other cells in which absence of a lamellipodium does not explicitly remove cellular migration capabilities (Gupton et al., 2005; Wu et al., 2012).

Linear actin arrays contribute to many specialized structures *in vivo,* such as muscle sarcomeres, stress fibers, and TAN lines that position nuclei (Luxton, Gomes, Folker, Worman, & Gundersen, 2011; Tojkander, Gateva, & Lappalainen, 2012). In *Drosophila*,

adult bristles are comprised of overlapping linear actin filaments (Tilney, Connelly, Smith, & Guild, 1996) shaped by capping (Hopmann et al., 1996) and bundling (Cant, Knowles, Mooseker, & Cooley, 1994). Below we use *Drosophila* oogenesis to look at the role of actin regulators in shaping the specialized linear actin structures required for holding the nucleus in place during cytoplasmic transfer.

At the cell periphery, actin networks comprised of linear, bundled actin, each containing 15-30 filaments (Lewis & Bridgman, 1992; Small & Celis, 1978), are found in long, thin cellular protrusions known as filopodia (Gupton & Gertler, 2007). Filopodia are promoted by elongation factors (reviewed in Gupton & Gertler, 2007), although recent work also suggests a possible role for stochastic capping of filaments in filopodia, as CP can localize within them (Sinnar, Antoku, Saffin, Cooper, & Halpain, 2014). While the first allusion to both filopodia and lamellipodia was made by Ramon y Cajal in 1890 in renderings of the growth cone in chick neurons, filopodia were not described in detail until 1910 (Harrison, 1959). From the first functional experiments of cells sending out filopodia to touch gold patches, followed by cell spreading preferentially toward the gold (Albrect-Buehler, 1976), to *in vivo* observations in sea urchin embryos where primary mesenchymal cells send out long filopodia to presumably receive positional information from the ectoderm (J. Miller, Fraser, & McClay, 1995), to a good deal of work on neuronal growth cones showing filopodia orient to chemotrophic gradients, filopodia have historically been thought of as sensory structures associated with directional cell movement (reviewed in Gupton & Gertler, 2007). However, as Chapter 4 and recent work by the Kornberg lab and others points out (Roy et al., 2014; Sanders, Llagostera, & Barna, 2013), we still do not completely understand how filopodia are formed, how their lifetime is governed, and we are still uncovering roles and functions of filopodia and filopodia-like structures *in vivo*.

There are currently two mechanisms of filopodia formation proposed, each using different actin-nucleating proteins: the Convergent Elongation model and the De-novo Filament Elongation model. These models share some commonalities, as each dictates

that an elongation factor binds to the barbed ends of a subset of actin filaments at the cell periphery to promote polymerization and slow depolymerization while protecting these ends from binding of capping protein, and both further suggest that these filaments are bundled (reviewed in Gupton & Gertler, 2007). De-novo Filament Elongation postulates that Dia is solely responsible for filopodia nucleation and elongation – consistent with this, Dia2 can promote filopodia in many cell types (J. Peng, Wallar, Flanders, Swiatek, & Alberts, 2003; Schirenbeck et al., 2005; Wallar et al., 2006) and Dia is required for filopodium formation in *Dictyostelium* (Schirenbeck et al., 2005). The more inclusive Convergent Elongation model postulates that filopodia form from filaments nucleated from branched networks (via Arp2/3 and CP activity) like those of the lamellipodia. To form filopodia, a subset of barbed ends of these filaments at the periphery are bound together, elongated, and at least partially bundled (Bachmann et al., 1999; Hüttelmaier et al., 1999; Schirenbeck et al., 2006) by Ena/VASP, and subsequently further bundled via Fascin (reviewed in Gupton & Gertler, 2007; Khurana & George, 2011).

As the filopodia field grows and research reveals more about the role of ABPs in many different cell types and thus filopodia with different functions, it's becoming more clear that the definition of filopodia solely through shape is, while necessary, also arbitrary, as different ABPs play varying roles in generating potentially quite different types of "filopodia" in different cell types (Yang & Svitkina, 2011). This variability between cell types suggests the De-novo and Convergent Elongation models are likely not mutually exclusive but each may be used in distinct situations (Yang & Svitkina, 2011). This highlights the current problem of understanding how basic cell structures like filopodia and their underlying actin networks are formed in different cell types that have access to the same genomically encoded ABP toolkit, but via differences in expression/ regulation utilize it differently. Further, understanding regulation of actin under normal developmental and signaling contexts helps us to understand what happens when this regulation goes awry.

Cell Migration: roles in Development and Disease

From individual cells to coordinated sheet migration, the ability of cells to migrate is integral for development and wound healing and when unregulated is associated with metastasis and cancer. As outlined above, the actin cytoskeleton is tightly regulated to maintain proper cell shape and behavior. This regulation can be hijacked by cancer cells to change cell growth, stiffness, proliferation, and movement (Lambrechts, Van Troys, & Ampe, 2004; Stevenson, Veltman, & Machesky, 2012). Alterations in expression and activity of many ABPs have been associated with cancer onset, progression and with metastasis (Ding et al., 2014; Philippar et al., 2008; Stevenson et al., 2012; Toyoda et al., 2011; Yamamoto et al., 2009).

The ability of cells to migrate is reliant on the remodeling and down regulation of the adhesive contacts between cells, the adherens junctions (AJS; Peglion, Llense, & Etienne-Manneville, 2014), as well as the adhesive contacts with the substrate (Mitra, Hanson, & Schlaepfer, 2005). Cell adhesion is a dynamic process and this is readily apparent at many places during normal development. A prime example of this is the epithelial to mesenchymal transition (EMT) that occurs at diverse times and places both in mammals and *Drosophila* (D'Souza-Schorey, 2005). During EMT cells down-regulate their adhesive potential, lose epithelial cell polarity, and concomitantly acquire migratory and invasive properties (reviewed in Thiery, Acloque, Huang, & Nieto, 2009). Examples of EMT and subsequent migratory behavior in development include single cells, as in primordial germ cell migration in zebrafish (Raz, 2003) or hemocytes in *Drosophila* (Evans & Wood, 2011), and also include collective cell migration events like those involved in the lateral line migration of zebrafish (Haas & Gilmour, 2006) and border cell migration in *Drosophila* (Montell, 2003). They also involve more partial EMT transitions during cell sheet migrations, like dorsal closure in *Drosophila* (Harden, 2002).

Both Ena and Dia localize to AJs in *Drosophila* and do so robustly during dorsal closure, and both also play critical roles in protrusive and migratory behavior (Gates et al., 2007; Homem & Peifer, 2008), making them excellent candidates for regulation and

interplay of junction actin regulation to protrusive actin regulation. In Chapter 2, I will describe the role of Ena and CP during a specific example of a cluster of cells undergoing EMT and migration, border cell migration in the *Drosophila* ovary, during which follicular epithelium cells at the anterior pole down regulate their adhesive properties and detach as a group of 6-8 cells that then directionally migrate towards the oocyte (Montell, 2003). In Chapter 2, I will also describe the role of Ena and Dia during the partial EMT occurring during stage 14 of *Drosophila* embryogenesis, where opposing sheets of epithelial cells change shape and migrate over another cell type to meet at the dorsal midline and cover the embryo in skin — a process known as dorsal closure (Belacortu & Paricio, 2011; Jacinto et al., 2000); Figure 4.1, p160). Both of these migratory events involve a restructuring of the AJs and an increase in protrusive behavior (Belacortu & Paricio, 2011; Montell, 2006). In order to study these complex *in vivo* migration events we need to work from the ground up.

Bottoms Up: Using Increasing Scale and Complexity to Inform Order and Test Hypotheses

Much of the work exploring actin regulation *in vivo* has followed in the footsteps of earlier actin work, which involved detailed biochemistry based on crystal structures. Technological advances from actin biochemistry and purified binding proteins along with harnessing new forms of microscopy like TIRF have enabled research to look at the flux state of single actin filaments upon addition of one or more actin binding proteins (we utilize these approaches in Chapter 3; reviewed in Pollard & Cooper, 2009). The ability to see and measure polymerization and flux of actin in this manner has revealed the nuts and bolts of many basic properties of actin regulatory proteins such as branching angle and nucleation rates by Arp2/3 (Fujiwara, Suetsugu, Uemura, Takenawa, & Ishiwata, 2002; Mullins, Heuser, & Pollard, 1998) or fascin-mediated bundling (Winkelman et al., 2014). Further, this technique is able to inform us about the relationship between multiple ABPs and actin, providing a clearer picture of how these machines work together in a setting stripped of the complexities of the cell. For example the recent work by our collaborators

detailed the interaction between Ena/VASP and Fascin (Winkelman et al., 2014). The information gained at this visual-biochemical level has been excellent for assigning values for mathematical modeling, which allows predictions to be made for testing both *in vitro* and in cell culture work. Understanding how these machines work together *in vitro* and in cell culture is subsequently able to provide a context for *in vivo* where the system is even more complex. We've harnessed this information pipeline in Chapters 3&4 to better understand how Ena and Dia work together and separately to shape protrusive behavior in different places within two different tissues *in vivo*.

Figure 1.1

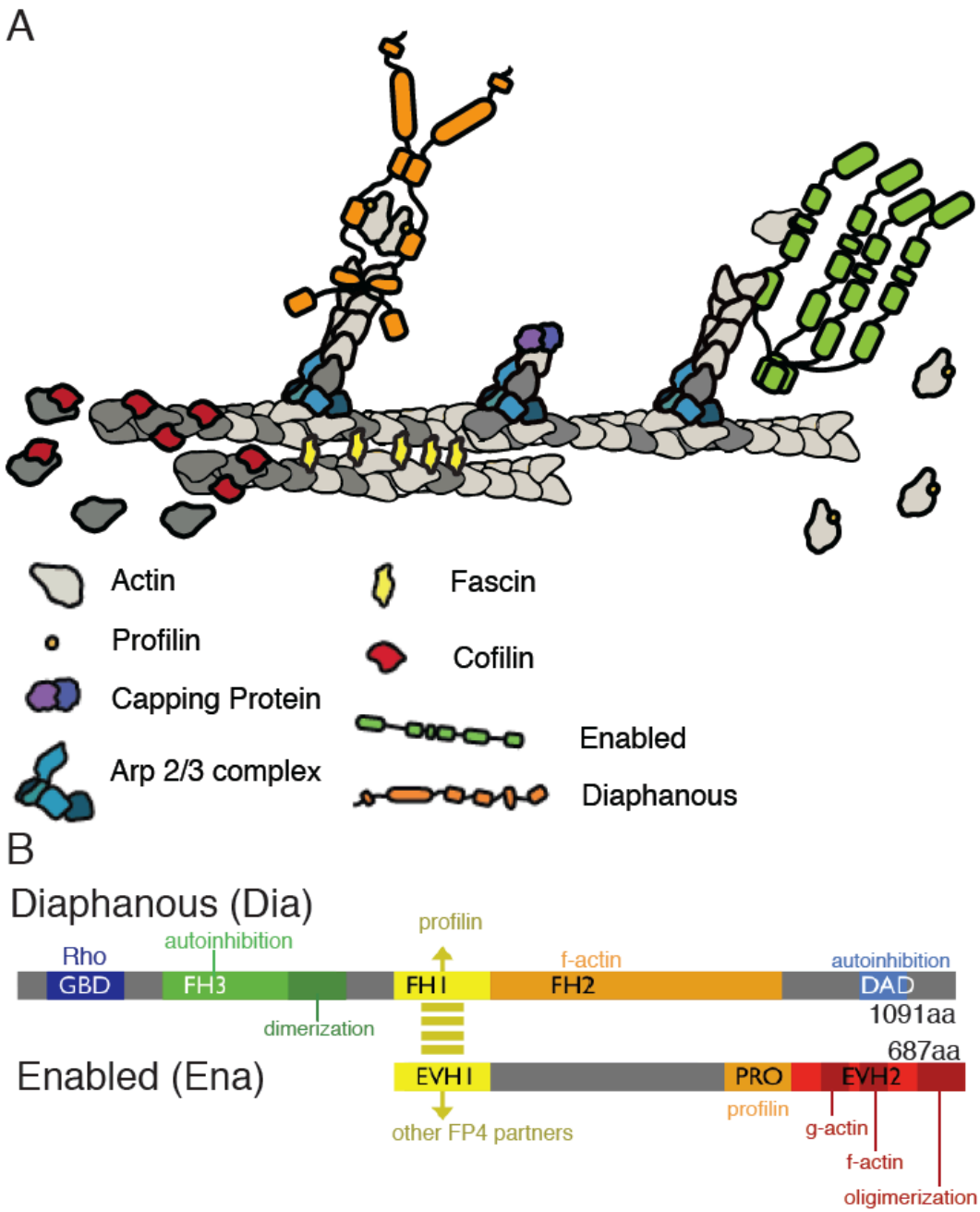

Figure 1.1 (A) Diagram of actin network with binding proteins. (B) Diagrams of Diaphanous and Enabled proteins with domains labeled and function/binding partners for domains noted.

REFERENCES

Afshar, K., Stuart, B., & Wasserman, S. A. (2000). Functional analysis of the Drosophila diaphanous FH protein in early embryonic development. *Development (Cambridge, England)*, *127*(9), 1887–1897.

Alberts, A. S. (2001). Identification of a carboxyl-terminal diaphanous-related formin homology protein autoregulatory domain. *The Journal of biological chemistry*, *276*(4), 2824–2830.

Alberts B, Johnson A, Lewis J, et al. Molecular Biology of the Cell. 4th edition. New York: Garland Science; 2002. *The Self-Assembly and Dynamic Structure of Cytoskeletal Filaments.* Available from http://www.ncbi.nlm.nih.gov/books/NBK26862/

Albrecht-Buehler, G. 1976. The function of filopodia in spreading 3T3 mouse fibroblasts. *In* Cell Motility. A. Book, T. Pollard, R. Goldman, and J. Rosenbaum, editors. Cold Spring Harbor Laboratory Press, Cold Spring Harbor, NY. 247–264.

Amândio, A. R., Gaspar, P., Whited, J. L., & Janody, F. (2014). Subunits of the Drosophila actin-capping protein heterodimer regulate each other at multiple levels. *PloS one*, *9*(5), e96326. doi:10.1371/journal.pone.0096326

Aragona, M., Panciera, T., Manfrin, A., Giulitti, S., Michielin, F., Elvassore, N., et al. (2013). A mechanical checkpoint controls multicellular growth through YAP/TAZ regulation by Actin-processing factors. *Cell*, *154*(5), 1047–1059. doi:10.1016/j.cell.2013.07.042

Austin, C. R. (1961). *The mammalian egg*. Oxford: Blackwell.

Bachmann, C., Fischer, L., Walter, U., & Reinhard, M. (1999). The EVH2 domain of the vasodilator-stimulated phosphoprotein mediates tetramerization, F-actin binding, and actin bundle formation. *The Journal of biological chemistry*, *274*(33), 23549–23557.

Barzik, M., Kotova, T. I., Higgs, H. N., Hazelwood, L., Hanein, D., Gertler, F. B., & Schafer, D. A. (2005). Ena/VASP proteins enhance actin polymerization in the presence of barbed end capping proteins. *The Journal of biological chemistry*, *280*(31), 28653–28662. doi:10.1074/jbc.M503957200

Bashaw, G. J., Kidd, T., Murray, D., Pawson, T., & Goodman, C. S. (2000). Repulsive axon guidance: Abelson and Enabled play opposing roles downstream of the roundabout receptor. *Cell*, *101*(7), 703–715.

Bear, J. E., Svitkina, T. M., Krause, M., Schafer, D. A., Loureiro, J. J., Strasser, G. A., et al. (2002). Antagonism between Ena/VASP proteins and actin filament capping regulates fibroblast motility. *Cell*, *109*(4), 509–521.

Beckingham, K. M., Armstrong, J. D., Texada, M. J., Munjaal, R., & Baker, D. A. (2005). Drosophila melanogaster--the model organism of choice for the complex biology of multi-cellular organisms. *Gravitational and space biology bulletin : publication of the American Society for Gravitational and Space Biology*, *18*(2), 17–29.

Begg, D. A., Rodewald, R., & Rebhun, L. I. (1978). The visualization of actin filament polarity in thin sections. Evidence for the uniform polarity of membrane-associated filaments. *The Journal of cell biology*, *79*(3), 846–852.

Belacortu, Y., & Paricio, N. (2011). Drosophila as a model of wound healing and tissue

regeneration in vertebrates. *Developmental dynamics : an official publication of the American Association of Anatomists*, *240*(11), 2379–2404. doi:10.1002/dvdy.22753

Bernstein, B. W., & Bamburg, J. R. (2010). ADF/cofilin: a functional node in cell biology. *Trends in cell biology*, *20*(4), 187–195. doi:10.1016/j.tcb.2010.01.001

Bianconi, E., Piovesan, A., Facchin, F., Beraudi, A., Casadei, R., Frabetti, F., et al. (2013). An estimation of the number of cells in the human body. *Annals of human biology*, *40*(6), 463–471. doi:10.3109/03014460.2013.807878

Bilancia, C. G., Winkelman, J. D., Tsygankov, D., Nowotarski, S. H., Sees, J. A., Comber, K., et al. (2014). Enabled negatively regulates diaphanous-driven actin dynamics in vitro and in vivo. *Developmental cell*, *28*(4), 394–408. doi:10.1016/j.devcel.2014.01.015

Blanchoin, L., Boujemaa-Paterski, R., Sykes, C., & Plastino, J. (2014). Actin dynamics, architecture, and mechanics in cell motility. *Physiological reviews*, *94*(1), 235–263. doi:10.1152/physrev.00018.2013

Breitsprecher, D., & Goode, B. L. (2013). Formins at a glance. *Journal of cell science*, *126*(Pt 1), 1–7. doi:10.1242/jcs.107250

Breitsprecher, D., Kiesewetter, A. K., Linkner, J., Vinzenz, M., Stradal, T. E. B., Small, J. V., et al. (2011). Molecular mechanism of Ena/VASP-mediated actin-filament elongation. *The EMBO journal*, *30*(3), 456–467. doi:10.1038/emboj.2010.348

Cant, K., Knowles, B. A., Mooseker, M. S., & Cooley, L. (1994). Drosophila singed, a fascin homolog, is required for actin bundle formation during oogenesis and bristle extension. *The Journal of cell biology*, *125*(2), 369–380.

Carl, U. D., Pollmann, M., Orr, E., Gertlere, F. B., Chakraborty, T., & Wehland, J. (1999). Aromatic and basic residues within the EVH1 domain of VASP specify its interaction with proline-rich ligands. *Current biology : CB*, *9*(13), 715–718.

Carlier, M. F., & Pantaloni, D. (1997). Control of actin dynamics in cell motility. *Journal of molecular biology*, *269*(4), 459–467. doi:10.1006/jmbi.1997.1062

Carlier, M. F., Laurent, V., Santolini, J., Melki, R., Didry, D., Xia, G. X., et al. (1997). Actin depolymerizing factor (ADF/cofilin) enhances the rate of filament turnover: implication in actin-based motility. *The Journal of cell biology*, *136*(6), 1307–1322.

Carlier, M.-F., Le Clainche, C., Wiesner, S., & Pantaloni, D. (2003). Actin-based motility: from molecules to movement. *BioEssays : news and reviews in molecular, cellular and developmental biology*, *25*(4), 336–345. doi:10.1002/bies.10257

Casella, J. F., Maack, D. J., & Lin, S. (1986). Purification and initial characterization of a protein from skeletal muscle that caps the barbed ends of actin filaments. *The Journal of biological chemistry*, *261*(23), 10915–10921.

Castrillon, D. H., & Wasserman, S. A. (1994). Diaphanous is required for cytokinesis in Drosophila and shares domains of similarity with the products of the limb deformity gene. *Development (Cambridge, England)*, *120*(12), 3367–3377.

Chakraborty, T., Ebel, F., Domann, E., Niebuhr, K., Gerstel, B., Pistor, S., et al. (1995). A focal adhesion factor directly linking intracellularly motile Listeria monocytogenes and

Listeria ivanovii to the actin-based cytoskeleton of mammalian cells. *The EMBO journal*, *14*(7), 1314–1321.

Chereau, D., & Dominguez, R. (2006). Understanding the role of the G-actin-binding domain of Ena/VASP in actin assembly. *Journal of structural biology*, *155*(2), 195–201. doi:10.1016/j.jsb.2006.01.012

Cooper, J A, Caldwell, J. E., Gattermeir, D. J., Torres, M. A., Amatruda, J. F., & Casella, J. F. (1991). Variant cDNAs encoding proteins similar to the alpha subunit of chicken CapZ. *Cell motility and the cytoskeleton*, *18*(3), 204–214. doi:10.1002/cm.970180306

Cooper, John A, & Sept, D. (2008). New insights into mechanism and regulation of actin capping protein. *International review of cell and molecular biology*, *267*, 183–206. doi:10.1016/S1937-6448(08)00604-7

D'Souza-Schorey, C. (2005). Disassembling adherens junctions: breaking up is hard to do. *Trends in cell biology*, *15*(1), 19–26. doi:10.1016/j.tcb.2004.11.002

del Valle Rodríguez, A., Didiano, D., & Desplan, C. (2012). Power tools for gene expression and clonal analysis in Drosophila. *Nature methods*, *9*(1), 47–55. doi:10.1038/nmeth.1800

Delalle, I., Pfleger, C. M., Buff, E., Lueras, P., & Hariharan, I. K. (2005). Mutations in the Drosophila orthologs of the F-actin capping protein alpha- and beta-subunits cause actin accumulation and subsequent retinal degeneration. *Genetics*, *171*(4), 1757–1765. doi:10.1534/genetics.105.049213

Dent, E. W., Kwiatkowski, A. V., Mebane, L. M., Philippar, U., Barzik, M., Rubinson, D. A., et al. (2007). Filopodia are required for cortical neurite initiation. *Nature cell biology*, *9*(12), 1347–1359. doi:10.1038/ncb1654

Ding, Z., Joy, M., Bhargava, R., Gunsaulus, M., Lakshman, N., Miron-Mendoza, M., et al. (2014). Profilin-1 downregulation has contrasting effects on early vs late steps of breast cancer metastasis. *Oncogene*, *33*(16), 2065–2074. doi:10.1038/onc.2013.166

Dominguez, R. (2009). Actin filament nucleation and elongation factors--structure-function relationships. *Critical reviews in biochemistry and molecular biology*, *44*(6), 351–366. doi:10.3109/10409230903277340

Dominguez, R., & Holmes, K. C. (2011). Actin structure and function. *Annual review of biophysics*, *40*, 169–186. doi:10.1146/annurev-biophys-042910-155359

Elliott, D. A., & Brand, A. H. (2008). The GAL4 system : a versatile system for the expression of genes. *Methods in molecular biology (Clifton, NJ)*, *420*, 79–95. doi:10.1007/978-1-59745-583-1_5

Euteneuer, U., & Schliwa, M. (1984). Persistent, directional motility of cells and cytoplasmic fragments in the absence of microtubules. *Nature*, *310*(5972), 58–61.

Evans, I. R., & Wood, W. (2011). Drosophila embryonic hemocytes. *Current biology : CB*, *21*(5), R173–4. doi:10.1016/j.cub.2011.01.061

Faix, J., & Grosse, R. (2006). Staying in shape with formins. *Developmental cell*, *10*(6), 693–706. doi:10.1016/j.devcel.2006.05.001

Fedorov, A. A., Fedorov, E., Gertler, F., & Almo, S. C. (1999). Structure of EVH1, a novel proline-rich ligand-binding module involved in cytoskeletal dynamics and neural

function. *Nature structural biology*, *6*(7), 661–665. doi:10.1038/10717

Fernández, B. G., Gaspar, P., Brás-Pereira, C., Jezowska, B., Rebelo, S. R., & Janody, F. (2011). Actin-Capping Protein and the Hippo pathway regulate F-actin and tissue growth in Drosophila. *Development (Cambridge, England)*, *138*(11), 2337–2346. doi:10.1242/dev.063545

Fernández, B. G., Jezowska, B., & Janody, F. (2014). Drosophila actin-Capping Protein limits JNK activation by the Src proto-oncogene. *Oncogene*, *33*(16), 2027–2039. doi:10.1038/onc.2013.155

Frank, D. J., Hopmann, R., Lenartowska, M., & Miller, K. G. (2006). Capping protein and the Arp2/3 complex regulate nonbundle actin filament assembly to indirectly control actin bundle positioning during Drosophila melanogaster bristle development. *Molecular biology of the cell*, *17*(9), 3930–3939. doi:10.1091/mbc.E06-06-0500

Fujiwara, I., Suetsugu, S., Uemura, S., Takenawa, T., & Ishiwata, S. (2002). Visualization and force measurement of branching by Arp2/3 complex and N-WASP in actin filament. *Biochemical and biophysical research communications*, *293*(5), 1550–1555. doi:10.1016/S0006-291X(02)00421-7

Furman, C., Sieminski, A. L., Kwiatkowski, A. V., Rubinson, D. A., Vasile, E., Bronson, R. T., et al. (2007). Ena/VASP is required for endothelial barrier function in vivo. *The Journal of cell biology*, *179*(4), 761–775. doi:10.1083/jcb.200705002

Gates, J., Mahaffey, J. P., Rogers, S. L., Emerson, M., Rogers, E. M., Sottile, S. L., et al. (2007). Enabled plays key roles in embryonic epithelial morphogenesis in Drosophila. *Development (Cambridge, England)*, *134*(11), 2027–2039. doi:10.1242/dev.02849

Gates, J., Nowotarski, S. H., Yin, H., Mahaffey, J. P., Bridges, T., Herrera, C., et al. (2009). Enabled and Capping protein play important roles in shaping cell behavior during Drosophila oogenesis. *Developmental biology*, *333*(1), 90–107. doi:10.1016/j.ydbio.2009.06.030

Gertler, F. B., Comer, A. R., Juang, J. L., Ahern, S. M., Clark, M. J., Liebl, E. C., & Hoffmann, F. M. (1995). enabled, a dosage-sensitive suppressor of mutations in the Drosophila Abl tyrosine kinase, encodes an Abl substrate with SH3 domain-binding properties. *Genes & development*, *9*(5), 521–533.

Gertler, F. B., Doctor, J. S., & Hoffmann, F. M. (1990). Genetic suppression of mutations in the Drosophila abl proto-oncogene homolog. *Science (New York, NY)*, *248*(4957), 857–860.

Giannone, G., Dubin-Thaler, B. J., Rossier, O., Cai, Y., Chaga, O., Jiang, G., et al. (2007). Lamellipodial actin mechanically links myosin activity with adhesion-site formation. *Cell*, *128*(3), 561–575. doi:10.1016/j.cell.2006.12.039

Gorelik, R., Yang, C., Kameswaran, V., Dominguez, R., & Svitkina, T. (2011). Mechanisms of plasma membrane targeting of formin mDia2 through its amino terminal domains. *Molecular biology of the cell*, *22*(2), 189–201. doi:10.1091/mbc.E10-03-0256

Gupton, S. L., & Gertler, F. B. (2007a). Filopodia: the fingers that do the walking. *Science's STKE : signal transduction knowledge environment*, *2007*(400), re5. doi:10.1126/stke.4002007re5

Gupton, S. L., Anderson, K. L., Kole, T. P., Fischer, R. S., Ponti, A., Hitchcock-DeGregori,

S. E., et al. (2005). Cell migration without a lamellipodium: translation of actin dynamics into cell movement mediated by tropomyosin. *The Journal of cell biology*, *168*(4), 619–631. doi:10.1083/jcb.200406063

Haas, P., & Gilmour, D. (2006). Chemokine signaling mediates self-organizing tissue migration in the zebrafish lateral line. *Developmental cell*, *10*(5), 673–680. doi:10.1016/j.devcel.2006.02.019

Halliburton, W. D. (1887). On Muscle-Plasma. *The Journal of physiology*, *8*(3-4), 133–202.

Hansen, S. D., & Mullins, R. D. (2010). VASP is a processive actin polymerase that requires monomeric actin for barbed end association. *The Journal of cell biology*, *191*(3), 571–584. doi:10.1083/jcb.201003014

Harbeck, B., Hüttelmaier, S., Schluter, K., Jockusch, B. M., & Illenberger, S. (2000). Phosphorylation of the vasodilator-stimulated phosphoprotein regulates its interaction with actin. *The Journal of biological chemistry*, *275*(40), 30817–30825.

Harden, N. (2002). Signaling pathways directing the movement and fusion of epithelial sheets: lessons from dorsal closure in Drosophila. *Differentiation; research in biological diversity*, *70*(4-5), 181–203. doi:10.1046/j.1432-0436.2002.700408.x

Harrison, R. G. (1959). The outgrowth of the nerve fiber as a mode of protoplasmic movement. *The Journal of experimental zoology*, *142*, 5–73.

Hart, M. C., Korshunova, Y. O., & Cooper, J. A. (1997). Vertebrates have conserved capping protein alpha isoforms with specific expression patterns. *Cell motility and the cytoskeleton*, *38*(2), 120–132. doi:10.1002/(SICI)1097-0169(1997)38:2<120::AIDCM2>3.0.CO;2-B

Hauser, W., Knobeloch, K. P., Eigenthaler, M., Gambaryan, S., Krenn, V., Geiger, J., et al. (1999). Megakaryocyte hyperplasia and enhanced agonist-induced platelet activation in vasodilator-stimulated phosphoprotein knockout mice. *Proceedings of the National Academy of Sciences of the United States of America*, *96*(14), 8120–8125.

Hensel, M., Klingauf, J., & Piehler, J. (2013). Imaging the invisible: resolving cellular microcompartments by superresolution microscopy techniques. *Biological chemistry*, *394*(9), 1097–1113. doi:10.1515/hsz-2012-0324

Hertwig, O. (1915). *Die Elemente der entwicklungslehre des Menschen und der Wirbeltiere.* Jena: Fischer.

Higashida, C., Miyoshi, T., Fujita, A., Oceguera-Yanez, F., Monypenny, J., Andou, Y., et al. (2004). Actin polymerization-driven molecular movement of mDia1 in living cells. *Science (New York, NY)*, *303*(5666), 2007–2010. doi:10.1126/science.1093923

Hightower, R. C., & Meagher, R. B. (1986). The molecular evolution of actin. *Genetics*, *114*(1), 315–332.

Homem, C. C. F., & Peifer, M. (2008). Diaphanous regulates myosin and adherens junctions to control cell contractility and protrusive behavior during morphogenesis. *Development (Cambridge, England)*, *135*(6), 1005–1018. doi:10.1242/dev.016337

Homem, C. C. F., & Peifer, M. (2009). Exploring the roles of diaphanous and enabled activity in shaping the balance between filopodia and lamellipodia. *Molecular biology of*

the cell, *20*(24), 5138–5155. doi:10.1091/mbc.E09-02-0144

Hooke, R., & Gunther, R. T. (1961). *Micrographia, or, Some physiological descriptions of minute bodies made by magnifying glasses: with observations and inquiries thereupon*. New York: Dover Publications.

Hopmann, R., & Miller, K. G. (2003). A balance of capping protein and profilin functions is required to regulate actin polymerization in Drosophila bristle. *Molecular biology of the cell*, *14*(1), 118–128. doi:10.1091/mbc.E02-05-0300

Hopmann, R., Cooper, J. A., & Miller, K. G. (1996). Actin organization, bristle morphology, and viability are affected by actin capping protein mutations in Drosophila. *The Journal of cell biology*, *133*(6), 1293–1305.

Hurst, S., Howes, E. A., Coadwell, J., & Jones, R. (1998). Expression of a testis-specific putative actin-capping protein associated with the developing acrosome during rat spermiogenesis. *Molecular reproduction and development*, *49*(1), 81–91. doi:10.1002/(SICI)1098-2795(199801)49:1<81::AID-MRD9>3.0.CO;2-K

Hüttelmaier, S., Harbeck, B., Steffens, O., Messerschmidt, T., Illenberger, S., & Jockusch, B. M. (1999). Characterization of the actin binding properties of the vasodilator-stimulated phosphoprotein VASP. *FEBS letters*, *451*(1), 68–74.

Iwasa, J. H., & Mullins, R. D. (2007). Spatial and temporal relationships between actinfilament nucleation, capping, and disassembly. *Current biology : CB*, *17*(5), 395–406. doi:10.1016/j.cub.2007.02.012

Jacinto, A., Wood, W., Balayo, T., Turmaine, M., Martinez-Arias, A., & Martin, P. (2000). Dynamic actin-based epithelial adhesion and cell matching during Drosophila dorsal closure. *Current biology : CB*, *10*(22), 1420–1426.

Janody, F., & Treisman, J. E. (2006). Actin capping protein alpha maintains vestigialexpressing cells within the Drosophila wing disc epithelium. *Development (Cambridge, England)*, *133*(17), 3349–3357. doi:10.1242/dev.02511

Jezowska, B., Fernández, B. G., Amândio, A. R., Duarte, P., Mendes, C., Brás-Pereira, C., & Janody, F. (2011). A dual function of Drosophila capping protein on DE-cadherin maintains epithelial integrity and prevents JNK-mediated apoptosis. *Developmental biology*, *360*(1), 143–159. doi:10.1016/j.ydbio.2011.09.016

Khurana, S., & George, S. P. (2011). The role of actin bundling proteins in the assembly of filopodia in epithelial cells. *Cell adhesion & migration*, *5*(5), 409–420. doi:10.4161/cam.5.5.17644

Kobielak, A., Pasolli, H. A., & Fuchs, E. (2004). Mammalian formin-1 participates in adherens junctions and polymerization of linear actin cables. *Nature cell biology*, *6*(1), 21–30.

Kovar, D. R., & Pollard, T. D. (2004). Insertional assembly of actin filament barbed ends in association with formins produces piconewton forces. *Proceedings of the National Academy of Sciences of the United States of America*, *101*(41), 14725–14730. doi:10.1073/pnas.0405902101

Kovar, D. R., Harris, E. S., Mahaffy, R., Higgs, H. N., & Pollard, T. D. (2006). Control of

the assembly of ATP- and ADP-actin by formins and profilin. *Cell*, *124*(2), 423–435. doi:10.1016/j.cell.2005.11.038

Kühne W. (1859) *Arch. f. Anat. Physiol. u. wissensch*. Med. 748
Kuhnel, K., Jarchau, T., Wolf, E., Schlichting, I., Walter, U., Wittinghofer, A., & Strelkov, S. V. (2004). The VASP tetramerization domain is a right-handed coiled coil based on a 15-residue repeat. *Proceedings of the National Academy of Sciences of the United States of America*, *101*(49), 17027–17032. doi:10.1073/pnas.0403069101

Kwiatkowski, A. V., Rubinson, D. A., Dent, E. W., Edward van Veen, J., Leslie, J. D., Zhang, J., et al. (2007). Ena/VASP Is Required for neuritogenesis in the developing cortex. *Neuron*, *56*(3), 441–455. doi:10.1016/j.neuron.2007.09.008

Lambrechts, A., Kwiatkowski, A. V., Lanier, L. M., Bear, J. E., Vandekerckhove, J., Ampe, C., & Gertler, F. B. (2000). cAMP-dependent protein kinase phosphorylation of EVL, a Mena/VASP relative, regulates its interaction with actin and SH3 domains. *The Journal of biological chemistry*, *275*(46), 36143–36151.

Lambrechts, A., Van Troys, M., & Ampe, C. (2004). The actin cytoskeleton in normal and pathological cell motility. *The international journal of biochemistry & cell biology*, *36*(10), 1890–1909. doi:10.1016/j.biocel.2004.01.024

Lanier, L. M., Gates, M. A., Witke, W., Menzies, A. S., Wehman, A. M., Macklis, J. D., et al. (1999). Mena is required for neurulation and commissure formation. *Neuron*, *22*(2), 313–325.

Laurent, V., Loisel, T. P., Harbeck, B., Wehman, A., Grobe, L., Jockusch, B. M., et al. (1999). Role of proteins of the Ena/VASP family in actin-based motility of Listeria monocytogenes. *The Journal of cell biology*, *144*(6), 1245–1258.

Le Clainche, C., & Carlier, M.-F. (2008). Regulation of actin assembly associated with protrusion and adhesion in cell migration. *Physiological reviews*, *88*(2), 489–513. doi:10.1152/physrev.00021.2007

Lee, Y.-J., Jeong, S.-H., Hong, S.-C., Cho, B.-I., Ha, W.-S., Park, S.-T., et al. (2013). Prognostic value of CAPZA1 overexpression in gastric cancer. *International journal of oncology*, *42*(5), 1569–1577. doi:10.3892/ijo.2013.1867

Lewis, A. K., & Bridgman, P. C. (1992). Nerve growth cone lamellipodia contain two populations of actin filaments that differ in organization and polarity. *The Journal of cell biology*, *119*(5), 1219–1243.

Li, F., & Higgs, H. N. (2003). The mouse Formin mDia1 is a potent actin nucleation factor regulated by autoinhibition. *Current biology : CB*, *13*(15), 1335–1340.

Loureiro, J. J., Rubinson, D. A., Bear, J. E., Baltus, G. A., Kwiatkowski, A. V., & Gertler, F. B. (2002). Critical roles of phosphorylation and actin binding motifs, but not the central proline-rich region, for Ena/vasodilator-stimulated phosphoprotein (VASP) function during cell migration. *Molecular biology of the cell*, *13*(7), 2533–2546. doi:10.1091/mbc.E01-10-0102

Luxton, G. W. G., Gomes, E. R., Folker, E. S., Worman, H. J., & Gundersen, G. G. (2011). TAN lines: a novel nuclear envelope structure involved in nuclear positioning. *Nucleus (Austin, Tex.)*, *2*(3), 173–181. doi:10.4161/nucl.2.3.16243

Maciver, S. K., & Weeds, A. G. (1994). Actophorin preferentially binds monomeric ADPactin

over ATP-bound actin: consequences for cell locomotion. *FEBS letters*, *347*(2-3), 251–256.

Maruyama, K., Kurokawa, H., Oosawa, M., Shimaoka, S., Yamamoto, H., Ito, M., & Maruyama, K. (1990). Beta-actinin is equivalent to Cap Z protein. *The Journal of biological chemistry*, *265*(15), 8712–8715.

Mehlen, P., & Puisieux, A. (2006). Metastasis: a question of life or death. *Nature reviews. Cancer*, *6*(6), 449–458. doi:10.1038/nrc1886

Menna, E., Fossati, G., Scita, G., & Matteoli, M. (2011). From filopodia to synapses: the role of actin-capping and anti-capping proteins. *The European journal of neuroscience*, *34*(10), 1655–1662. doi:10.1111/j.1460-9568.2011.07897.x

Miller, J., Fraser, S. E., & McClay, D. (1995). Dynamics of thin filopodia during sea urchin gastrulation. *Development (Cambridge, England)*, *121*(8), 2501–2511.

Mitchison, T. J., & Cramer, L. P. (1996). Actin-based cell motility and cell locomotion. *Cell*, *84*(3), 371–379.

Mitra, S. K., Hanson, D. A., & Schlaepfer, D. D. (2005). Focal adhesion kinase: in command and control of cell motility. *Nature reviews. Molecular cell biology*, *6*(1), 56–68. doi:10.1038/nrm1549

Montell, D. J. (2003). Border-cell migration: the race is on. *Nature reviews. Molecular cell biology*, *4*(1), 13–24. doi:10.1038/nrm1006

Montell, D. J. (2006). The social lives of migrating cells in Drosophila. *Current opinion in genetics & development*, *16*(4), 374–383. doi:10.1016/j.gde.2006.06.010

Mullins, R. D., Heuser, J. A., & Pollard, T. D. (1998). The interaction of Arp2/3 complex with actin: nucleation, high affinity pointed end capping, and formation of branching networks of filaments. *Proceedings of the National Academy of Sciences of the United States of America*, *95*(11), 6181–6186.

Niebuhr, K., Ebel, F., Frank, R., Reinhard, M., Domann, E., Carl, U. D., et al. (1997). A novel proline-rich motif present in ActA of Listeria monocytogenes and cytoskeletal proteins is the ligand for the EVH1 domain, a protein module present in the Ena/VASP family. *The EMBO journal*, *16*(17), 5433–5444. doi:10.1093/emboj/16.17.5433

Otomo, T., Otomo, C., Tomchick, D. R., Machius, M., & Rosen, M. K. (2005). Structural basis of Rho GTPase-mediated activation of the formin mDia1. *Molecular cell*, *18*(3), 273–281. doi:10.1016/j.molcel.2005.04.002

Pantaloni, D., & Carlier, M. F. (1993). How profilin promotes actin filament assembly in the presence of thymosin beta 4. *Cell*, *75*(5), 1007–1014.

Peglion, F., Llense, F., & Etienne-Manneville, S. (2014). Adherens junction treadmilling during collective migration. *Nature cell biology*, *16*(7), 639–651. doi:10.1038/ncb2985

Peng, J., Wallar, B. J., Flanders, A., Swiatek, P. J., & Alberts, A. S. (2003). Disruption of the Diaphanous-related formin Drf1 gene encoding mDia1 reveals a role for Drf3 as an effector for Cdc42. *Current biology : CB*, *13*(7), 534–545.

Peng, Y., Han, C., & Axelrod, J. D. (2012). Planar polarized protrusions break the symmetry of EGFR signaling during Drosophila bract cell fate induction. *Developmental cell*,

23(3), 507–518. doi:10.1016/j.devcel.2012.07.016

Perrin, B. J., & Ervasti, J. M. (2010). The actin gene family: function follows isoform. *Cytoskeleton (Hoboken, NJ)*, *67*(10), 630–634. doi:10.1002/cm.20475

Perry, S. V. (2003). When was actin first extracted from muscle? *Journal of muscle research and cell motility*, *24*(8), 597–599.

Philippar, U., Roussos, E. T., Oser, M., Yamaguchi, H., Kim, H.-D., Giampieri, S., et al. (2008). A Mena invasion isoform potentiates EGF-induced carcinoma cell invasion and metastasis. *Developmental cell*, *15*(6), 813–828. doi:10.1016/j.devcel.2008.09.003

Pollard, T. D., & Borisy, G. G. (2003). Cellular motility driven by assembly and disassembly of actin filaments. *Cell*, *112*(4), 453–465.

Pollard, T. D., & Cooper, J. A. (2009). Actin, a central player in cell shape and movement. *Science (New York, NY)*, *326*(5957), 1208–1212. doi:10.1126/science.1175862

Pollard, T. D., Blanchoin, L., & Mullins, R. D. (2001). Actin dynamics. *Journal of cell science*, *114*(Pt 1), 3–4.

Pruyne, D., Evangelista, M., Yang, C., Bi, E., Zigmond, S., Bretscher, A., & Boone, C. (2002). Role of formins in actin assembly: nucleation and barbed-end association. *Science (New York, NY)*, *297*(5581), 612–615. doi:10.1126/science.1072309

Raz, E. (2003). Primordial germ-cell development: the zebrafish perspective. *Nature reviews. Genetics*, *4*(9), 690–700. doi:10.1038/nrg1154

Reinhard, M., Halbrugge, M., Scheer, U., Wiegand, C., Jockusch, B. M., & Walter, U. (1992). The 46/50 kDa phosphoprotein VASP purified from human platelets is a novel protein associated with actin filaments and focal contacts. *The EMBO journal*, *11*(6), 2063–2070.

Rogers, S. L., Wiedemann, U., Stuurman, N., & Vale, R. D. (2003). Molecular requirements for actin-based lamella formation in Drosophila S2 cells. *The Journal of cell biology*, *162*(6), 1079–1088. doi:10.1083/jcb.200303023

Romero, S., Le Clainche, C., Didry, D., Egile, C., Pantaloni, D., & Carlier, M.-F. (2004). Formin is a processive motor that requires profilin to accelerate actin assembly and associated ATP hydrolysis. *Cell*, *119*(3), 419–429. doi:10.1016/j.cell.2004.09.039

Rose, R., Weyand, M., Lammers, M., Ishizaki, T., Ahmadian, M. R., & Wittinghofer, A. (2005). Structural and mechanistic insights into the interaction between Rho and mammalian Dia. *Nature*, *435*(7041), 513–518. doi:10.1038/nature03604

Rotty, J. D., Wu, C., & Bear, J. E. (2013). New insights into the regulation and cellular functions of the ARP2/3 complex. *Nature reviews. Molecular cell biology*, *14*(1), 7–12. doi:10.1038/nrm3492

Roy, S., Huang, H., Liu, S., & Kornberg, T. B. (2014). Cytoneme-mediated contactdependent transport of the Drosophila decapentaplegic signaling protein. *Science (New York, NY)*, *343*(6173), 1244624. doi:10.1126/science.1244624

Russell, B. (1945). *A history of western philosophy, and its connection with political and social circumstances from the earliest times to the present day*. New York: Simon and

Schuster.

Sahai, E., & Marshall, C. J. (2002). ROCK and Dia have opposing effects on adherens junctions downstream of Rho. *Nature cell biology*, *4*(6), 408–415.

Sanders, T. A., Llagostera, E., & Barna, M. (2013). Specialized filopodia direct long-range transport of SHH during vertebrate tissue patterning. *Nature*, *497*(7451), 628–632. doi:10.1038/nature12157

Sansores-Garcia, L., Bossuyt, W., Wada, K.-I., Yonemura, S., Tao, C., Sasaki, H., & Halder, G. (2011). Modulating F-actin organization induces organ growth by affecting the Hippo pathway. *The EMBO journal*, *30*(12), 2325–2335. doi:10.1038/emboj.2011.157

Schafer, D. A., Jennings, P. B., & Cooper, J. A. (1996). Dynamics of capping protein and actin assembly in vitro: uncapping barbed ends by polyphosphoinositides. *The Journal of cell biology*, *135*(1), 169–179.

Schirenbeck, A., Arasada, R., Bretschneider, T., Stradal, T. E. B., Schleicher, M., & Faix, J. (2006). The bundling activity of vasodilator-stimulated phosphoprotein is required for filopodium formation. *Proceedings of the National Academy of Sciences of the United States of America*, *103*(20), 7694–7699. doi:10.1073/pnas.0511243103

Schirenbeck, A., Bretschneider, T., Arasada, R., Schleicher, M., & Faix, J. (2005). The Diaphanous-related formin dDia2 is required for the formation and maintenance of filopodia. *Nature cell biology*, *7*(6), 619–625. doi:10.1038/ncb1266

Schleiden, M. (1838). *Beiträge zur Phytogenesis.*

Schwann, T. (1847). *Microscopical researches into the accordance in the structure and growth of animals and plants*. London: The Sydenham society.

Sept, D., & McCammon, J. A. (2001). Thermodynamics and kinetics of actin filament nucleation. *Biophysical journal*, *81*(2), 667–674. doi:10.1016/S0006-3495(01)75731-1

Severson, A. F., Baillie, D. L., & Bowerman, B. (2002). A Formin Homology protein and a profilin are required for cytokinesis and Arp2/3-independent assembly of cortical microfilaments in C. elegans. *Current biology : CB*, *12*(24), 2066–2075.

Shaner, N. C., Patterson, G. H., & Davidson, M. W. (2007). Advances in fluorescent protein technology. *Journal of cell science*, *120*(Pt 24), 4247–4260. doi:10.1242/jcs.005801

Sinnar, S. A., Antoku, S., Saffin, J.-M., Cooper, J. A., & Halpain, S. (2014). CAPPING PROTEIN IS ESSENTIAL FOR CELL MIGRATION IN VIVO AND FOR FILOPODIAL MORPHOLOGY AND DYNAMICS. *Molecular biology of the cell*. doi:10.1091/mbc.E13-12-0749

Small, J. V., & Celis, J. E. (1978). Filament arrangements in negatively stained cultured cells: the organization of actin. *Cytobiologie*, *16*(2), 308–325.

Stevenson, R. P., Veltman, D., & Machesky, L. M. (2012). Actin-bundling proteins in cancer progression at a glance. *Journal of cell science*, *125*(Pt 5), 1073–1079. doi:10.1242/jcs.093799

Straub FB (1942) *Actin.* Stud Inst Med Chem Univ Szeged II: 1–15.

Svitkina, T. M., & Borisy, G. G. (1999). Arp2/3 complex and actin depolymerizing factor/cofilin in dendritic organization and treadmilling of actin filament array in lamellipodia. *The Journal of cell biology*, *145*(5), 1009–1026.

Svitkina, T. M., Bulanova, E. A., Chaga, O. Y., Vignjevic, D. M., Kojima, S.-I., Vasiliev, J. M., & Borisy, G. G. (2003). Mechanism of filopodia initiation by reorganization of a dendritic network. *The Journal of cell biology*, *160*(3), 409–421.

Swan, K. A., Severson, A. F., Carter, J. C., Martin, P. R., Schnabel, H., Schnabel, R., & Bowerman, B. (1998). cyk-1: a C. elegans FH gene required for a late step in embryonic cytokinesis. *Journal of cell science*, *111 (Pt 14)*, 2017–2027.

Szent-Gyorgyi A (1941–42a) *The contraction of myosin threads.* Stud Inst Med Chem Univ Szeged I: 6–15.

Szent-Gyorgyi A (1941–42b) *Discussion.* Stud Inst Med Chem Univ Szeged I: 67–71.

Tanizaki, H., Egawa, G., Inaba, K., Honda, T., Nakajima, S., Moniaga, C. S., et al. (2010). Rho-mDia1 pathway is required for adhesion, migration, and T-cell stimulation in dendritic cells. *Blood*, *116*(26), 5875–5884. doi:10.1182/blood-2010-01-264150

Theriot, J. A., & Mitchison, T. J. (1991). Actin microfilament dynamics in locomoting cells. *Nature*, *352*(6331), 126–131. doi:10.1038/352126a0

Thiery, J. P., Acloque, H., Huang, R. Y. J., & Nieto, M. A. (2009). Epithelial-mesenchymal transitions in development and disease. *Cell*, *139*(5), 871–890. doi:10.1016/j.cell.2009.11.007

Thumkeo, D., Shinohara, R., Watanabe, K., Takebayashi, H., Toyoda, Y., Tohyama, K., et al. (2011). Deficiency of mDia, an actin nucleator, disrupts integrity of neuroepithelium and causes periventricular dysplasia. *PloS one*, *6*(9), e25465. doi:10.1371/journal.pone.0025465

Tilney, L. G., Connelly, P., Smith, S., & Guild, G. M. (1996). F-actin bundles in Drosophila bristles are assembled from modules composed of short filaments. *The Journal of cell biology*, *135*(5), 1291–1308.

Tojkander, S., Gateva, G., & Lappalainen, P. (2012). Actin stress fibers--assembly, dynamics and biological roles. *Journal of cell science*, *125*(Pt 8), 1855–1864. doi:10.1242/jcs.098087

Toyoda, A., Yokota, A., Saito, T., Kawana, H., Higashi, M., Suzuki, Y., et al. (2011). Overexpression of human ortholog of mammalian enabled (hMena) is associated with the expression of mutant p53 protein in human breast cancers. *International journal of oncology*, *38*(1), 89–96.

Verkhovsky, A. B., Svitkina, T. M., & Borisy, G. G. (1999). Self-polarization and directional motility of cytoplasm. *Current biology : CB*, *9*(1), 11–20.

Vinson, V. K., La Cruz, De, E. M., Higgs, H. N., & Pollard, T. D. (1998). Interactions of Acanthamoeba profilin with actin and nucleotides bound to actin. *Biochemistry*, *37*(31), 10871–10880. doi:10.1021/bi980093l

Walders-Harbeck, B., Khaitlina, S. Y., Hinssen, H., Jockusch, B. M., & Illenberger, S. (2002). The vasodilator-stimulated phosphoprotein promotes actin polymerisation

through direct binding to monomeric actin. *FEBS letters*, *529*(2-3), 275–280.

Wallar, B. J., Stropich, B. N., Schoenherr, J. A., Holman, H. A., Kitchen, S. M., & Alberts, A. S. (2006). The basic region of the diaphanous-autoregulatory domain (DAD) is required for autoregulatory interactions with the diaphanous-related formin inhibitory domain. *The Journal of biological chemistry*, *281*(7), 4300–4307. doi:10.1074/jbc.M510277200

Watanabe, S., De Zan, T., Ishizaki, T., Yasuda, S., Kamijo, H., Yamada, D., et al. (2013). Loss of a Rho-regulated actin nucleator, mDia2, impairs cytokinesis during mouse fetal erythropoiesis. *Cell reports*, *5*(4), 926–932. doi:10.1016/j.celrep.2013.10.021

Wear, M. A., & Cooper, J. A. (2004). Capping protein: new insights into mechanism and regulation. *Trends in biochemical sciences*, *29*(8), 418–428. doi:10.1016/j.tibs.2004.06.003

Wear, M. A., Yamashita, A., Kim, K., Maéda, Y., & Cooper, J. A. (2003). How capping protein binds the barbed end of the actin filament. *Current biology : CB*, *13*(17), 1531–1537.

Wills, Z., Bateman, J., Korey, C. A., Comer, A., & Van Vactor, D. (1999). The tyrosine kinase Abl and its substrate enabled collaborate with the receptor phosphatase Dlar to control motor axon guidance. *Neuron*, *22*(2), 301–312.

Winkelman, J. D., Bilancia, C. G., Peifer, M., & Kovar, D. R. (2014). Ena/VASP Enabled is a highly processive actin polymerase tailored to self-assemble parallel-bundled F-actin networks with Fascin. *Proceedings of the National Academy of Sciences of the United States of America*, *111*(11), 4121–4126. doi:10.1073/pnas.1322093111

Wu, C., Asokan, S. B., Berginski, M. E., Haynes, E. M., Sharpless, N. E., Griffith, J. D., et al. (2012). Arp2/3 is critical for lamellipodia and response to extracellular matrix cues but is dispensable for chemotaxis. *Cell*, *148*(5), 973–987. doi:10.1016/j.cell.2011.12.034

Yamamoto, S., Tsuda, H., Honda, K., Onozato, K., Takano, M., Tamai, S., et al. (2009). Actinin-4 gene amplification in ovarian cancer: a candidate oncogene associated with poor patient prognosis and tumor chemoresistance. *Modern pathology : an official journal of the United States and Canadian Academy of Pathology, Inc*, *22*(4), 499–507. doi:10.1038/modpathol.2008.234

Yang, C., & Svitkina, T. (2011). Filopodia initiation: focus on the Arp2/3 complex and Formins. *Cell adhesion & migration*, *5*(5), 402–408. doi:10.4161/cam.5.5.16971

Zigmond, S. H., Evangelista, M., Boone, C., Yang, C., Dar, A. C., Sicheri, F., et al. (2003). Formin leaky cap allows elongation in the presence of tight capping proteins. *Current biology : CB*, *13*(20), 1820–1823.

CHAPTER 2: ENABLED AND CAPPING PROTEIN PLAY IMPORTANT ROLES IN SHAPING CELL BEHAVIOR DURING *DROSOPHILA* OOGENESIS

Julie Gates[a,c], Stephanie H. Nowotarski[a], Hongyan Yin[b], James P. Mahaffey[a], Tina Bridges[b], Cristina Herrera[c], Catarina C.F. Homem[a], Florence Janody[d], Denise J. Montell[b], Mark Peifer[a,*]

[a] Lineberger Comprehensive Cancer Center and Department of Biology; University of North Carolina at Chapel Hill, Chapel Hill, NC 27599, USA; [b] Department of Biological Chemistry, Center for Cell Dynamics, Johns Hopkins School of Medicine, Baltimore, MD 21205, USA; [c] Department of Biology, Bucknell University, Lewisburg, PA 17837, USA; [d] Instituto Gulbenkian de Ciencia, Oeiras, Portugal

Preface

For my second chapter I have included a second author paper constituting a large portion of my early work in the lab. This work was published by Developmental Biology in 2009 and is entitled: "Enabled and Capping Protein play important roles in shaping cell behavior during *Drosophila* oogenesis." This paper built off of Julie Gates' 2007 paper describing how Ena contributes to embryonic morphogenesis by pursuing an oogenesis defect observed in mutants. Julie Gates, James Mahaffey and Cristina Herrera completed the embryo hatch rates and fixed analysis of *ena* mutant egg chambers. Hongyan Yin and Tina Bridges from Denise Montell's laboratory and Catarina Homem completed the border cell migration assays.Florence Janody generously provided capping protein fly stocks. This work was completed under the direction of

Mark Peifer.

My contributions to the following work are: (1) I found loss of Ena's negative regulator, Abl leads to premature nurse cell dumping and some de-regulation of Ena. I carried out work detailing CP phenotypes in germline clones and transheterozygotic mutants finding: (2) cytoplasmic actin filaments are disrupted upon loss of CP, (3) CP is required for nurse cell cortical integrity as well as for (4) proper oocyte specification. The latter finding is most likely through CPs role in the dynein-dynactin complex- providing one of the first *in vivo* roles for CP in this complex.

Abstract

During development, cells craft an impressive array of actin-based structures, mediating events as diverse as cytokinesis, apical constriction, and cell migration. One challenge is to determine how cells regulate actin assembly and disassembly to carry out these cell behaviors. During *Drosophila* oogenesis diverse cell behaviors are seen in the soma and germline. We used oogenesis to explore developmental roles of two important actin regulators: Enabled/VASP proteins and Capping protein. We found that Enabled plays an important role in cortical integrity of nurse cells, formation of robust bundled actin filaments in late nurse cells that facilitate nurse cell dumping, and migration of somatic border cells. During nurse cell dumping, Enabled localizes to barbed ends of the nurse cell actin filaments, suggesting its mechanism of action. We further pursued this mechanism using mutant Enabled proteins, each affecting one of its protein domains. These data suggest critical roles for the EVH2 domain and its tetramerization subdomain, while the EVH1 domain appears less critical. Enabled appears to be negatively regulated during oogenesis by Abelson kinase. We also explored the function of Capping protein. This revealed important roles in oocyte determination, nurse cell cortical integrity and nurse cell dumping, and support the idea that Capping protein and Enabled act antagonistically during dumping. Together these data reveal places that these actin regulators shape oogenesis.

Introduction

Animal tissues and their constituent cells undergo dynamic changes during embryonic development and during homeostasis and remodeling of adult tissues. The actin cytoskeleton plays a key role in the dynamic behavior of individual cells during morphogenesis, mediating cell shape change and migration. One key challenge is to understand how actin dynamics are regulated during normal development.

Elegant biochemical and biophysical studies in vitro and cell biological analyses in cultured cells have begun to reveal the toolkit cells use to regulate actin dynamics. Actin filaments are asymmetric polymers that extend by monomer addition at the barbed end. An impressive array of proteins regulates actin nucleation, polymerization or capping, bundling and severing (Pollard and Borisy, 2003). One key regulated event is the decision to continue polymerization or terminate this process. Capping protein (CP) binds barbed ends to prevent further addition of actin monomers (Wear and Cooper, 2004).In contrast, Enabled (Ena)/VASP proteins act at barbed ends to promote continued polymerization, thus antagonizing CP (Bear *et al.*, 2002; Barzik *et al.*, 2005). Ena/VASP proteins can also accelerate polymerization by recruiting Profilin/actin complexes (Sechi and Wehland, 2004) and can bundle actin filaments in filopodia (Schirenbeck *et al.*, 2006; Applewhite *et al.*, 2007).

To understand how these proteins shape cell behavior, the roles of Ena/VASP proteins and CP were dissected in cultured fibroblasts and epithelial cells. In fibroblasts, Ena/VASP proteins regulate cell motility (Bear *et al.*, 2000). Inactivating Ena/VASP proteins speeds cell migration while recruiting Ena/VASP proteins to the plasma membrane slows it, suggesting they restrain fibroblast migration. Recruiting Ena/VASP proteins to the plasma membrane leads to longer, unbranched actin filaments in lamellipodia, which may not provide sufficient mechanical strength for sustained lamellipodial extension.

In keratinocytes (Vasioukhin *et al.*, 2000) and mammary epithelial cells (Scott *et al.*, 2006), inactivating Ena/VASP proteins impairs establishment of cadherin-based cell–cell contacts, potentially by reducing filopodial extensions that initiate adhesion. In contrast,

depleting CP in mammalian (Mejillano *et al.*, 2004) or Drosophila (Gates *et al.*, 2007) cultured cells triggers explosive formation of filopodia, confirming that CP is a major player in limiting filament extension. In mammalian cells, this response requires Ena/VASP proteins (Mejillano *et al.*, 2004; Applewhite *et al.*, 2007), further supporting an antagonistic relationship between Ena/VASP and CP.

Ena/VASP proteins are critical for normal development. They play important roles in axon outgrowth and guidance in mice, *Drosophila* and *C. elegans* (reviewed in Korey and Van Vactor, 2000; Krause *et al.*, 2003).They also regulate epithelial morphogenesis. While *C. elegans* epithelial development is normal in the absence of its single Ena/ VASP protein UNC-34, animals double mutant for UNC-34 and the Arp2/3 regulator WASP have severe defects in morphogenesis, suggesting redundant roles (Withee *et al.*, 2004; Sheffield *et al.*, 2007). Mice double or triple mutant for Ena/VASP proteins have defects in neural tube closure, craniofacial development, and endothelial barrier function (Menzies *et al.*, 2004; Furman *et al.*, 2007), while knockdown of *Xenopus* Ena disrupts neural tube closure (Roffers-Agarwal *et al.*, 2008). Removal of maternal and zygotic Ena from *Drosophila* embryos (Gates *et al.*, 2007) disrupts or alters many events in embryonic morphogenesis, including germband retraction, dorsal closure and head involution, but does not disrupt cell adhesion or the overall cortical actin cytoskeleton. Less is known about the roles of CP *in vivo*. Functional CP is a dimer of α- and β-subunits. Null mutations in *Drosophila* capping protein β (cpb) are zygotically larval lethal; presumably maternal contribution rescues embryogenesis. Adult mutants for weaker cpb alleles have defects in bristle development, and are female sterile (Hopmann *et al.*, 1996). In bristles CP has antagonistic relationships with the actin monomer binding protein Profilin and the actin-nucleating Arp2/3 complex (Frank and Rushlow, 1996; Hopmann and Miller, 2003). In imaginal discs, precursors of the adult eye and epidermis, loss of CP leads to increased actin accumulation (Delalle *et al.*, 2005; Janody and Treisman, 2006). In the eye, this is followed by late neural degeneration, while in the wing disc a subset of cells degenerate. Phenotypes of CP mutants in mice or worms have not been reported.

Together, these data provide a glimpse of some biological events that require Ena/VASP proteins and CP *in vivo*. To obtain additional insight into how they influence cell behavior during development, we turned to *Drosophila* oogenesis (Hudson and Cooley, 2002a).The ovary is a relatively simple tissue, with a small number of germline and somatic cell types (Spradling, 1993). Each ovariole is an egg assembly line, with egg chambers of different developmental stages along its length (Fig. 2.1A). Oogenesis involves a stereotyped set of cell behaviors driven, in part, by the actin cytoskeleton. In the germarium (Fig. 2.1A), germline stem cells divide asymmetrically to produce cystocytes, which undergo four rounds of cell division without fully completing cytokinesis, producing a cyst of 16 germ cells interconnected by cytoplasmic bridges called ring canals. One cell becomes the oocyte and 15 become nurse cells. Each cyst is then encapsulated by a polarized epithelial sheet of somatic follicle cells joined by adherens junctions (AJs). Nurse cells and the oocyte also have AJ proteins at the cortex, underlain by cortical actin. Cadherin-based adhesion between germ and follicle cells is critical for posterior oocyte positioning (Peifer *et al.*, 1993; Godt and Tepass, 1998; González-Reyes and St Johnston, 1998). Cadherins and cortical actin also maintain nurse cell integrity, likely resisting force exerted by muscles surrounding each ovariole. In the absence of AJs (Peifer *et al.*, 1993) or when the germline is mutant for actin regulators such as Profilin (Verheyen and Cooley, 1994), the Arp2/3 complex (Hudson and Cooley, 2002b), or its regulator Scar (Zallen *et al.*, 2002), the cortical plasma membrane is disrupted, leading to multinucleate nurse cells.

Nurse cells produce nutrients and macromolecules needed in oocytes for embryogenesis. These are transferred into the oocyte in two stages—early slow cytoplasmic transfer, and rapid late “dumping” when nurse cells transfer their entire contents into the egg, leaving only nuclei behind. Nurse cell dumping is driven by actomyosin contraction (Wheatley *et al.*, 1995), and also requires adhesive proteins and additional cytoskeletal structures. Just prior to dumping, the nurse cell actin cytoskeleton is dramatically remodeled. Arrays of bundled actin filaments, referred to as cytoplasmic filaments, extend from the plasma membrane toward the nucleus, immobilizing it (Gutzeit, 1986; Guild *et al.*, 1997). These filaments initiate at the

plasma membrane as filopodia/microvilli, with barbed ends oriented outward. By an unknown mechanism, many of these initial filament bundles are cross-linked together to form the full-length cytoplasmic filaments. When the germline is mutant for Profilin (Cooley *et al.*, 1992), or the actin bundling proteins Fascin (Cant *et al.*, 1994; 1998), Villin (Drosophila Quail; (Mahajan-Miklos and Cooley, 1994), or Filamin (Li et al., 1999), cytoplasmic filaments fail to form properly. Similar failure occurs when the germline lacks AJs (Peifer *et al.*, 1993). As a result, dumping is reduced or halted, in part because nuclei physically block the ring canals.

Follicle cells also undergo morphogenetic movements. For example, anterior polar follicle cells recruit a group of neighboring cells, undergo a partial epithelial–mesenchymal transition, leave the follicular epithelium and migrate between nurse cells to the anterior end of the oocyte (Rørth, 2002; Montell, 2003). These cells are called border cells (Fig. 2.1A). Cell adhesion and actin dynamics also regulate border cell migration. However, despite extensive genetic studies, essential regulators of actin dynamics in border cells have not been fully characterized. The actin-depolymerizer ADF/cofilin is required for border cell migration (Chen *et al.*, 2001), and other actin regulators are expressed in migrating border cells (Wang *et al.*, 2006). However, most proteins with well-characterized biochemical functions in actin dynamics have not been functionally tested in border cell migration.

Here we examine how Ena/VASP and CP influence cell behavior, using *Drosophila* oogenesis as a model. This revealed important roles for Ena in maintaining nurse cell cortical integrity, in forming the robust bundled cytoplasmic actin filaments in nurse cells during dumping, and in border cell migration. We examined the requirement for different domains of Ena in each process, suggesting mechanisms by which Ena acts, and explored its antagonism with CP and regulation by Abelson (Abl) kinase. We also analyzed the role of CP during germline development, revealing novel insights into events where it plays a critical role.

Results

Ena's dynamic localization during oogenesis suggests possible roles in actin regulation

Current models suggest that Ena/VASP proteins regulate actin capping, accelerate actin polymerization and regulate actin bundling (see Introduction). To assess when and where Ena is required during Drosophila oogenesis we examined its localization. In the germarium, Ena is weakly cortical in all cells (Fig. 2.1B, arrowhead). As follicle cells envelop the germ cells, Ena becomes enriched at follicle cell AJs (Fig. 2.1B, arrows), where it remains as egg chambers mature (Figs. 2.1C–E, white arrows). During border cell migration, Ena accumulates in both central and peripheral cells in the cluster (Fig. 2.1I). In germline cells Ena accumulates in the cytoplasm (Figs. 2.1C–H) and is weakly cortically enriched during early stages (Figs. 2.1C, E, arrowheads); cortical enrichment increases as dumping approaches (Figs. 2.1F, H, arrow- heads) and remains high through this process (Fig. 2.1G, arrowhead). Ena is also enriched at the posterior end of the oocyte, the follicle cells that abut it, or both (Fig. 2.1E, red arrow).

Oogenesis requires multiple actin structures, and to gain insight into Ena's role we closely examined Ena localization relative to these. During late oogenesis, the nurse cell cortical actomyosin network contracts, pushing the nurse cell contents into the oocyte through the ring canals. Just prior to dumping a set of very robust unbranched, bundled actin filaments forms between the plasma membranes and nurse cell nuclei (Fig. 2.2A; Guild *et al.*, 1997). These cytoplasmic filaments are anchored in plasma membrane projections (Fig. 2.2C), with their barbed ends membrane proximal (Guild *et al.*, 1997). They hold the nuclei in place, preventing them from being pushed into the ring canals and blocking transport.

The formation of cytoplasmic actin filaments requires several actin regulators, including Profilin (Cooley *et al.*, 1992), and the actin bundling proteins Fascin (Cant *et al.*, 1994), Villin (Drosophila Quail; Mahajan-Miklos and Cooley, 1994), and Filamin (Li et al., 1999). We thus examined whether Ena localization is consistent with a role in regulating filament formation. Interestingly, just as cytoplasmic actin filaments form, a cloud of punctate Ena

appears bracketing the nurse cell cortex (Fig. 2.2A, white arrows, 2.2B, bracket) and at the nurse cell– oocyte interface (Fig. 2.2A, blue arrows). Strikingly, this Ena is concentrated at membrane-associated barbed ends of these bundled cytoplasmic filaments (Figs. 2.2B, D, arrows). During later stages, Ena also accumulates around ring canals (Figs. 2.1F, H, blue arrows, 2A, arrowheads). Ring canals are large assemblies of actin and other proteins (Robinson and Cooley, 1997) that are surrounded by plasma membrane rich in membrane projections (Riparbelli and Callaini, 1995; Tilney *et al.*, 1996). During dumping, actin filaments form baskets around ring canals (inset Fig. 2.2E). Ena is not enriched in the ring canal proper (Fig. 2.2E, arrowhead), but is concentrated in the surrounding plasma membrane (Fig. 2.2E, arrows), and at the tips of the basket of actin filaments (Fig. 2.2E inset, arrows). Thus Ena is positioned to potentially help modulate the assembly of the cytoplasmic actin filaments as well as the actin filaments that surround the ring canals.

Loss of Ena results in defects in nurse cell dumping

We next examined whether Ena plays important roles in the germline during oogenesis. We inactivated Ena function using two approaches. We first adapted an approach from cultured mammalian cells, which uses the FP4mito fusion protein (Fig. 2.3A, top; Bear *et al.*, 2000) to relocalize endogenous Ena/VASP proteins to mitochondria, and thus sequester them away from their normal sites of action. For use in Drosophila we put FP4mito under control of the Gal4-UAS system to allow us to express it at different times and/or places in development. Expression of FP4mito rapidly relocalizes Ena to mitochondria, and in embryos this leads to a very strong to complete loss of Ena function (Gates *et al.*, 2007). We expressed FP4mito in the female germline using the matα4-Gal4-VP16 driver (matGal4), resulting in Ena sequestration (Fig. 2.1J) beginning at ~ stage 6 of oogenesis. In our second approach, we generated females with germlines mutant for three different loss of function ena alleles from the onset of oogenesis; each affects a different protein domain (Fig. 2.3A, bottom; Ahern-Djamali *et al.*, 1998; Li *et al.*, 2005). The N-terminal EVH1 domain binds protein partners carrying the consensus sequence D/EFPPPPXD/E (“FP4”; Ball *et al.*, 2002),

and is thought to mediate Ena localization. The C-terminal EVH2 domain carries several functional subdomains that bind G-actin, F-actin and mediate homotetramerization. ena^{210} encodes a missense change in the EVH1 domain (A97V; Fig. 2.3A), and prevents interaction with one of Ena's FP4 partners, Zyxin, *in vitro* (Ahern-Djamali *et al.*, 1998). ena^{23} truncates the EVH2 domain, deleting the tetramerization motif but not removing the actin binding sites (Fig. 2.3A). ena^{46} truncates the protein at the very beginning of the EVH2 domain (Fig. 2.3A), produces only a very low level of this truncated protein, and behaves genetically like a null allele (Li *et al.*, 2005).

When we reduced germline Ena function by either approach, female fertility was dramatically reduced; many eggs were smaller than wildtype (Fig. 2.3B vs. C) and most were not fertilized. These eggs exhibited the “dumpless” phenotype characteristic of failure to fully transfer the nurse cell contents into the oocyte (Hudson and Cooley, 2002b). Similar phenotypes are seen when germline cells are mutant for other cytoskeletal regulators including Ena's binding partner Profilin (Cooley *et al.*, 1992), the actin bundling proteins Fascin (Cant *et al.*, 1994) or Villin (Mahajan-Miklos and Cooley, 1994), a component of the Arp2/3 complex (Hudson and Cooley, 2002a), or when they are mutant for the AJ proteins DE-cadherin (DE-cad; Godt and Tepass, 1998) or Armadillo (Arm = fly β-catenin; Peifer *et al.*, 1993). The dumpless phenotype of Ena sequestration using FP4mito is most severe, with nearly complete penetrance (Fig. 2.3F). ena^{23}, deleting Ena's tetramerization domain, and ena^{46}, deleting the EVH2 domain (Fig. 2.3A), both display a similar intermediate dumpless phenotype (Fig. 2.3F), while ena^{210}, a point mutation in the EVH1 domain (Fig. 2.3A), is relatively weak in phenotype (Fig. 2.3F). Thus Ena function is critical for nurse cell dumping.

Ena stimulates formation of nurse cell cytoplasmic actin filaments

Our localization studies suggested that Ena is positioned to potentially regulate the cortical actin network, the bundled cytoplasmic actin filaments extending from the cortex to nuclei (referred to below as cytoplasmic filaments for simplicity) or the ring canals. We hypothesized that Ena might play a role at each of these places, mediating ring canal formation or maintenance, cortical actin formation or contractility, and cytoplasmic filament formation or maintenance. Defects in any of these actin structures could potentially explain the dumping defects we saw when Ena function was reduced in the germline. To explore the mechanisms by which Ena regulates nurse cell dumping, we examined the cell biological consequences of reduced Ena function during oogenesis.

In wildtype egg chambers cytoplasmic filaments first appear in early-mid stage 10B, in nurse cells adjacent to the oocyte (Figs. 2.4D1,2, arrows; staging was by morphogenetic movements of follicle cells, which do not express FP4mito). Cytoplasmic filaments are often most prominent at junctions where three nurse cells meet (Figs. 2.4A, B arrows), or at the periphery of ring canals (Figs. 2.4A, C, arrowheads); interestingly, both are sites of Ena enrichment (Fig. 2.4A). As egg chambers mature further, cytoplasmic filaments increase in number and appear in more anterior nurse cells (Figs. 2.4D3, D4, arrows), and by stage 11 nurse cells near the oocyte have already expelled much of their contents (Fig. 2.4D4).

We first examined egg chambers expressing FP4mito using matGal4 (mat-FP4mito). MatGal4 drives expression of FP4mito in nurse cells after ring canal formation but prior to dumping, pulling Ena from the cortex to presumptive mitochondria (Fig. 2.1J). Based on our work with FP4mito in embryos (Gates *et al.*, 2007), this should very strongly reduce Ena function. We did not see obvious alterations in cortical actin levels or organization prior to dumping (Fig. 2.4D1 vs. E1), but did observe a striking difference in the cytoplasmic filaments. Many fewer cytoplasmic filaments formed in FP4mito-expressing egg chambers, and those that formed did so later and were usually restricted to nurse cells nearest the oocyte (Figs. 2.4E1–4, arrows); these filaments resembled those in wildtype chambers in their

banding pattern after phalloidin staining (Fig. 2.5J vs. K, arrows), reflecting the assembly of these filaments from short segments (Guild *et al.*, 1997). FP4mito expression also reduced and delayed formation of ring canal-associated actin filaments (Fig. 2.4D2–3 vs. E3–4, arrowheads). In other dumpless mutants such as chickadee (Drosophila profilin; Cooley *et al.*, 1992), reducing cytoplasmic filaments allows nurse cell nuclei to be forced into ring canals, blocking cytoplasmic transport. Most mat-FP4mito egg chambers display nurse cell nuclei that protrude into ring canals (Figs. 2.5B, D, red arrows). As a result of these defects, nurse cells in terminal chambers expressing FP4mito often retain cytoplasm (Fig. 2.5B, white arrow vs. 5C). Thus Ena plays an important role in the formation of the cytoplasmic actin filaments and plays a key role in nurse cell dumping.

Differential effects of Ena's EVH1 and EVH2 domains in nurse cell cytoplasmic filament formation

We next explored the mechanisms by which Ena acts in the formation of cytoplasmic actin filaments, by examining the requirement for different parts of the protein. We assessed roles of the EVH1 and EVH2 domains by examining females with germlines homozygous mutant for the three ena mutants described above, ena^{23}, ena^{210}, or ena^{46}. The ena^{23} and ena^{210} alleles generate stable proteins (Ahern-Djamali *et al.*, 1998); cortical recruitment of both mutant proteins in the germline was substantially reduced but not eliminated (Figs. 2.1K, L). ena^{23} (Figs. 2.4F1–4), ena^{46}(data not shown), and ena^{210} (Figs. 2.4G1–4) mutant germlines all had defects in cytoplasmic filaments, but these phenotypes were less severe than mat-FP4mito, with increased numbers of filaments and less delay in their appearance. ena^{23} had a more severe cytoplasmic filament phenotype than ena^{210} (Fig. 2.4F vs. G), consistent with its higher penetrance dumpless phenotype (24%, N = 920 vs. 4%, N = 627; Fig. 2.3F). ena^{46} is no more severe than ena^{23}, consistent with the similar penetrance of their dumpless phenotypes (Fig. 2.3F). These data suggest that a functional EVH1 domain

may not be essential for formation of nurse cell cytoplasmic filaments, but that the EVH2 domain and its tetramerization subdomain are more critical.

Ena is required for cortical actin integrity in nurse cells but is dispensable for ring canal formation

Ena's localization suggested it also might mediate ring canal formation or maintenance, or cortical actin formation or contractility. We observed no defects in ring canal formation or growth in mat- FP4mito, ena^{23}, ena^{46}, or ena^{210} mutant egg chambers. They accumulated the ring canal markers actin, Hts, Kelch, and tyrosine phosphorylated proteins normally (Suppl. Figs. 2.1A–J). These data suggest that Ena is not essential for ring canal assembly.

Ena also localizes to the nurse cell cortex. Interestingly, cortical actin in ena^{23} and ena^{210} mutant egg chambers exhibited an additional defect not seen in mat-FP4mito: some egg chambers contained multinucleate nurse cells (Figs. 2.5E–G, arrows). We suspect that this resulted from rupture of the plasma membrane and cortical actin, since both actin (Figs. 2.5E–G) and DE-cad (data not shown) staining were lost. Consistent with this, multinucleate nurse cells often contained actin aggregates that may be ring canal remnants (Fig. 2.5E, arrowhead), and we occasionally saw nurse cell membranes apparently in the process of breaking down (Fig. 2.5F, arrow). Multinucleate nurse cells appeared at ~ stage 7, when slow transport of nurse cell contents begins (ena^{23}6% of egg chambers, N = 77; ena^{210}3%, N = 30), but defect frequency increased dramatically by stage 10, when dumping is initiated (ena^{23}25%, N = 105; ena^{210}12%, N = 19). A similar phenotype is seen when the germline is mutant for AJ proteins (Arm, Peifer *et al.*, 1993), Profilin (Cooley *et al.*, 1992), or the Arp2/3 complex (Arp3; Hudson and Cooley, 2002a). Loss of Ena does not, however, grossly affect nurse cell AJs, as DE-cad levels and localization resembled wildtype (Fig. 2.5H vs. I). Some nurse cells successfully expelled cytoplasm even in egg chambers with multinucleate nurse cells (Fig. 2.5G, arrowhead), suggesting that cortical actin can retain enough integrity to allow contraction. Since cortical defects are not seen in mat-FP4mito ovaries, in which Ena

inactivation does not begin until stage 6, Ena may help reorganize and strengthen cortical actin prior to contraction, so that ena mutant nurse cells are unable to cope with the mechanical stress of dumping.

Loss of Capping protein affects oocyte determination

As a further test of the hypothesis that regulated actin capping is important for oogenesis, we explored the function of CP. CP is a dimer of α- and β-subunits, both of which are essential for function (Cooper and Sept, 2008). Null alleles of either capping proteinα (cpa) or capping proteinβ (cpb) are lethal (Hopmann *et al.*, 1996; Delalle *et al.*, 2005). Analysis of mosaics in imaginal discs revealed that loss of CP function leads to a striking increase in actin levels, and in some regions of the disc this leads to cell death (Delalle *et al.*, 2005; Janody and Treisman, 2006). We thus anticipated that eliminating CP function in the germline would elevate actin polymerization. To test this hypothesis we generated germlines mutant for a null allele of the α-subunit, cpa^{69E} (Janody and Treisman, 2006). We marked mutant germline cells by loss of GFP (e.g. Fig. 2.6B).

To our surprise, early development of egg chambers and many features of actin accumulation in cpa^{69E} mutant germline cells were relatively normal (Fig. 2.6B vs. A, C–E; wildtype oocytes are marked with an arrowhead, mutant oocytes with an arrow). Mutant germ cells formed 16-cell cysts, were encapsulated by follicle cells relatively normally, and initially grew in size at a rate relatively similar to wild- type (Fig. 2.6B). As they reached stage 6, mutant egg chambers became morphologically abnormal, taking on a spindle shape (Figs. 2.6C–E, arrows). At this point egg chambers ceased increasing in size, and ultimately degenerated. No mutant egg chambers later than ~ stage 6/ 7 were observed. Through stage 6/7, however, overall actin levels were relatively normal in cpa69E mutant germ cells (Figs. 2.6B–E, arrows). When we looked at higher magnification, we could some- times discern a slight increase in the number and length of fine actin filaments at the nurse cell cortex (Fig. 2.6I vs. J), but this was much less striking than previously observed in cpa^{69E} mutant

imaginal disc epithelia (Delalle *et al.*, 2005; Janody and Treisman, 2006) or than we observed in cpa^{69E} mutant follicle cells (see below). Ring canals also appeared to form normally, accumulating, Kelch, Hts and tyrosine phosphorylated proteins as in wildtype (Suppl. Figs. 2.1K–P).

There was one striking difference in cpa69E mutant germlines: many did not contain a recognizable oocyte. Normally, one of the 16 cells in the germline cyst is specified as the oocyte soon after cyst formation. This cell accumulates the oocyte determinant Orb (Figs. 2.6A, B white arrowheads; Lantz *et al.*, 1994). Most mutant egg chambers failed to accumulate Orb at higher levels in any particular cell (22/30; 73%; Figs. 2.6B, C, arrows; ~30% of mutant egg chambers did determine an oocyte; Figs. 2.6F–H, arrows). We observed a similar defect in oocyte specification in animals whose germlines were mutant for a second null allele, cpa^{107E} (data not shown). In wildtype, Orb enrichment in a single cell in each cyst can be detected in the germarium, sometimes as early the distal end of region 2b (with disc-shaped germline cysts; Fig. 2.6K, blue arrow). Orb enrichment is readily apparent in stage 1 (Fig. 2.6K, white arrows). In contrast, we did not observe Orb enrichment in any cells in many mutant germaria (Fig. 2.6L). As oogenesis proceeds, nurse cell genomes become highly polyploid and their nuclei enlarge, while the oocyte retains a small diploid nucleus (Fig. 2.6A, left inset red arrowhead). Strikingly, most cpa^{69E} mutant egg chambers did not contain a properly differentiated oocyte; instead they had 16 nuclei that were all larger than expected for the oocyte (73%; 19/26; we confirmed this by serial sectioning; an example is in Suppl. Fig. 2.2; the oocyte is one of the cells with 4 ring canals, indicated in violet). Of those without a properly differentiated oocyte, in some the 16 nuclei were equal in size (32%; 6/19; Fig. 2.6E, arrow), and in others one nucleus, likely the oocyte, was smaller, but not nearly as small as a normal oocyte nucleus (68%; 13/19; Suppl Fig. 2.2). We also saw a second defect in cpa^{69E} mutant egg chambers at a lower penetrance. Normally, the oocyte is tightly positioned at the posterior end of the egg chamber. However, in about half the mutant egg chambers (15/ 26; ~61%), the oocyte was not precisely positioned at the posterior (Figs.

2.6G, H)—this included egg chambers that did and did not display a specified oocyte. These data suggest CP plays roles in oocyte specification and positioning.

In wildtype egg chambers, the oocyte is easily distinguished by stage 3 because it accumulates more actin at its cortex than the nurse cells (Fig. 2.6A, arrowheads). In cpa mutant egg chambers lacking a differentiated oocyte, no germline cell had extra actin (Figs. 2.6B–E, arrows). However, in the fraction of cpa mutant egg chambers that did have a properly differentiated oocyte (indicated by a small oocyte nucleus or proper Orb accumulation), actin was enriched surrounding the oocyte (Figs. 2.6G, H). Thus the failure to enrich actin in most cpa mutant egg chambers is likely a secondary consequence of failed oocyte determination rather than a direct effect of loss of CP.

Reducing levels of Capping protein disrupts nurse cell dumping and disrupts integrity of the cortical membrane of nurse cells

These results revealed an important role for CP in oocyte specification, but the degeneration of mutant egg chambers after stage 7 precluded analysis of later stages, during nurse cell dumping. However, Miller and colleagues identified a transheterozygous combination of weak cpb alleles ($cpb^{F19}/cpb^{6.15}$) that produces viable but female sterile flies (Hopmann *et al.*, 1996). We used these animals to examine effects of reducing CP function on oogenesis—because these are not null alleles, we cannot rule out additional roles for CP not revealed in this hypomorphic situation.

We first examined whether $cpb^{F19}/cpb^{6.15}$ transheterozygotes lay eggs, and if so, whether these eggs are defective. Most $cpb^{F19}/cpb^{6.15}$ eggs are shorter than wildtype (Fig. 2.3D), suggesting defects in nurse cell dumping. 97% were dumpless (Fig. 2.3F), similar to or more severe than we saw when disrupting Ena function using FP4mito. Thus reducing CP function disrupts nurse cell dumping.

To begin to determine mechanisms by which CP acts during dumping at the cellular level, we examined actin organization and Ena localization during oogenesis in $cpb^{F19}/cpb^{6.15}$ mutants. Early stage egg chambers appeared largely or completely normal

(Figs. 2.7A, B). We observed the first defects beginning at stage 8, with the appearance of occasional egg chambers with multinucleate nurse cells (17%; N = 6). As egg chamber development progressed, multinucleate nurse cells became more frequent (57% at stage 9 were multinucleate; N = 7; Fig. 2.7C, pink arrow). As in ena mutants, this defect occurred without obvious overall defects in levels or localization of nurse cell cortical actin prior to the onset of nurse cell dumping (Fig. 7B), at least at the level of light microscopy. By stage 10 and later, most egg chambers had multinucleate nurse cells (66%; N = 32; Figs. 2.7D, G pink arrows), and many late stage egg chambers, which should have already begun dumping (Fig. 2.7G), exhibited little or no transfer of cytoplasm to the oocyte. There were also defects in the nurse cell–oocyte border. In wildtype this is straight (Fig. 2.7B, arrow), but in $cpb^{F19}/cpb^{6.15}$ mutant egg chambers nurse cells often bulged into the oocyte (Figs. 2.7C, E, G, yellow arrows), and at times the nurse cell–oocyte interface ruptured (Fig. 2.7F, arrowhead) or nurse cell nuclei were found in the oocyte (data not shown). We do not think multinucleate nurse cells result from defects in cytokinesis, as we did not observe them before stage 8. Instead, we believe they reflect breakdown of the cortical membrane. Consistent with this, we sometimes found actin aggregates in the oocyte, at least some of which appear to be ring canal remnants (Fig. 2.7F, white arrow). These data suggest that CP plays an important role in nurse cell cortical integrity, and in its absence these defects contribute to the highly penetrant defects in nurse cell dumping.

Capping protein is important for correct organization of cytoplasmic actin filaments in nurse cells

While cortical integrity defects are likely to explain part of the problem with nurse cell dumping in $cpb^{F19}/cpb^{6.15}$ mutants, the frequency of dumping defects (97%) is higher than that of cortical defects (~65% by stage 10). We thus examined another actin structure, the cytoplasmic actin filaments, defects in which might affect dumping. There are striking differences in cytoplasmic actin filaments in $cpb^{F19}/cpb^{6.15}$. Prior to the onset of

dumping, cortical actin appeared relatively normal in $cpb^{F19}/cpb^{6.15}$ nurse cells that did not have defects in cortical integrity (Figs. 2.8A, B). Unlike ena mutants, cpb hypomorphs did not have substantial delays in cytoplasmic filament production or large reductions in filament number (Figs. 2.4H1–4; Figs. 2.8H, I vs. F, G). However, the morphology and organization of the cytoplasmic filaments were substantially different from wildtype. As filaments formed, the oocyte (Fig. 2.8C, bottom arrow) and nurse cell (Fig. 2.8E) cortex of cpb hypomorphs appeared “furry”, with excess actin accumulating both cortically and in the form of short filaments; this contrasted with what we observed in wildtype (Fig. 2.8C, top arrow; D). As filament growth proceeded, the distribution of longer cytoplasmic filaments in cpb hypomorphs was less uniform around the cortex (Figs. 2.8I, M yellow arrows, vs. Figs. 2.8G, J) and filaments were more disorganized (Figs. 2.8L, M vs. K, J). This asymmetric filament accumulation was not effective in restraining the nurse cell nuclei, which were often positioned against the cortex, or protruding through and thus blocking ring canals (Figs. 2.8N, O). These defects likely contribute to the significant reduction in nurse cell dumping observed (e.g., Fig. 2.8I). Interestingly, despite the disorganization of the cytoplasmic actin filaments and the disruption of dumping, Ena cortical localization was not dramatically altered (Figs. 2.8H″, M″ vs. F″, J″). Together, these data suggest that Ena and CP are essential for dumping, likely via affects on both cortical actin and cytoplasmic filaments.

Most models suggest that one function of Ena/VASP proteins is to functionally antagonize CP. These models would predict that reducing CP levels might ameliorate the reduction of Ena function. We tested this during nurse cell dumping by generating females expressing FP4mito and also heterozygous for a null mutation in CP, and comparing them to FP4mito alone. Reduction of the levels of CP reduced the severity of the dumpless phenotype from 84% to 57% (Fig. 2.3G), consistent with an antagonistic relationship.

Does Abl regulate Ena and actin architecture during nurse cell dumping?

During embryonic development, the tyrosine kinase Abl is a key negative regulator of Ena activity (Gertler *et al.*, 1995). In its absence, de-regulated Ena activity leads to disruption of morphogenetic events and embryonic lethality (Grevengoed *et al.*, 2001; 2003; Fox and Peifer, 2007). We thus explored whether Abl acts as a negative regulator of Ena activity during oogenesis.

We generated females whose germlines are homozygous for the null abl allele abl^4, and examined the actin cytoskeleton, staining them together with wildtype egg chambers marked with histone- GFP as a control. Early to mid-stages of oogenesis in abl^4 mutants were indistinguishable from wildtype in morphology and actin localization (Fig. 2.9A). abl^4 mutants assembled relatively normal nurse cell actin structures (Fig. 2.9B vs. C). There were only slight differences from wildtype. First, while most wildtype egg chambers do not assemble cytoplasmic filaments until stage 10 (Fig. 2.9E; we occasionally see wildtype egg chambers with filaments in stage 9; Fig. 2.9F), 3/3 stage 9 abl^4 mutants already had cytoplasmic filaments (Fig. 2.9D), suggesting a possible acceleration in initiating filament formation. Second, we occasionally noticed ectopic accumulations of Ena and actin in the oocyte of abl^4 mutants (Figs. 2.9G, H arrows). Finally, late stage cytoplasmic filaments sometimes appeared more robust than wild- type, with additional Ena at their barbed ends (Fig. 2.9I vs. J). Thus, loss of Abl results in mild phenotypes consistent with modest deregulation of Ena function. These defects are associated with defects in dumping, though not as frequent as those seen upon inactivation of Ena or CP—14% of eggs laid by females whose germlines were abl^4 mutant were dumpless (Figs. 2.3E, F). Given this evidence that Abl restrains Ena activity during oogenesis, we explored whether reducing Abl levels might alleviate the effects of Ena inactivation on dumping.

In fact, heterozygosity for abl partially suppressed the effects of Ena inactivation by FP4mito, reducing the frequency of dumpless eggs from 83% to 68% (Fig. 2.3G). Together

these data are consistent with a role for Abl in negatively regulating Ena during oogenesis.

Exploring roles for Ena and Capping protein in follicle cell epithelia

Work in cultured mammalian cells suggested that Ena plays an important role in cell adhesion in cultured keratinocytes and mammary epithelial cells (Vasioukhin *et al.*, 2000; Scott *et al.*, 2006). In *Drosophila*, earlier work suggested it plays a role in epithelial integrity in follicle cells, as there were apical actin defects in follicle cells mutant for ena^{210} or ena^{23} (Baum and Perrimon, 2001). However, embryonic and imaginal epithelia in Drosophila do not require Ena function for epithelial organization or cell adhesion (Gates *et al.*, 2007). To understand this difference and test the hypothesis that Ena is required for epithelial integrity in follicle cells, we re-examined Ena function in this tissue.

Follicle cells form a polarized epithelial sheet surrounding the germ cells, with its apical surface facing inward. Follicle cells assemble an actin ring underlying the AJs, which in cross section makes a line across the apical end of the sheet (Suppl. Fig. 2.3B, arrowheads). We generated clones of follicle cells mutant for ena^{23}—homozygous mutant cells lost expression of a GFP-marker on the other chromo- some. Loss of Ena in early egg chambers (stages 2–7) did not usually cause significant disruptions in either epithelial organization (Suppl. Fig. 2.3A; blue lines demarcate mutant clones), or in the assembly of cortical actin into follicle cell AJs, as illustrated in Suppl. Fig. 2.3B, where almost all follicle cells are mutant, or Suppl. Figs. 2.3C–E, illustrating boundaries between mutant and wildtype follicle cells. However, in later egg chambers, we did observe clones with reduced cortical actin (Suppl. Figs. 2.3F, G) and at times with disruptions in epithelial integrity (Suppl. Fig. 2.3H, arrowhead). These data are more consistent with a role for Ena in morphogenetic movements of follicle cells rather than in epithelial integrity per se.

In contrast, loss of CP had more dramatic consequences. Follicle cells mutant for the null allele cpa^{69E} began to accumulate excess actin on their apical and lateral surfaces in early stage egg chambers (Suppl. Fig. 2.3I; mutant cells lack GFP). By stages 6–8, some mutant

cells began to lose their monolayer organization, especially in clones positioned near the posterior end of the egg chamber (Suppl. Figs. 2.3J, K, arrows). Mutant cells accumulated very high levels of actin around their entire circumference (Suppl. Figs. 2.3K, K′), similar to what was observed in imaginal discs mutant for CP (Delalle *et al.*, 2005; Janody and Treisman, 2006). As wildtype cells began to accumulate basal actin in oriented filaments at stage 9 (Suppl. Fig. 2.3N′, arrow; Gutzeit, 1990), the excess actin phenotype in cpa69E mutant cells became even more accentuated (Suppl. Fig. 2.3L, arrow, M,N′, arrowhead). Thus CP is essential for maintaining proper levels of apical actin in follicle cells, and for epithelial architecture in at least a subset of cells.

Ena regulates speed of border cell migration

The phenotypes observed in ena mutant follicle cells suggest that Ena may play a role in their morphogenetic movements. The best-characterized follicle cell movement is migration of the border cells, a cluster of 6–8 follicle cells surrounding the two anterior polar cells, which undergo a dramatic and stereotypical migration of 150–200 μm (Rørth, 2002; Montell, 2003). Early in stage 9, these cells extend long and dynamic actin-rich protrusions between the nurse cells (Murphy and Montell, 1996; Fulga and Rørth, 2002; Prasad and Montell, 2007) and then delaminate from the rest of the follicle cell epithelium and migrate towards the oocyte. They reach the anterior border of the oocyte by stage 10.

Ena/VASP proteins regulate the speed of migration of cultured fibroblasts; in this cell type they inhibit cell migration (Bear *et al.*, 2000). Unlike cultured fibroblasts, border cells migrate as a group, use a cellular substrate, and must force their way in between tightly apposed nurse cells. Thus their mechanisms of migration and their requirement for Ena function may be different. To examine Ena function in border cells we inactivated it by expressing FP4mito using slow border cells (slbo)-Gal4 (Rørth *et al.*, 1998),which drives expression in border cells, centripetal follicle cells and posterior follicle cells, but not polar cells (Fig. 2.10A; Geisbrecht and Montell, 2002). As a negative control, we expressed AP4mito, which localizes to mitochondria but does not bind or sequester Ena (Bear *et al.*, 2000; Gates *et al.*, 2007). In wildtype and AP4mito expressing border cells, Ena was largely

cytoplasmic (Fig. 2.10A″; data not shown). When FP4mito was expressed using slbo-Gal4, it altered Ena localization in follicle cells (Fig. 2.10B″ vs. A″), consistent with its expected mitochondrial sequestration.

In contrast to what was observed in fibroblasts (Bear *et al.*, 2000), inactivating Ena in border cells did not accelerate migration but rather slowed migration. Although the long cellular extensions required to initiate migration appeared normal (Fig. 2.10C vs. D), ~ 50% of FP4mito- expressing border cell clusters failed to reach the oocyte by early stage 10 (Fig. 2.10B vs. A; quantified in 10E), compared to b10% in control AP4mito or wildtype egg chambers (Fig. 2.10E).

This defect in arrival time could result from a change in the time required to detach from the follicle cell epithelium or an actual change in migration speed. To distinguish these, we analyzed border cells live. This confirmed that FP4mito-expressing border cells extend long protrusions seemingly normally, and detach from the follicle cell monolayer (Suppl. Fig. 2.4; Movie 1 vs. 2). However, migration after detachment occurred significantly more slowly than normal (Figs. 2.10F,G; Suppl. Fig. 2.4); for AP4mito-expressing controls the duration of migration was 129 min±8.1 min (Movie 2.1), while it was 198 min ± 17.9 min for FP4mito (Movie 2.2). Thus migration speed for border cells expressing FP4mito (1.06 ± 0.056 μm per min) was significantly slower than that of AP4mito-expressing controls (1.56 ± 0.26 μm per min; p = 0. 038). These results indicate that Ena plays a positive role in promoting cell migration in border cells.

To explore Ena function in border cells further, we assessed effects of overexpressing Ena on border cell morphology and migration. Interestingly, Ena overexpression also delayed/disrupted migration (Fig. 2.11A vs. B; G; ~40% of border cell clusters did not complete migration in a timely fashion). To investigate the mechanism by which this might occur, we examined the morphology of border cell clusters, using antibodies against Failed Axonal Connections (Fax) and Singed (Sn), which are enriched in border cells (Figs. 2.11A, C). Wildtype border cell clusters at the beginning of migration generally exhibit one prominent protrusion in the direction of the oocyte (Figs. 2.11C, D). In contrast border cell

clusters overexpressing Ena showed many fine protrusions (Fig. 2.11E). To observe actin distribution following Ena overexpression, we co-expressed Ena and GFP-actin using slbo-Gal4. Overexpression of GFP-actin by itself increases the frequency and length of the long cellular extensions from the border cell cluster (Fig. 2.11D vs. C), and inhibits border cell migration (Fig. 2.11G). When we co- expressed Ena together with GFP-actin, ~50% of border cell clusters showed numerous fine actin-rich protrusions (Fig. 2.11F), and border cell migration was further inhibited (Fig. 2.11G). Thus the proper level of Ena activity is required for border cells to generate the correct sort of protrusions and migrate effectively.

In parallel, we examined effects on border cell migration of overexpressing Cpb in border cells using slbo-Gal4. Strikingly, over- expression of Cpb resulted in premature arrival of border cells at the oocyte (Fig. 2.11). In wildtype, we never saw border cells arrive at the oocyte during stage 9 (0/19), while in UAS-Cpb ovaries border cells had already reached the oocyte during stage 9 in 100% of those observed (28/28; p b 10− 12 by Fisher's Exact test). We also assessed border cell migration in cpb hypomorphs. Border cells reached the oocyte in 28/28 stage 10 egg chambers scored. In 9/28 cases border cells arrived somewhat off-center, but this is likely due to the breakdown of some nurse cell membranes. Thus follicle cell morphogenesis is less sensitive to reduction of CP than is nurse cell dumping. However, the residual CP in the hypomorphs precludes any stronger conclusions.

Discussion

As cell biological studies provide increasing information about the toolkit cells use to modulate actin dynamics, our challenge is to determine how this toolkit is used to create diverse cell structures and behaviors during development. Drosophila oogenesis provides an outstanding model for assessing this, with diverse cell types and stereotyped cell behaviors. Our work provides new insights into the developmental mechanisms that allow Ena and CP to create a wide- range of actin structures.

Ena helps mold diverse actin structures

To address the challenge outlined above, we eliminated the function of two key actin regulators and examined the effect on the diverse actin structures cells produce during development. In the case of Ena, the results are surprising: cells use this tool to craft a diverse array of different actin assemblies that contribute to many different cell behaviors. In cultured fibroblasts (Bear *et al.*, 2000), neurons (Lebrand *et al.*, 2004) and epithelial cells (Mejillano *et al.*, 2004), Ena restrains migration by modulating actin dynamics at the leading edge, and generates filopodia by anti-capping and filament bundling. Ena also regulates axon outgrowth and guidance, manipulating actin assembly in growth cones (reviewed in Krause *et al.*, 2003), and plays roles in dendrite branching (Li *et al.*, 2005; Lin *et al.*, 2007). During *Drosophila* morphogenesis Ena plays many roles (Gates *et al.*, 2007). Some, like promoting leading edge filopodia and thus epithelial zippering during dorsal closure, fit well with Ena's anti-capping function. In other roles (segmental groove formation and head involution), the cell biological basis is less clear, but affected cell types exhibit striking patterns of Ena localization. Our analysis of oogenesis further broadens the diversity of cell behaviors requiring Ena, highlighting roles in nurse cell cortical integrity, formation of nurse cell cytoplasmic filaments during dumping, and border cell migration.

In the case of the cytoplasmic filaments, our analysis combined with Ena's postulated biochemical functions provides interesting mechanistic insights into filament assembly. Ena is thought to promote filopodia by providing anti-capping activity (Bear *et al.*, 2002; Barzik *et al.*, 2005), promoting filament elongation (Sechi and Wehland, 2004), and helping bundle filaments (Schirenbeck *et al.*, 2006; Applewhite *et al.*, 2007). Work from the Tilney/Guild labs revealed that nurse cell cytoplasmic filaments form from bundled actin filaments projecting from the plasma membrane, with their barbed ends membrane proximal (Guild *et al.*, 1997). Ena localizes to these bundled barbed ends and filament formation is depressed in its absence, supporting the idea that it plays an important role in promoting filament elongation/bundling. Consistent with anti-capping being critical, reducing CP levels partially

suppressed the effects of Ena inactivation.

We used three ena mutants to begin to dissect mechanisms by which Ena acts. Ena^{23} protein lacks the tetramerization domain (Ahern-Djamali *et al.*, 1998). In nurse cells, Ena tetramerization may help collect individual actin filaments into the robust bundled cytoplasmic filaments, as was suggested for filopodia in mammalian cells (Schirenbeck *et al.*, 2006; Applewhite *et al.*, 2007). Consistent with this, the Ena^{23}mutant protein, which should be able to act in anti-capping but should be reduced in the ability to bundle capped filaments, displayed a significant decrease in its ability to mediate filament formation. Ena^{23}'s phenotype was similar to that of Ena^{46}, which completely lacks the EVH2 domain, suggesting tetramerization is a key part of EVH2 function. Both appeared to retain some residual function in filament assembly, however, as their phenotypes were less severe than that of FP4mito. Alternately, FP4mito sequestration of Ena may also sequester some protein partners, thereby increasing phenotypic severity. Ena^{210}mutant protein, with a point mutation in the EVH1 domain impairing binding to EVH1 ligands (Ahern-Djamali *et al.*, 1998), retained significant function. This suggests either that Ena's role in this process is largely independent of an EVH1 ligand (perhaps it is recruited to the cortex by other protein interactions), or that the point mutation in ena^{210} does not fully inactivate EVH1 function.

None of our methods of disrupting Ena function fully eliminated cytoplasmic filaments. This may suggest either that none of our approaches completely eliminate all functional Ena (our data in embryos suggest that FP4mito produces a nearly null or null phenotype; Gates *et al.*, 2007), or that Ena is not absolutely essential for filament assembly, although it does clearly regulate the rate/ success of filament initiation or polymerization. It will be interesting to further explore how Ena's structure dictates its function in future experiments.

The mechanistic role of Ena in nurse cell cortical integrity must remain more speculative, as actin substructure at this position has not been closely investigated. Cortical integrity also requires Ena's partner Profilin (Cooley *et al.*, 1992) and Ena's antagonist CP (our data), as

well as the actin-nucleating/branching Arp2/3 complex (Hudson and Cooley, 2002a). Thus correct structural integrity of cortical actin appears to require balance between anti-capping and branching. Nurse cell cortical integrity also requires the cadherin–catenin complex (Peifer *et al.*, 1993); it may anchor cortical actin, or may have a more active role in regulating actin assembly through α- catenin (Drees *et al.*, 2005) and other actin regulators associated with AJs (Gates and Peifer, 2005).

Ena also plays a role in border cell migration. This role has an interesting twist. While decreasing Ena/VASP function increases speed of fibroblast migration in cell culture (Bear *et al.*, 2000), it slows migration of border cells. These two cell types migrate in quite different settings. Fibroblasts move over an extracellular matrix substrate by lamellipodial protrusion, adhesion, and tail retraction. In contrast, border cells migrate by squeezing in between nurse cells, and thus their substrate is cellular rather than matrix, and the shape of the leading process is constrained by the presence of other cells surrounding it. The shapes of border cell leading protrusions (Fulga and Rørth, 2002; Prasad and Montell, 2007) are quite different from fibroblast leading edge lamella, so perhaps the differential requirements for Ena are not so surprising. In fibroblasts, too much Ena activity increases lamellipodial dynamics but prevents production of a leading edge strong enough to promote stable protrusion (Bear *et al.*, 2000; Bear, 2008). In border cells Ena inactivation may inhibit migration by several mechanisms. Ena inactivation could, in principle, affect ability of cells to protrude; however protrusions appeared relatively normal following Ena sequestration. Ena inactivation could reduce formation of finer protrusions like filopodia (as it did during *Drosophila* dorsal closure; Gates *et al.*, 2007), and filopodia might serve a sensory function in migration. Finally, as Ena localizes to AJs in epithelia, Ena inactivation might affect DE-cadherin-mediated adhesion, which promotes border cell migration (Niewiadomska *et al.*, 1999). It will be important to test these alternatives, for example by exploring the migration of wildtype border cells through a germline that is ena mutant.

Overexpressing Ena also causes border cell migration defects, as well as formation of excess filopodia. Neurons (Lebrand *et al.*, 2004) and leading edge cells during *Drosophila*

dorsal closure (Gates *et al.*, 2007) also exhibit excess filopodia following Ena up-regulation, while fibroblasts do not. Interestingly, neurons and border cells express high levels of the actin bundler Fascin (Singed in Drosophila), whereas fibroblasts do not. Since Fascin is thought to be a key regulator of filopodia (Vignjevic *et al.*, 2006), perhaps the explosive filopodia phenotype depends upon Fascin-mediated bundling. This remains to be tested. singed mutants (Cant *et al.*, 1994) do not have border cell migration defects, however, suggesting that it acts redundantly with other regulators of actin bundling under normal circumstances. Excess filopodia may slow migration several ways, from reducing the ability to produce a single leading process to altering chemosensory cues received via filopodia. More detailed analysis wildtype and mutant border cell protrusions will help address these issues.

Balancing capping and anti-capping in generating cytoplasmic actin filaments?

The simplest model of Ena/VASP protein function suggests it acts as a CP antagonist (Bear *et al.*, 2002; Barzik *et al.*, 2005), promoting filament elongation while CP prevents this. Studies in cultured cells support this basic hypothesis: in both mammalian B16F1 melanoma cells and *Drosophila* D16 cells, CP depletion triggers explosive formation of filopodia (Mejillano *et al.*, 2004; Gates *et al.*, 2007), and in melanoma cells this largely depends on Ena/VASP activity (Mejillano *et al.*, 2004). In contrast Ena depletion prevents filopodial formation in both mammalian MVD7 cells and *Drosophila* D16 cells (Mejillano *et al.*, 2004; Gates *et al.*, 2007). *In vivo*, it is likely that cell behavior is regulated by differences in relative ratios of CP and Ena/ VASP activity in the context of other actin regulators.

Nurse cell cytoplasmic filaments provide an interesting system in which to examine this balance. Ena plays an important though possibly not essential role in filament initiation, and this role appears to be restrained by negative regulation by Abl kinase. Naively, we initially thought CP depletion might have the opposite phenotype, producing more or more robust filaments. However, reducing CP function produced a more complex phenotype. Filaments were produced, but they were not uniformly distributed around the cortex, and were not effective at anchoring nuclei during dumping. The number of filaments extending to the

nuclei did not seem increased, but instead the entire nurse cell cortex became “furry” with actin.

What mechanism might explain this phenotype? Perhaps depleting CP produces so many elongating, “anti-capped” actin filaments that they exceed the available Ena and/or other tip complex proteins. This may consume much of the available G-actin in producing numerous relatively short filaments, giving the cortex its furry appearance. Recent work supports this idea of “monomer channeling” *in vitro* (Akin and Mullins, 2008). Another speculative possibility, which is not mutually exclusive, is that in the absence of CP, the individual “units” from which the cytoplasmic actin filaments are assembled (Guild *et al.*, 1997) grow longer than usual, compromising their mechanical strength and leading to the disorganization observed. Similar models were offered for the reduced lamellipodial persistence in fibroblasts with too much Ena activity (Bear, 2008). Reducing CP levels suppressed the effects of Ena inactivation on dumping, consistent with an antagonistic relationship. Future experiments, including further exploring epistatic relationships between Ena and CP, are required to test these hypotheses and further explore Ena, CP and their joint mechanisms of action.

An unexpected role for Capping protein in oocyte determination

When we generated CP null germlines, we hypothesized this would dramatically increase cortical actin, as was observed in imaginal discs (Delalle *et al.*, 2005; Janody and Treisman, 2006) and follicle cells (our data). However, this was not the case—there may be a modest increase in cortical actin, but it is not dramatic. This suggests that other factors limit actin accumulation at the cortex—these may include activity of nucleating factors like the Arp2/3 complex and Formins.

However, loss of CP function in the germline did have one dramatic and surprising consequence: oocyte determination was often disrupted, and the oocyte determinant Orb was no longer enriched in the presumptive oocyte. Two other genes have very similar phenotypes: BicaudalD and Egalitarian. Both are thought to be co-factors for Dynein, modulating microtubule organization and mediating transport of cargos into the oocyte

(Pearson and González-Reyes, 2004). Consistent with this, microtubule depolymerization also disrupts oocyte specification. It remains unclear why loss of CP impairs this process. Eliminating CP may impair function of the dynein–dynactin complex, of which it is a part (Cooper and Sept, 2008). Alternately, cross-regulatory interactions between actin and microtubules may be important for proper cytoskeletal structure and transport in the germarium, as is true later in oogenesis (e.g., Dahlgaard *et al.*, 2007). Finally, CP may play a more direct role in transporting or anchoring Orb, or in some other step important for oocyte determination. This can now be examined in more detail.

Together these data provide insights into the developmental mechanisms that regulate the diverse actin structures critical for oogenesis. Future explorations of the detailed mechanisms of action of Ena and CP during these dynamic events and how they cooperate with other actin regulators like Formins and the Arp2/3 complex will help further extend our understanding of this important topic.

Acknowledgements

We thank K. Miller, E. Liebl, P. Garrity, the Bloomington Drosophila Stock Center, and the Developmental Studies Hybridoma Bank for reagents, S. Beckwith, N. Kaplan and T. Tedeschi for technical assistance, and D. Applewhite, E. Rogers and G. Shemer for helpful comments.

This work was supported by NIHGM47857 to MP and NIHGM73164 to DJM. JG was a Leukemia and Lymphoma Society Special Fellow. JG was supported by NIH5F32GM068337 and Bucknell University's Swanson Fellowship, SHN by Cell and Molecular Biology Training Grant T32 GM008581, JPM by the Smallwood Foundation and a Goldwater Scholarship, and MP by the Hooker Distinguished Professorship.

Materials and Methods

Fly stocks and clone generation

All mutations are described at Flybase (flybase.bio.indiana.edu). ena^{23}, ena^{46} and

ena^{210} germline clones were generated by heat shocking 48–72 hour old hsflp12;FRT42Bena/FRT42BovoD1 larvae for 3 h at 37°C. abl^{4} germline clones were generated in the same manner with hsflp12;+;FRT79Dabl^{4}/FRT79DovoD1larvae. Only homozygous ena or abl mutant germ cells develop in these females. ena^{23} follicle cell clones were generated by heat shocking 48–72 hour old hsflp12; FRT42B ena^{23}/FRT42B Ubi-GFP larvae for 3 h at 37°C. CP mutant follicle and germline clones were generated by heat shocking 48 hour old hsflp12; FRT42D cpa^{69E}/FRT42D Ubi-GFP larvae for 1 h at 37°C every 24 h until they eclose. Homozygous ena^{23}and cpa^{69E} follicle and germ cells are marked by a lack of GFP. Stocks used to generate ena germline clones (hsflp12; Sco/CyO and w; FRT42B ovoD1/CyO), ena follicle cell clones (w; FRT42B UBi-GFP-nls), as well as matα4-Gal4- VP16, slbo-Gal4, UAS-GFP-actin, and the hypomorphic cpb alleles were from the Bloomington Stock Center. FRT42D cpa^{69E} was from F. Janody, and UAS-cpb from P. Garrity.

Antibodies and Image Acquisition

ArmN27A1 (1:100), mouse anti-htsRC (1:100), mouse anti-kel1B (1:10), rat anti-DE-cad DCAD2 (1:200, all DSHB), and rabbit anti-Fax (1:500, a gift of Dr. Eric Liebl). DNA was visualized with DAPI (1:1000, Sigma-Aldrich) and actin with Alexa Fluor®568 phalloidin (Invitrogen). Secondary antibodies (Invitrogen) were Alexa Fluor®488, Alexa Fluor®568 and Alexa Fluor®647. Tissues were mounted in Aqua Polymount (Polysciences) or Vectashield (Vector Laboratories; border cell experiments). All images were acquired using a laser scanning confocal microscope (model 510, Carl Zeiss MicroImaging), LSM510 AIM acquisition software and a 40Å~ (Plan-Neo-Fluar: NA 1.3) or 63Å~ (Plan-Apochromat; NA 1.4) objectives. Adobe Photoshop® 7.0 was used to adjust levels to use the full range of pixel values, and used to adjust brightness and contrast. Modifications were made on entire panel.

When levels were compared, brightness and contrast alterations were performed identically on wildtype and experimental images.

Figure 2.1

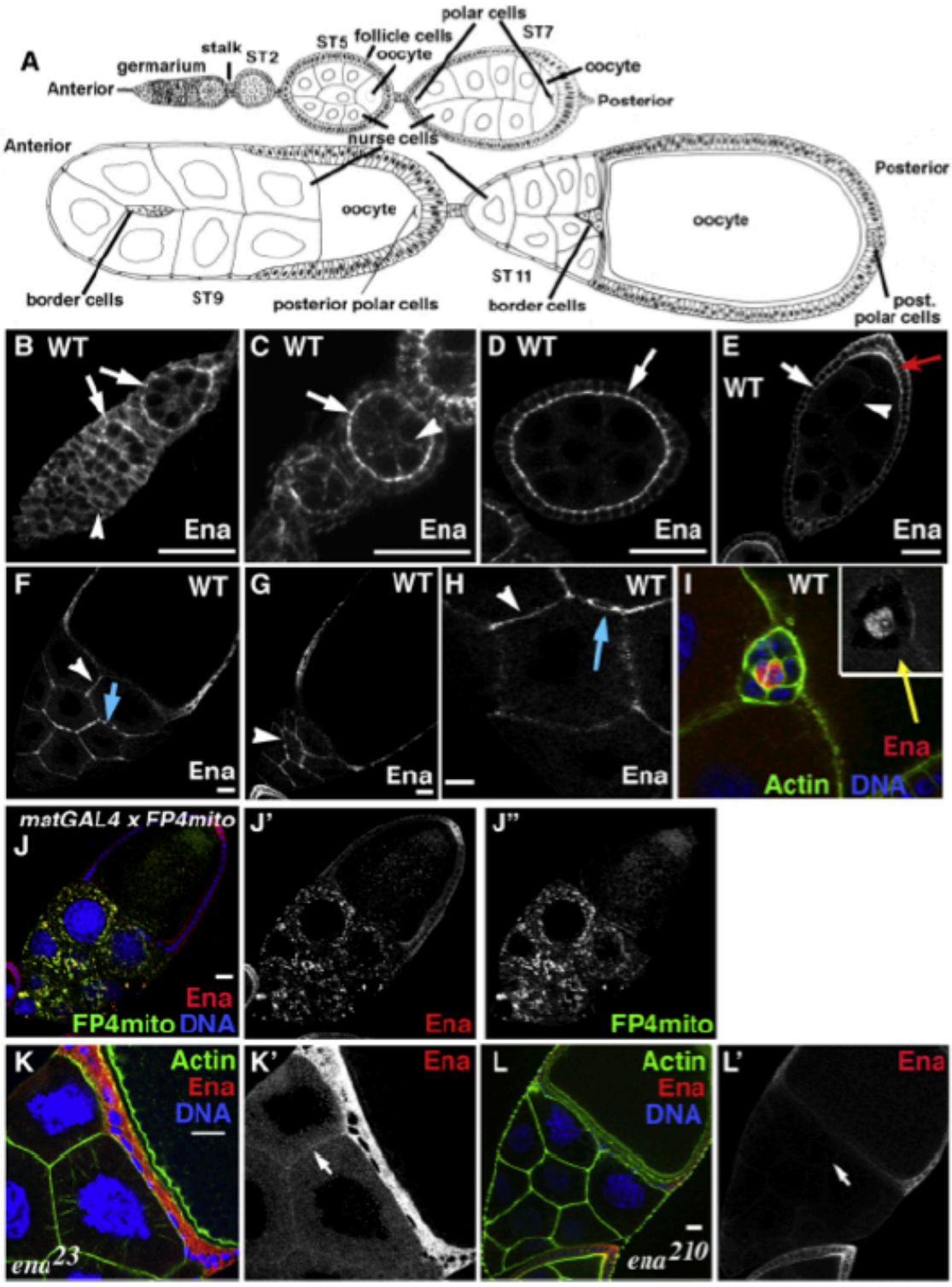
A
Anterior
germarium
stalk
ST2
ST5
follicle cells
oocyte
polar cells
ST7
oocyte
Posterior
Anterior
nurse cells
Posterior
oocyte
oocyte
ST 11
border cells
ST9
posterior polar cells
border cells
post.
polar cells
B WT
Ena
C WT
Ena
D WT
Ena
E
WT
Ena
F
WT
Ena
G
WT
Ena
H
WT
Ena
I
WT
Ena
Actin
DNA
matGAL4 x FP4mito
J
Ena
FP4mito
DNA
J'
Ena
J''
FP4mito
K
Actin
Ena
DNA
ena23
K'
Ena
L
Actin
Ena
DNA
ena210
L'
Ena

Fig. 2.1. Ena localization and mislocalization during oogenesis. Egg chambers, anterior to left. Genotypes and antigens indicated. (A) Diagram of an ovariole, showing stages of egg chamber development. Stages and cell types labeled. Modified with permission from Peifer et al., 1993. (B–H) Ena. (B) Germarium. Arrowhead = proliferating cystoblasts. Arrows = AJs in follicle cells that are encapsulating germline cells. (C–G) Stages 4, 5, 8, late 10b, and 12, respectively. (H) close-up, late stage 10b. White arrows = Ena at follicle cell AJs. Arrowheads = Ena at nurse cell cortex. Red arrow = Ena at posterior pole of oocyte. Blue arrow = Ena around ring canals. (I) Stage 9, showing border cell cluster. (J) mat-FP4mito expression relocalizes Ena to mitochondria. (K, L) Mutant ena^{23} (K) and ena^{210} (L) protein accumulation at cortex (arrows) is strongly reduced relative to wild-type (F) but not abolished. Scale bars=20 μm.

Figure 2.2

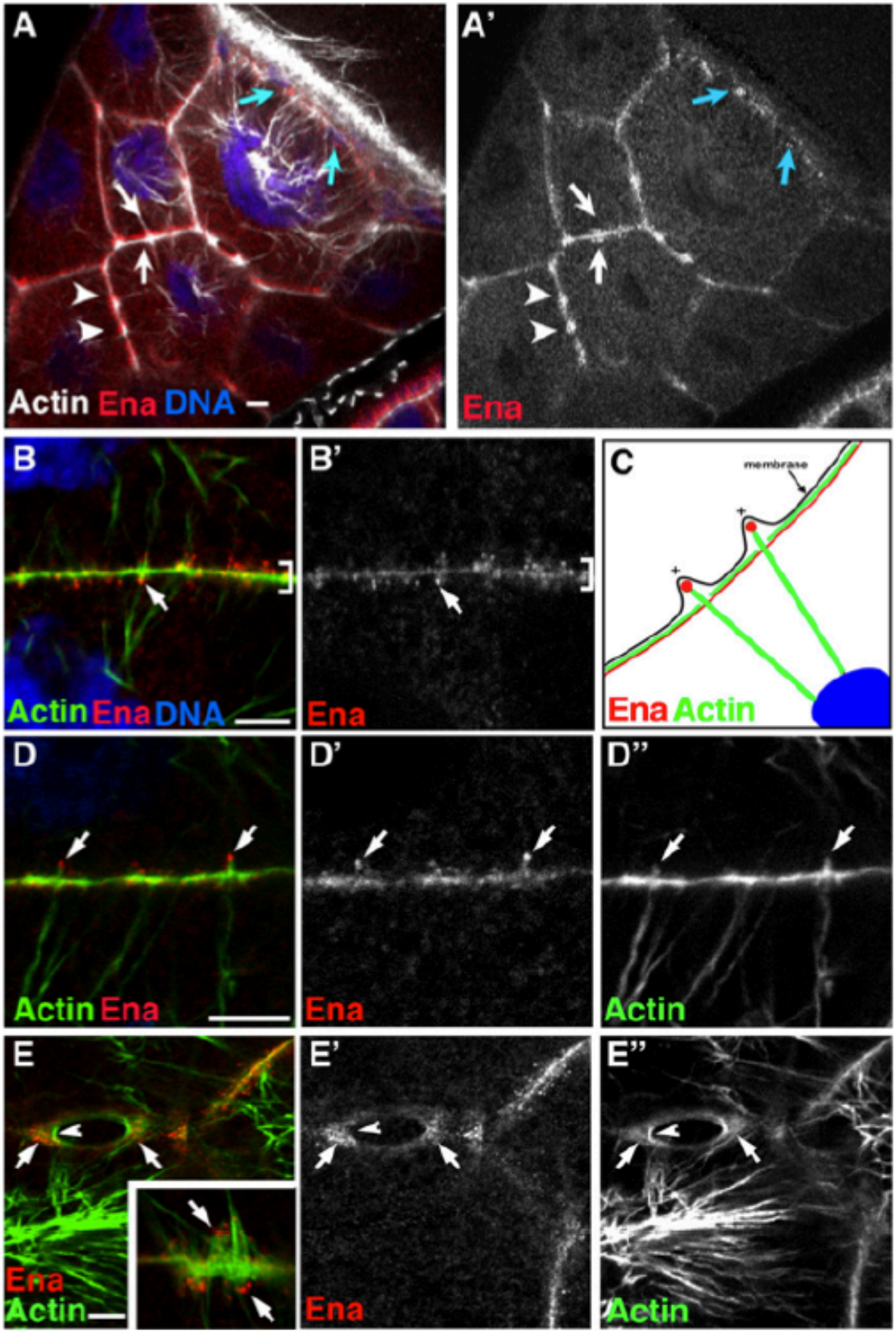
A
Actin Ena DNA
A'
Ena
B
Actin Ena DNA
B'
Ena
C
membrane
Ena Actin
D
Actin Ena
D'
Ena
D''
Actin
E
Ena
Actin
E'
Ena
E''
Actin

Fig. 2.2. Ena localization suggests roles in regulating nurse cell actin filaments. Wildtype stage 10B egg chambers, anterior lower left. Antigens indicated. (A) As cytoplasmic actin filaments form in nurse cells, Ena localizes in a cloud near the nurse cell–nurse cell (white arrows) and nurse cell–oocyte cortex (blue arrows) and around ring canals (arrowheads). (B, D) Successively more close-up views of nurse cell cortex. Ena surrounding nurse cell:nurse cell cortex (bracket) and at barbed ends of bundled actin filaments (arrows). (C) Diagram illustrating (B, D) (E) Ena localizes to microvillar-rich membrane (arrows) surrounding ring canals (arrowhead). (E) Inset. Ena at ends (arrows) of basket of actin filaments projecting from ring canal. Scale bars=5 μm.

Figure 2.3

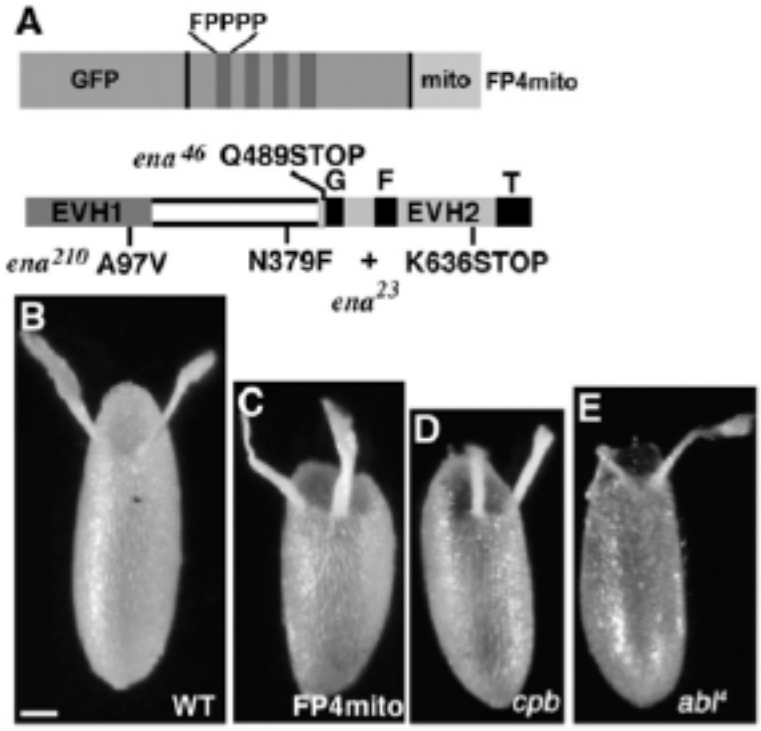

F	Normal	Dumpless	N
FP4mito	11%	89%	400
ena^{23}	76%	24%	920
ena^{210}	96%	4%	627
ena^{46}	78%	22%	816
cpb^{F19}/*cpb*$^{6.15}$	3%	97%	514
abl^{4}	86%	14%	212

G	Normal	Dumpless	N
FP4mito	16%	84%	852
FP4mito; cpb^{1}/+	43%	57%	900
FP4mito; TM3/+	17%	83%	300
FP4mito; abl^{4}/+	32%	68%	450

Fig. 2.3. Reducing function of either Ena or CP leads to a "dumpless" phenotype. (A) Diagrams of the FP4mito construct and of Ena, showing lesions in ena alleles. ena23 has two lesions—the first is a missense change in a non-conserved amino acid and may be a polymorphism. F = F-actin binding domain, G = G-actin binding domain, T = tetramerization domain. B. Wild-type egg. (C–E) Dumpless eggs from mat-FP4mito (C) cpb hypomorphic (D) mutant, or abl4 (E) germline mutant mothers. (F) Frequencies of dumping defects in mat-FP4mito, ena maternal mutants, cpb hypomorphs, and abl4 maternal mutants are indicated. N = number of eggs scored. (G) Test for modification of dumping defects of FP4mito by heterozygosity for cpb or abl. Scale bar = 50 μm.

Figure 2.4

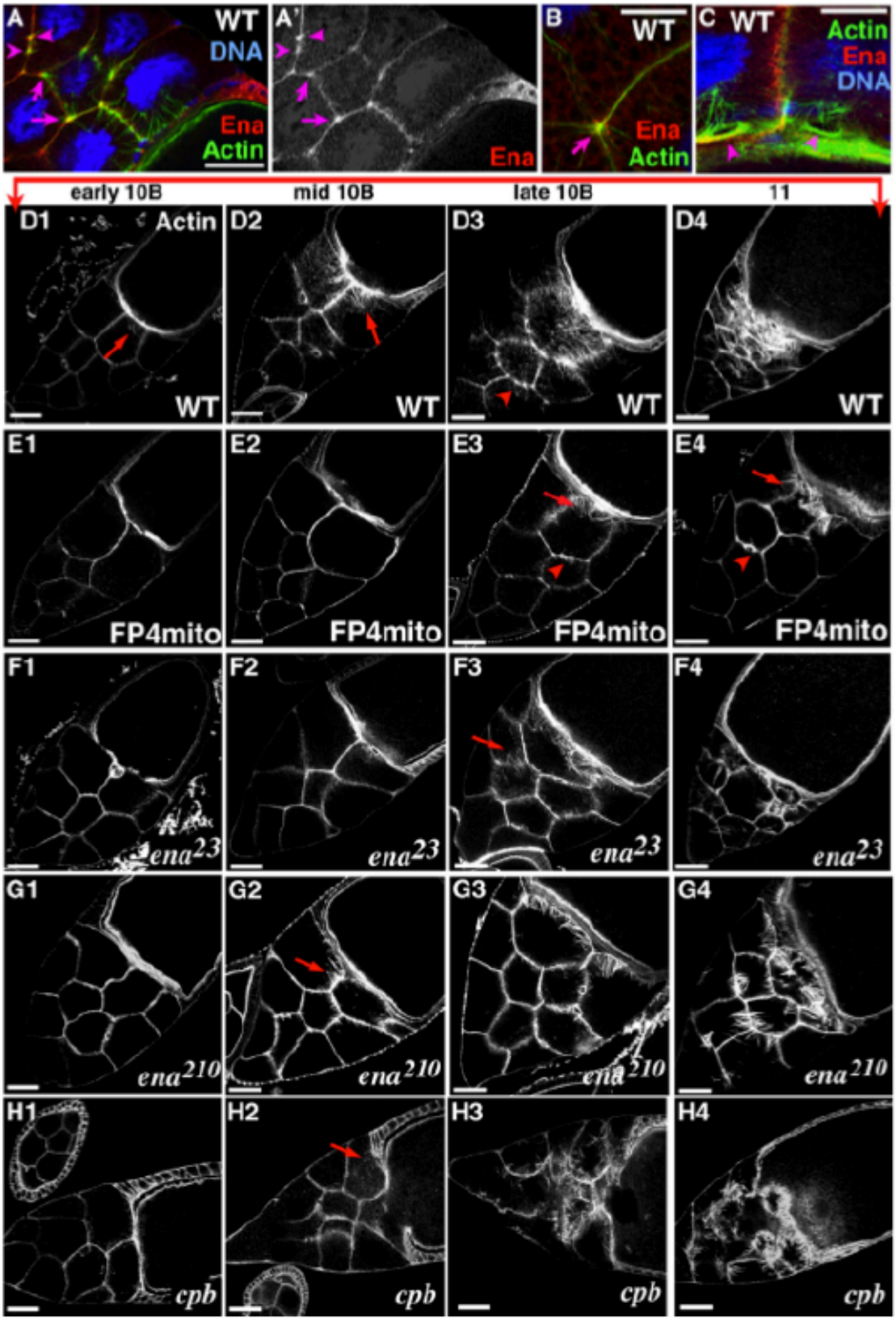
A
WT
DNA
Ena
Actin
A'
Ena
B
WT
Ena
Actin
C WT
Actin
Ena
DNA
early 10B
mid 10B
late 10B
11
D1
Actin
WT
D2
WT
D3
WT
D4
WT
E1
FP4mito
E2
FP4mito
E3
FP4mito
E4
FP4mito
F1
ena23
F2
ena23
F3
ena23
F4
ena23
G1
ena210
G2
ena210
G3
ena210
G4
ena210
H1
cpb
H2
cpb
H3
cpb
H4
cpb

Fig. 2.4. Ena inactivation disrupts formation of cytoplasmic actin filaments. Egg chambers, anterior lower left, except C where anterior is at bottom. (A–C) Wild-type, antigens indicated. Arrows, filaments at tricellular junctions. Arrowheads = filaments at ring canals. (D–H) Actin. Arrows = first filaments. D1–D4. Wild-type. D3. Arrowhead = ring canal filaments. E1–E4. Ena inactivation delays formation and reduces number of cytoplasmic (arrows) and ring canal filaments (arrowheads). F1–F4. ena^{23} germline mutants. G1–G4. ena^{210} germline mutants. ena mutants have delays in filament formation (arrows) matching the severity of their dumpless phenotype. H1–4. cpb hypomorphs. Filaments are not substantially reduced in number but are abnormal in organization. Scale bars = 40 μm.

Figure 2.5

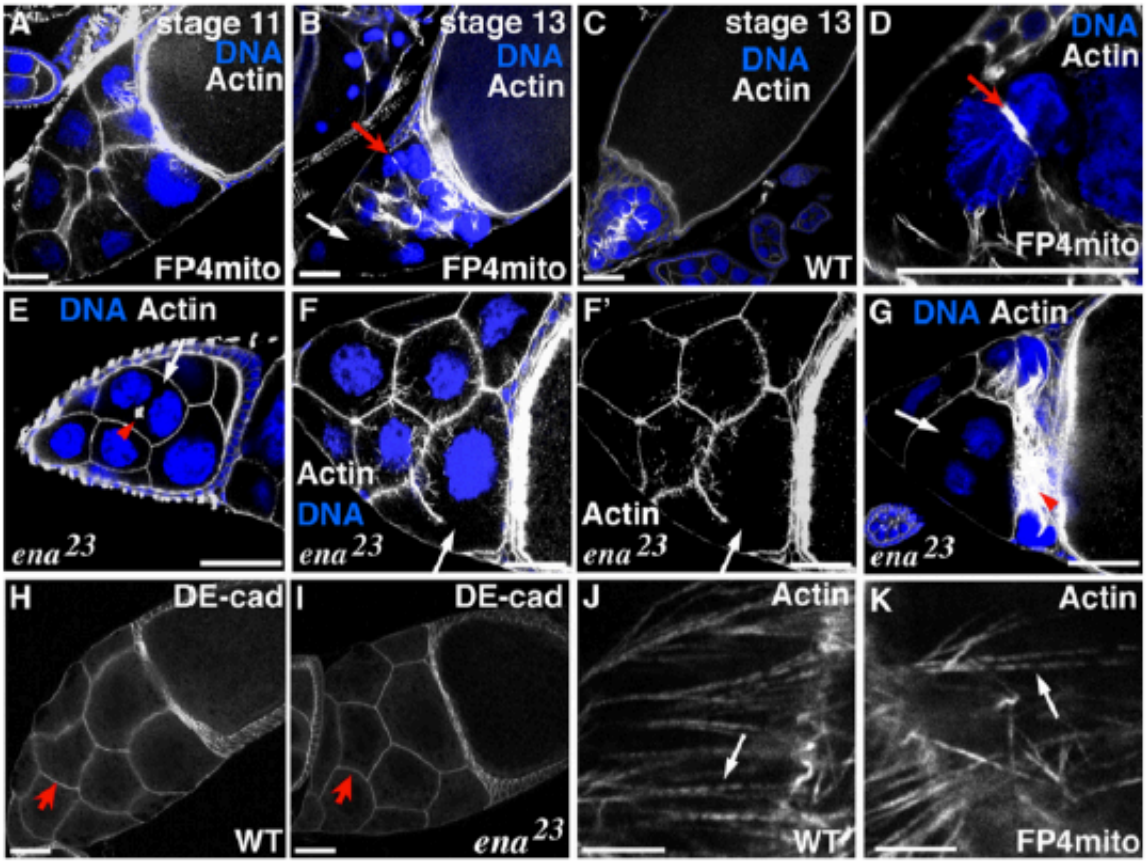

Fig. 2.5. Ena's roles in nurse cell dumping and nurse cell cortical integrity. Egg chambers, anterior left. Genotypes and antigens indicated. (A, B, D) mat-FP4mito. C. Wildtype. Note failure to transfer nurse cell contents (B, white arrow) and nuclei blocking ring canals (B, D, red arrows). E–G. ena^{23} germline mutants. Note failure of cortical actin and multinucleate nurse cells (arrows). (E) Arrowhead = Putative ring canal remnant. (G) Arrowhead = nurse cells that successfully dumped. (H, I) Wild-type (H) and ena^{23} germline mutant (I). DE-cad appears normal. (J, K) Wild-type (J), mat-FP4mito (K). Note similar banding pattern of filaments (arrows). Scale bars = 40 μm (A–I); 5 μm (J,K).

Figure 2.6

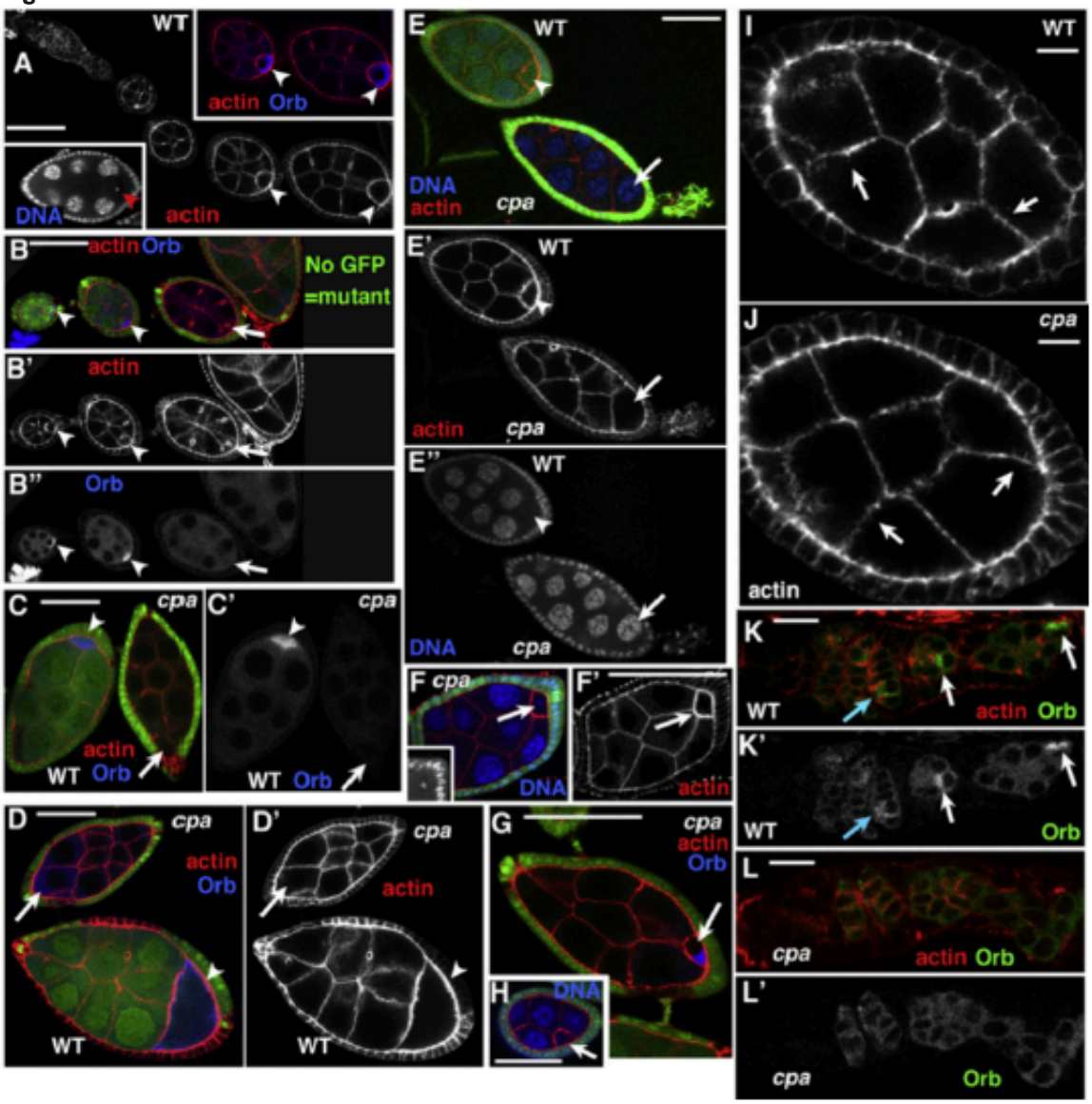

Fig. 2.6. CP is required for correct oocyte determination. Egg chambers, anterior left. Genotypes and antigens indicated. (A) Wildtype. Arrowheads = actin and Orb accumulation in oocyte, and small oocyte nucleus. (B–L) cpa^{69E} mosaic ovarioles. Cpa loss detected by absence of GFP. (B–D) Arrowheads= wildtype oocytes. Note lack of Orb accumulation in mutant egg chambers (arrows). Nurse cell cortical actin is relatively normal. (E) Arrowhead= wildtype oocyte with normal elevated actin. Arrow= mutant egg chamber with large nucleus and no actin elevation. F. Arrow= mutant egg chamber with normal elevated actin and small nucleus. (G, H) Arrows = mutant egg chambers with normal oocyte determination but mispositioned oocyte. (I, J) Cortical actin is slightly more “furry” in mutant (J, arrows). (K, L) Germaria. In wildtype (K) Orb accumulation in the oocyte begins in region 2b (blue arrow) and is clear in stage 1(white arrows). In mutant (L) no obvious Orb accumulation is seen. Scale bars=50μm(A–H); 10 μm (I–L).

Figure 2.7

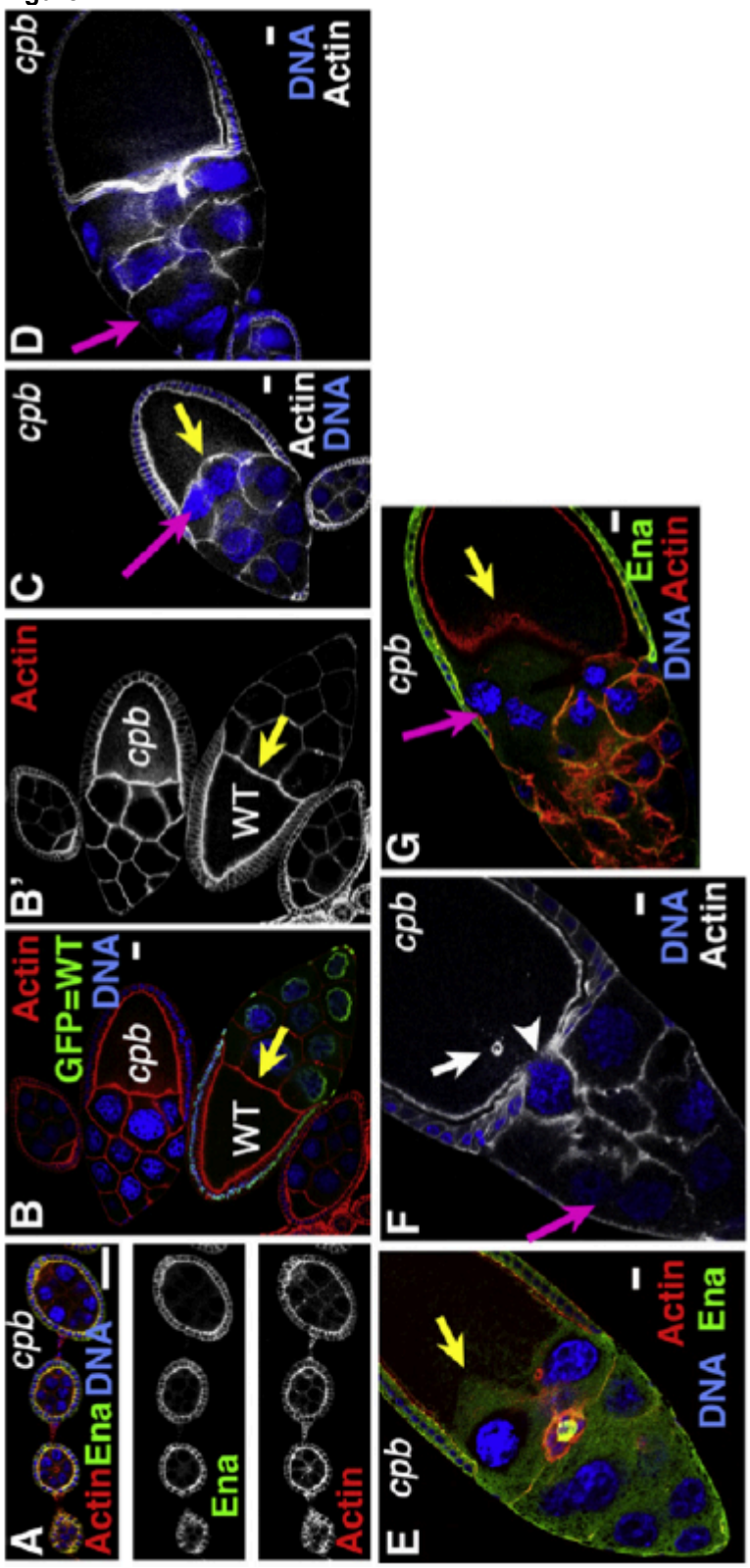
A
cpb
Actin Ena DNA
Ena
Actin
B
Actin
GFP=WT
DNA
cpb
WT
B'
Actin
cpb
WT
C
cpb
Actin
DNA
D
cpb
DNA
Actin
E
cpb
Actin
DNA Ena
F
cpb
DNA
Actin
G
cpb
Ena
DNA Actin

Fig. 2.7. CP is essential for nurse cell cortical integrity. Egg chambers, anterior left, antigens and genotypes indicated. (A) Early egg chambers are normal. (B) Prior to dumping cortical actin levels are unchanged. (C–G) Stage 9 (C), stage 10 (D–F), or stage 11 (G) egg chambers with multinucleate nurse cells (pink arrows) or bulging nurse cells (yellow arrows). (F) White arrow, ring canal floating in oocyte. Arrowhead, breakdown of nurse cell–oocyteborder. Scale Bars = 20 μm.

Figure 2.8

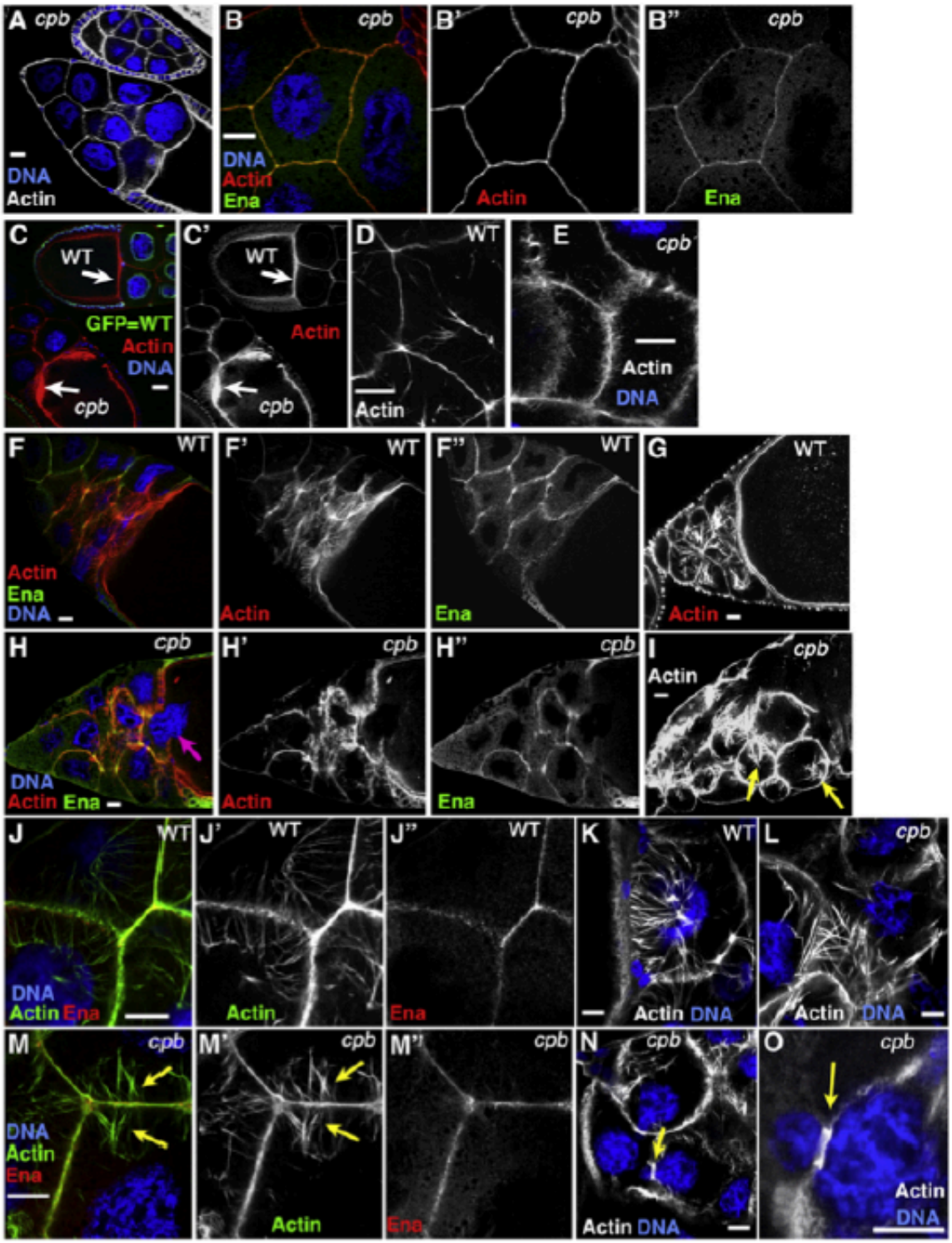
A cpb
DNA
Actin
B cpb
DNA
Actin
Ena
B' cpb
Actin
B'' cpb
Ena
C WT
GFP=WT
Actin
DNA
cpb
C' WT
Actin
cpb
D WT
Actin
E cpb
Actin
DNA
F WT
Actin
Ena
DNA
F' WT
Actin
F'' WT
Ena
G WT
Actin
H cpb
DNA
Actin Ena
H' cpb
Actin
H'' cpb
Ena
I cpb
Actin
J WT
DNA
Actin Ena
J' WT
Actin
J'' WT
Ena
K WT
Actin DNA
L cpb
Actin DNA
M cpb
DNA
Actin
Ena
M' cpb
Actin
M'' cpb
Ena
N cpb
Actin DNA
O cpb
Actin
DNA

Fig. 2.8. In cpb mutants cytoplasmic actin filaments form but are disorganized. Egg chambers, anterior left, antigens and genotypes indicated. (A, B) Just prior to dumping. Actin and Ena localization are roughly normal. (C–E) When dumping begins excess actin accumulates at oocyte (C, bottom arrow) and nurse cell (E) cortex relative to wild-type (C, top arrow and D). (F, G) Mid and late stages of dumping in wild-type. (H, I) cpb mutant, mid- and late-dumping. (H) Arrow = nurse cell nucleus protruding into oocyte. (I) Arrows = disorganized actin filaments. (J–M) cpb. Filaments have a non-uniform distribution (M, yellow arrows) relative to wild-type (J), and filaments are less well organized (L vs. K). N,O.cpb. Nurse cell nuclei sometimes block ring canals (arrows). Scale Bars=20 μm.

Figure 2.9

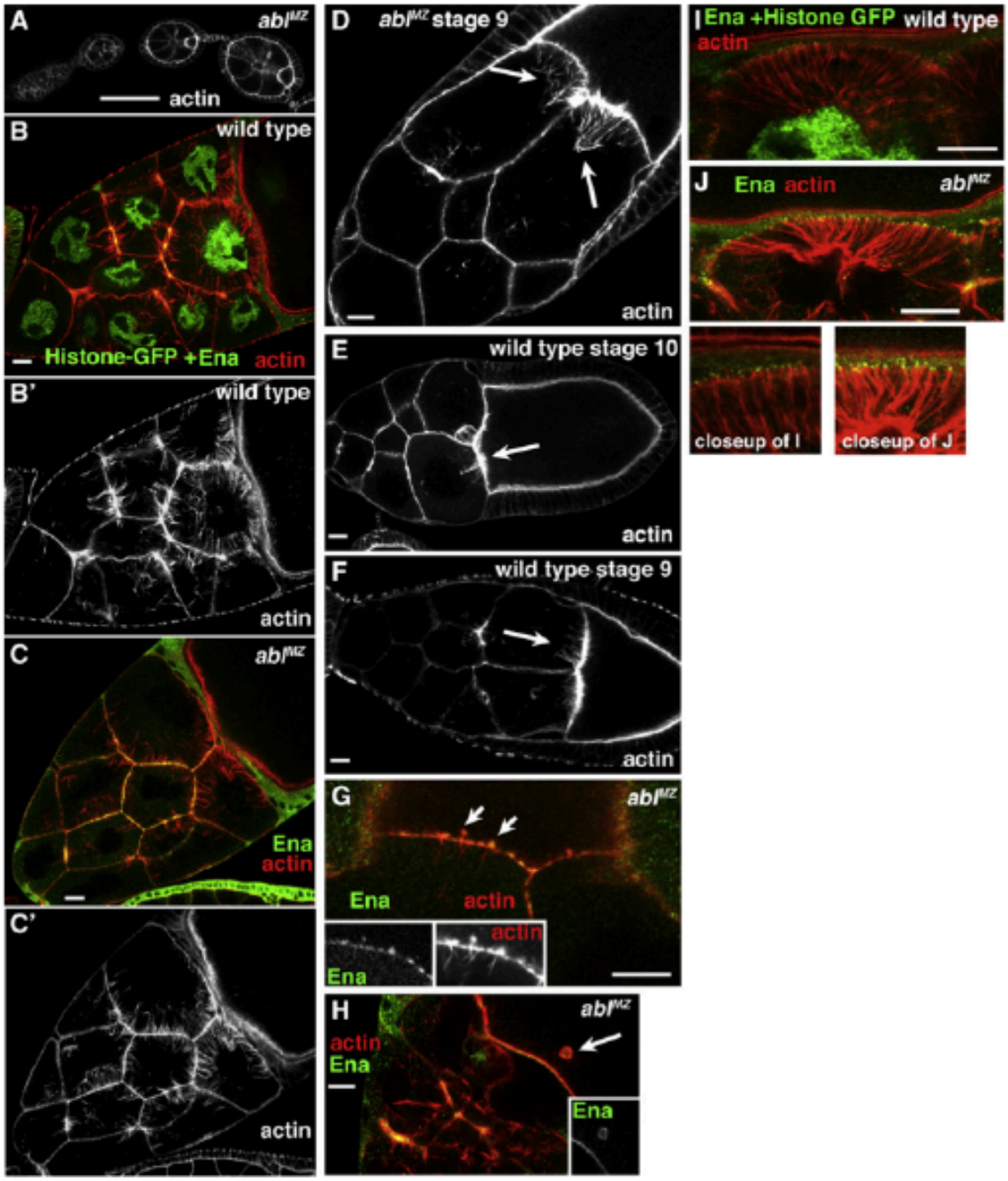

Fig. 2.9. Loss of Abl leads to premature dumping and some Ena de-regulation. Egg chambers, anterior left, antigens and genotypes indicated. (A) Germarium to stage 5. (B, C) Stage 11. abl mutants form relatively normal cytoplasmic nurse cell filaments. (D–F) abl mutant with premature nurse cell filaments at stage 9 (D) contrasts with most wildtype chambers where filaments are initiated in stage 10 (E). Only rarely do wildtype chambers initiate filaments in stage 9 (F). (G, H) abl mutants occasionally accumulated ectopic actin and Ena containing structures at the oocyte–nurse cell interface (G, arrows, insets) or inside the oocyte (H, arrow, inset). (I, J) More robust actin filaments with more Ena at their barbed ends in abl mutant (J) vs. wild-type (I). Scale bars=20 μm.

Figure 2.10

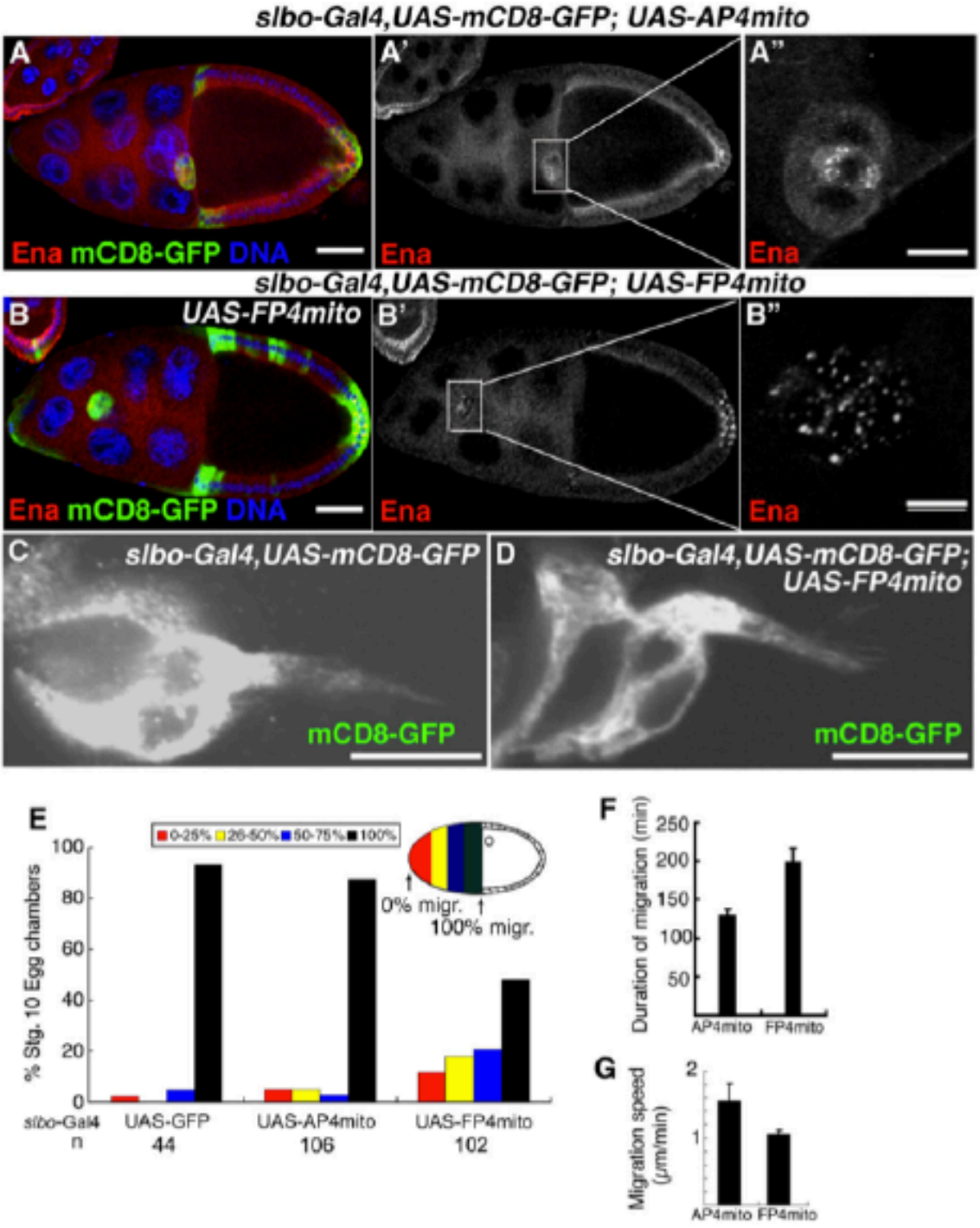
slbo-Gal4,UAS-mCD8-GFP; UAS-AP4mito
A
A'
A''
Ena mCD8-GFP DNA
Ena
Ena
slbo-Gal4,UAS-mCD8-GFP; UAS-FP4mito
B
UAS-FP4mito
B'
B''
Ena mCD8-GFP DNA
Ena
Ena
C
slbo-Gal4,UAS-mCD8-GFP
mCD8-GFP
D
slbo-Gal4,UAS-mCD8-GFP;
UAS-FP4mito
mCD8-GFP
E
0-25% 26-50% 50-75% 100%
0% migr.
100% migr.
% Stg. 10 Egg chambers
100
80
60
40
20
0
slbo-Gal4
UAS-GFP
UAS-AP4mito
UAS-FP4mito
n
44
106
102
F
Duration of migration (min)
250
200
150
100
50
AP4mito
FP4mito
G
Migration speed (μm/min)
2
1
AP4mito
FP4mito

Fig. 2.10. Ena regulates border cell migration. Genotypes and antigens indicated. (A–D) Stage 10 egg chambers. (A) slboGal4; UAS-A4Pmito negative control. (B) slboGal4; UASF4Pmito. A″, B″. High magnification views indicated in A′ and B′, showing sequestration of Ena in border cells by FP4mito but not by AP4mito. (C, D) High magnification views of border cell protrusions in (C) slboGal4,UAS-MCD8GFP and (D) slboGal4,UAS-MCD8GFP; UAS-F4Pmito. (E) Quantification of border cell migration in stage 10 egg chambers expressing indicated genes using slbo-Gal4. n=number of egg chambers scored. (F) Border cell migration duration after detachment from follicle cell epithelium (+/−s.d.). (G) Border cell migration speed (+/−s.d.). Scale bars=50 μm (A, B); 10 μm (C, D).

Figure 2.11

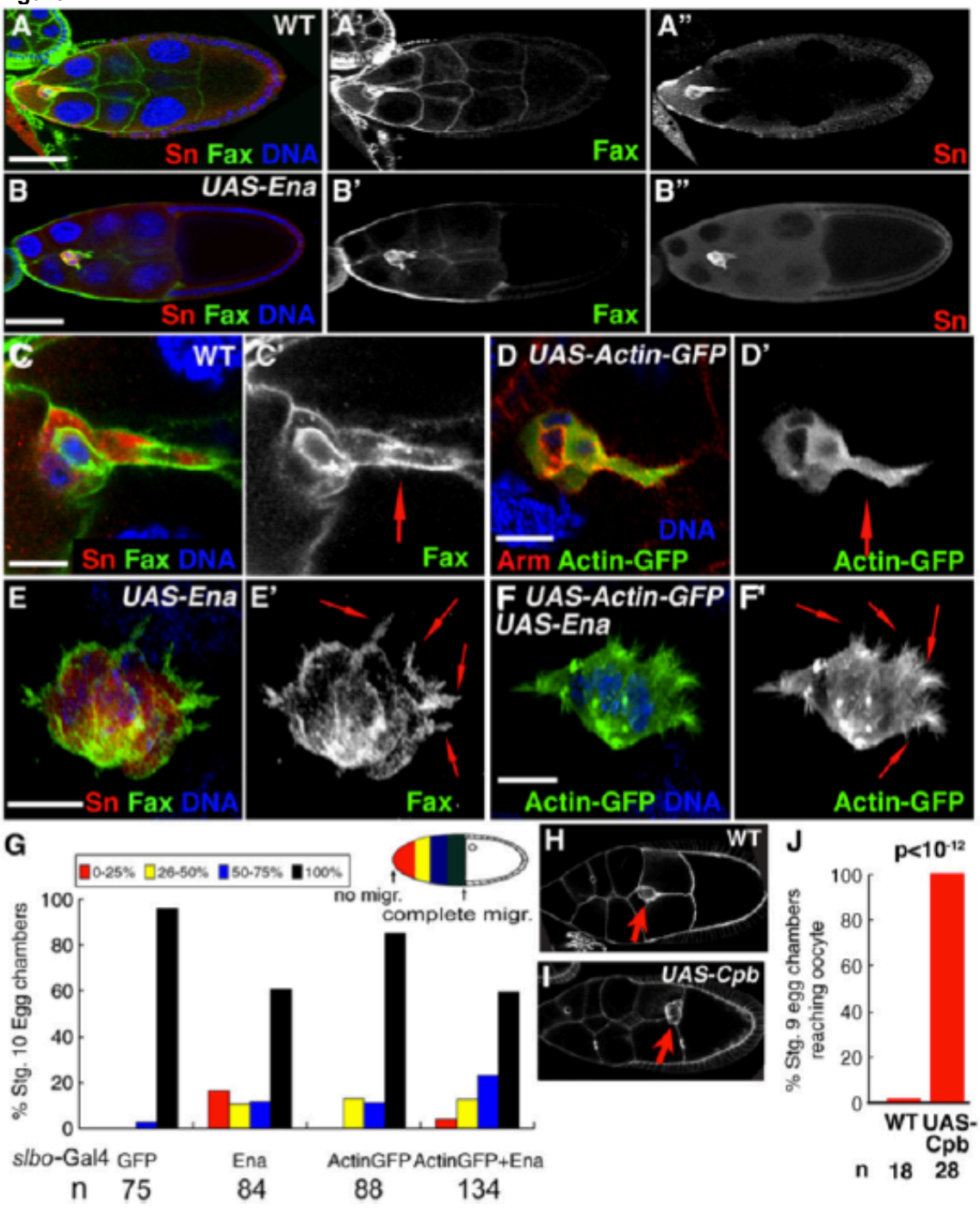
A
WT
Sn Fax DNA
A'
Fax
A''
Sn
B
UAS-Ena
Sn Fax DNA
B'
Fax
B''
Sn
C
WT
Sn Fax DNA
C'
Fax
D UAS-Actin-GFP
DNA
Arm Actin-GFP
D'
Actin-GFP
E
UAS-Ena
Sn Fax DNA
E'
Fax
F UAS-Actin-GFP
UAS-Ena
Actin-GFP DNA
F'
Actin-GFP
G
0-25%
26-50%
50-75%
100%
no migr.
complete migr.
% Stg. 10 Egg chambers
100
80
60
40
20
0
slbo-Gal4 GFP
Ena
ActinGFP
ActinGFP+Ena
n 75
84
88
134
H
WT
I
UAS-Cpb
J
p<10-12
% Stg. 9 egg chambers reaching oocyte
100
80
60
40
20
0
WT
UAS-Cpb
n 18
28

Fig. 2.11. Overexpression of Ena leads to border cell migration defects and altered protrusiveness. Genotypes and antigens indicated. (A) Wild-type (w1118), early stage 9. (B) slbo-Gal4; UAS-Ena late stage 9/early stage 10. (C–F) High magnification view of border cell cluster. Red arrows = leading cells with prominent protrusion. (C) Wild-type. D. slboGal4; UAS- Actin-GFP. (E) slboGal4; UAS-Ena. (F) slboGal4; UAS-ActinGFP/UASEna. (E, F) Arrows = numerous protrusions induced by Ena overexpression; they are even more numerous and/or more evident in the presence of Actin-GFP. G. Quantification of border cell migration in stage 10 egg chambers following overexpression of indicated genes using slbo-Gal4. n = number of egg chambers scored. (H) Wild-type stage 9 egg chamber showing incomplete border cell migration (arrow). Egg chambers staged by degree of retraction of follicle cells from nurse cells to oocyte. (I) slboGal4; UAS-Cpb stage 9 egg chamber showing border cells having reached oocyte (arrow). (J) Quantitation of completion of border cell migration during stage 9 (n = number of egg chambers scored). p value calculated using Fisher's exact test. Scale bars=50 μm (A, B); 10 μm (C–F).

REFERENCES

Ahern-Djamali, S. M., Comer, A. R., Bachmann, C., Kastenmeier, A. S., Reddy, S. K., Beckerle, M. C., Walter, U., and Hoffmann, F. M. (1998). Mutations in Drosophila enabled and rescue by human vasodilator-stimulated phosphoprotein (VASP) indicate important functional roles for Ena/VASP homology domain 1 (EVH1) and EVH2 domains. Mol Biol Cell *9*, 2157–2171.

Akin, O., and Mullins, R. D. (2008). Capping protein increases the rate of actin-based motility by promoting filament nucleation by the Arp2/3 complex. Cell *133*, 841–851.

Applewhite, D. A., Barzik, M., Kojima, S.-I., Svitkina, T. M., Gertler, F. B., and Borisy, G. G. (2007). Ena/VASP proteins have an anti-capping independent function in filopodia formation. Mol Biol Cell *18*, 2579–2591.

Ball, L. J., Jarchau, T., Oschkinat, H., and Walter, U. (2002). EVH1 domains: structure, function and interactions. FEBS Lett *513*, 45–52.

Barzik, M., Kotova, T. I., Higgs, H. N., Hazelwood, L., Hanein, D., Gertler, F. B., and Schafer, D. A. (2005). Ena/VASP proteins enhance actin polymerization in the presence of barbed end capping proteins. J Biol Chem *280*, 28653–28662.

Baum, B., and Perrimon, N. (2001). Spatial control of the actin cytoskeleton in Drosophila epithelial cells. Nat Cell Biol *3*, 883–890.

Bear, J. E. (2008). Follow the monomer. Cell *133*, 765–767.

Bear, J. E. *et al.* (2002). Antagonism between Ena/VASP proteins and actin filament capping regulates fibroblast motility. Cell *109*, 509–521.

Bear, J. E., Loureiro, J. J., Libova, I., Fässler, R., Wehland, J., and Gertler, F. B. (2000). Negative regulation of fibroblast motility by Ena/VASP proteins. Cell *101*, 717–728.

Cant, K., Knowles, B. A., Mahajan-Miklos, S., Heintzelman, M., and Cooley, L. (1998). Drosophila fascin mutants are rescued by overexpression of the villin-like protein, quail. J Cell Sci *111 (Pt 2)*, 213–221.

Cant, K., Knowles, B. A., Mooseker, M. S., and Cooley, L. (1994). Drosophila singed, a fascin homolog, is required for actin bundle formation during oogenesis and bristle extension. J Cell Biol *125*, 369–380.

Chen, J., Godt, D., Gunsalus, K., Kiss, I., Goldberg, M., and Laski, F. A. (2001). Cofilin/ADF is required for cell motility during Drosophila ovary development and oogenesis. Nat Cell Biol *3*, 204–209.

Cooley, L., Verheyen, E., and Ayers, K. (1992). chickadee encodes a profilin required for intercellular cytoplasm transport during Drosophila oogenesis. Cell *69*, 173–184.

Dahlgaard, K., Raposo, A. A. S. F., Niccoli, T., and St Johnston, D. (2007). Capu and Spire assemble a cytoplasmic actin mesh that maintains microtubule organization in the Drosophila oocyte. Dev Cell *13*, 539–553.

Delalle, I., Pfleger, C. M., Buff, E., Lueras, P., and Hariharan, I. K. (2005). Mutations in the Drosophila orthologs of the F-actin capping protein alpha- and beta-subunits cause actin accumulation and subsequent retinal degeneration. Genetics *171*, 1757–1765.

Drees, F., Pokutta, S., Yamada, S., Nelson, W. J., and Weis, W. I. (2005). Alpha-catenin is a molecular switch that binds E-cadherin-beta-catenin and regulates actin-filament assembly.Cell *123*, 903–915.

Fox, D. T., and Peifer, M. (2007). Abelson kinase (Abl) and RhoGEF2 regulate actin organization during cell constriction in Drosophila. Development *134*, 567–578.

Frank, L. H., and Rushlow, C. (1996). A group of genes required for maintenance of the amnioserosa tissue in Drosophila. Development *122*, 1343–1352.

Fulga, T. A., and Rørth, P. (2002). Invasive cell migration is initiated by guided growth of long cellular extensions. Nat Cell Biol *4*, 715–719.

Furman, C., Sieminski, A. L., Kwiatkowski, A. V., Rubinson, D. A., Vasile, E., Bronson, R. T., Fässler, R., and Gertler, F. B. (2007). Ena/VASP is required for endothelial barrier function in vivo. J Cell Biol *179*, 761–775.

Gates, J., and Peifer, M. (2005). Can 1000 reviews be wrong? Actin, alpha-Catenin, and adherens junctions. Cell *123*, 769–772.

Gates, J., Mahaffey, J. P., Rogers, S. L., Emerson, M., Rogers, E. M., Sottile, S. L., Van Vactor, D., Gertler, F. B., and Peifer, M. (2007). Enabled plays key roles in embryonic epithelial morphogenesis in Drosophila. Development *134*, 2027–2039.

Geisbrecht, E. R., and Montell, D. J. (2002). Myosin VI is required for E-cadherin-mediated border cell migration. Nat Cell Biol *4*, 616–620.

Gertler, F. B., Comer, A. R., Juang, J. L., Ahern, S. M., Clark, M. J., Liebl, E. C., and Hoffmann, F. M. (1995). enabled, a dosage-sensitive suppressor of mutations in the Drosophila Abl tyrosine kinase, encodes an Abl substrate with SH3 domain-binding properties. Genes Dev *9*, 521–533.

Godt, D., and Tepass, U. (1998). Drosophila oocyte localization is mediated by differential cadherin-based adhesion. Nature *395*, 387–391.

González-Reyes, A., and St Johnston, D. (1998). The Drosophila AP axis is polarised by the cadherin-mediated positioning of the oocyte. Development *125*, 3635–3644.

Grevengoed, E. E., Fox, D. T., Gates, J., and Peifer, M. (2003). Balancing different types of actin polymerization at distinct sites: roles for Abelson kinase and Enabled. J Cell Biol *163*,1267–1279.

Grevengoed, E. E., Loureiro, J. J., Jesse, T. L., and Peifer, M. (2001). Abelson kinase regulates epithelial morphogenesis in Drosophila. J Cell Biol *155*, 1185–1198.

Guild, G. M., Connelly, P. S., Shaw, M. K., and Tilney, L. G. (1997). Actin filament cables in Drosophila nurse cells are composed of modules that slide passively past one another during dumping. J Cell Biol *138*, 783–797.

Gutzeit, H. O. (1986). The role of microfilaments in cytoplasmic streaming in Drosophila follicles. J Cell Sci *80*, 159–169.

Gutzeit, H. O. (1990). The microfilament pattern in the somatic follicle cells of midvitellogenic ovarian follicles of Drosophila. Eur. J. Cell Biol. *53*, 349–356.

Hopmann, R., and Miller, K. G. (2003). A balance of capping protein and profilin functions is required to regulate actin polymerization in Drosophila bristle. Mol Biol Cell *14*, 118–

128.

Hopmann, R., Cooper, J. A., and Miller, K. G. (1996). Actin organization, bristle morphology, and viability are affected by actin capping protein mutations in Drosophila. J Cell Biol *133*, 1293–1305.

Hudson, A. M., and Cooley, L. (2002a). A subset of dynamic actin rearrangements in Drosophila requires the Arp2/3 complex. J Cell Biol *156*, 677–687.

Hudson, A. M., and Cooley, L. (2002b). Understanding the function of actin-binding proteins through genetic analysis of Drosophila oogenesis. Annu. Rev. Genet. *36*, 455–488.

Janody, F., and Treisman, J. E. (2006). Actin capping protein alpha maintains vestigialexpressing cells within the Drosophila wing disc epithelium. Development *133*, 3349–3357.

Korey, C. A., and Van Vactor, D. (2000). From the growth cone surface to the cytoskeleton: one journey, many paths. J. Neurobiol. *44*, 184–193.

Krause, M., Dent, E. W., Bear, J. E., Loureiro, J. J., and Gertler, F. B. (2003). Ena/VASP proteins: regulators of the actin cytoskeleton and cell migration. Annu. Rev. Cell Dev. Biol. *19*, 541–564.

Lantz, V., Chang, J. S., Horabin, J. I., Bopp, D., and Schedl, P. (1994). The Drosophila orb RNA-binding protein is required for the formation of the egg chamber and establishment of polarity. Genes Dev *8*, 598–613.

Lebrand, C., Dent, E. W., Strasser, G. A., Lanier, L. M., Krause, M., Svitkina, T. M., Borisy, G. G., and Gertler, F. B. (2004). Critical role of Ena/VASP proteins for filopodia formation in neurons and in function downstream of netrin-1. Neuron *42*, 37–49.

Li, W., Li, Y., and Gao, F.-B. (2005). Abelson, enabled, and p120 catenin exert distinct effects on dendritic morphogenesis in Drosophila. Dev Dyn *234*, 512–522.

Lin, H.-P., Chen, H.-M., Wei, S.-Y., Chen, L.-Y., Chang, L.-H., Sun, Y.-J., Huang, S.-Y., and Hsu, J.-C. (2007). Cell adhesion molecule Echinoid associates with unconventional myosin VI/Jaguar motor to regulate cell morphology during dorsal closure in Drosophila. Dev Biol *311*, 423–433.

Mahajan-Miklos, S., and Cooley, L. (1994). The villin-like protein encoded by the Drosophila quail gene is required for actin bundle assembly during oogenesis. Cell *78*, 291–301.

Mejillano, M. R., Kojima, S.-I., Applewhite, D. A., Gertler, F. B., Svitkina, T. M., and Borisy, G. G. (2004). Lamellipodial versus filopodial mode of the actin nanomachinery: pivotal role of the filament barbed end. Cell *118*, 363–373.

Menzies, A. S., Aszodi, A., Williams, S. E., Pfeifer, A., Wehman, A. M., Goh, K. L., Mason, C. A., Fässler, R., and Gertler, F. B. (2004). Mena and vasodilator-stimulated Phosphoprotein are required for multiple actin-dependent processes that shape the vertebrate nervous system.J Neurosci *24*, 8029–8038.

Montell, D. J. (2003). Border-cell migration: the race is on. Nat. Rev. Mol. Cell Biol. *4*, 13–24.

Murphy, A. M., and Montell, D. J. (1996). Cell type-specific roles for Cdc42, Rac, and RhoL in Drosophila oogenesis. J Cell Biol *133*, 617–630.

Niewiadomska, P., Godt, D., and Tepass, U. (1999). DE-Cadherin is required for intercellular

motility during Drosophila oogenesis. J Cell Biol *144*, 533–547.

Pearson, J., and González-Reyes, A. (2004). Egalitarian and the case of the missing link. Nat Cell Biol *6*, 381–383.

Peifer, M., Orsulic, S., Sweeton, D., and Wieschaus, E. (1993). A role for the Drosophila segment polarity gene armadillo in cell adhesion and cytoskeletal integrity during oogenesis. Development *118*, 1191–1207.

Pollard, T. D., and Borisy, G. G. (2003). Cellular motility driven by assembly and disassembly of actin filaments. Cell *112*, 453–465.

Prasad, M., and Montell, D. J. (2007). Cellular and molecular mechanisms of border cell migration analyzed using time-lapse live-cell imaging. Dev Cell *12*, 997–1005.

Riparbelli, M. G., and Callaini, G. (1995). Cytoskeleton of the Drosophila egg chamber: new observations on microfilament distribution during oocyte growth. Cell Motil Cytoskeleton *31*, 298–306.

Robinson, D. N., and Cooley, L. (1997). Genetic analysis of the actin cytoskeleton in the Drosophila ovary. Annu. Rev. Cell Dev. Biol. *13*, 147–170.

Roffers-Agarwal, J., Xanthos, J. B., Kragtorp, K. A., and Miller, J. R. (2008). Enabled (Xena) regulates neural plate morphogenesis, apical constriction, and cellular adhesion required for neural tube closure in Xenopus. Dev Biol *314*, 393–403.

Rørth, P. (2002). Initiating and guiding migration: lessons from border cells. Trends Cell Biol *12*, 325–331.

Rørth, P. *et al.* (1998). Systematic gain-of-function genetics in Drosophila. Development *125*, 1049–1057.

Schirenbeck, A., Arasada, R., Bretschneider, T., Stradal, T. E. B., Schleicher, M., and Faix, J. (2006). The bundling activity of vasodilator-stimulated phosphoprotein is required for filopodium formation. Proceedings of the National Academy of Sciences of the United States of America *103*, 7694–7699.

Scott, J. A., Shewan, A. M., Elzen, den, N. R., Loureiro, J. J., Gertler, F. B., and Yap, A. S. (2006). Ena/VASP proteins can regulate distinct modes of actin organization at cadherin adhesive contacts. Mol Biol Cell *17*, 1085–1095.

Sheffield, M., Loveless, T., Hardin, J., and Pettitt, J. (2007). C. elegans Enabled exhibits novel interactions with N-WASP, Abl, and cell-cell junctions. Curr Biol *17*, 1791–1796.

Tilney, L. G., Connelly, P., Smith, S., and Guild, G. M. (1996). F-actin bundles in Drosophila bristles are assembled from modules composed of short filaments. J Cell Biol *135*, 1291–1308.

Vasioukhin, V., Bauer, C., Yin, M., and Fuchs, E. (2000). Directed actin polymerization is the driving force for epithelial cell-cell adhesion. Cell *100*, 209–219.

Verheyen, E. M., and Cooley, L. (1994). Profilin mutations disrupt multiple actin-dependent processes during Drosophila development. Development *120*, 717–728.

Vignjevic, D., Kojima, S.-I., Aratyn, Y., Danciu, O., Svitkina, T., and Borisy, G. G. (2006). Role of fascin in filopodial protrusion. J Cell Biol *174*, 863–875.

Wang, X., Bo, J., Bridges, T., Dugan, K. D., Pan, T.-C., Chodosh, L. A., and Montell, D. J. (2006). Analysis of cell migration using whole-genome expression profiling of migratory cells in the Drosophila ovary. Dev Cell *10*, 483–495.

Wear, M. A., and Cooper, J. A. (2004). Capping protein: new insights into mechanism and regulation. Trends Biochem. Sci. *29*, 418–428.

Wheatley, S., Kulkarni, S., and Karess, R. (1995). Drosophila nonmuscle myosin II is required for rapid cytoplasmic transport during oogenesis and for axial nuclear migration in early embryos. Development *121*, 1937–1946.

Withee, J., Galligan, B., Hawkins, N., and Garriga, G. (2004). Caenorhabditis elegans WASP and Ena/VASP proteins play compensatory roles in morphogenesis and neuronal cell migration. Genetics *167*, 1165–1176.

Zallen, J. A., Cohen, Y., Hudson, A. M., Cooley, L., Wieschaus, E., and Schejter, E. D. (2002). SCAR is a primary regulator of Arp2/3-dependent morphological events in Drosophila. J Cell Biol *156*, 689–701.

CHAPTER 3: ENABLED NEGATIVELY REGULATES DIAPHANOUS-DRIVEN ACTIN DYNAMICS *IN VITRO* AND *IN VIVO*

Colleen G. Bilancia,[1] Jonathan D. Winkelman,[3] Denis Tsygankov,[4] Stephanie H. Nowotarski,[1] Jennifer A. Sees,[3] Kate Comber,[5] Iwan Evans,[5] Vinal Lakhani,[4] Will Wood,[5] Timothy C. Elston,[4] David R. Kovar',[3,6] and Mark Peifer[1,2,*]

[1]Biology Department, University of North Carolina at Chapel Hill, Chapel Hill, NC 27599, USA [2]Lineberger Comprehensive Cancer Center, University of North Carolina at Chapel Hill, Chapel Hill, NC 27599, USA [3]Department of Molecular Genetics and Cell Biology, The University of Chicago, Chicago, IL 60637, USA 4Department of Pharmacology, University of North Carolina at Chapel Hill, Chapel Hill, NC 27599, USA [5]Department of Biology and Biochemistry, University of Bath, Bath BA2 7AY, UK [6]Department of Biochemistry and Molecular Biology, The University of Chicago, Chicago, IL 60637, USA

Preface

For my third chapter I am including a large collaborative work I was a part of detailing an interaction between Ena and Dia that influenced and underpinned my first author paper. This work was published by Developmental Cell in 2014 and is entitled: " Enabled negatively regulates Diaphanous-driven actin dynamics in vitro and in vivo." This paper built off of previous work in the lab by Catarina Homem, which suggested Ena and Dia interact by showing they directly interact and that Ena negatively regulates Dia biochemically *in vitro* and *in vivo*. Colleen Bilancia carried out the yeast two hybrid assay, pulldown assays and cell

culture. Denis Tsygankov with Vinal Lakhani from Timothy Elston's lab developed filopodia-tracking software and analyzed cell culture data sets. Jonathan Winkleman with Jennifer Sees from Dave Kovar's lab performed the *in vitro* actin assays. Kate Comer and Iwan Evans from Will Wood's lab contributed the *Droso*phila hemocyte analysis. This work was completed under the direction of Mark Peifer.

My contributions to the following work were initial cell culture experiments and the *in vivo* analysis during *Drosophila* dorsal closure. This *in vivo* support to our cell culture and *in vitro* data, revealed areas with high levels of Dia and low levels of Ena produced long-lived protrusions, while tissue locations with high levels of endogenous Ena produced filopodia that were shorter-lived. I followed up on *in vivo* filopodia and the kinds of protrusions Ena and Dia promote during dorsal closure for my first author paper (Chapter 4).

Abstract

Actin regulators facilitate cell migration by controlling cell protrusion architecture and dynamics. As the behavior of individual actin regulators becomes clear, we must address why cells require multiple regulators with similar functions and how they cooperate to create diverse protrusions. We characterized Diaphanous (Dia) and Enabled (Ena) as a model, using complementary approaches: cell culture, biophysical analysis, and Drosophila morphogenesis. We found that Dia and Ena have distinct biochemical properties that contribute to the different protrusion morphologies each induces. Dia is a more processive, faster elongator, paralleling the long, stable filopodia it induces *in vivo*, while Ena promotes filopodia with more dynamic changes in number, length, and lifetime. Acting together, Ena and Dia induce protrusions distinct from those induced by either alone, with Ena reducing Dia-driven protrusion length and number. Consistent with this, EnaEVH1 binds Dia directly and inhibits DiaFH1FH2-mediated nucleation *in vitro*. Finally, Ena rescues hemocyte migration defects caused by activated Dia.

Introduction

Actin-based cell protrusions are a hallmark of migrating cells during development and disease. Migrating cells use two protrusion types: lamellipodia, broad protrusions supported by short -branched actin filaments, and filopodia, narrow processes containing parallel, unbranched actin filaments. Filopodia are thought to be exploratory environment sensors, while lamellipodia provide the driving force for motility.

Key regulators shape the actin cytoskeletal architecture required for protrusions. Functions of individual actin regulators *in vitro* and in simple cell types are well studied, but how cells utilize different suites of actin regulators, some with similar functions, to make functionally distinct protrusions remains unclear. It is also unknown how the regulatory network is controlled by crosstalk among proteins to modify their activities and protrusion dynamics. We used two unbranched actin filament polymerases, Diaphanous (Dia) and Enabled (Ena), as a model to understand mechanistic differences between individual actin regulators with similar functions and how they work together to regulate actin dynamics and protrusions.

Dia is a Diaphanous-related formin (DRF), which nucleate and elongate unbranched actin filaments (Breitsprecher and Goode, 2013). *Drosophila* Dia plays many important roles in development, driving cellularization (Grosshans *et al.*, 2005), regulating myosin, adhesion, and protrusive behavior during epithelial morphogenesis (Homem and Peifer, 2008; 2009), and controlling polarized epithelial secretion (Massarwa *et al.*, 2009). Mammalian DRFs are also important actin regulators, controlling adhesion and cell protrusive behavior in culture (e.g., (Gupton and Gertler, 2007; Yang *et al.*, 2007)); via these roles they are implicated in human disease (DeWard *et al.*, 2010).

DRFs share conserved domains (Figure 3.1A): the guanosine triphosphatase binding domain (GBD), Dia interacting domain (DID), dimerization domain, formin homology 1 and 2 (FH1 and FH2), and Dia autoinhibitory domain (DAD). DRFs are autoinhibited by association of the DAD and DID and activated when guanosine-triphosphate-bound Rho

binds the GBD, releasing autoinhibition and allowing cortical recruitment (Alberts, 2001; Li and Higgs, 2003; Otomo *et al.*, 2005; Rose *et al.*, 2005; Gorelik *et al.*, 2011). Once activated, the FH2 nucleates actin filaments (Sagot et al., 2002; Pruyne *et al.*, 2002) and remains processively associated with barbed ends to promote monomer addition and block capping (Zigmond *et al.*, 2003; Higashida *et al.*, 2004; Kovar and Pollard, 2004; Romero *et al.*, 2004). The FH1, a polyproline motif that binds profilin (Chang *et al.*, 1997), increases barbed end elongation (Romero *et al.*, 2004; Kovar *et al.*, 2006).

DRF FH1 and FH2 domains cooperate to polymerize actin, making them targets for negative regulators. A wide range of proteins negatively regulate formins, e.g., yeast Bnr1's FH2 is bound by Smy1 to slow elongation or by Bud14 to displace it from filaments (Chesarone and Goode, 2009; Chesarone-Cataldo *et al.*, 2011). Diaphanous interacting protein binds mDia2 and can inhibit filopodia and actin assembly(Eisenmann *et al.*, 2007), while Cip4 antagonizes Dia by inhibiting nucleation (Yan et al., 2013). Less is known about how multiple actin-binding proteins work together to regulate each other's activity. WAVE and the Arp2/3 complex, primary players in branched actin networks, can interact with mDia2 to inhibit filopodia (Beli *et al.*, 2008), suggesting important regulatory interactions between proteins responsible for opposing actin structures. However, the nature and role of interactions between proteins generating similar actin structures, like Dia and Ena/vasodilator-stimulated phosphoprotein (VASP), remain to be seen.

Ena/VASP proteins promote unbranched actin filament elongation by antagonizing Capping Protein (Bear *et al.*, 2002; Barzik *et al.*, 2005; Applewhite *et al.*, 2007) and riding processively on barbed ends, promoting actin monomer addition (Breitsprecher *et al.*, 2008; Hansen and Mullins, 2010). VASP also bundles actin filaments and may prevent Arp2/3-induced branching (reviewed in (Bear and Gertler, 2009). Ena/VASP proteins, including the single Drosophila Ena/VASP, Ena (Gertler *et al.*, 1990), share several conserved domains (Figure 3.1A). The Ena/VASP Homology 1 (EVH1) domain binds partners like Zyxin or Testin, often through a consensus FP4 motif (Phenylalanine and 4 Prolines). A Proline rich region (Pro) recruits profilin-actin for barbed end addition. The EVH2 domain has G- and Factin

binding sites and a coiled-coil for tetramerization. Like Dia, Ena/VASP proteins regulate filopodia and lamellipodia in cell culture, and during development and disease (e.g., (Gertler *et al.*, 1996; Bear *et al.*, 2002; Schirenbeck *et al.*, 2006; Gates *et al.*, 2007; Philippar *et al.*, 2008).

Ena/VASP and Dia coimmunoprecipitate in flies, mice, and *Dictyostelium* (Grosse *et al.*,2003; Schirenbeck *et al.*, 2005; Homem and Peifer, 2009). In *Drosophila* both localize at the leading edge of migrating epidermal cells, and their interplay modulates the function of each *in vivo*, as varying relative levels of Ena and Dia changes the protrusion profile during dorsal closure (Homem and Peifer, 2009). Thus, both Dia and Ena are important for shaping protrusions *in vivo*, but current data suggest they interact in complex ways to balance filopodia and lamellipodia during morphogenesis.

We explored how Dia and Ena regulate cell protrusions both individually and together, using cell biology and biophysical approaches. We found that Ena and Dia drive distinct protrusive behaviors that reflect differences in their processive actin filament assembly abilities. Ena and Dia directly bind through Ena's EVH1 and Dia's FH1 domains. When coexpressed, they induce protrusions distinct from those induced by either alone, and this seems largely explained by Ena's EVH1 inhibiting Dia activity *in vivo*. Biophysical studies confirm that Ena's EVH1 inhibits Dia nucleation but not elongation. Using *Drosophila*, we provide evidence that Ena modulates Dia activity and its effects on protrusive behavior in vivo during both dorsal closure and hemocyte migration.

Results

Dia and Ena Drive Distinct Filopodial Dynamics

Dia and Ena both promote unbranched processive actin filament elongation, leading us to ask why cells have two proteins performing similar functions. We hypothesized each has distinct properties, tailoring their activities to produce specific types of actin dynamics and cell protrusions. To test this, we characterized how they work individually to drive cell protrusions in culture. We used *Drosophila* D16 cells as a model, as they naturally form filopodia and lamellipodia (Figures 3.1B–1E). Furthermore, Dia is the single fly DRF and

Ena the single Ena/VASP, eliminating redundancy. D16 cells express both Ena and Dia. Ena has a large cytoplasmic pool, but is enriched at the cortex, filopodia, and lamellipodia edges (Figures 3.1B–1B’’’). Dia localizes similarly, with cytoplasmic staining and enrichment cortically and in filopodia (Figures 3.1C–1C’’’). Surprisingly, despite similar roles in promoting filament elongation, only 9% of filopodia (n = 529; Figure 3.1E) had Ena and Dia colocalized at their tips. The most prominent class of filopodia contained only Ena (47%), while 32% had Ena at the tip and Dia in the shaft. Only a small fraction had Dia alone (4%) or Dia at the tip and Ena in the shaft (9%). Thus Ena seems dominant in D16 cells.

We next examined how each protein controls protrusion dynamics (Movie S1 available online). We expressed fluorescent actin alone (Figures 3.2A and 3.2A’), with GFPDiaDDAD (activated Dia lacking the DAD; Figures 3.2B–2D’ and S1F; expressed ~30- fold over endogenous Dia), or with mCherry-Ena (mCh-Ena; Figures 3.2E–2G’ and S1F; expressed ~3-fold over endogenous Ena). We hypothesized each would induce filopodia, but that number, length, or lifetime may differ. Consistent with this, DiaDDAD (Figures 3.2B and 2B’) and Ena (Figures 3.2E and 2E’ ; Movie S1) drove ectopic filopodia and localized to filopodia tips (Figures 3.2D’ and 2G’). To determine if these filopodia differ, we quantified cell protrusions using a novel computational method, CellGeo (Tsygankov *et al.*, 2014). CellGeo automatically identifies and tracks cell protrusions using a tree-graph representation of cell shape, allowing users to set mathematically precise definitions of filopodia and broad protrusions and to track and quantify them over time (Supplemental Experimental Procedures).

As expected, both DiaDDAD and Ena significantly increased mean filopodial number and length relative to actin-only controls (Figures 3.2L and 2M). However, DiaDDAD protrusion morphology and dynamics differed significantly from those driven by Ena. In DiaDDAD, long filopodia (>1.5 mm) often emerged directly from the cell body (Figures 3.2B and 3.2B’; 8.1 filopodia/cell [n = 30] versus 0.9 filopodia/cell for actin-only [n = 11], Figure 3.2N), and the filopodia produced were strikingly stable (mean lifetime = 97 s versus 59 s for wild-type; Figure 3.2O and Movie S1). In contrast, Ena-driven filopodia were seen to

emerge from fan- like broad protrusions by a process resembling convergent elongation, and multiple filopodia merged into fans (Figure 3.2G'; 2.7 events/movie, n = 18 movies; fans with Ena at the edge were rare in wild-type cells, being observed in 2/62 fixed cells stained with Ena). These ''fans'' had linear actin structures extending into the cell body, in contrast to wild-type cells (Figure 3.2A' versus Figure 3.2E'). Ena also stimulated long filopodia emerging from the cell body (3.1/cell, n = 31; Figure 3.2N), but not as effectively as Dia. Ena-driven filopodia had a mean lifetime comparable to wildtype (68 s; Figure 3.2O). Thus, while Dia and Ena both elongate unbranched actin, they drive filopodia with distinct morphology and dynamics. This suggests their roles in filopodia are not redundant, but that each plays a distinct role as different cells create unique protrusion profiles.

Different Actin Assembly Properties of Dia and Ena Might Underlie Their Ability to Drive Protrusions with Distinct Morphology and Dynamics

We hypothesized that the different biochemical properties of Dia and Ena account for the distinct protrusions they drive in vivo. To test this, we purified derivatives of Drosophila Dia and Ena and tested their actin assembly ability. As expected, Dia's FH1FH2 domains (DiaFH1FH2) stimulated rapid pyrene actin assembly (Figures 3.5F, 3.6A, and S4D). Total internal reflection fluorescence microscopy (TIRF) with Oregon-green-labeled actin and quantum-dot-clustered (QD-clustered) DiaFH1FH2 revealed that DiaFH1FH2 accelerates actin filament elongation in the presence of profilin (Figures 3.3C–3E; Movie S2), relative to actin- only controls (Figure 3.3A; Movie S2; Romero et al., 2004; Jaiswal et al., 2013; Yan et al., 2013). DiaFH1FH2 rides processively on filament barbed ends, increasing the elongation rate $6-fold to 72.6 subunits/s versus 11.9 subunits/s for actin only (Figure 3.3F). We assessed Dia's processivity by calculating the barbed end residence time of DiaFH1FH2, which averaged 709 s (Figure 3.3G). This would allow Dia to add $50,000 subunits/association, making it a very processive and efficient filament elongator, comparable to other DRFs (Romero et al., 2004; Kovar and Pollard, 2004; Kovar et al., 2006; Neidt et al., 2008).

We next examined Ena's biochemical properties. We used an Ena derivative lacking the

poorly conserved Linker (EnaDLinker) because it was more stable than full-length Ena and stimulated comparable actin assembly (Figures S2A and S2B). Two-color TIRF of actin and QD-clustered EnaDLinker revealed that Ena binds and rides processively on actin filament barbed ends (Figures 3.3B, 3F, and 3G; Movie S2), increasing the elongation rate 2.4-fold to 34.4 subunits/s (14.1 subunits/s for actin only; Figure 3.3F). We calculated the barbed end residence time for EnaDLinker as 95.2 s (Figure 3.3G), yielding $3,200 subunits/ association. Thus, both Dia and Ena promote actin filament elongation, but Dia remains processively associated with barbed ends $7-fold longer (709.2 s versus 95.2 s) and elongates them $2-fold faster (72.6 versus 34.4 subunits/s). These differences may help explain the distinct filopodial morphology and dynamics we observed. Dia induced longer, more persistent filopodia, while Ena stimulated shorter filopodia with wildtype lifetimes (Figures 3.2M–2O). In this model, once DiaDDAD binds a barbed end, it is highly processive and quickly elongates filaments, resulting in long, stable filopodia. In contrast, Ena is less processive, which might make filaments susceptible to other actin regulators, resulting in more dynamic changes in filopodia number, length, and lifetime.

Dia and Ena Together Produce Protrusions Distinct from Those They Induce Separately

Our previous work in embryos suggests Dia and Ena interact in a complex way to balance filopodia and lamellipodia (Homem and Peifer, 2009). To identify the mechanism by which they cooperate, we coexpressed DiaDDAD and Ena in D16 cells. Strikingly, double overexpression (Figures 3.2H and 3.2H'; Movie S1) produced protrusions with morphology and dynamics distinct from those induced by Ena (Figures 3.2E and 2E') or DiaDDAD (Figures 3.2B and 3.2B') alone. Morphologically, filopodia appeared thicker than wildtype but shorter than filopodia in DiaDDAD cells (Figures 3.2A' , 3.2B' , and 3.2H'). Furthermore, while there were some broad protrusions, the fan-like regions of apparent convergent elongation induced by Ena alone were strikingly reduced (0.9/movie in DiaDDad+Ena [n = 11] versus 2.7/movie for Ena alone; Figures 3.2H and 3.2H' versus

Figures 3.2E and 3.2E'). Coexpressing Ena and DiaDDAD reduced mean filopodia number and length relative to DiaDDAD alone (Figures 3.2L and 2M). Filopodia lifetimes are also reduced relative to DiaDDAD or Ena cells alone (Figure 3.2O). There was also a striking effect on the number of long filopodia (>1.5 mm) emerging directly from the cell body, which was reduced from 8.1/cell to 2.25/cell (n = 16; Figure 3.2N). Ena does not need to be highly overexpressed relative to DiaDDAD to have this effect (Figure S1F). These results are consistent with work in Drosophila embryos, where Ena coexpression reduced DiaDDADdriven filopodia number (Homem and Peifer, 2009). Thus, when coexpressed, Ena reduces filopodia number and length induced by active Dia, consistent with a model where Ena's interaction with Dia is part of a negative regulatory mechanism.

When Ena and Active Dia Colocalize, Filopodia Retract

D16 cells have cortical regions where endogenous Dia and Ena colocalize and other areas where only Ena or Dia localize (Figure 3.1D). Most filopodia are dominated by Ena, and they only occasionally colocalized at filopodial tips (Figures 3.1D and 3.1E). Our differential function hypothesis predicts that structures where they colocalize will exhibit different dynamics from those with only one or the other. We tested this by coexpressing GFPDiaDDAD and mCh-Ena and observing protrusion dynamics when they colocalize. As we saw in fixed cells (Figures 3.1D and 3.1E), most filopodia had DiaDDAD or Ena alone (94% of 539 filopodia; Figures 3.2I–2K; Movie S3), and strong cortical colocalization correlated with regions of few filopodia. This is consistent with quantification showing a reduction in filopodia number by coexpressing DiaDDAD and Ena, relative to DiaDDAD alone (Figure 3.2L).

A small fraction of filopodia (6% of 539 filopodia) had strong DiaDDAD and Ena colocalization (Figures S3.1A–S1C; Movie S4). Quantification revealed that Ena and DiaDDAD colocalized on these filopodia tips for an average of 20 s, shorter than their individual tip residence times (DiaDDAD = 95 s; Ena = 56 s; Figure S3.1E). After colocalization, most filopodia retracted (67%), folded back into the cortex (12%), or stalled

(3%) (Figure S3.1D). These data are consistent with quantification of filopodia length, which is reduced by DiaDDAD and Ena coexpression (Figure 3.2M). This is strikingly different from DiaDDAD-only filopodia in the same cells, with mean lifetimes ≥190 s, supporting the idea that Dia and Ena can act separately or together to control distinct protrusion dynamics.

Dia and Ena Directly Interact through Ena's EVH1 and Dia's FH1 Domains

Our data are consistent with the hypothesis that Ena negatively regulates Dia with important consequences for filopodia dynamics. To define mechanisms by which this occurs, we explored whether their colocalization and coimmunoprecipitation reflect indirect or direct interactions. We found that Ena's EVH1 interacts with Dia's FH1 domain in both yeast twohybrid (Figure 3.4A; Table S1) and glutathione S-transferase (GST) pull- down assays (Figures 3.4B and 3.4C). DiaFH1-carboxyl-terminus (Cterm) binds EnaEVH1 with an equilibrium dissociation constant of 13.3 mM, consistent with a physiologically relevant interaction and similar to Ena/VASP EVH1 affinity for ActA (Holtzman *et al.*, 2007). We next tested whether Ena and Dia interact in D16 cells, using split yellow fluorescent protein (YFP) bimolecular fluorescence complementation, in which the two halves of YFP, which are not individually fluorescent, reconstitute fluores- cence if fused to proteins that bring them into close proximity (Kerppola, 2008); Gohl et al., 2010). We tagged DiaFH1FH2 with the N-terminal region of YFP (NYFP) and EnaEVH1 with the C-terminal region (CYFP). NYFP+CYFP does not reconstitute fluorescence (Figures 3.4D and 3.4D'), and neither NYFP- DiaFH1FH2 (Figures 3.4E and 3.4E') nor CYFP-EnaEVH1 (Figure 3.4F and 3.4F') fluoresces alone. However, coexpressing NYFP- DiaFH1FH2 and CYFP-EnaEVH1 resulted in YFP fluorescence internally and at filopodia tips (Figures 3.4G–4G''). These data confirm that EnaEVH1 and DiaFH1FH2 come into close proximity in cells and, with the data above, suggest direct Ena:Dia binding is important for regulating cell protrusions.

Ena EVH1 is Sufficient to Reduce Dia-Driven Actin Dynamics

Ena and DiaDDAD coexpression reduces filopodia number and length, and their colocalization correlates with low filopodia number or retraction (Figures 3.2 and S1D). We

hypothesized that direct EnaEVH1:Dia binding allows Ena to modulate Dia activity. To test this, we coexpressed GFP-DiaDDAD (Figures 3.5B and 3.5B'') with mCh-EnaEVH1 (Figures 3.5B' and 3.5B'') in D16 cells, comparing them to DiaDDAD-only cells (Figure 3.5A). EnaEVH1 expression is sufficient to significantly reduce the number of DiaDDAD induced filopodia (Figure 3.5D). Consistent with this, although full-length Ena significantly reduced filopodia induced by DiaDDad (Figure 3.2L), EnaProEVH2, lacking the EVH1 domain, did not do so (Figure 3.5D).

We next took this exploration in vitro. EnaDLinker inhibits stimulation of actin assembly by DiaFH1FH2 in pyrene assays (Figure S3A), consistent with reduced filopodia induction in cells. We next tested if EnaEVH1 is sufficient to alter Dia activity, by performing actin assembly assays with DiaFH1FH2 and profilin with or without EnaEVH1. Bulk assays showed that EnaEVH1 has no effect on spontaneous actin assembly (Figures S4A and S4B) but inhibits stimulation of actin polymerization by DiaFH1FH2 (Figures 3.5F and 3.5G). Thus, EnaEVH1 alone is sufficient to reduce Dia-driven actin dynamics *in vitro* and in cell culture.

To test if Dia inhibition requires direct binding via EnaEVH1, we used the EVH1 domain crystal structure (Prehoda et al., 1999; (Ball *et al.*, 2000)to design mutants predicted to reduce ligand binding. We mutated the canonical ligand-binding phenylalanine 77 to glutamic acid to create the EnaEVH1F77E mutant. GST pull-downs with EnaEVH1F77E showed reduced binding to DiaFH1 (Figure 3.5E), suggesting EnaEVH1 binding re- quires the canonical ligand-binding site. We tested if the EnaEVH1F77E mutation reduced Ena's ability to inhibit Dia-driven actin dynamics, coexpressing GFP-DiaDDAD and mCh-EnaEVH1F77E in D16 cells (Figure 3.5C). Unlike EnaEVH1, EnaEVH1F77E did not significantly reduce mean filopodia number induced by DiaDDAD (Figure 3.5D). We also examined the effect of EnaEVH1F77E in pyrene assays, assessing whether direct association is required for EnaEVH1 to reduce Dia-mediated actin assembly *in vitro.* Consistent with cell experiments, EnaEVH1F77E had a significantly reduced ability to inhibit DiaFH1FH2 actin assembly (Figures 3.5F and 3.5G). Taken together, these data show that EnaEVH1 is

sufficient to negatively regulate Dia and suggest that it acts through canonical EnaEVH1 ligand-binding residues. Our functional assays also suggest the possibility that EnaEVH1F77E reduces, but does not eliminate, Ena:Dia interactions and thus acts as a hypomorph. Our data support a model where negative regulation of Dia by direct binding of EnaEVH1 is part of the complex mechanism regulating actin assembly and cell protrusions. Ena and Dia also may affect one another by additional mechanisms, such as competition for barbed ends. Consistent with this, EnaProEVH2 also can reduce actin assembly by DiaFH1FH2 in pyrene assays (Figures S3B and S3C).

Ena's EVH1 Domain Inhibits Dia-Mediated Nucleation

Our data reveal that EnaEVH1 can inhibit Dia function by direct binding, but how it inhibits actin assembly remained unclear. DiaFH1 also binds to profilin-actin, which is the rate-limiting step of formin-mediated barbed end elongation (Vavylonis *et al.*, 2006; Paul *et al.*, 2008). Therefore, we hypothesized that EnaEVH1:DiaFH1 association interferes with elongation by disrupting profilin binding to DiaFH1. To test this, we repeated actin assembly assays with DiaFH1FH2 and EnaEVH1 without profilin, but found that EnaEVH1 still inhibited DiaFH1FH2 (Figures 3.6A and S4G). Thus, blocking profilin is not the main role of EnaEVH1 binding.

To further probe mechanism, we performed TIRF, using Oregon-green-labeled actin and red-labeled SNAP-549-DiaFH1FH2 to assess actin filament elongation in the presence and absence of EnaEVH1. In the absence of profilin, DiaFH1FH2 (Figure 3.6E; Movie S5) increased barbed end actin filament elongation from 12.5 to 24.3 subunits/s (Figure 3.6B; this was surprising since other formins slow elongation in the absence of profilin, and it will need to be explored further) and had a mean residence time of 600 s (Figure 3.6C). EnaEVH1 alone caused actin puncta formation (Figure 3.6F; Movie S5), but this had little effect on actin assembly (Figures S4A and S4B). EnaEVH1 did not alter the DiaFH1FH2 elongation rate (24.2 subunits/s; Figure 3.6B), residence time (806.5 s; Figure 3.6C), or its effect in seeded actin assembly assays (Figures S4D and S4E), showing that EnaEVH1 does not inhibit Dia's ability to processively elongate actin filaments. Similarly, EnaDLinker did not

alter Dia's elongation rate (Figures S4C and S4F).

We next tested whether EnaEVH1 inhibits actin nucleation by Dia. Knowing the barbed end elongation rate from TIRF allowed us to calculate barbed end concentrations from pyrene actin assembly assays (Figures 3.6A, 3.6D, and S4H; as in (Higgs *et al.*, 1999). We found that increasing concentrations of EnaEVH1 significantly reduced the concentration of DiaFH1FH2-nucleated barbed ends (e.g., 1.0 nM without EnaEVH1 to 0.27 nM at 5.8 mM EnaEVH1; Figures 3.6D and S4H). These data suggest that only 20% of DiaFH1FH2 dimers nucleate a new filament under these conditions. Thus, EnaEVH1 reduces the nucleation efficiency of DiaFH1FH2. TIRF revealed that EnaEVH1 recruits DiaFH1FH2 to actin puncta; most do not initiate actin assembly, but occasionally Dia-associated barbed ends elongated away from these puncta (Figures 3.6G and 6H; Movie S5), suggesting that Dia can escape inhibition and initiate actin assembly. These data, together with the lack of change in elongation, support a model where EnaEVH1 binds DiaFH1 and actin to inhibit Dia nucleation (Figure 3.6I), but do not rule out the possibility that EnaEVH1 also interacts with the FH2 domain.

Dia-Driven Protrusions Are More Dynamic in Areas of High Endogenous Ena during Drosophila Dorsal Closure

We next tested whether Ena plays the same negative regulatory role in the complex environment *in vivo* (Figure 3.7A). Ena and Dia shape the suite of protrusions formed during Drosophila dorsal closure *in vivo*; notably, Ena coexpression reduced DiaDDAD-induced filopodia, and reducing Ena activity increased DiaDDAD-induced filopodia number and length (Homem and Peifer, 2009), consistent with our D16 cell results. To explore the role of endogenous Ena in regulating Dia-driven actin dynamics *in vivo*, we imaged wildtype embryos (Movie S6) and those expressing DiaDDAD, which induced ectopic filopodia at all cell borders (Figures 3.7C and 3.7C' versus Figures 3.7D and 3.7D'; Movie S7). We compared protrusion dynamics in areas of the cortex with low or high endogenous Ena levels (Figures 3.7B and 3.7B'), comparing the leading edge and tricellular junctions (high Ena) with lateral borders (low Ena). This revealed two distinct filopodia populations with different

dynamics, depending on endogenous Ena levels. Strikingly, Dia-induced filopodia at lateral cell borders, where Ena levels were low, were long lived (Figure 3.7K) and emerged directly from the cell body (Figures 3.7D and 3.7D', arrowheads), reminiscent of long, stable DiaDDAD filopodia in D16 cells (Figure 3.2B'). In contrast, filopodia Dia induced from tricellular junctions (Figures 3.7D and 3.7D', green arrows), areas with high endogenous Ena levels, were shorter lived (Figure 3.7K) and emerged from dynamic structures with both lamellipodial and filopodial character, thus resembling those at the leading edge where Ena levels are also high (Fig- ure 3.7C, red arrow). These data are consistent with the hypothesis that Ena can alter Dia activity *in vivo*.

Ena Rescues Dia∆DAD-Induced Defects in Filopodia Number, Actin Bundle Formation, and Migration Speed in Hemocytes

Dorsal closure is driven by a sheet of planar polarized adherent and collectively migrating epithelial cells, which are distinct from the D16 cells we used as a model. To test whether Ena:Dia interactions play a role in other tissues *in vivo*, we examined Drosophila hemocytes, immune cells roughly analogous to macrophages. These cells undergo stereotypical migration throughout the embryo and exhibit chemotactic migration to wounds (Wood and Jacinto, 2007). Ena promotes filopodia number and length, lamellipodial dynamics, and migration speed in hemocytes (Tucker *et al.*, 2011). However, Dia's role and interaction with Ena remained unclear.

We thus examined whether DiaDDAD can promote filopodia in hemocytes and assessed whether Ena can negatively regulate that activity. We analyzed inflammatory recruitment of hemocytes on the ventral side of stage 15 embryos, comparing wildtype (Figures 3.7E, 3.7E', and 3.7I), Ena overexpression (Figures 3.7F and 3.7F'), DiaDDAD (Figures 3.7G, 3.7G' , 3.7J, and 3.7J'), and DiaDDAD+Ena (Figures 3.7H and 3.7H') hemocytes. Ena overexpression increased filopodia number and migration speed to wounds (Figures 3.7L and 3.7N). Ena also increases actin bundles in hemocyte lamellipodia (Figure 3.7M). DiaDDAD localized to filopodia tips (Figures 3.7J and 3.7J') and increased filopodia number more effectively than Ena (Figure 3.7L), but those filopodia lacked the actin bundles induced by

Ena.

This *in vivo* tissue also allowed us to assess the functional consequences of manipulating Ena and Dia activity. Strikingly, while Ena expression enhanced migration velocity, activated Dia reduced it (Figure 3.7N). Thus, increasing filopodia number alone cannot enhance migration speed, suggesting that Ena-induced bundled actin architecture in lamellipodia might be an important driver of hemocyte migration. Finally, we examined whether coexpressing Ena was sufficient to rescue the DiaDDAD phenotypes. Ena coexpression reduced filopodia number to Ena-only levels (Figure 3.7L), matching our D16 cell results (Figure 3.2L). Inflammatory migration speed was also rescued, with DiaDDAD+Ena hemocytes migrating at speeds similar to those overexpressing Ena alone (Figure 3.7N). Surprisingly, while actin bundles were significantly increased in DiaDDAD+Ena cells, they did not reach wildtype or Ena-only numbers (Figure 3.7M), suggesting that a few actin bundles are sufficient to drive migration or that they only function minimally to promote migration speed. Together with our dorsal closure work, these data support the idea that Ena can negatively regulate Dia *in vivo* to control cell protrusions and migration during morphogenesis.

Discussion

As actin regulator functions become clearer, we must address how they work in parallel or together in vivo. Ena and Dia provide a superb model; both are key actin regulators that facilitate processive unbranched actin filament assembly, and our work in vivo suggests they work together to promote protrusions during embryogenesis via a complex mechanism. We used an interdisciplinary approach to explore how Ena and Dia's biochemical properties and direct interaction shape their effects on actin dynamics and cell behavior *in vivo.*

Since Ena and Dia both promote unbranched actin polymerization, we first asked why cells use two similar machines. We found both Ena and Dia promote filopodia in cell culture, but Ena- and Dia-driven filopodia had substantially different morphology and dynamics. Our data suggest these differences reflect distinct biochemical properties. Dia is a faster and more processive elongator than Ena, helping explain why Dia-based filopodia are more persistent

and Ena-based protrusions more dynamic. Ena and Dia may also elongate filaments nucleated by different proteins (e.g., Ena elongating Arp2/3 complex-initiated filaments and Dia elongating filaments it nucleated itself; (Chesarone and Goode, 2009). Tuning the balance of Ena and Dia activity helps cells produce different suites of protrusions and diverse cell behaviors (Figure 3.6I).

We next examined how Ena and Dia work together. Our data are consistent with a model in which cells modulate Dia activity through negative regulation by Ena. EnaEVH1 binds to and inhibits Dia actin assembly *in vitro*. Inhibition occurs in the absence of profilin, and Dia's elongation rate and processivity are not affected by EnaEVH1 or EnaDLinker. Instead, we found EnaEVH1 inhibits DiaFH1FH2 nucleation. As VASP's EVH1 binds mDia2's FH2 (F. Gertler, personal communication), this might be a conserved mechanism for inhibiting formins. Since both Ena's EVH1 and Dia's FH1 domains have other partners that are essential for their functions, it will be important to generate mutants specifically blocking Ena:Dia interaction to further test these hypotheses.

How does EnaEVH1 binding inhibit actin nucleation by Dia? Several ‘‘stepping models’’ of formin actin assembly all share a role for conformational changes in the FH2 domain and actin (Paul and Pollard, 2009). One attractive but speculative hypothesis is that EnaEVH1:DiaFH1 binding inhibits conformational changes needed for nucleation and initiation of processive elongation. Indeed, the plant formin AFH1's FH1 domain has a profilin-independent effect on barbed end elongation, likely by affecting FH2 domain conformation (Michelot *et al.*, 2005). Actin may also play a role as DiaFH1FH2 is recruited to EnaEVH1- induced actin puncta seen in our TIRF assays, suggesting that EnaEVH1-actin association might stabilize Dia binding or help block nucleation. It will be important to examine how all three proteins interact to regulate Dia activity as part of a broader effort to determine mechanisms by which Ena inhibits Dia.

How does Ena regulation of Dia control cell protrusions? In TIRF, we observed that DiaFH1FH2 accumulated at EnaEVH1- dependent actin puncta, but could escape and elongate filaments (Figures 3.6G and 3.6H). Such an inhibitory mechanism might allow

quick modulation of active Dia, allowing it to be paused and released to promote actin nucleation and long, stable filopodia without multiple rounds of autoinhibition and cortical localization. Second, actin and nucleation promoting factors (NPFs) can bind formin DADs to enhance actin assembly (Moseley *et al.*, 2004; Okada *et al.*, 2010; Gould *et al.*, 2011; Graziano *et al.*, 2011; Heimsath and Higgs, 2012; Jaiswal *et al.*, 2013) ; Breitsprecher et al., 2012. Ena inhibition might counterbalance this mechanism by blocking Dia nucleation or interfering with the ‘‘rocket launcher’’ mechanism. Examining whether the DAD domain also modulates interactions among Ena, Dia, and actin will be important to further elucidate this negative regulatory interaction.

Our studies provide a foundation for future work, both *in vitro* and *in vivo*. For example, studying Ena and Dia with NPFs in vitro will be crucial to understanding mechanisms controlling the broad network of actin regulators. It will also be important to expand this work in vivo. Our mechanistic data support a model in which Ena and Dia play distinct roles when acting alone or together. In the simplest version of our model, Ena inhibits Dia, allowing cells to switch from long, persistent protrusions to a more dynamic mix of lamellipodia and filopodia. This fits well with our data in D16 cells and also helps explain what we observed in hemocytes *in vivo*; however, these may represent relatively simple systems, as our data and earlier work (Tucker *et al.*, 2011; Tsygankov *et al.*, 2014) suggest Ena plays the primary role in these cells. This model does not fully explain results observed in more complex tissues like leading edge cells during dorsal closure. In these cells, Ena and Dia are both required for the proper balance of filopodia and lamellipodia that ensures dorsal closure, and relative levels of Ena and Dia activity help regulate this balance (Gates *et al.*, 2007; Homem and Peifer, 2009). Some features of leading edge cell behavior fit our simplest model, e.g., Ena overexpression reduces the number of filopodia induced by DiaDDad and reducing Ena levels increases DiaDDAD-induced filopodia, consistent with a negative regulatory role of Ena *in vivo* (Homem and Peifer, 2009). However, in this complex environment we observed other effects not predicted by our simplest model, e.g., coexpressing Ena and DiaDDad significantly increased lamellipodial area (Homem and

Peifer, 2009). These complexities likely reflect the presence and activity of other players like the Arp2/3 complex, which may compete with Ena and Dia for a limiting pool of actin. Ena may also be channeled away from Dia and to the ends of Arp2/3 generated branches. It will be important to examine how Ena and Dia are integrated with other actin regulators during dorsal closure.

Dorsal closure also provides a place to examine mechanisms driving polarized protrusive behavior. The restriction of filopodia to the dorsal side of leading edge cells is due in part to limited Dia activation, as activated Dia induces filopodia on all surfaces of all epidermal cells. Our work suggests that the types of Dia-driven protrusions are regulated by the localization of endogenous Ena. At places with low cortical Ena like lateral cell borders, Dia induces long-lived filopodia emerging from the cell body. In contrast, at dorsal cell borders, where Ena is enriched, activated Dia induces a dynamic mix of lamellipodia and filopodia like those at the leading edge. These data are consistent with the idea that polarized Ena localization and localized Dia activation help regulate leading edge polarization and protrusion dynamics. It will be exciting to define mechanisms leading to this asymmetry.

Material and Methods

Cell Analysis

D16C3 cells were cultured in Schneider's Media+FBS+insulin, transfected with FugeneHD, and imaged on glass-bottom dishes after 48–72 hr every 2 s for 2–6 min on a Wallac Ultraview Confocal. Expressing tagged proteins versus endogenous shows Ena is $3-fold overexpressed (24% transfected cells) and Dia is $30-fold overexpressed (16% transfected cells; Figure S1F). For fixed images, cells were plated on coverslips, fixed with 32% paraformaldehye solution (EM Sciences) diluted to 10% in PBS, and stained for Ena, Dia, or tetrarhodamine-isothiocyanate-phalloidin. Antibodies are in Supplemental Experimental Procedures. ImageJ (National Institutes of Health) was used to adjust brightness/contrast. We quantified >60 fr from 11–35 cells using CellGeo (number/length) or manually (lifetime/persistence). Filopodia definition was >1 mm long and <0.77 mm wide.

Protein Purification

Dia or Ena were induced with 0.5 mM isopropylthio-b-galactoside (IPTG) for 16 hr at 16_C and purified from Talon Metal Affinity Resin. Ena was gel purified on S20010/300GL and Dia was dialyzed against formin buffer and stored at _80_C. SNAP tagging used SNAPtag-T7-2(NEB) with a flexible linker (GGSGGS) between tag and start codon, and labeling was per manufacturer.

TIRF

Images were collected every 2–4 s with an iXon electron-multiplying charge- coupled device (CCD) camera (Andor) on an Olympus IX-71 microscope with through-the-objective TIRF. Mg-ATP-actin (15% Oregon green) was mixed with 2XTIRF buffer and Ena or Dia ± 3.0 mM profilin, and imaged in a flow cell at 23_C. Biotinylated SNAP-tagged proteins were labeled with streptavidin-conjugated QDs. Ena or Dia were tracked manually for barbed end residence times. Filament elongation rates were calculated by measuring filament length over time in ImageJ. Nucleation was calculated as in Higgs et al. (1999). Curve fits and plots were generated with KaleidaGraph.

Fluorescence Spectroscopy

Pyrene-actin fluorescence was measured with Safire2 fluorescent plate reader. The 10% pyrene-labeled Mg-ATP-actin monomer assembly was initiated by adding 50 mM KCl, 1 mM MgCl2, 1 mM EGTA, 10 mM imidazole pH 7.0, and Ena/Dia constructs.

Yeast Two-Hybrid

Yeast two-hybrid used the LexA system and LacZ reporter strain EGY48. Constructs were tested pairwise for growth in selective media and in liquid b-galactosidase (bgal) assays. Bait constructs with activation domain alone were controls. Greater than or equal to three assays were performed per bait-prey pair.

GST Pull-Down

N-terminally GST-tagged or maltose binding protein (MBP)-tagged proteins in BL-21 cells were induced by 0.5 mM IPTG and grown overnight at 18_C, and lysates were incubated with glutathione-Sepharose-4B for 2 hr at 4_C. Supernatants and bead eluates were analyzed by SDS-PAGE and Coomassie, or Dia immunoblot. For pull-downs with purified proteins, DiaFH1-Cterm and glutathione-Sepharose bead concentrations were kept constant and increasing amounts of GST-EVH1 were added, incubated for 20 min at 25_. Supernatants were analyzed by SDS-PAGE, and the bound faction of DiaFH1-Cterm was fit to a quadratic equation to give the equilibrium dissociation constant.

Drosophila

Stocks are in Supplemental Experimental Procedures. Dorsal closure images were acquired every 5 s using 100X1.4NA PlanApoVC objective on a TE2000-E microscope (Nikon) with a VTHawk (VisiTech) and OrcaR2 CCD camera (Hammamatsu). GFPexpressing hemocytes images were acquired every 1 min for 1 hr postwounding on a spinning disc confocal (PerkinElmer). ImageJ was used for filopodia quantification and to track hemocytes. Hemocyte morphology, filopodia, and actin bundles were quantified from still images of LifeAct-expressing hemocytes.

Statistical Analysis

Statistical comparisons were done by Student's t test (Figures 3.2, 3.5, 3.7K, 7N, and S1) or Mann Whitney U test (Figures 3.4, 3.7L, and 7M).

Supplemental Information

Supplemental Information includes Supplemental Experimental Procedures, four figures, one table, and seven movies and can be found with this article online at http://dx.doi.org/10.1016/j.devcel.2014.01.015.

Aknowledgements

We thank S. Rogers, the Drosophila Genomics Resource Center, J. Dangl, S. Wasserman, S. Bogdan, P. Martin, and B. Stramer for reagents; P. Maddox and T. Salmon for microscopy

help; Johanna Bischof and Philippa Tucker for initial hemocyte work; Andrea Brady and Kyle Smith for technical help; and K. Slep, D. Applewhite, A. Fanning, J. Bear, and the Peifer laboratory for discussions. This work was supported by NIH R01GM47857 (to M.P.); R01GM0079265 and ACS RSG-11-126-01-CSM (to D.R.K.); R01GM079271, NCI 200079604, and the Army Research Office (to T.C.E.); and the Wellcome Trust (to W.W.). C.G.B. was supported by NIH 5T32HD046369 and J.D.W. by GM007183.

Figure 3.1

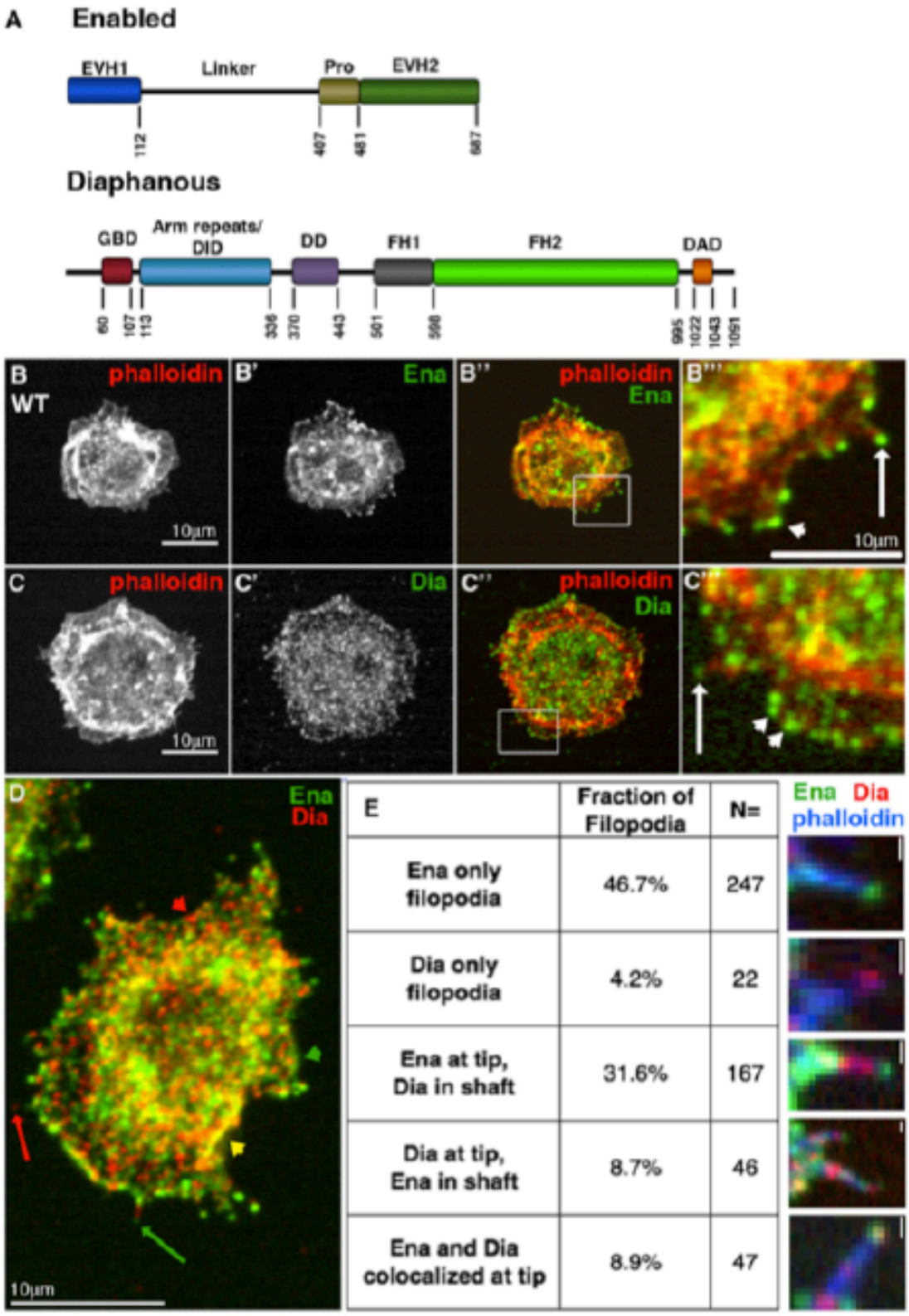
A
Enabled
EVH1
Linker
Pro
EVH2
112
407
481
687
Diaphanous
GBD
Arm repeats/ DID
DD
FH1
FH2
DAD
60
107
113
336
370
443
501
598
995
1022
1043
1091
B
WT
phalloidin
10µm
B'
Ena
B''
phalloidin
Ena
B'''
10µm
C
phalloidin
10µm
C'
Dia
C''
phalloidin
Dia
C'''
D
Ena
Dia
10µm
E
Fraction of Filopodia
N=
Ena only filopodia
46.7%
247
Dia only filopodia
4.2%
22
Ena at tip, Dia in shaft
31.6%
167
Dia at tip, Ena in shaft
8.7%
46
Ena and Dia colocalized at tip
8.9%
47
Ena Dia
phalloidin

Figure 3.1. Endogenous Ena and Dia in D16 Cells
(A) Drosophila Ena and Dia. (B–E) Drosophila D16 cells; arrows, filopodia; whitearrowheads, lamellipodia.

Figure 3.2

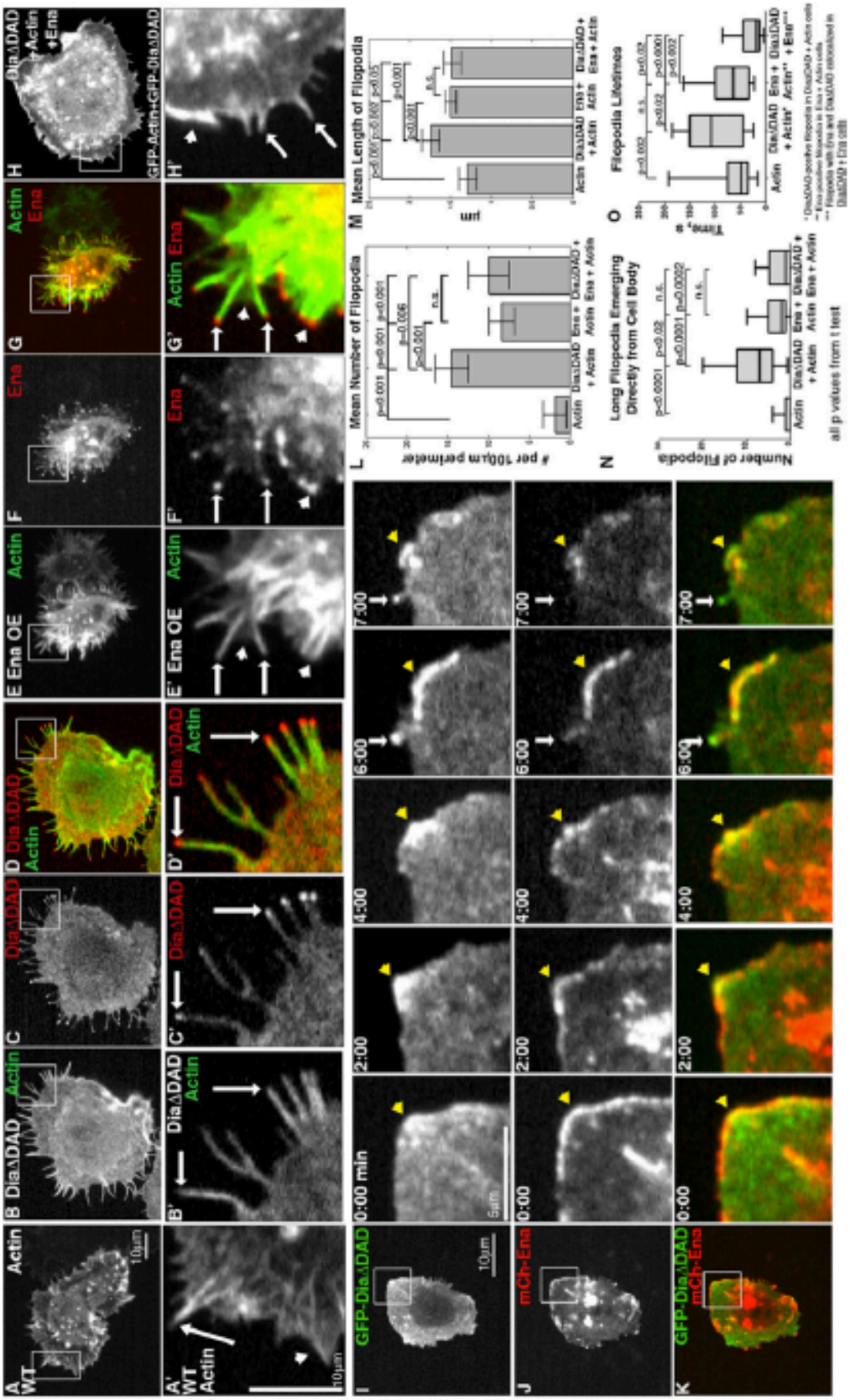
A WT Actin
B DiaΔDAD Actin
C DiaΔDAD
D DiaΔDAD Actin
E Ena OE Actin
F Ena
G Actin Ena
H DiaΔDAD +Actin +Ena
A' WT Actin
B' DiaΔDAD Actin
C' DiaΔDAD
D' DiaΔDAD Actin
E' Ena OE Actin
F' Ena
G' Actin Ena
H' GFP-Actin-GFP-DiaΔDAD
10μm
I GFP-DiaΔDAD
J mCh-Ena
K GFP-DiaΔDAD mCh-Ena
0:00 min
2:00
4:00
6:00
7:00
5μm
L Mean Number of Filopodia
per 100μm perimeter
Actin
DiaΔDAD
DiaΔDAD + Actin
Ena + Actin
DiaΔDAD Ena + Actin
M Mean Length of Filopodia
μm
N Long Filopodia Emerging Directly from Cell Body
Number of Filopodia
O Filopodia Lifetimes
Time, s
Actin
DiaΔDAD
DiaΔDAD + Actin*
Ena + Actin
DiaΔDAD Ena + Actin*
Actin
DiaΔDAD
Ena + Actin
DiaΔDAD Ena + Actin*
Actin
DiaΔDAD
Ena + Actin
DiaΔDAD Ena + Actin*
all p values from t test

Figure 3.2. Ena and Activated Dia Coexpression Drives Protrusion Dynamics Distinct from Either Alone. (A–O) D16 cells: arrows, filopodia; white arrowheads, lamellipodia; yellow arrowheads, Ena and Dia cortical colocalization. Transfection efficiency ranged from 10%–25% and expression levels were variable. Cells with midrange expression were used for all experiments. (A–H') D16 cells (Movie S1) expressing GFP-actin (A and A'), GFPDiaDDAD+ RFP-actin (B–D'), mCh-Ena+GFP-actin (E–G'), or GFP-DiaDDAD+mCh-Ena+GFP- actin (H and H'). (I–K) Movie stills of GFP-DiaDDAD (I and K) + mCh-Ena (J and K; Movie S3). Arrowhead, cortical colocalization in region without filopodia; white arrows, DiaDDAD only filopodium. (L and M) Mean filopodia number (L) and length (M) for Actin (n = 16), DiaDDAD (n = 34), Ena (n = 31), or DiaDDAD+Ena (n = 28). Error bars = 95% confidence interval. (N) The 95th percentile box and whisker plot, number of long filopodia (>1.5 mm) emerging from the cell body (actin, n = 11; DiaDDAD, n = 30; Ena, n = 31; DiaDDAD+Ena, n = 16). (O) Filopodia lifetimes (actin, n = 34; DiaDDAD, n = 31; Ena, n = 33; DiaDDAD+Ena, n = 14). See also Figure S1 and Movies S1, S3, and S4.

Figure 3.3

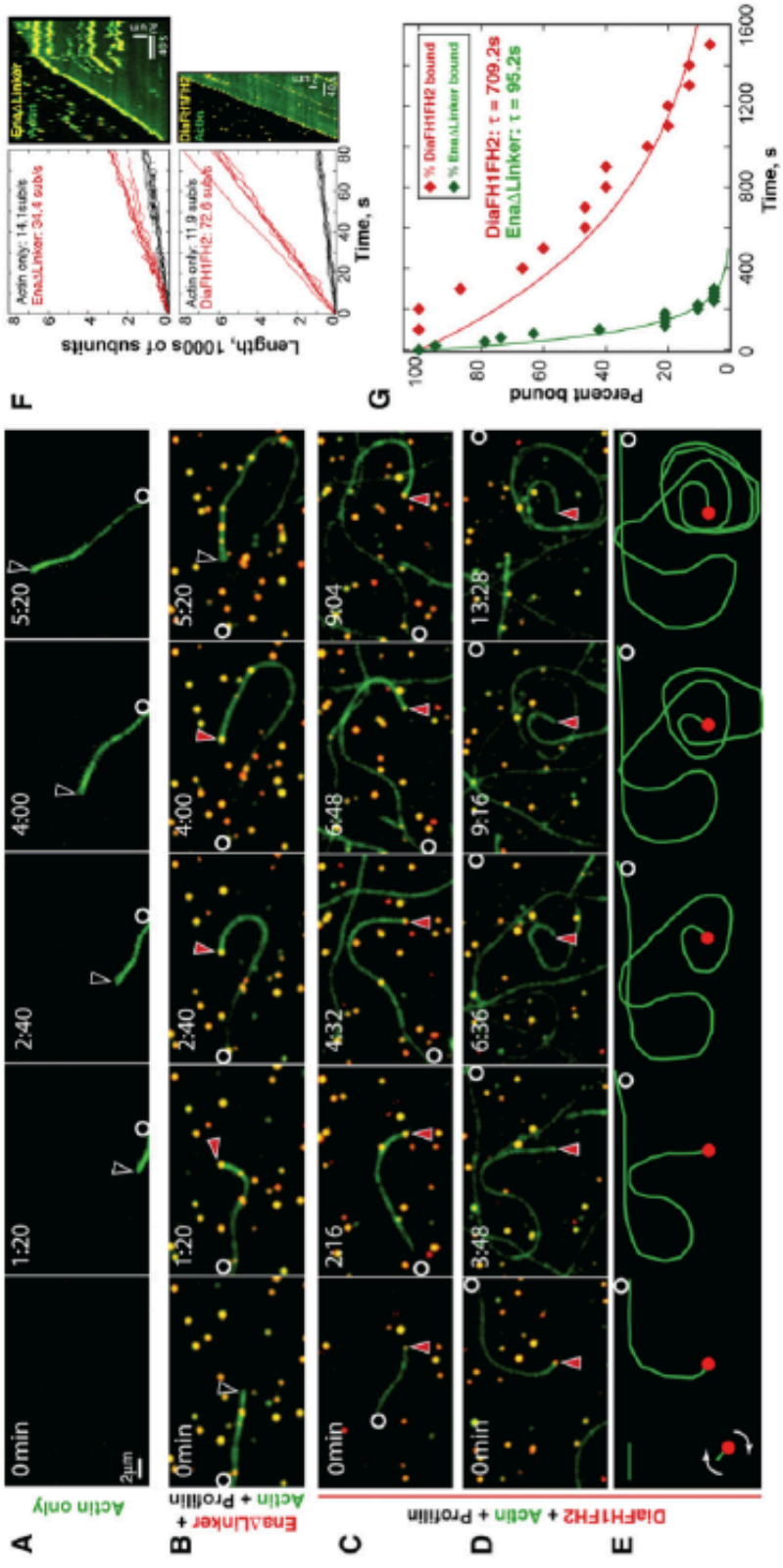
A
Actin only
0min
1:20
2:40
4:00
5:20
2μm
B
EnaΔLinker + Profilin + Actin
0min
1:20
2:40
4:00
5:20
C
DiaFH1FH2 + Profilin + Actin
0min
2:16
4:32
6:48
9:04
D
0min
3:48
6:36
9:16
13:28
E
F
Length, 100s of subunits
Actin only: 14.1subs/s
EnaΔLinker: 34.4 subs/s
Actin only: 11.9 subs/s
DiaFH1FH2: 72.6 subs/s
Time, s
G
Percent bound
% DiaFH1FH2 bound
% EnaΔLinker bound
DiaFH1FH2: τ = 709.2s
EnaΔLinker: τ = 95.2s
Time, s

Figure 3.3. Dia Is a Faster Elongator and Is More Processive than Ena.(A–D) TIRF montages, Movie S2: Oregon-green-labeled actin alone (A). Actin and Drosophila profilin with QD-biotin-SNAP-EnaDLinker (B) or QD-biotin-SNAP- DiaFH1FH2 (C and D). Circles, filament pointed end; arrows, free filament barbed ends (open) or with EnaDLinker or DiaFH1FH2 (red). QD blinks off in (D), but DiaFH1FH2 is present. (E) Filament in (D) traced (green); QD (red). (F) Filament elongation rates for controls (QDfree, black), EnaDLinker (top left, red), or DiaFH1FH2 (bottom left, red). Representative kymographs (right) show single filaments with EnaDLinker (top) or DiaFH1FH2 (bottom) processively bound to barbed end. Scale bars represent 2 mm (vertical) and 40 s (horizontal). (G) Single exponential fit of percent bound versus time gives mean residence time (t) for DiaFH1FH2 (red) and EnaDLinker (green). See also Figure S2 and Movie S2.

Figure 3.4

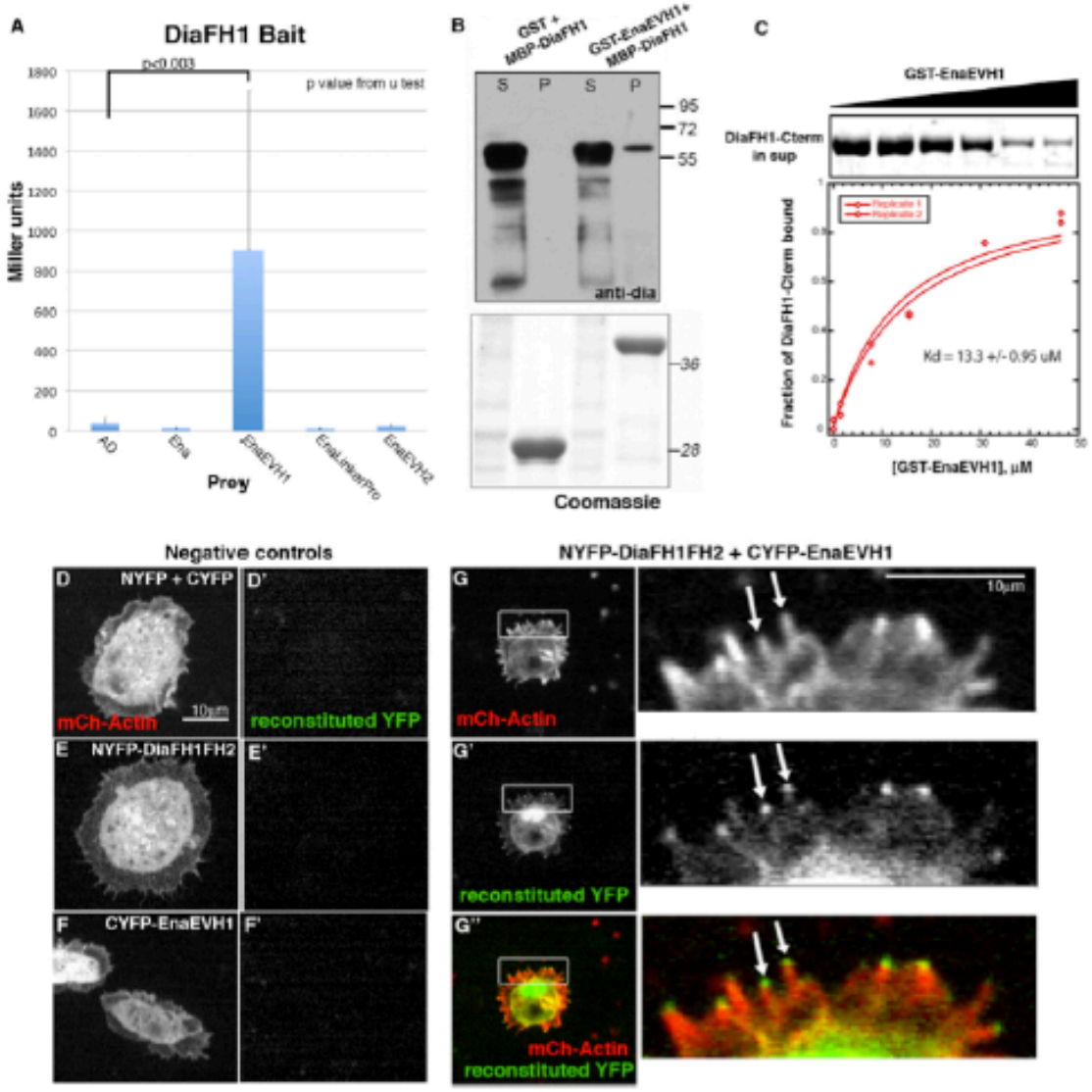

Figure 3.4. Ena and Dia Directly Bind and Interact in D16 Cells. (A) Yeast two-hybrid bgal assays with DiaFH1 bait. Mean Miller units ± SD. (B) Top: GST-EnaEVH1 pulls down MBP-DiaFH1; S, supernatant; p, pellet. Bottom: Coomassie verifying equal loading. (C) Purified DiaFH1-Cterm is pulled down by GST-EnaEVH1. Top: Coomassie stained gel of DiaFH1-Cterm recruitment from supernatant with increasing concentrations of GSTEnaEVH1. Bottom: plot of dependence of DiaFH1-Cterm bound over a range of GSTEnaEVH1 concentrations. Average equilibrium dissociation constant = 13.3 mM. (D–G'') Split YFP in D16 cells. mCh-Actin (D, E, F, G) and reconstituted YFP fluorescence (D', E', F', and G') in NYFP+CYFP (D and D'), NYFP-DiaFH1FH2 alone (E and E'), CYFPEnaEVH1 alone (F and F'), and NYFP-DiaFH1FH2+CYFP-EnaEVH1 (G–G''). Arrows in inset, YFP at filopodia tips. See Table S1.

Figure 3.5

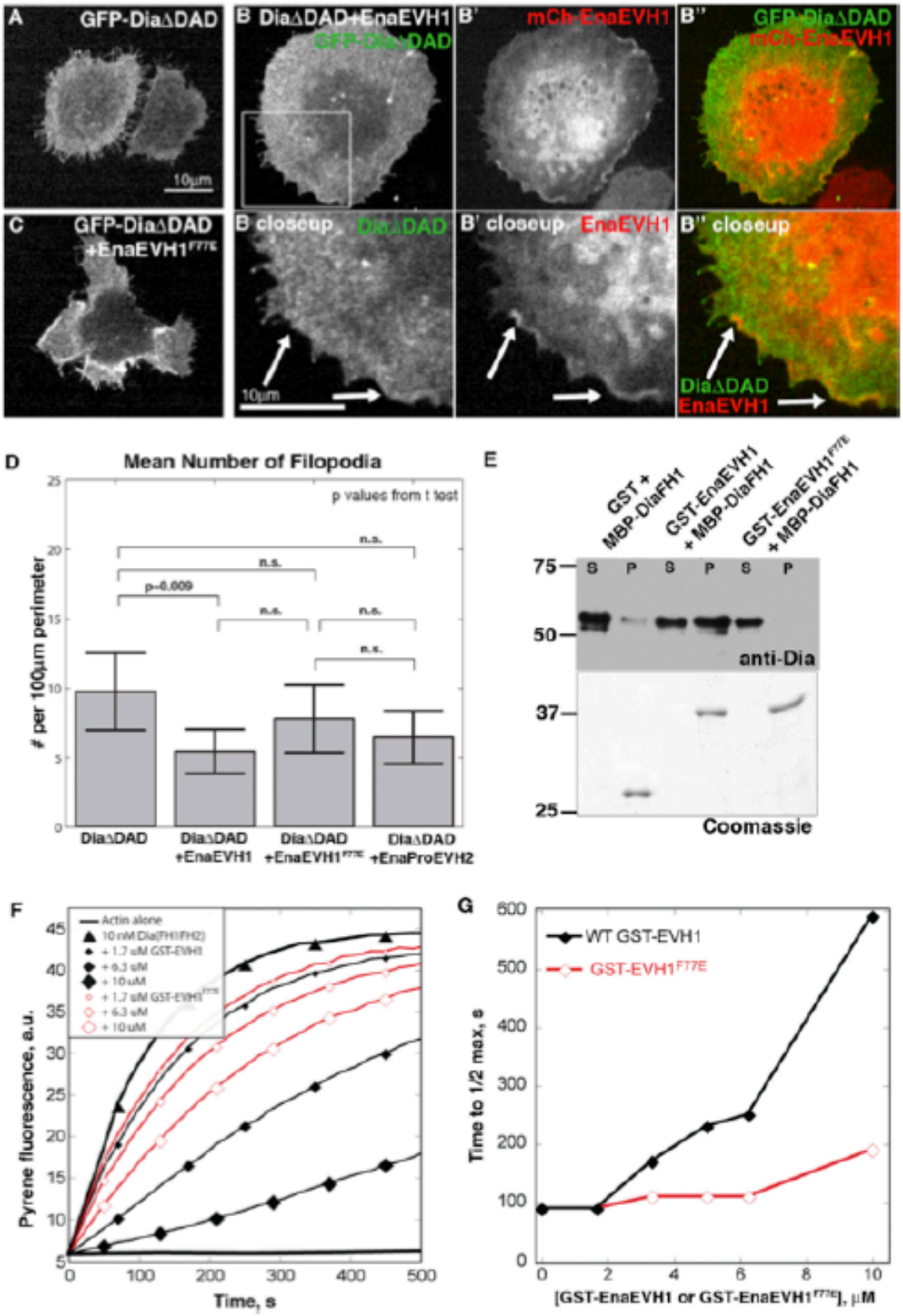
A
GFP-DiaΔDAD
10μm
B DiaΔDAD+EnaEVH1
GFP-DiaΔDAD
B'
mCh-EnaEVH1
B''
GFP-DiaΔDAD
mCh-EnaEVH1
C
GFP-DiaΔDAD
+EnaEVH1F77E
B closeup
DiaΔDAD
10μm
B' closeup
EnaEVH1
B'' closeup
DiaΔDAD
EnaEVH1
D
Mean Number of Filopodia
p values from t test
# per 100μm perimeter
p=0.009
n.s.
DiaΔDAD
DiaΔDAD +EnaEVH1
DiaΔDAD +EnaEVH1F77E
DiaΔDAD +EnaProEVH2
E
GST + MBP-DiaFH1
GST-EnaEVH1 + MBP-DiaFH1
GST-EnaEVH1F77E + MBP-DiaFH1
75
50
37
25
S
P
anti-Dia
Coomassie
F
Actin alone
10 nM Dia(FH1FH2)
+ 1.7 uM GST-EVH1
+ 6.3 uM
+ 10 uM
+ 1.7 uM GST-EVH1F77E
+ 6.3 uM
+ 10 uM
Pyrene fluorescence, a.u.
Time, s
G
WT GST-EVH1
GST-EVH1F77E
Time to 1/2 max, s
[GST-EnaEVH1 or GST-EnaEVH1F77E], μM

Figure 3.5. EnaEVH1 is Sufficient to Reduce Dia-Driven Filopodia. (A–C) D16 cells with GFP-DiaDDAD alone (A), GFP-DiaDDAD (B, B00, and B closeup) + mCh-EnaEVH1 (B', B'', and B' closeup), or GFP-DiaDDAD+mCh- EnaEVH1F77E (C). Arrows, cortical EnaEVH1. (D) Mean filopodia number, DiaDDAD alone (n = 27), DiaDDAD+EnaEVH1 (n = 28), DiaDDAD+EnaEVH1F77E (n = 26), and GFP-DiaDDAD+EnaProEVH2 (n = 29); error bars = 95% confidence interval. (E) GST pull-down of DiaFH1 by GST, GSTEnaEVH1, or GST-EnaEVH1F77E. S, supernatant; p, pellet. Bottom: Coomassie verifying equal load. (F) Pyrene actin assembly with profilin and 10 nM DiaFH1FH2 (triangles), plus GST-EnaEVH1 (black diamonds) or GST-EnaEVH1F77E (red diamonds). (G) Time it takes 10 nM DiaFH1FH2 to stimulate 1/2 max steady-state pyrene fluorescence (maximum actin assembly) versus concentration of GST-EVH1 constructs. See Figure S3.

Figure 3.6

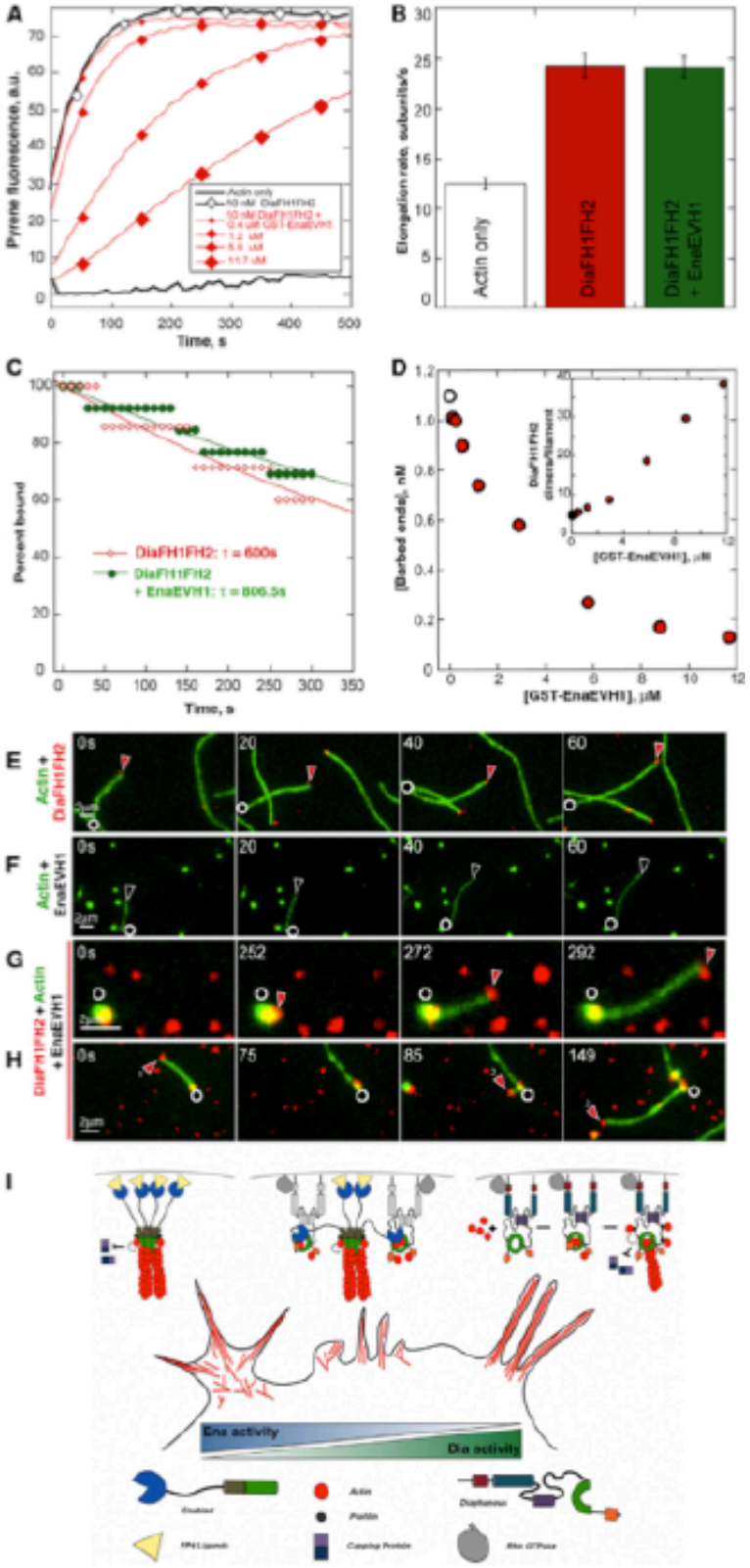
A
Pyrene fluorescence, a.u.
Time, s
Actin only
10 nM DiaFH1FH2
10 nM DiaFH1FH2 +
0.4 uM GST-EnaEVH1
1.2 uM
5.5 uM
11.7 uM
B
Elongation rate, subunits/s
Actin only
DiaFH1FH2
DiaFH1FH2
+ EnaEVH1
C
Percent bound
Time, s
DiaFH1FH2: τ = 600s
DiaFH1FH2
+ EnaEVH1: τ = 806.5s
D
[Barbed ends], nM
[GST-EnaEVH1], μM
DiaFH1FH2
dimers/Filament
E
Actin +
DiaFH1FH2
F
Actin +
EnaEVH1
G
DiaFH1FH2 + Actin
+ EnaEVH1
H
I
Ena activity
Dia activity
Actin
Profilin
Capping Protein
Diaphanous

Figure 3.6. EnaEVH1 Inhibits Dia Nucleation. All assays without profilin. (A) Pyrene actin assembly; 10 nM DiaFH1FH2+increasing GST-EnaEVH1. (B) Actin elongation rates calculated from TIRF. Actin alone (white), actin+DiaFH1FH2 (red), or actin+DiaFH1FH2+ GST-EnaEVH1(green); n = 2; error bars = ±SEM. (C) Percent of barbed ends remaining bound to SNAP-549- DiaFH1FH2 in absence (red) or presence (green) of 5 mM GSTEnaEVH1. Single exponential fits show mean resi- dence time (t). (D) DiaFH1FH2 nucleation calculated from pyrene assays in (A). Concentration of barbed ends nucleated by 10 nM DiaFH1FH2 in the absence (white) or increasing concen- trations of GST-EnaEVH1 (red). Inset: mean number of DiaFH1FH2 dimers required to nucleate a filament in the absence or presence of increasing GST-EnaEVH1. (E–H) TIRF montages: 1.5 mM Oregongreen actin with SNAP-549-DiaFH1FH2 (red) (E), GST-EnaEVH1 (F), or GST-EnaEVH1 and SNAP-549-DiaFH1FH2 (G and H) (Movie S5); circles, filament pointed end; arrows, free filament barbed ends (open) or with DiaFH1FH2 (red). (I) Model of Ena inhibition of Dia and effects on protrusions. See also Figure S4 and Movie S5.

Figure 3.7

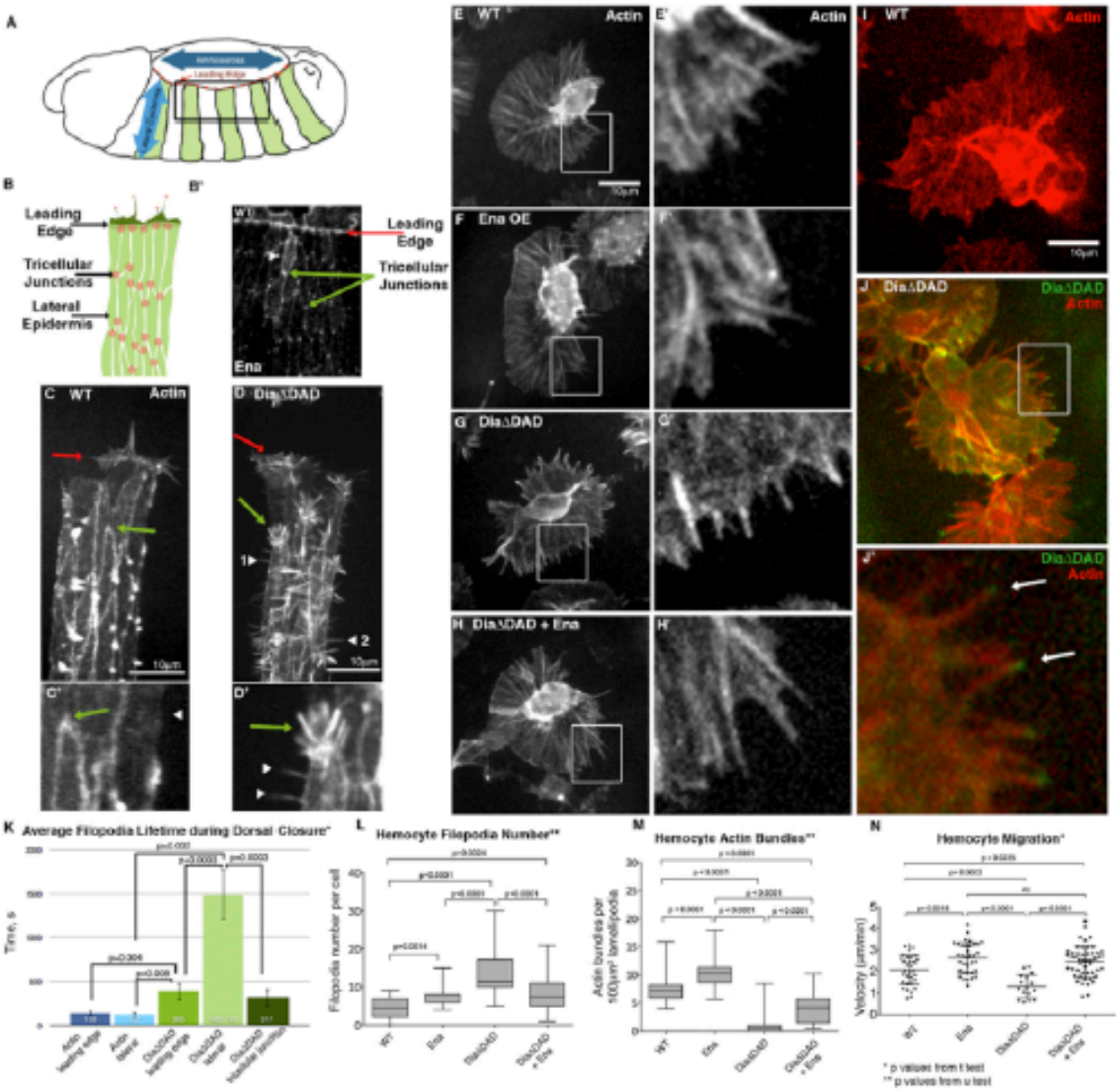

Figure 3.7. Ena Negatively Regulates Activated Dia during Drosophila Development (A) Dorsal closure; green stripes, enGAL4-driven Actin-expressing epidermis in (C)–(D'). (B) Single Actin-expressing stripe with leading edge protrusions (dark green), lateral epidermis (light green), and high Ena localization (red). (B') Ena staining at leading edge (red arrow), lateral cell border (white arrowhead), and tricellular junctions (green arrows). (C–D') Dorsal closure imaged by GFP-Actin for wild-type (C and C') (Movie S6) and DiaDDAD (D and D') (Movie S7). Leading edge, red arrows; tricellular junctions, green arrows; lateral cell borders, white arrowheads. (E–H') F-actin (LifeActGFP) in wild-type (E and E'), Ena (F and F'), DiaDDAD (G and G'), and DiaDDAD+Ena (H and H') hemocytes. (I–J') F-actin (mCh-Moesin) in wild-type (I) or GFP-DiaDDAD-expressing (J and J') hemocytes. DiaDDAD at filopodia tips (arrows). (K) Mean filopodia lifetime: actin leading edge, n = 95; actin lateral, n = 28; DiaDDAD leading edge, n = 140; DiaDDAD lateral, n = 110; and DiaDDAD tricellular junctions, n = 68. Error bars ± SEM. (L and M) Number of hemocyte filopodia and actin bundles: wild-type, n = 34; Ena, n = 37; DiaDDAD, n = 36; DiaDDAD+Ena, n = 38. Median and interquartile range. (N) Hemocyte migration speed: wild-type, n = 34; Ena, n = 35; DiaDDAD, n = 16; DiaDDAD+Ena, n = 50. Mean ± SD. See also Movies S6 and S7.

REFERNCES

Alberts, A. S. (2001). Identification of a carboxyl-terminal diaphanous-related formin homology protein autoregulatory domain. J Biol Chem *276*, 2824–2830.

Applewhite, D. A., Barzik, M., Kojima, S.-I., Svitkina, T. M., Gertler, F. B., and Borisy, G. G. (2007). Ena/VASP proteins have an anti-capping independent function in filopodia Formation. Mol Biol Cell *18*, 2579–2591.

Ball, L. J. *et al.* (2000). Dual epitope recognition by the VASP EVH1 domain modulates polyproline ligand specificity and binding affinity. Embo J *19*, 4903–4914.

Barzik, M., Kotova, T. I., Higgs, H. N., Hazelwood, L., Hanein, D., Gertler, F. B., and Schafer, D. A. (2005). Ena/VASP proteins enhance actin polymerization in the presence of barbed end capping proteins. J Biol Chem *280*, 28653–28662.

Bear, J. E. *et al.* (2002). Antagonism between Ena/VASP proteins and actin filament capping regulates fibroblast motility. Cell *109*, 509–521.

Bear, J. E., and Gertler, F. B. (2009). Ena/VASP: towards resolving a pointed controversy at the barbed end. J Cell Sci *122*, 1947–1953.

Beli, P., Mascheroni, D., Xu, D., and Innocenti, M. (2008). WAVE and Arp2/3 jointly inhibit filopodium formation by entering into a complex with mDia2. Nat Cell Biol *10*, 849–857.

Breitsprecher, D., and Goode, B. L. (2013). Formins at a glance. J Cell Sci *126*, 1–7.
Breitsprecher, D., Kiesewetter, A. K., Linkner, J., Urbanke, C., Resch, G. P., Small, J. V., and Faix, J. (2008). Clustering of VASP actively drives processive, WH2 domain-mediated actin filament elongation. Embo J *27*, 2943–2954.

Chang, F., Drubin, D., and Nurse, P. (1997). cdc12p, a protein required for cytokinesis in fission yeast, is a component of the cell division ring and interacts with profilin. J Cell Biol *137*, 169–182.

Chesarone, M. A., and Goode, B. L. (2009). Actin nucleation and elongation factors: mechanisms and interplay. Curr Opin Cell Biol *21*, 28–37.

Chesarone-Cataldo, M., Guerin, C., Yu, J. H., Wedlich-Soldner, R., Blanchoin, L., and Goode, B. L. (2011). The myosin passenger protein Smy1 controls actin cable structure and dynamics by acting as a formin damper. Dev Cell *21*, 217–230.

DeWard, A. D., Eisenmann, K. M., Matheson, S. F., and Alberts, A. S. (2010). The role of formins in human disease. Biochim Biophys Acta *1803*, 226–233.

Eisenmann, K. M., Harris, E. S., Kitchen, S. M., Holman, H. A., Higgs, H. N., and Alberts, A. S. (2007). Dia-interacting protein modulates formin-mediated actin assembly at the cell cortex. Curr Biol *17*, 579–591.

Gates, J., Mahaffey, J. P., Rogers, S. L., Emerson, M., Rogers, E. M., Sottile, S. L., Van Vactor, D., Gertler, F. B., and Peifer, M. (2007). Enabled plays key roles in embryonic epithelial morphogenesis in Drosophila. Development *134*, 2027–2039.

Gertler, F. B., Doctor, J. S., and Hoffmann, F. M. (1990). Genetic suppression of mutations in the Drosophila abl proto-oncogene homolog. Science *248*, 857–860.

Gertler, F. B., Niebuhr, K., Reinhard, M., Wehland, J., and Soriano, P. (1996). Mena, a relative of VASP and Drosophila Enabled, is implicated in the control of microfilament dynamics. Cell *87*, 227–239.

Gorelik, R., Yang, C., Kameswaran, V., Dominguez, R., and Svitkina, T. (2011). Mechanisms of plasma membrane targeting of formin mDia2 through its amino terminal domains. Mol Biol Cell *22*, 189–201.

Gould, C. J., Maiti, S., Michelot, A., Graziano, B. R., Blanchoin, L., and Goode, B. L. (2011). The formin DAD domain plays dual roles in autoinhibition and actin nucleation. Curr Biol *21*, 384–390.

Graziano, B. R., DuPage, A. G., Michelot, A., Breitsprecher, D., Moseley, J. B., Sagot, I., Blanchoin, L., and Goode, B. L. (2011). Mechanism and cellular function of Bud6 as an actin nucleation-promoting factor. Mol Biol Cell *22*, 4016–4028.

Grosse, R., Copeland, J. W., Newsome, T. P., Way, M., and Treisman, R. (2003). A role for VASP in RhoA-Diaphanous signalling to actin dynamics and SRF activity. Embo J *22*, 3050–3061.

Grosshans, J., Wenzl, C., Herz, H.-M., Bartoszewski, S., Schnorrer, F., Vogt, N., Schwarz, H., and Muller, H.-A. (2005). RhoGEF2 and the formin Dia control the formation of the furrow canal by directed actin assembly during Drosophila cellularisation. Development *132*, 1009–1020.

Gupton, S. L., and Gertler, F. B. (2007). Filopodia: the fingers that do the walking. Sci STKE *2007*, re5.

Hansen, S. D., and Mullins, R. D. (2010). VASP is a processive actin polymerase that requires monomeric actin for barbed end association. J Cell Biol *191*, 571–584.

Heimsath, E. G., and Higgs, H. N. (2012). The C terminus of formin FMNL3 accelerates actin polymerization and contains a WH2 domain-like sequence that binds both monomers and filament barbed ends. J Biol Chem *287*, 3087–3098.

Higashida, C., Miyoshi, T., Fujita, A., Oceguera-Yanez, F., Monypenny, J., Andou, Y., Narumiya, S., and Watanabe, N. (2004). Actin polymerization-driven molecular movement of mDia1 in living cells. Science *303*, 2007–2010.

Higgs, H. N., Blanchoin, L., and Pollard, T. D. (1999). Influence of the C terminus of Wiskott-Aldrich syndrome protein (WASp) and the Arp2/3 complex on actin polymerization. Biochemistry *38*, 15212–15222.

Holtzman, J. H., Woronowicz, K., Golemi-Kotra, D., and Schepartz, A. (2007). Miniature protein ligands for EVH1 domains: interplay between affinity, specificity, and cell motility. Biochemistry *46*, 13541–13553.

Homem, C. C. F., and Peifer, M. (2008). Diaphanous regulates myosin and adherens junctions to control cell contractility and protrusive behavior during morphogenesis. Development *135*, 1005–1018.

Homem, C. C. F., and Peifer, M. (2009). Exploring the roles of diaphanous and enabled activity in shaping the balance between filopodia and lamellipodia. Mol Biol Cell *20*, 5138–5155.

Jaiswal, R., Stepanik, V., Rankova, A., Molinar, O., Goode, B. L., and McCartney, B. M. (2013). Drosophila homologues of adenomatous polyposis coli (APC) and the formin diaphanous collaborate by a conserved mechanism to stimulate actin filament assembly. J Biol Chem *288*, 13897–13905.

Kerppola, T. K. (2008). Bimolecular fluorescence complementation (BiFC) analysis as a probe of protein interactions in living cells. Annu Rev Biophys *37*, 465–487.

Kovar, D. R., and Pollard, T. D. (2004). Insertional assembly of actin filament barbed ends in association with formins produces piconewton forces. Proceedings of the National Academy of Sciences of the United States of America *101*, 14725–14730.

Kovar, D. R., Harris, E. S., Mahaffy, R., Higgs, H. N., and Pollard, T. D. (2006). Control of the assembly of ATP- and ADP-actin by formins and profilin. Cell *124*, 423–435.

Li, F., and Higgs, H. N. (2003). The mouse Formin mDia1 is a potent actin nucleation factor regulated by autoinhibition. Curr Biol *13*, 1335–1340.

Massarwa, R., Schejter, E. D., and Shilo, B.-Z. (2009). Apical secretion in epithelial tubes of the Drosophila embryo is directed by the Formin-family protein Diaphanous. Dev Cell *16*, 877–888.

Michelot, A., Guerin, C., Huang, S., Ingouff, M., Richard, S., Rodiuc, N., Staiger, C. J., and Blanchoin, L. (2005). The formin homology 1 domain modulates the actin nucleation and bundling activity of Arabidopsis FORMIN1. Plant Cell *17*, 2296–2313.

Moseley, J. B., Sagot, I., Manning, A. L., Xu, Y., Eck, M. J., Pellman, D., and Goode, B. L. (2004). A conserved mechanism for Bni1- and mDia1-induced actin assembly and dual regulation of Bni1 by Bud6 and profilin. Mol Biol Cell *15*, 896–907.

Okada, K., Bartolini, F., Deaconescu, A. M., Moseley, J. B., Dogic, Z., Grigorieff, N., Gundersen, G. G., and Goode, B. L. (2010). Adenomatous polyposis coli protein nucleates actin assembly and synergizes with the formin mDia1. J Cell Biol *189*, 1087–1096.

Otomo, T., Otomo, C., Tomchick, D. R., Machius, M., and Rosen, M. K. (2005). Structural basis of Rho GTPase-mediated activation of the formin mDia1. Mol Cell *18*, 273–281.

Paul, A. S., and Pollard, T. D. (2009). Review of the mechanism of processive actin filament elongation by formins. Cell Motil Cytoskeleton *66*, 606–617.

Paul, A. S., Paul, A., Pollard, T. D., and Pollard, T. (2008). The role of the FH1 domain and profilin in formin-mediated actin-filament elongation and nucleation. Curr Biol *18*, 9–19.

Philippar, U. *et al.* (2008). A Mena invasion isoform potentiates EGF-induced carcinoma cell invasion and metastasis. Dev Cell *15*, 813–828.

Pruyne, D., Evangelista, M., Yang, C., Bi, E., Zigmond, S., Bretscher, A., and Boone, C. (2002). Role of formins in actin assembly: nucleation and barbed-end association. Science *297*, 612–615.

Romero, S., Le Clainche, C., Didry, D., Egile, C., Pantaloni, D., and Carlier, M.-F. (2004). Formin is a processive motor that requires profilin to accelerate actin assembly and associated ATP hydrolysis. Cell *119*, 419–429.

Rose, R., Weyand, M., Lammers, M., Ishizaki, T., Ahmadian, M. R., and Wittinghofer, A. (2005). Structural and mechanistic insights into the interaction between Rho and

mammalian Dia. Nature *435*, 513–518.

Schirenbeck, A., Arasada, R., Bretschneider, T., Stradal, T. E. B., Schleicher, M., and Faix, J. (2006). The bundling activity of vasodilator-stimulated phosphoprotein is required for filopodium formation. Proceedings of the National Academy of Sciences of the United States of America *103*, 7694–7699.

Schirenbeck, A., Bretschneider, T., Arasada, R., Schleicher, M., and Faix, J. (2005). The Diaphanous-related formin dDia2 is required for the formation and maintenance of filopodia.Nat Cell Biol *7*, 619–625.

Tsygankov, D., Bilancia, C. G., Vitriol, E. A., Hahn, K. M., Peifer, M., and Elston, T. C. (2014). CellGeo: a computational platform for the analysis of shape changes in cells with complex geometries. J Cell Biol *204*, 443–460.

Tucker, P. K., Evans, I. R., and Wood, W. (2011). Ena drives invasive macrophage migration in Drosophila embryos. Dis Model Mech *4*, 126–134.

Vavylonis, D., Kovar, D. R., O'Shaughnessy, B., and Pollard, T. D. (2006). Model of formin associated actin filament elongation. Mol Cell *21*, 455–466.

Yang, C., Czech, L., Gerboth, S., Kojima, S.-I., Scita, G., and Svitkina, T. (2007). Novel roles of formin mDia2 in lamellipodia and filopodia formation in motile cells. PLoS Biol *5*, e317.

Zigmond, S. H., Evangelista, M., Boone, C., Yang, C., Dar, A. C., Sicheri, F., Forkey, J., and Pring, M. (2003). Formin leaky cap allows elongation in the presence of tight capping proteins. Curr Biol *13*, 1820–1823.

CHAPTER 4: ENABLEDAND DIAPHANOUS EACH DIRECT DISTINCTIVE PROTRUSIVE BEHAVIORS IN NEIGHBORING TISSUE TYPES DURING *DROSOPHILA* DORSAL CLOSURE.

Stephanie H. Nowotarski*, Natalie McKeon*, Rachel J. Moser*

and Mark Peifer*†‡

*Department of Biology

University of North Carolina at Chapel Hill

Chapel Hill, NC 27599-3280

†Lineberger Comprehensive Cancer Center

University of North Carolina at Chapel Hill, Chapel Hill, NC 27599

Preface

Chapter 4 includes my first author paper that is currently accepted with minor revisions at *Molecular Biology of the Cell*, entitled: " Enabled and Diaphanous each direct distinctive protrusive behaviors in neighboring tissue types during *Drosophila* development. This paper built directly off of the work described in the previous chapter as well as on previous work in the lab carried out by Catarina Homem exploring how Ena and Dia shift protrusive behavior along the epidermal leading edge during dorsal closure. I carried out all experimental design, high magnification and bleach movies, all quantification, and wrote the manuscript with Mark Peifer. Natalie McKeon and Rachel Moser were undergraduates working with me who carried out the majority of the low magnification movies for dorsal closure rates.

Abstract

Actin-based protrusions are important for signaling and migration during development and tissue homeostasis. Defining how different tissues craft diverse protrusive behaviors using the same genomic toolkit of actin regulators is a current challenge. The actin elongation factors Diaphanous and Enabled both promote barbed-end actin polymerization, and can stimulate filopodia in cultured cells. However, redundancy in mammals and Diaphanous' role in cytokinesis limited analysis of whether and how they regulate protrusions during development. We use two tissues driving *Drosophila* dorsal closure, migratory leading-edge (LE) and non-migratory amnioserosal (AS) cells, as models to define how cells shape distinct protrusions during morphogenesis. We found the non-migratory AS cells produce filopodia that are morphologically and dynamically distinct from those of LE cells. We hypothesized that differing Enabled and/or Diaphanous activity drive these differences. A combination of gain- and loss-of-function with quantitative approaches revealed Diaphanous and Enabled each regulate filopodial behavior *in vivo* and defined a quantitative "fingerprint", the protrusive profile, characteristic of each actin regulator. Our data suggest LE protrusiveness is primarily Enabled-driven, while Diaphanous plays the primary role in AS filopodial dynamics, and reveal each has roles in dorsal closure, but its robustness ensures timely completion in their absence.

Introduction

From bundled myofibrils in muscle to dynamic filopodia and lamellipodia in migratory axons, proper development requires cells to build distinct actin-based structures. A host of actin regulatory proteins govern the underlying geometries of actin structures, mediating elongation, nucleation, branching, capping and severing (Pollard and Borisy, 2003). Elegant studies have characterized biochemical properties and interactions of these regulators *in vitro* or in simple, single cell systems, but we still lack a clear understanding of how they work together or separately to produce protrusions *in vivo* during development. Filopodia, first

described on neuronal growth cones (Harrison 1910), were historically viewed as sensory structures associated with migratory cell types, helping drive guided cell migration (Wood and Martin, 2002; Gupton and Gertler, 2007). A century later we are still uncovering filopodial roles *in vivo* (Sanders *et al.*, 2013; Roy *et al.*, 2014). Defining the mechanisms by which filopodia are formed within a single cell type and how they differ between different cell types during development remains a key challenge.

Filopodia formation is thought to rely on actin elongation factors such as Diaphanous related formins (DRFs) and Enabled (Ena)/VASP proteins (Michelot and Drubin, 2011). Both protein families bind to actin filament barbed ends to promote polymerization and block capping, and members of both protein families can, when overexpressed or activated in cultured cells or neurons, promote formation of filopodia (Bachmann *et al.*, 1999; Lanier *et al.*, 1999; Rottner *et al.*, 1999; Bear *et al.*, 2002; Svitkina *et al.*, 2003; Lebrand *et al.*, 2004; Barzik *et al.*, 2005; Applewhite *et al.*, 2007; Pasic *et al.*, 2008; Chesarone and Goode, 2009; Hansen and Mullins, 2010) Cell protrusive behavior is crucial in many developmental events (Rørth, 2009) and current models suggest Ena/VASP proteins and DRFs should play key roles in regulating this (Gupton and Gertler, 2007). One puzzle has been why cells have these two different families of actin elongation factors. The roles of Ena/VASP proteins in filopodia formation and protrusive behavior have been confirmed in cell culture and *in vivo* by loss-of-function approaches (Bear *et al.*, 2000; Loureiro *et al.*, 2002; Schirenbeck *et al.*, 2006; Gonçalves-Pimentel *et al.*, 2011). In contrast, while activated DRFs clearly can induce filopodia and localize to their tips (Yang *et al.*, 2007; Block *et al.*, 2008), assessing whether DRFs are essential for protrusive behavior and filopodia during development has been more challenging, due to their conserved roles in cytokinesis and the partial redundancy of mammalian DRFs.

DRFs play a wide variety of roles *in vivo*. They were first identified via their conserved roles in cytokinesis (Castrillon and Wasserman, 1994; Chang *et al.*, 1997; Imamura *et al.*, 1997; Swan *et al.*, 1998; Tominaga *et al.*, 2000; Tolliday *et al.*, 2002; Peng *et al.*, 2003; Echard *et al.*, 2004; Ingouff *et al.*, 2005). Subsequent work in cultured mammalian cells

identified a diverse array of functions, ranging from stress fiber assembly, to coordinating microtubules and actin, to targeted secretion and organelle dynamics, to modulating cell adhesion and phagocytosis (Faix and Grosse, 2006). Knockdown studies clearly implicate DRFs in directional cell migration (Yamana *et al.*, 2006; Gupton *et al.*, 2007; Lai *et al.*, 2008; Shi *et al.*, 2009; Dong *et al.*, 2013; Daou *et al.*, 2014), but, with the exception of work in *Dictyostelium* and *Drosophila* epidermal cells (Schirenbeck *et al.*, 2005; Homem and Peifer, 2009), their roles in protrusive behavior and filopodia formation *in vivo* remain less well established. In cultured cells, mDia1 knockdown reduces filopodia formation induced by IRSp53 or Rif (Goh *et al.*, 2011; Goh and Ahmed, 2012), while mDia2 antibody blockade or knockdown in B16F1 cells reduces both filopodia and lamellipodia (Peng *et al.*, 2003; Yang *et al.*, 2007). The roles of mammalian DRFs in protrusive behavior during development remain even less clear. Mammals have three DRFs, complicating analysis. *mDia1* mutants have immune system defects (Tanizaki *et al.*, 2010), while compound *mDia1; mDia3* mutants have defects in neuronal migration (Thumkeo *et al.*, 2011), and *mDia2* knockout mice have multinucleate erythroblasts (Watanabe *et al.*, 2013). In none of these cases were clear effects on protrusive behavior defined.

Drosophila provides a simple system for studying these proteins, as there is only one Ena/VASP protein, Ena, and one DRF, Diaphanous (Dia). In *Drosophila*, Dia's early role in the modified form of cytokinesis known as cellularization (Afshar *et al.*, 2000; Grosshans *et al.*, 2005) obscured the search for later functions. However, use of RNAi or examination of animals in which maternal protein had run down revealed roles in apical protein secretion in tracheae (Massarwa *et al.*, 2009), cytoskeletal regulation during wound healing (Antunes *et al.*, 2013; Abreu-Blanco *et al.*, 2014), segmental groove formation (Mulinari *et al.*, 2008), and synapse growth (Pawson *et al.*, 2008). However, once again, *in vivo* roles for Ena in protrusive behavior proved more elusive.

Recent work revealed that these two processive actin elongators, Ena and Dia, are biochemically distinct. Dia is a more efficient elongation factor than Ena, being 7x more processive and elongating twice as fast (Bilancia *et al.*, 2014). This difference in biochemical

properties is reflected in the filopodia each stimulates in cell culture, with Dia-driven filopodia having longer lifetimes and Ena-driven filopodia being more dynamic. Further, Ena and Dia directly interact via their EVH1 and FH1 domains, and through this interaction Ena can negatively regulate Dia, most likely at filament initiation (Bilancia *et al.*, 2014). These data suggest there are distinct roles for each of these elongation factors in filopodia. However, we still lack a clear understanding of how actin-elongation proteins work together or separately to initiate and elongate protrusions *in vivo* and how these protrusions contribute to major developmental processes. Our desire to define the roles of Dia in protrusive behavior were further sharpened by the discovery earlier this year of a likely role for Dia in generating cytonemes, "signaling filopodia" whose roles in paracrine signaling are becoming increasingly apparent (Roy *et al.*, 2014).

To study the regulation and roles of protrusive behavior in embryonic development, we use *Drosophila* dorsal closure as a model (Jacinto *et al.*, 2002b; Heisenberg, 2009). During this process, two lateral sheets of epidermal cells move dorsally to meet at the dorsal midline, displacing the central amnioserosal (AS) cells and enclosing the embryo in skin (Figure 1A, B). As closure proceeds, lateral epidermal cells elongate along their dorsal-ventral axes and move towards the midline. Closure is partially powered by an actin-based supracellular cable at the leading edge (LE) of the epidermis, which acts as a purse string to draw the two sheets together (Young *et al.*, 1991; Kiehart *et al.*, 2000; Jacinto *et al.*, 2002a), while the central AS cells undergo waves of apical constriction (Kiehart *et al.*, 2000; Gorfinkiel *et al.*, 2009; Solon *et al.*, 2009), drastically reducing their area. Actin-based protrusions from LE cells play key roles in closure, aligning the two contralateral sheets as they meet at the anterior and posterior canthi (Supplemental Movie 1, Jacinto *et al.*, 2002a; Millard and Martin, 2008). While LE cells are not classical migrating cells, their filopodia and lamellipodia are likely to serve a similar purpose, helping sense the cellular environment and provide protrusive force, matching the epidermal sheets on the two sides and zippering them closed, akin to the role of filopodia in junction formation in primary keratinocytes, endothelial cells or *C. elegans* ventral enclosure (Raich *et al.*, 1999; Vasioukhin *et al.*, 2000; Woolner *et al.*, 2005;

Millard and Martin, 2008; Hoelzle and Svitkina, 2012). Surprisingly, the non-migratory cells of the amnioserosa also make actin-based protrusions, though they have not been characterized nor their roles defined.

We used the LE and AS tissues to uncover whether and how Ena and Dia regulate protrusive behavior during development, assessing whether the roles these proteins can have in stimulating filopodial behavior after overexpression or activation play out in important roles during normal development. Combining detailed quantitative analysis of cell behavior with both loss-of-function and gain-of function genetic tools helped reveal the mechanisms by which regulated Ena and Dia activity shape protrusive behavior in these two cell types, one migratory and one not, and to assess their contributions to the tissue level process of dorsal closure.

Results

The AS and LE cells provide a model for differential regulation of protrusive behavior during normal development

Protrusions produced by LE cells during dorsal closure provide a model for how different actin regulators shape protrusive activity within a single cell type (Figure 1, A-C; Jacinto *et al.*, 2000; Woolner *et al.*, 2005; Gates *et al.*, 2007; Millard and Martin, 2008; Homem and Peifer, 2009; Bilancia *et al.*, 2014). During dorsal closure LE cells elongate and migrate to meet contralateral partners, producing protrusions that are a mix of broad lamellipodia (Figure 1C, arrowheads) and filopodia (Figure 1C, arrows). Their nearest neighbors, the AS cells (Figure 1B) also use the actin cytoskeleton to drive oscillatory behavior resulting in net apical constriction (Kiehart *et al.*, 2000; Jacinto *et al.*, 2002b; Solon *et al.*, 2009). Previous work suggested AS cells, although they are non-migratory, also produce filopodia (Figure 1D; Jacinto *et al.*, 2000), but their characteristics and dynamics have not been assessed. These two cell types provide a setting to test the hypothesis that Ena and Dia act separately

and together to help shape the distinctive protrusive behaviors of different cell types in normal development. Our first task was to determine if filopodial dynamics differ in these two cell types, which undergo very different cell shape changes, by characterizing AS cell protrusions and comparing them to those in the LE.

We visualized protrusions through labeling f-actin structures by expressing the moesin actin binding domain fused to GFP (Moe-GFP) via the myosin light chain promoter *(spaghetti squash (sqh),* driving expression both in the AS and the lateral epidermis and by using the UAS-GAL4 system to drive Moe-GFP along the LE in stripes (Table 1). We then used live confocal imaging to visualize filopodia dynamics in both tissues. This revealed AS cells produced thin, actin-based, filopodia (Figure 1D, arrows). However, because AS cells protrude over one another (Figure 1D), quantifying AS filopodial number, length and lifetime was initially obstructed by lack of contrast against which to accurately measure individual filopodia. To better visualize AS filopodia we developed a bleaching assay, photobleaching individual AS cells (Figure 1E). Bleaching allowed us to correctly assign protrusions to neighboring cells, and to reliably discern spatial and temporal properties of individual protrusions, facilitating direct quantitative comparison of AS and LE cell protrusions. Our initial impression was that AS cells produced more and longer filopodia than LE cells (Figure 1, C vs D, Supplemental Movie 2). However, when we quantitated the number of filopodia formed per μm of cell perimeter per hour in both AS and LE cells, we found AS cells produce 4X fewer filopodia than LE cells (Figure 1F, 1.0±0.01 vs. 4.3±0.9, p=0.013) and that the mean maximum lengths of filopodia in each tissue were similar (Figure 1G, 3.7± 0.5μm, vs. 3.5 ± 0.5μm).

What then accounts for the obvious differences in protrusive behavior of LE and AS cells? Two parameters were strikingly different in the two tissues. Filopodia along the LE most often arise from a broad lamellipodium (Figure 1C, arrow; Gates *et al.*, 2007; Homem and Peifer, 2009), but the actin-based structures associated with AS filopodia remained largely unexplored. To test the hypothesis that differences in the filopodia/lamellipodial balance might help account for the visual difference between the two tissues (Ebbinghaus 1902), we quantified lamellipodial area. There was significantly less lamellipodial area/cell

perimeter in AS versus LE cells (Figure 1I, 0.4±0.01μm2/μm perimeter, n= 6 embryos vs. 2.4±0.55μm2/μm perimeter, n=5 embryos). Thus AS filopodia largely emerge directly from the cell cortex, while LE filopodia emerge from lamellipodia (Figure 1D,E vs C).

The difference in lamellipodial area accounted for part of the visual difference between protrusive behaviors in the two tissues, but a second, subtler dynamic parameter also played an important role. AS cell filopodia had significantly longer mean lifetimes than their LE cell counterparts (Figure 1H, AS 459± 52s, n= 9 embryos, 567 filopodia vs. LE 294± 27s, n=7 embryos, 429 filopodia; p=0.014). This difference in lifetime prompted us to look closely at the relationship between filopodial length and lifetime, which could be influenced in part by barbed end polymerization rates. To explore this, we plotted the maximum length versus lifetime for each wildtype LE or AS filopodium, generating a “protrusive profile” of individual filopodia (Figure 1J). We applied a linear regression fit to each dataset, the slope of which revealed the relationship between filopodial length and lifetime. As expected, longer filopodia generally have longer lifetimes in all cases. However, the relationship between these two parameters differed significantly in the two tissues (p=0.0001). This suggested possible differences in filopodial extension rates, which may reflect differences in activity of the actin regulators governing filopodial behavior in the AS and LE. Comparing LE and AS filopodial protrusive profiles also revealed an outlier population of AS cell filopodia that are both longer and longer-lived (Figure 1J, yellow bar brackets). This is prominently illustrated by comparing the top 20% longest-lived filopodia in LE versus AS cells (Figure 1K)—the mean lifetime of the longest-lived filopodia differs by almost two-fold (Figure 1L, 564±68s vs. 985±108s). Thus these two tissues have distinct filopodial dynamics as revealed by their protrusion profiles. AS filopodia are longer-lived than LE filopodia of the same length, and a subset of the AS filopodia have significantly longer lifetimes overall. This difference was intriguing, given our recent results in cultured cells in which Dia-driven filopodia had longer lifetimes and often emerged directly from the cell body, while Enadriven filopodia were more dynamic and emerged from broad lamellipodia (Bilancia *et al.*, 2014), suggesting Ena and Dia have properties that might allow them to drive filopodia with

distinct dynamic properties *in vivo*.

Ena and Dia have distinct localization patterns in the AS versus the LE

The simplest prediction of the hypothesis that Dia and Ena drive different types of protrusive behavior in different cell types is that either Ena or Dia would predominate in one or the other tissue. In fixed embryos, both Ena and Dia are present in both cell types but localize differently in each. In LE cells, Ena localizes robustly with f-actin to LE "dots" where LE cells abut one another and project over the AS (Figure 2A,A'',C,C',E-E'' cyan arrowheads), as well as to the tips of LE filopodia (in images where these are preserved; Figure 2E-E'' yellow arrows). In epidermal cells ventral to the LE, Ena is planar polarized, enriched at tricellular junctions and with lower levels at the lateral cortex (Figure 2A'' cyan arrows vs brackets; Bilancia *et al.*, 2014). Dia is cortical in all cells of the lateral epidermis (Figure 2B) and less polarized than Ena, though there is enrichment just ventral to the LE 142 dots (Figure 2B'',C'' cyan arrowheads) and somewhat elevated accumulation at dorsalventral cell borders (Figure 2B,B" arrows). Co-staining for Ena and Dia revealed Ena is localized more proximal to the AS cell interface, closer to LE protrusions than Dia (Figure 2C,D). Together, these localization patterns suggest there may be differential activity of these two elongation factors in the lateral epidermis versus the LE. In the AS, Ena localizes robustly to the cell cortex (Figure 2A,A' yellow arrowheads), even from early stages (data not shown), at levels roughly comparable to the cortex of LE cells. However, in contrast to the LE, Ena's localization in AS cells was radially symmetric. Dia was also cortically localized in the AS, at levels roughly comparable to the LE cell cortex, and also was radially symmetric (Figure 2B,B'). Thus both proteins are present in both the LE cells and the AS cells and are potentially poised to play roles in filopodia formation and elongation in both tissues.

Ena is preferentially enriched in LE filopodia.

This analysis of fixed embryos provided insights into potential localization differences of these two actin regulators *in vivo*, but did not capture the dynamic cell protrusions we study. To assess this, we used live analysis of fluorescently-tagged proteins. Both endogenous and GFP-tagged Ena can localize to filopodia tips in LE cells (Figure 2E,F; Gates *et al.*, 2007). RFP-tagged Ena also localizes robustly to tips of LE filopodia (Figure 2F arrows). Preserving endogenous Dia localization to filopodia proved impossible, as fixation conditions preserving LE filopodia fail to preserve Dia antibody signal. To assess Dia's ability to localize to filopodia tips we live imaged embryos expressing a GFP-tagged constitutively active version of Dia (DiaΔDAD, lacking the DAD auto inhibitory domain). Active Dia was also enriched at tips of LE filopodia (Figure 2I arrows; Homem and Peifer, 2009); thus both elongation factors can localize to filopodia tips along the LE.

Since we cannot reliably preserve AS cell protrusions after fixation, we assessed the ability of Ena and Dia to localize to AS filopodia tips by live imaging. Surprisingly, expressing RFP-Ena in the AS using the c381-GAL4 driver revealed strong localization to the AS cortex (Figure 2G, arrowheads) but did not reveal clear enrichment in AS filopodia. When we expressed RFP-Ena using the *engrailed*-GAL4 driver, we saw robust localization to LE filopodia (Figure 2F, H cyan arrow left) and to LE filopodial "fans" (Figure 2H, cyan arrows right). In the rare, isolated AS cells expressing both Actin and RFP-Ena via this driver, we saw RFP-Ena localization to the cortex (Figure 2H, yellow arrowheads) and occasional localization to the tips of AS cell filopodia (Figure 2H inset), but the ratio of RFPEna at AS filopodial tips relative to the AS cell cortex was lower than in LE cells (Figure 2H yellow arrowheads and arrow vs cyan arrows). This is not solely due to reduced filopodia number as Ena over-expression increases the number of AS filopodia (see below). In contrast, GFP-tagged active Dia localized robustly to the tips of AS filopodia (Figure 2J arrows). Together these data demonstrate both Ena and Dia can localize to the tips of filopodia in both AS and LE cells, but suggest Ena enrichment to filopodial tips may be more

robust at the LE.

Roles for Ena levels in governing filopodia number and dynamics along the LE

Our assessment of the biochemical properties of Ena and Dia and their effects on protrusive behavior in cultured *Drosophila* cells revealed Dia generates longer, longer-lived filopodia while Ena generates shorter-lived filopodia that emerge from lamellipodia (Bilancia *et al.*, 2014). Based on this, we hypothesized Ena is responsible for the more dynamic LE filopodia while Dia might play a more dominant role in the AS. Consistent with this, reducing Ena function using loss-of-function mutants substantially reduced LE filopodial number (Homem and Peifer, 2009).

To further test this hypothesis, we used quantitative tools to assess the dynamic properties of filopodia driven by either Ena or activated Dia. To do so, we expressed tagged versions of Ena or active Dia (DiaΔDAD; Homem and Peifer, 2009) along with Actin-GFP in epidermal stripes using *engrailed*-GAL4. Wildtype LE protrusions are a mix of lamellipodia (Figure 3A, arrowheads) and their associated filopodia (Figure 3A, arrows). Both Ena and activated Dia can promote formation of filopodia along the LE (this data; Gates *et al.*, 2007; Homem and Peifer, 2009). Overexpressing RFP-Ena in the lateral epidermis altered LE protrusive behavior, promoting both excess filopodia (Figure 3B, arrows, H; Gates *et al.*, 2007) and "filopodial-fans," which appear to be many closely packed filopodia elongating in concert presumably within in a common membrane (Figure 3B, arrowheads, Supplemental Movie 3). Both filopodia and fan-like protrusions have RFP-Ena at the tips (Figure 2H, cyan arrows). When we quantitated LE filopodia induced by Ena overexpression (excluding fan protrusions to allow direct comparisons), we found higher filopodia number, indicative of increased filopodia initiation (Figure 3H; Gates *et al.*, 2007). However, mean filopodial lifetime and length were not different from control LEs (Figure 3I,J). We next examined the protrusive profile, comparing filopodia length and lifetime. The protrusive profile of Ena-induced filopodia was not significantly different than wildtype (Figure 3K, green versus blue dots and lines). The observation that elevating Ena along the LE increases filopodia initiation without

changing filopodia dynamics is consistent with the idea that Ena initiates and governs elongation of LE filopodia, while the elevation of filopodia number after elevation of Ena levels suggests Ena may be limiting for LE filopodial initiation.

Active Dia induces long-lived LE filopodia that mimic AS filopodia

We then contrasted filopodia induced by Ena at the LE with filopodia induced by active Dia. Overexpressing HA-tagged DiaΔDAD had a dramatic affect, triggering filopodia-like protrusions all along the epidermal cell cortex of all lateral epidermal cells (Figure 3F, Supplemental Movie 3; Homem and Peifer, 2009). Like Ena, active Dia also significantly increased the number of filopodia initiated along the LE (Figure 3C arrows, H), and induced filopodial fans (Figure 3C, arrowhead). However, in contrast to Ena, Dia substantially altered the dynamic properties of LE filopodia, with length significantly decreased and lifetime significantly increased (Figure 3I,J). We thus examined the protrusive profile, plotting maximum length versus lifetime for each wildtype LE filopodium, as well as those induced by Ena over-expression or activated Dia (Figure 3K). The protrusive profile of Ena-induced filopodia was not significantly different than wildtype (Figure 3K, green versus blue dots, blue versus yellow lines). In contrast, the protrusive profile of Dia-induced LE filopodia was significantly shifted, with active Dia inducing shorter, longer-lived filopodia (Figure 3K). Thus, in contrast to Ena, Dia does not seem to be a strong candidate for playing a dominant role in LE filopodial dynamics.

Ena activity in the lateral epidermis is polarized

In the wildtype, Ena is strongly enriched at LE dots (Figure 2A, A” arrowheads) and robustly but more weakly enriched at tricellular junctions in more ventral epidermal cells (Figure 2A, A’’ arrows). Overexpressing RFP-Ena in lateral epidermal stripes also induced ectopic filopodia at tricellular junctions in more ventral cells (Figure 3E, cyan arrowheads, Supplemental Movie 4), with RFP-Ena localized to their tips (Supplemental Figure 1A

arrows) This allowed us to ask questions about the polarization of Ena activity. At the LE, protrusions are restricted to the dorsal sides of the LE cells. The ectopic filopodia induced by RFP-Ena in more ventral epidermal cells also appeared to be oriented dorsally. To directly test if these filopodia were polarized, we co-expressed RFP-Ena and GFP-Actin, photobleached the GFP-Actin in a subset of lateral epidermal cells and watched over time as filopodia appeared on unbleached neighbors. These filopodia emerged from the dorsal tricellular junctions of unbleached cells (100%, n=5, Supplemental Figure 1B, yellow arrows). Controls in the same tissue (ventral tricellular junctions in more dorsal unbleached cells) never produced filopodia (Supplemental Figure 1B, cyan arrows). Thus the lateral epidermis is polarized towards the LE, suggesting Ena's activity at tricellular junctions is polarized.

Active Dia also induced filopodia in cells ventral to the LE—like Ena, Dia induced filopodia at tricellular junctions and active Dia also induced filopodia along the lateral cortex (Figure 3F cyan versus yellow arrowheads). Dia-induced filopodia at the lateral cortex, where Ena levels are low, have exceptionally long lifetimes (Bilancia *et al.*, 2014) consistent with our hypothesis that Dia promotes longer-lived filopodia. Dia-induced filopodia at tricellular junctions, where Ena levels are higher, were shorter-lived. We analyzed and compared protrusive profiles of filopodia at tricellular junctions. The occasional wildtype filopodia observed at tricellular junctions and those induced by Ena had similar protrusive profiles (Supplemental Figure 1C), and the protrusive profiles of both resembled those of wildtype LE cells (Figure 3L). In contrast, Dia-induced filopodia at tricellular junctions had a significantly different protrusive profile, being longer-lived with respect to length (Figure 3L) and thus more similar to the wildtype AS filopodia. Therefore, even in this ectopic location, Ena induced filopodia more resembled those at the wildtype LE.

Elevating Ena expression in the AS induces filopodia with LE characteristics while active Dia promotes long-lived filopodia in the AS with AS-like dynamics

The data above combined with our earlier work suggest Ena may be the dominant actin

elongator acting at the LE. The differences in protrusive profile between the wildtype LE and AS, along with the shift in protrusive profile induced by Dia at the LE, led us to hypothesize Dia may be more important in the AS. To begin to test this we elevated either Ena or Dia activity in AS cells, expressing RFP-Ena or HA-DiaΔDAD specifically in the AS using c381-GAL4 (plus *sqh*-Moe-GFP to visualize protrusions; Figure 4,A-C; Supplemental Movie 5). Neither RFP-Ena nor HA-DiaΔDAD substantially changed either the overall process of dorsal closure (Supplemental Figure 2A-C) or its timing, as assessed by area change or canthi migration within the last 90 minutes of closure (Supplemental Figure 2A-E; Supplemental Movie 6). Both RFP-Ena and HA-DiaΔDAD expression increased AS filopodia number (Figure 4D). Unexpectedly, Ena expression in the AS did not induce the fan-like protrusions driven by Ena overexpression along the LE (Figure 4B vs 4B inset, Supplemental Movie 3 vs Supplemental Movie 5). However, elevating Ena levels significantly altered filopodial behavior. While Ena overexpression increased filopodia number, as it did when overexpressed at the LE, both filopodial length and lifetime decreased (Figure 4E,F). Analysis of the protrusive profile of AS filopodia after Ena expression provided an interesting insight into this difference. Ena overexpression in the AS altered the relationship between filopodial length and lifetime, with lifetime reduced for filopodia of the same length, relative to AS controls (Figure 4G). As a result, the protrusive profile of Enainduced AS filopodia strongly resembles that of filopodia produced by Ena expression along the LE (Figures 3K versus 4H), and is statistically indistinguishable from wildtype LE filopodia (Figure 4H). The fact that Ena overexpression induces “LE-like” filopodia in the AS is consistent with the hypothesis that Ena governs wildtype filopodia dynamics along the LE.

To begin to test if Dia governs the longer-lived AS filopodia, we examined effects of expressing DiaΔDAD in the AS, predicting it would increase filopodia lifetime. Indeed, both lifetime and maximum length of filopodia are significantly increased (Figure 4E,F). The increase in length is readily apparent, with occasional filopodia spanning the cortex of one to several AS cells, a length never seen in controls (Figure 4C, arrowheads, Supplemental

Movie 5). However, despite this, the slope of the protrusive profile of DiaΔDAD induced filopodia in the AS is the same as that of wildtype AS cells, as length and lifetime increased in parallel (Figure 4I). These data are consistent with the model that Dia normally drives wildtype AS cell filopodial behavior, helping make them longer-lived.

Ena/Dia relocalization via FP4mito expression alters and delays dorsal closure and drastically reduces filopodia number, length and lifetime

Both elongation factors are thus poised play roles in filopodia in each tissue, and each can influence filopodia in distinctive ways. However, the integral test for whether Ena and Dia truly regulate normal filopodial behavior during development is to ask if and how filopodia are altered when each elongation factor is reduced or removed. We first reduced function of both Ena and Dia by sequestering Ena away from the cell cortex by expressing FP4mito, a high affinity Ena-EVH1 domain binding site tethered to mitochondria (Bear *et al.*, 2000). FP4mito efficiently recruits Ena to mitochondria in *Drosophila*, leading to loss-of-function (Figure 5B'' inset arrows, Gates *et al.*, 2007). FP4mito also recruits some Dia to mitochondria, while some remains at the cortex (Figure 5B'''inset arrows vs arrowhead; Homem and Peifer, 2009). FP4mito drastically reduces filopodia in LE cells (Gates *et al.*, 2007).

To explore the effect of depleting Ena and Dia in the AS, we expressed FP4mito specifically there, and visualized protrusions using Moe-GFP (Figure 5A,B,D; Supplemental Movie 6). FP4mito substantially reduced AS filopodia number (Figure 5C vs. D, E; 0.53+/-0.12 filopodia/μm perimeter per hour vs 1.0+/-0.12 in wildtype; p=0.03), and dramatically reduced the maximum length and lifetime of the remaining filopodia, relative to controls (Figure 5F,G). Interestingly, however, the slope of the protrusive profile of the remaining filopodia was unchanged from wildtype (Figure 5I). In contrast, lamellipodial area increased relative to wildtype (Figure 5D, H; 0.58±0.05 um2/um perimeter vs, 0.42±-0.01 in wildtype, p=0.03). These data suggest some combination of Ena and Dia is important for filopodia initiation in AS cells, and, because FP4mito more effectively recruits Ena relative to Dia, are

consistent with the idea that the filopodia remaining after FP4mito expression may be driven by residual cortical Dia.

We next explored how depleting Ena and Dia from the AS affected the larger scale process of dorsal closure. The AS provides a significant but partially redundant contribution to the forces required to ensure completion of dorsal closure (Kiehart *et al.*, 2000; Hutson *et al.*, 2003), resulting, at least in part, from pulsatile apical constrictions of each AS cell that reduce AS area. However, the role of AS cell protrusions in dorsal closure has remained untested. Filopodial protrusions of LE cells do play an important role in late dorsal closure, helping zipper the two sheets together and correctly matching contralateral partners (Woolner *et al.*, 2005a; Gates *et al.*, 2007; Millard and Martin, 2008).

To explore the hypothesis that AS cell protrusions are also important for dorsal closure, we assessed morphogenetic movements and dorsal closure timing in embryos expressing FP4mito in the AS. These embryos completed dorsal closure, as lethality was negligible (96% embryonic viable, n= 327), suggesting either the few remaining filopodia are sufficient or that filopodia in the AS are not essential for dorsal closure. However, our movies revealed substantial alterations in the process. In wildtype, the advancing epidermis encloses an eye-shaped opening (Figure 6A,G) with zippering occurring at the canthi (Figure 6A, arrows) and a straight leading edge (Figure 6A, arrowhead). In contrast, embryos expressing FP4mito had very abnormally-shaped openings, with apparent difficulties in zippering at the canthi (Figure 6B, arrow, G). Some regions along the leading edge progressed toward the dorsal midline more rapidly than others (Figure 6B, 60 and 30 min white vs blue arrows), and as closure was completed, the epidermis was puckered (Figure 6B, 30 and 0 min, yellow arrows). In a subset of embryos there was ripping between the AS and LE, (2/8 embryos; Figure 6B, asterisk) though this was repaired and closure completed. Ripping between the AS and LE is also characteristic of mutants lacking the integrin βPS subunit in both tissues (Narasimha and Brown, 2004; Gorfinkiel *et al.*, 2009). Finally, in a subset of embryos expressing FP4mito in the AS there was a slight delay in dorsal closure. In normal development, dorsal closure precedes the initiation of muscle constriction. If dorsal closure is delayed, the muscles begin to twitch *before* the epidermis fully encloses the embryo. While

muscle contraction never precedes closure in wildtype (n=13), in embryos expressing FP4mito in the AS, muscles started to twitch just prior to closure in half of the embryos (3/6, Supplemental Movie 7); this delay is likely restricted to early stages, as mean rates of area change and canthi advancement in late closure were not significantly altered (Figure 6 E,F, Supplemental Movie 6). Thus depleting Ena and Dia substantially alters dorsal closure, but the robustness of the morphogenesis program allows closure to go to completion despite their depletion.

Ena regulates AS filopodial length and lifetime and is required for proper dorsal closure

We next sought to determine which elongation factor was responsible for these changes in dorsal closure and in AS protrusions upon expression of FP4mito, by examining embryos zygotically mutant for either *ena* or *dia*. For *ena,* we examined embryos trans-heterozygous for *enaGC1,* a null allele (Gertler *et al.*, 1995) and *ena46* , that truncates Ena and eliminates the EVH2 domain responsible for Ena's interaction with actin (Li *et al.*, 2005). In transheterozygotes Ena levels and cortical localization in fixed embryos were substantially reduced by dorsal closure (Supplemental Figure 3A).

Ena reduction did not significantly alter AS filopodial number relative to wildtype (Figure 7A,B,D), indicating either Ena is not responsible for most filopodia initiation in the AS, or that residual maternal Ena is sufficient. This is in marked contrast to the LE, where reducing Ena significantly reduces filopodia number (Homem and Peifer, 2009). We next addressed the requirement of Ena for AS filopodia lifetime and length. Loss of zygotic Ena significantly reduced filopodial maximum length and lifetime (Figure 7B,E,F), while lamellipodial area remained statistically indistinguishable from wildtype (Figure 7G). This partially phenocopied FP4mito expression (Supplemental Movie 8), suggesting Ena does, in fact, help regulate filopodial behavior in this tissue. Analysis of the protrusive profile of filopodia in *ena* mutants revealed they are both shorter and shorter-lived, and thus the slope of the protrusion profile remained unchanged (Figure 7H). This result suggested to us that Dia might elongate the remaining filopodia, consistent with the idea that Dia normally

regulates the wildtype AS protrusion profile.

We then assessed the requirement for Ena for dorsal closure, analyzing the dynamics of the process using live imaging (Figure 6C). As expected from analysis of fixed embryos (Gates *et al.*, 2007), *ena* zygotic mutants displayed obvious defects in dorsal closure, many of which were shared with FP4mito expressing embryos. These varied in severity, and most prominently affected the normally "eye-shaped" dorsal closure front, with delays in zippering at the canthi (Figure 6C, 90 min, yellow arrow, G), and uneven progress of the leading edge (Figure 6G), with some LE cells in the same sheet slowed compared to neighbors (Figure 6C, 90 min, blue vs white arrows, Supplemental Movie 6). We next assessed whether these differences in morphogenetic movements slowed the overall rate of closure, by measuring the average rate of area change and advancement of canthi during the last 90 min of closure. Surprisingly, despite the obvious visual defects in dorsal closure shape, the change in area over time was not different from wildtype (Figure 6E). However, canthi migration rate was increased (Figure 6F), perhaps because the wavy, elongated LE initially lags behind in zippering and then quickly increases it's rate in last 30-60 min before closure (Figure 6C- 60 min vs 30 min). Further in contrast to embryos expressing FP4mito, only 10% (n=1/10) of *ena* mutants displayed twitching prior to complete closure. Thus while reducing Ena dramatically alters the process of dorsal closure, it is not required for either completing closure or for its correct timing, suggesting that the timing defects seen after FP4mito expression in the AS are not solely a result of Ena loss in that tissue.

Dia regulates AS filopodia protrusive profile and plays a role in normal dorsal closure

Dia and its family members can induce filopodia, and cultured cell studies are consistent with a role in protrusive behavior. However, Dia's essential role in cytokinesis and the redundancy of mammalian family members have largely precluded assessment of whether Dia-class formins regulate protrusive behavior during normal development. To assess this, we reduced Dia levels by examining zygotic loss of function using the null allele *dia2* (Castrillon and Wasserman, 1994). We found that zygotic *dia2* mutants have substantially

reduced cortical Dia at dorsal closure (Supplemental Figure 3B). Further, *dia2* mutants are embryonic lethal and display significant phenotypes by the time they initiated dorsal closure, including severe head involution defects (Supplemental Figure 4A,B). These mutants also had the characteristic defect associated with *dia* loss in other tissues (Castrillon and Wasserman, 1994; Afshar *et al.*, 2000) fewer and larger cells with correspondingly large nuclei (Supplemental Figure 4C, D, E yellow arrows), which in other cases result from cytokinesis failure. Importantly, because AS cells do not divide after the blastoderm stage (Frank and Rushlow, 1996; Reim *et al.*, 2003), AS cells and nuclei were of normal size in *dia2* mutants (Supplemental Figure 4E, magenta arrows). We thus used *dia2* zygotic mutants to assess Dia's role in filopodial behavior and in the overall process of dorsal closure.

We first looked at Dia's role in AS filopodia number. Unexpectedly, *dia2* mutants had significantly more AS filopodia (Figure 7C,D). This increase is in direct contrast to the effects of either FP4mito or loss of Ena, where filopodia number was either reduced or remained the same (Figures 5E,7D, Supplemental Movie 8). This is also in contrast to the LE where reducing Dia reduced filopodia number (Homem and Peifer, 2009). We consider possible explanations for this in the Discussion. Reducing Dia also affected other parameters of protrusive behavior. Like Ena reduction, reducing Dia reduced both the maximum length and lifetime of filopodia (Figure 7E,F). However, unlike what we observed in *ena* mutants, the AS protrusive profile of *dia* mutants significantly differed from wildtype–*dia* mutant AS filopodia had a significantly lower lifetime per length relative to either control or *ena* mutant filopodia (Figure 7I). Strikingly, the protrusive profile of AS filopodia in *dia* mutants was shifted to resemble that of wildtype LE filopodia (Figure 6J), where, as we discussed above, Ena largely drives protrusive behavior. These data are consistent with a model in which Dia activity shapes the protrusive profile of filopodia in AS cells, as Ena does at the LE, and when Dia is reduced, Ena confers upon the AS cells filopodial behavior like it drives at the LE.

Like Ena, Dia is not essential for completion of dorsal closure, as *dia* zygotic mutants close (9/9 live embryos). However, closure was morphologically very different. The shape

of the dorsal opening was substantially altered in many embryos (Figure 6D,G), with delays in zippering both anterior and posterior (Figure 6D, 90 min, blue and yellow arrows). Unlike *ena* mutants, but reminiscent of FP4mito expression in the AS, *dia* mutants displayed ripping along the LE (10/13 embryos; Figure 6H, arrows). Additionally, during the last hour of closure, when the AS, the LE cable, and the LE cells in wildtype embryos are normally in roughly the same position in the z-axis, in *dia* mutants both the LE cable and the AS drop below the level of the LE cells (Figure 6D bracket, 6I-I", Supplemental Movie 6). This is not due to premature AS cell apoptosis, as we can still visualize both the cable and the AS cells in lower z planes (Figure 6I',I"). Despite these morphological differences, the rate of closure as assessed by the rate of change in area or reduction in canthi distance was not affected (Figure 6E,F), and only occasional (1/9) *dia* mutants had muscle twitching prior to closure. Together, these data are consistent with the hypothesis that the AS-LE ripping seen after FP4mito expression results in part from Dia reduction and suggest the delay in dorsal closure seen after FP4mito expression is an additive result of reducing both Ena and Dia in the AS.

In recent work, we found Ena and Dia directly bind one another and that Ena can inhibit Dia, both *in vitro* and *in vivo* (Bilancia *et al.*, 2014). In examining the lateral epidermis of *dia* zygotic mutants, we saw a surprising phenotype that suggested this relationship may be even more complex. While protrusive behavior in wildtype is essentially restricted to the dorsal surface of LE cells, in *dia* zygotic embryos we observed frequent ectopic protrusions at tricellular junctions of more ventral cells (Fig 3G,arrows- 14/17 embryos), reminiscent of the effects of Ena overexpression (Figure 3E). One possible explanation is that Dia can also inhibit Ena. We consider this further in the Discussion.

Discussion

Cell protrusions help drive many cell behaviors, including cell migration. We are interested in how different cells craft distinct suites of cell protrusions using the same genomic toolkit of actin regulators, and how these distinct cell behaviors contribute to large scale morphogenesis. We addressed these questions using gain- and loss-of-function approaches during embryonic morphogenesis to alter the function of two actin elongation

factors with known roles in cultured cells, to assess how their biochemical properties and activities in simpler systems play out in the more complex environment *in vivo.*

Both Ena and Dia play important roles in regulating protrusive behavior during normal development

Studies *in vitro* and in cultured cells demonstrated both Ena/VASP and DRFs bind to barbed ends and accelerate filament elongation, and gain-of-function studies revealed both can stimulate formation of filopodia (see Introduction). However, the contributions of these proteins to protrusive behavior during normal development remain significantly less clear. Ena/VASP proteins have clearly defined roles *in vivo* in filopodia formation in several settings: *Dictyostelium*, (Schirenbeck *et al.*, 2006), *Xenopus* retinal ganglion cells (Dwivedy *et al.*, 2007), *Drosophila* primary neurons (Gonçalves-Pimentel *et al.*, 2011), LE cells (Homem and Peifer, 2009), and hemocytes (Tucker *et al.*, 2011). In contrast, functional redundancy of mammalian DRFs and their essential role in cytokinesis limit loss-of-function studies during normal development. As a result there are only a handful of examples suggesting important roles for DRFs in protrusive behavior *in vivo*: these include roles in planar polarized protrusions during *Drosophila* bract cell induction (Peng *et al.*, 2012), a role in LE protrusions during dorsal closure (Homem and Peifer, 2009) and a recently described role in promoting cytonemes, the long signaling filopodia in fly imaginal disc cells (Roy *et al.*, 2014).

Our data provide new insights into these issues, allowing us to directly compare the roles of Ena and Dia in shaping the dynamics of protrusive behavior during normal development within the same cell types. Our quantitative analyses of both gain- and loss-of-function mutants reveal that Ena and Dia each induce filopodia with characteristic dynamic behaviors that are most clearly depicted by their distinct “protrusive profiles,” which relate filopodial length and lifetime and thus provide a filopodial fingerprint for each actin regulator. Our data reveal Dia promotes filopodia with longer lifetimes, while Ena-driven filopodia are shorter-lived. These differences in filopodial dynamics regulated by Ena and Dia during embryogenesis parallel the biochemical differences we recently documented for these two

proteins: *Drosophila* Dia is a more effective actin elongation factor than Ena, promoting actin elongation 2x more efficiently, and remaining at the barbed end 7x longer (Bilancia *et al.*, 2014). The ability to assess the roles of Ena and Dia in parallel at all levels of complexity from purified proteins to cultured cells to tissues *in vivo* during morphogenesis is beginning to provide a picture of why cells retain two different proteins that both promote actin filament elongation, by suggesting cells use them differentially to craft distinct protrusive behaviors.

Different elongation factors play predominant roles in shaping filopodia in different tissues

Dorsal closure is driven by two cell types that differ dramatically in many ways: the migratory LE cells and the apically constricting but non-migratory AS cells. The protrusive behavior of LE cells has served as a model for understanding the role of filopodia in collective cell migration (Woolner *et al.*, 2005; Gates *et al.*, 2007; Millard and Martin, 2008; Homem and Peifer, 2009) but the nature and role of cell protrusions of AS cells remained mysterious. Our quantitative comparison revealed the two cell types differ in protrusive behavior in specific ways: (1) AS cells produce significantly fewer filopodia and substantially less lamellipodia, and (2) AS filopodia had significantly longer lifetimes. Extending this analysis beyond simply comparing mean values of individual parameters further revealed that the relationship between length and lifetime of individual filopodia, the protrusive profile, highlighted differences in filopodial dynamics between these two tissues. The differences in dynamics of LE and AS filopodia led us to hypothesize the longer-lived AS filopodia were governed by Dia while the more dynamic LE filopodia were governed by Ena.

A combination of gain- and loss-of-function approaches allowed us to test this hypothesis. Elevating Ena levels promoted dynamic, shorter-lived filopodia in both cell types, with protrusive profiles matching those of wildtype LE cells, while active Dia induced longer-lived filopodia at all locations we examined, whose protrusive profiles were more

similar to wildtype AS cells. This is consistent with the idea that Ena is responsible for the normal protrusive profile of the LE cells. In contrast, while *ena* loss-of-function did not alter the slope of the protrusive profile of AS filopodia, *dia* loss-of-function converted the AS cell protrusive profile slope to one resembling that of LE cells, consistent with the idea that Dia is normally the dominant player in the AS. However, the full picture that emerged is not that simple—our current and previous (Homem and Peifer, 2009) loss-of-function analysis reveal that both actin regulators play roles in both tissues—for example, the data are consistent with a model in which Dia is important for elongation of AS filopodia, while Ena may play a supporting role−perhaps helping regulate filopodia initiation and working in concert with fascin-based bundling (Winkelman *et al.*, 2014). It will be important to define mechanistic underpinnings of these differences.

How might cells differentially deploy these two actin regulators? Our analysis ruled out the simplest model, in which one or the other cell type expressed only Ena or Dia. However, the two tissues do localize both actin regulators in distinctive fashions, with both Ena and to a lesser extent Dia having polarized localizations in the lateral epidermis, while both proteins are uniformly cortical in the AS. These differences in localization could reflect direct recruitment of Ena or Dia to these discrete places by distinct actin architectures, or indirect recruitment via binding partners, such binding partners of Ena's EVH1 domain like Lamellipodin or Zyxin (Krause *et al.*, 2004; Drees *et al.,*2000). Another potential clue emerged from examination of fluorescently tagged Ena and Dia. GFP-DiaΔDad localized effectively to filopodia tips in both the AS and at the LE. However, RFP-Ena localized distinctly differently in the two tissues. In LE cells it readily localized to both filopodia tips and to the "filopodial fans" that it induced. However, in the AS, RFP-Ena was largely cortical rather than strongly localized to filopodial tips, and did not readily induce filopodial fans. Perhaps Ena localization and/or activity is differentially regulated in these two tissues. Defining the mechanisms differentially regulating Ena at different subcellular locations will be of interest as we move forward.

Both actin elongation factors are important for proper dorsal closure but the process is robust to their depletion

While AS cells are not migratory, they still produce dynamic filopodia and some lamellipodia. Why do these non-migratory cells have filopodia, and are they important for dorsal closure? FP4mito expression specifically in the AS, which sequesters Ena and some Dia, substantially reduced filopodia length and lifetime. It also led to striking alterations in the shape/movement of the LE, along with more subtle changes in proper timing of closure and tissue integrity. *ena* and *dia* zygotic mutants, which each exhibited alterations in AS and LE filopodial behavior, also close in a manner morphologically quite distinct from wildtype, though the timing of closure remains unaltered. Together these data are consistent with the possibility that AS filopodia may help regulate dorsal closure. However, AS cells also undergo dramatic cycles of actomyosin-based apical constriction and relaxation, which play important roles in driving closure and presumably use the same actomyosin machinery that drives migration (Franke *et al.*, 2005; Solon *et al.*, 2009; David *et al.*, 2010). Since we lack a method for depleting cell protrusions without affecting cortical actin and the actomyosin network involved in cell constriction, it remains unclear if the altered closure process we observed is directly related to filopodia loss or occurs via effects on another structure/process altered by elongation factor loss. The ability of FP4mito expressing embryos and *ena* and *dia* zygotic mutants to close in a time frame largely similar to wildtype despite considerable larger scale defects also highlights the robustness of the dorsal closure process.

The question of why non-migratory AS cells have filopodia is intriguing. The dynamic LE filopodia are important for neighbor sensing and alignment as the epithelial sheets meet at the midline (Millard and Martin 2008). One possible role for the long-lived filopodia in the non-migratory AS cells is in cell-cell signaling over the course of the closure process. Cytonemes, long basally-associated filopodia-like structures present in the non-migratory but shape-changing *Drosophila* wing disc cells, play a role in Dpp signaling, and Dia is required for proper cytoneme elongation (Roy *et al.*, 2014). JNK and Dpp signaling regulate dorsal closure (Reed *et al.*, 2001; Fernández *et al.*, 2007), and thus it will be of interest to look at the

relationship between AS cell filopodia and signaling. Alternately, filopodia might play an entirely different function in the AS– as AS cells rapidly reduce their apical area in each pulse of apical constriction, these long-lived protrusions may simply function as external membrane storage to allow time for the endocytic machinery to catch up. Assessing coordination of constriction with protrusive behavior will be of interest in the future.

Integrating Ena, Dia and other actin regulators

Cells rely on arrays of actin regulators to accomplish complex tasks. Even the seemingly simple process of antagonizing actin capping and promoting filament elongation involves Ena and Dia working together in complex ways, based in part on their direct physical interaction (Homem and Peifer, 2009; Bilancia *et al.*, 2014). *In vitro* and cultured cell assays revealed Ena can negatively regulate Dia activity, and, consistent with this, active Dia induces long-lived filopodia at lateral borders of epidermal cells, where Ena levels are low, and more dynamic filopodia at tricellular junctions where Ena levels are high (Bilancia *et al.*, 2014). However, Dia can also influence Ena localization and perhaps activity. DiaΔDAD expression induced fan-like protrusions along the LE –these structures are never seen in wildtype but are also induced upon Ena overexpression. One possible mechanism by which active Dia could mimic Ena activation is suggested by the fact that active Dia triggers Ena localization from LE “dots” to the protrusive front (Homem and Peifer, 2009). We observed a similar relationship at tricellular junctions in the lateral epidermis: both overexpressing Ena and expressing active Dia induce similar ectopic protrusions. However, paradoxically, zygotic *dia2* mutants also exhibit ectopic protrusions at tricellular junctions in the lateral epidermis, and also produce more AS filopodia. Both effects closely resemble Ena overexpression, suggesting Dia may also negatively regulate Ena at those locations. Perhaps reduced Dia levels release Ena from Ena:Dia complexes, allowing it to interact with other partners and stimulate protrusive behavior. Thus while Ena and Dia are both important in each tissue, their relationship is not a simple one. Finally, filament elongation does not exist in a vacuum– instead actin regulators work in competition and synergy with each other, making the network plastic. Ena and Dia are likely to be heavily influenced by other actin

regulators, and vice versa. Competition for actin monomers with the Arp2/3 complex and the roles of filament bundling and severing are likely to be critical. It will be of interest moving forward to probe integration of multiple players using quantitative tools to assess the dynamics of protrusions induced by different combinations of actin regulators.

Materials and Methods

Fly Stocks

All experiments were performed at 25°C. Mutations are described at http://flybase.org. Wildtype was *y w* for fixed imaging and either *sqh* promoter driven Moesin actin binding domain fused to GFP (Moe-GFP), UAS driven Moe-GFP, or UAS Actin GFP for live imaging. Zygotic mutants were selected using the *Cy twiGFP* balancer. A full length Ena transgene was cloned into a derivative of pUASp modified for Gateway® cloning by T. Murphy for an N-terminal mRFP tag. Males carrying UAS-transgenes were crossed to females with a GAL4 driver. See 1 for additional fly stock information.

Image Acquisition and Analysis

The following fixations were used: Dia and Nrt: heat methanol (Müller and Wieschaus, 1996; Laplante and Nilson, 2006) and held in methanol for at least 48 hours at 4°C before antibody application. All other immunohistochemistry used a 4% formaldehyde fix for 1 hour. Phalloidin staining required hand-devittilinzed embryos. All fixed embryos were incubated in primary antibodies overnight with agitation at 4°C, in secondary antibodies (Alexa, Molecular Probes) for 2h at room temperature, then mounted in Aquapolymount (Poly-sciences, Warrington, PA) and imaged with a Zeiss 710 Confocal (Thornwood, NY). Antibodies and concentrations used are in Table 1.

For live imaging, embryos were bleach-dechorionated in 50% bleach, and mounted in halocarbon oil (series 700; Halocarbon Products, River Edge, NJ) between a coverslip and a permeable membrane (Petriperm; Sartorius, Edgewood, NJ or Lumox; Starsdet, GE). For high resolution movies single-plane images or 0.5uM z stacks were acquired every 5s using a

100X 1.4 NA Plan Apo VC Nikon objective on an inverted TE2000-E microscope (Nikon) with a Visitech VTHawk confocal system (Sunderland, UK) and an Orca R2 (Hammamatsu Photonics K.K.) CCD camera. Image J (http://rsb.info.nih.gov/ ij/) was used to quantitate filopodial lifetime and maximum length. Movies with z stacks were compiled as maximum intensity projections for quantification. Filopodia were manually tracked and defined as any thin protrusion (width <1.25 μm, length >1.15 μm) extending beyond the lamellipodium or leading edge. Lamellipodia were defined as protrusions >1.25 μm in width. For leading edge cells, quantitation was performed on 1 or more pairs of contralateral *engrailed* expressing stripes (as the leading edge moved from 30-15 μm apart) per embryo. For amnioserosl cells, quantitation was performed on one to two bleached cells per embryo during the mid stage of closure. In both tissues n=number of embryos analyzed per genotype. For low magnification movies, single plane images were acquired every 15 seconds using a 40X 1.3NA Plan Fluor Nikon objective on a Perkin Elmer Wallac Ultraview System (Norwalk, CT). Direct comparison of top 20% of filopodia lifetimes utilized a random number generator function in MatLab (MathWorks ,Natic MA) to reduce the n of AS cells by 12 in a non-biased manner to match that of LE cells. Statistical significance for averaged, normally distributed, datasets were determined using an unpaired student's t test or ANOVA when comparing more than two samples, while a Mann Whitney U test was used for the non-normal distribution data set associated with the 20% lifetime data. Analysis of covariance for linear regression (ANCOVA) was determined using MatLab (MathWorks,Natic MA).

Acknowledgments

We thank all members of our lab and R. Cheney for helpful discussions. We are very grateful to Dr. Tony Perdue for assistance with imaging and life, Kyle Smith for help with timelapse imaging and good taste in music, Jim Dale's accent and the BBC version of Pride and Prejudice for assistance with data analysis and Ted Salmon for emergency microscope help. Additional thanks go to D. Tatomer, C. Bilancia, S. Rogers and A. Maddox for constructive comments on the manuscript. These experiments were supported by NIH grant GM47857

Table 4.1. Fly Stocks, Antibodies and probes

Stock	Source	
Sqh Moesin-GFP	D. Kichart (Duke University, Durham, NC,USA)	
UAS-GFP-Actin	P.Martin (university of Bristol, Bristol, UK)	
UAS Moesin-GFP	D. Kichart	
UASGFPDiaΔDAD	P. Rorth (EMBL, Heidelberg, GE)	
UASHADiaΔDAD	Homem and Peifer, 2009	
GAL4 Drivers	**Expression Pattern**	
C381-GAL4	Expression starts at stage 12 in the amnioserosa	
engrailed-GAL4	Expression starting at stage 12 in engrailed expressing epidermal cells in the posterior of each segment. Occasionally a few amnioserosa cells.	
Antibody	**Dilution**	**Source**
Anti-Enabled	1:100	Developmental Studies Hybridoma Bank (DSHB)
Anti-Diaphanous	1:5000	S. Wasserman, UCSD
Anti-DE-CAD2	1:100	DSHB
Anti-Neurotactin	1:100	DSHB
Anti-Phospho-Tyrosine	1:1000	Upstate Biotechnology
Anti-lamin	1:500	DSHB
TRITC-Phalloidin	1:500	Molecular Probes
Secondary Antibodies: Alexas 488,568,647	1:500	Molecular Probes

Figure 4.1

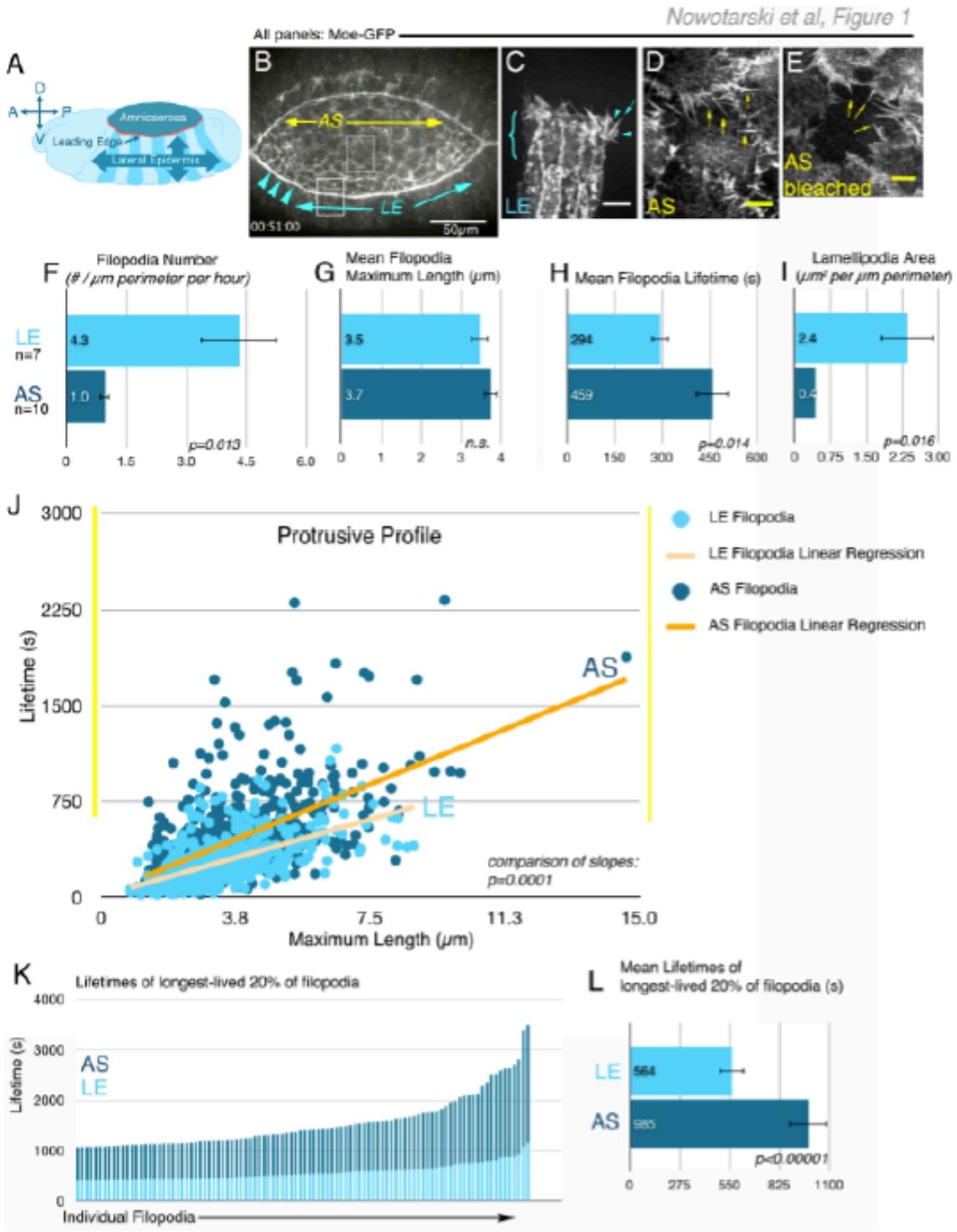
Nowotarski et al, Figure 1
All panels: Moe-GFP
A
B
C
D
E
AS
LE
AS bleached
Filopodia Number (# / µm perimeter per hour)
Mean Filopodia Maximum Length (µm)
Mean Filopodia Lifetime (s)
Lamellipodia Area (µm² per µm perimeter)
LE n=7
AS n=10
4.3
1.0
3.5
3.7
294
459
2.4
0.4
p=0.013
n.s.
p=0.014
p=0.016
J
Protrusive Profile
Lifetime (s)
Maximum Length (µm)
LE Filopodia
LE Filopodia Linear Regression
AS Filopodia
AS Filopodia Linear Regression
comparison of slopes: p=0.0001
K
Lifetimes of longest-lived 20% of filopodia
Individual Filopodia
L
Mean Lifetimes of longest-lived 20% of filopodia (s)
564
585
p<0.00001

Figure 4.1. The AS and LE cells as a model for differential regulation of protrusive behavior during normal development. For all images anterior is left. (A) Schematic, stage 14 embryo during dorsal closure (B) Maximum intensity projection movie still. dorsal closure in an embryo expressing the moesin actin binding domain fused to GFP driven in both AS and LE via *spaghetti squash* promoter. LE cells (blue), LE actin cable (arrowheads), AS cells (yellow region). Boxes indicate regions of embryo like those shown in C vs D,E. (C-E) Scale bars=5μm (C) Lateral epidermal cells expressing Moe-GFP in *engrailed* stripes. LE cells (bracket) produce filopodia (arrow) that often arise from lamellipodia (arrowheads). (D,E) AS cells (D, before bleaching; E, after bleaching central cell) produce filopodia (arrows) and fewer lamellipodia. (F-I) Quantitation of protrusive parameters of LE vs AS cells. Error Bars=SEM, n≥5 embryos. (F) LE cells produce more filopodia than AS cells. (G) Filopodia mean maximum length is the same. (H) AS cell filopodia have a longer mean lifetime than LE filopodia. (I) LE cells produce more lamellipodial area per um of perimeter. (J) Protrusive profiles of AS and LE cells=plot of filopodium maximum length vs lifetime. Slopes of linear regression illustrate AS filopodia are longer lived per unit length. Longerlived subset of AS cell filopodia indicated by yellow bars. (K) Top 20% of filopodia by lifetime from each tissue. (L) The longest lived 20% AS cell filopodia have a lifetime almost double that of the longest-lived LE filopodia.

Figure 4.2

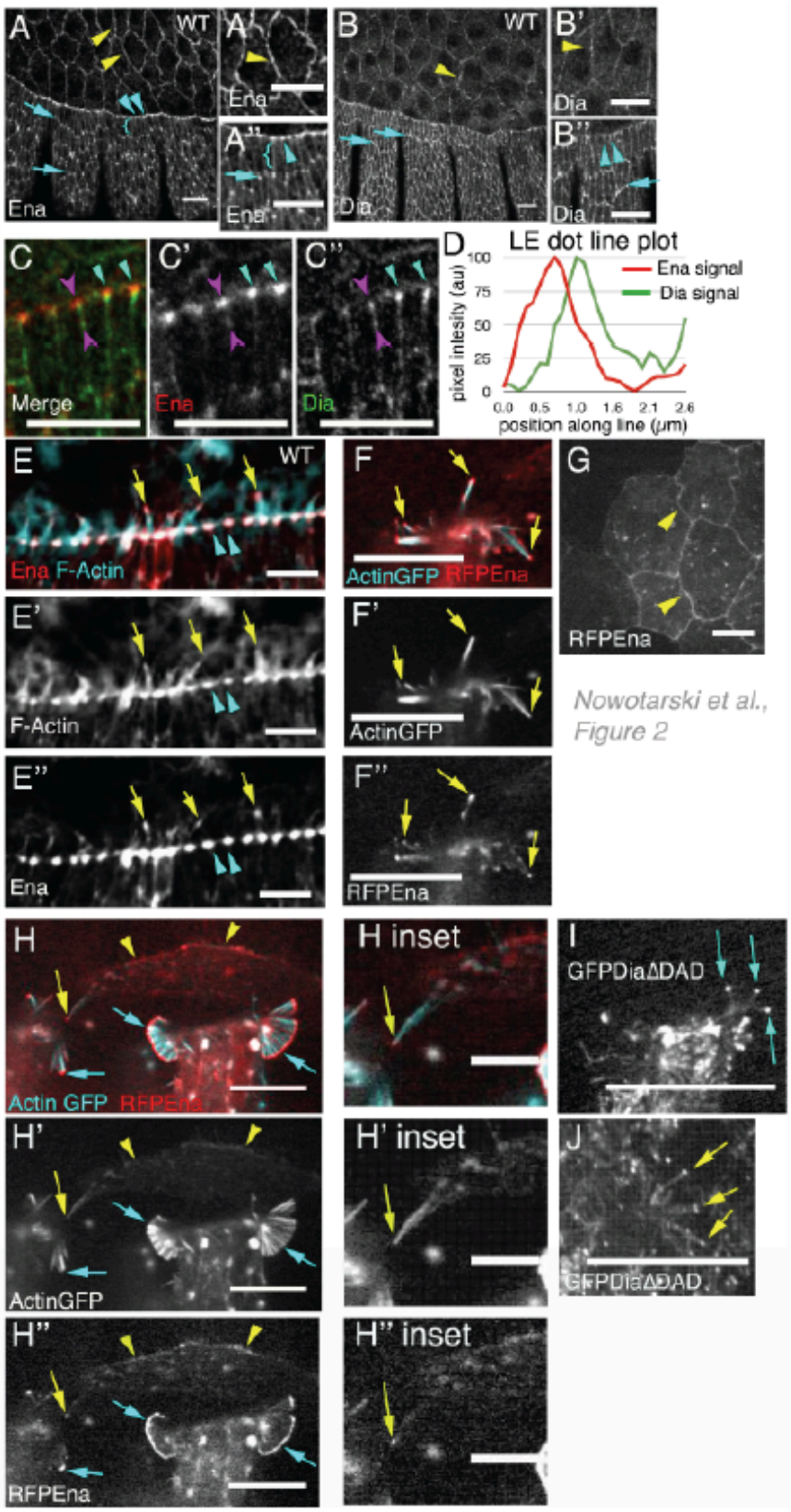
A
WT
A'
Ena
A''
Ena
Ena
B
WT
B'
Dia
B''
Dia
Dia
C
Merge
C'
Ena
C''
Dia
D
LE dot line plot
Ena signal
Dia signal
pixel intesity (au)
100
75
50
25
0
0.0 0.5 1.0 1.6 2.1 2.6
position along line (μm)
E
WT
Ena F-Actin
F
ActinGFP RFPEna
G
RFPEna
E'
F-Actin
F'
ActinGFP
E''
Ena
F''
RFPEna
Nowotarski et al.,
Figure 2
H
Actin GFP RFPEna
H inset
I
GFPDiaΔDAD
H'
ActinGFP
H' inset
J
GFPDiaΔDAD
H''
RFPEna
H'' inset

Figure 4.2. Ena and Dia localization in AS and LE cells: similarities and distinctions. Embryos, stage 13-14, anterior left and dorsal up, antigens indicated. (F-J) express the indicated protein using *engrailed* (F,H,I) or *c381* AS (G,J) GAL4 drivers. (A-A'') Ena localizes circumferentially to the AS cortex (yellow arrowheads), and in the lateral epidermis is enriched in LE dots in LE cells (cyan arrowheads) and at tricellular junctions (cyan arrows) in more ventral epidermal cells, relative to the lateral cell cortex (cyan bracket, A''). (B-B'') Dia localizes cortically in the AS (yellow arrowheads), and is cortical in the lateral epidermis with some enrichment just behind the LE (B'', cyan arrowheads) and at dorsal/ventral cell borders (arrows). (C) Ena localizes more proximal to the AS than Dia at the LE (cyan arrows) (D) Line plot of magenta arrowhead path in C. Pixel intensities normalized to a 1-100 arbitrary unit range. (E-E'') Endogenous Ena localizes to filopodia tips along the LE (arrows) and robustly localizes to LE dots (arrowheads). (F-F'') RFP-Ena also localizes to tips of LE cell filopodia (arrows). (G) When expressed in the AS RFP-Ena localizes predominantly to the cell cortex (arrowheads). (H-H'') RFP-Ena robustly localizes to tips of LE cell filopodia and filopodial fans (cyan arrows) while in an adjacent AS cell it is cortical (arrowheads) and occasionally localizes to filopodial tips (yellow arrows). (I,J) Constitutively active GFPDiaΔDAD can localize to LE filopodia tips (I, arrows) and localizes robustly to tips of AS cell filopodia (J, arrows). All scale bars=20 um except H insets which=10um.

Figure 4.3

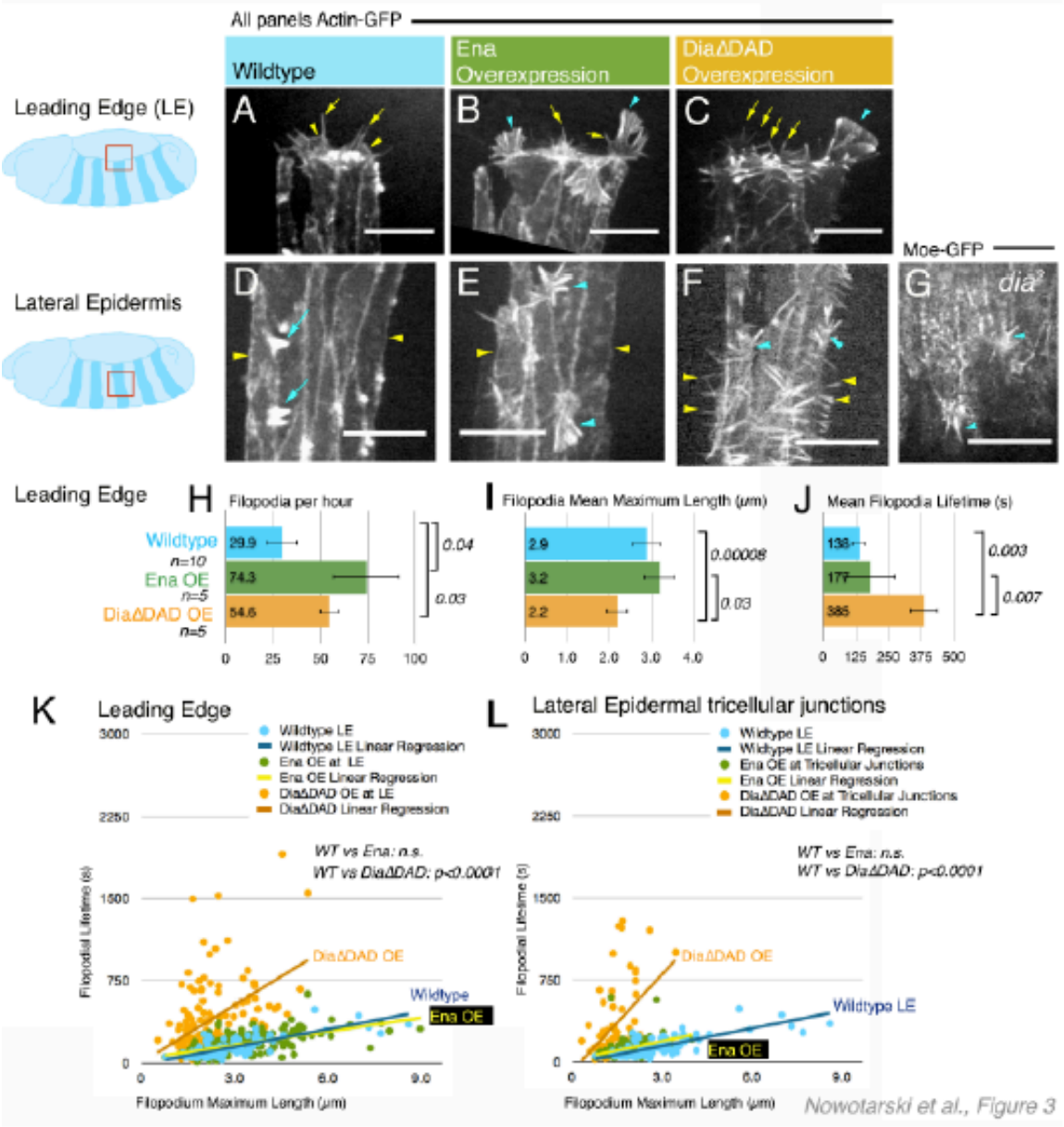
All panels Actin-GFP
Wildtype
Ena Overexpression
DiaΔDAD Overexpression
Leading Edge (LE)
A
B
C
Moe-GFP
Lateral Epidermis
D
E
F
G
dia²
Leading Edge
H
Filopodia per hour
Wildtype n=10
Ena OE n=5
DiaΔDAD OE n=5
29.9
74.3
54.6
0.04
0.03
I
Filopodia Mean Maximum Length (μm)
2.9
3.2
2.2
0.00008
0.03
J
Mean Filopodia Lifetime (s)
138
177
385
0.003
0.007
K
Leading Edge
Wildtype LE
Wildtype LE Linear Regression
Ena OE at LE
Ena OE Linear Regression
DiaΔDAD OE at LE
DiaΔDAD Linear Regression
WT vs Ena: n.s.
WT vs DiaΔDAD: p<0.0001
Filopodial Lifetime (s)
DiaΔDAD OE
Wildtype
Ena OE
Filopodium Maximum Length (μm)
L
Lateral Epidermal tricellular junctions
Wildtype LE
Wildtype LE Linear Regression
Ena OE at Tricellular Junctions
Ena OE Linear Regression
DiaΔDAD OE at Tricellular Junctions
DiaΔDAD Linear Regression
WT vs Ena: n.s.
WT vs DiaΔDAD: p<0.0001
Filopodial Lifetime (s)
DiaΔDAD OE
Wildtype LE
Ena OE
Filopodium Maximum Length (μm)
Nowotarski et al., Figure 3

Figure 4.3. Expressing Ena or active Dia at the LE induces filopodia with distinct dynamic behaviors. Schematics indicate locations of LE cells and more ventral epidermal cells and expression pattern of *engrailed* driver (dark stripes). (A-G) Stage 14 embryos expressing GFP-actin in stripes in the ventral epidermis under control of *en*-GAL4 (A-F) or moe-GFP ubiquitously (G). Scale bars=10μm (A-C) LE cells. (A) Wild-type, revealing normal filopodia (arrows) that arise from broad lamellipodia (arrowheads). (B) Overexpressing Ena yields filopodia (arrows) and morphologically distinct filopodial-fan protrusions (arrowheads). (C) Expressing constitutively active DiaΔDAD induces short filopodia (arrows) as well as fan-like structures (arrowheads). (D-G) Lateral epidermal cells. (D) Wildtype epidermal cells ventral to the LE normally do not form filopodia or lamellipodia, either laterally (arrowheads) or at tricellular junctions, but do produce actinbased dorsal hairs at the posterior borders of cells by late closure (arrows). (E) Ena overexpression yields filopodia and filopodial-fan-like protrusions at tricellular junctions (cyan arrowhead) but no lateral filopodia (yellow arrowheads) (F) DiaΔDAD overexpression induces numerous lateral filopodia (yellow arrowheads) and filopodia emerging from lamellipodia at tricellular junctions (cyan arrowheads). (G) *dia2* zygotic mutants also have filopodia emerging from tricellular junctions (cyan arrowheads). (H) Mean number of filopodia produced per hour along the LE, in the genotypes indicated. Statistics=T-test. (I) Mean maximum filopodia length (μm). (J) Mean filopodia lifetime(s). (K-L) Protrusive profile plots of maximum length (μm) vs lifetime (s) with linear regression analysis. p value by ANCOVA for slopes. (K) LE filopodia, genotypes indicated. (L) Filopodia induced at tricellular junctions.

Figure 4.4

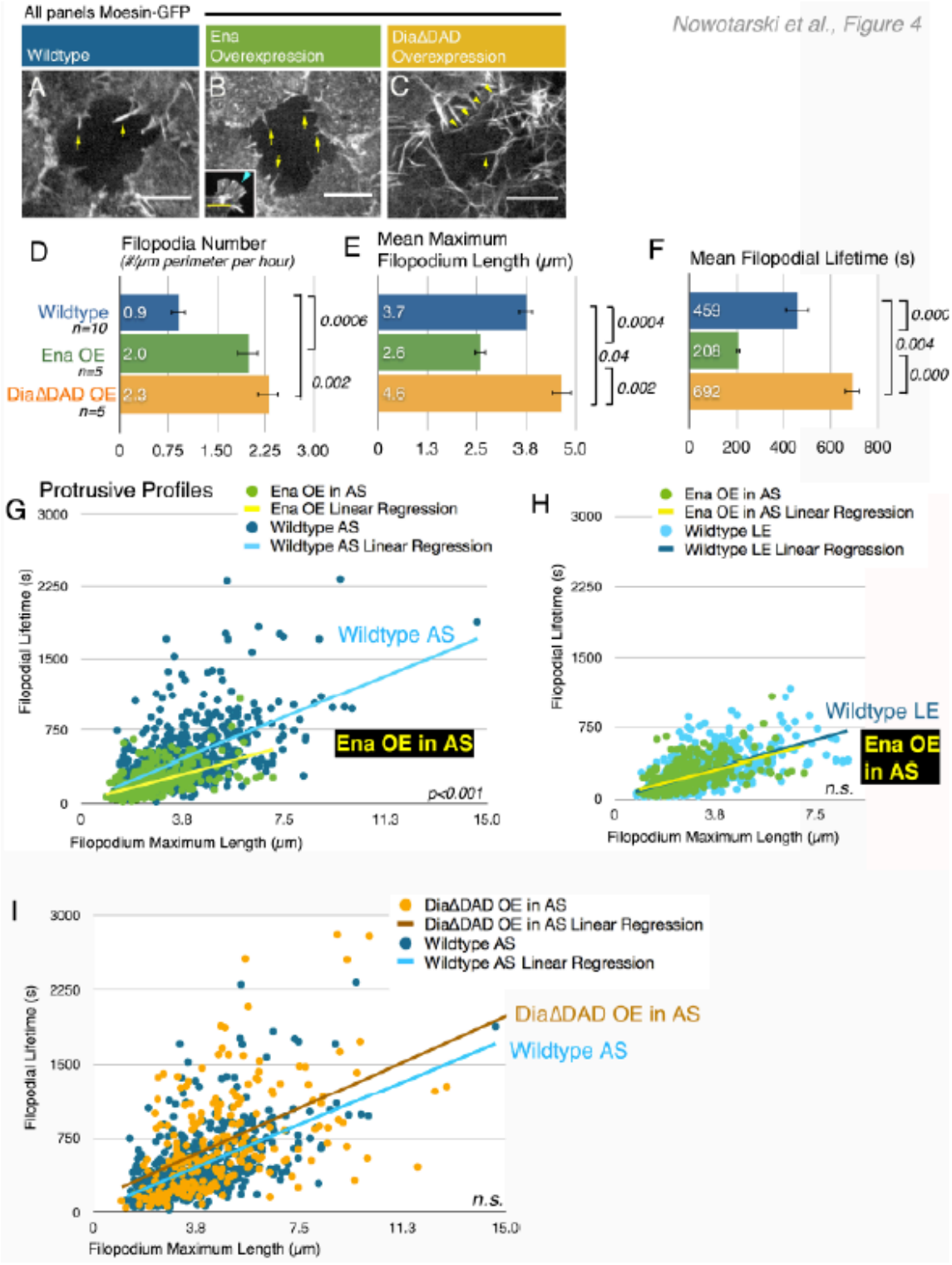
All panels Moesin-GFP
Nowotarski et al., Figure 4
Wildtype
Ena Overexpression
DiaΔDAD Overexpression
A
B
C
D
Filopodia Number
(#/μm perimeter per hour)
Wildtype n=10
Ena OE n=5
DiaΔDAD OE n=5
0.9
2.0
2.3
0.0006
0.002
0 0.75 1.50 2.25 3.00
E
Mean Maximum Filopodium Length (μm)
3.7
2.6
4.6
0.0004
0.04
0.002
0 1.3 2.5 3.8 5.0
F
Mean Filopodial Lifetime (s)
459
208
692
0.000
0.004
0.000
0 200 400 600 800
G
Protrusive Profiles
Ena OE in AS
Ena OE Linear Regression
Wildtype AS
Wildtype AS Linear Regression
Filopodial Lifetime (s)
3000
2250
1500
750
0
Wildtype AS
Ena OE in AS
p<0.001
0 3.8 7.5 11.3 15.0
Filopodium Maximum Length (μm)
H
Ena OE in AS
Ena OE in AS Linear Regression
Wildtype LE
Wildtype LE Linear Regression
Wildtype LE
Ena OE in AS
n.s.
0 3.8 7.5
Filopodium Maximum Length (μm)
I
DiaΔDAD OE in AS
DiaΔDAD OE in AS Linear Regression
Wildtype AS
Wildtype AS Linear Regression
DiaΔDAD OE in AS
Wildtype AS
n.s.
0 3.8 7.5 11.3 15.0
Filopodium Maximum Length (μm)

Figure 4.4. Elevating Ena or Dia activity in the AS have effects on protrusive behavior distinct from one another and from their effects at the LE. (A-C) Representative movie stills of AS cell bleach experiments in stage 14 embryos ubiquitously expressing Moe-GFP in genotypes indicated. Yellow arrows note filopodia. Scale Bars =10μm, except B inset= 5μm. (A) Wildtype AS cells produce filopodia (arrows) without much lamellipodia. (B) Ena overexpression increases filopodia number (arrows) but does not induce the filopodial fans seen in LE cells (B inset, arrowhead). (C) DiaΔDAD induces long filopodia (arrow, arrowheads). (D-F) Statistics via T-test (D) Mean filopodia number per um perimeter per hour. (E) Mean maximum filopodium length (μm) (F) Mean filopodial lifetime (s). (G-I) Statistical test: ANCOVA for slopes (G) Ena overexpression in the AS alters the protrusive profile, leading to shorter-lived filopodia when controlled for length. (H) Ena overexpression in the AS yields filopodia with a protrusive profile resembling that of wildtype LE cells. (I) Expressing DiaΔDAD in the AS does not significantly alter the protrusive profile slope of AS cell filopodia.

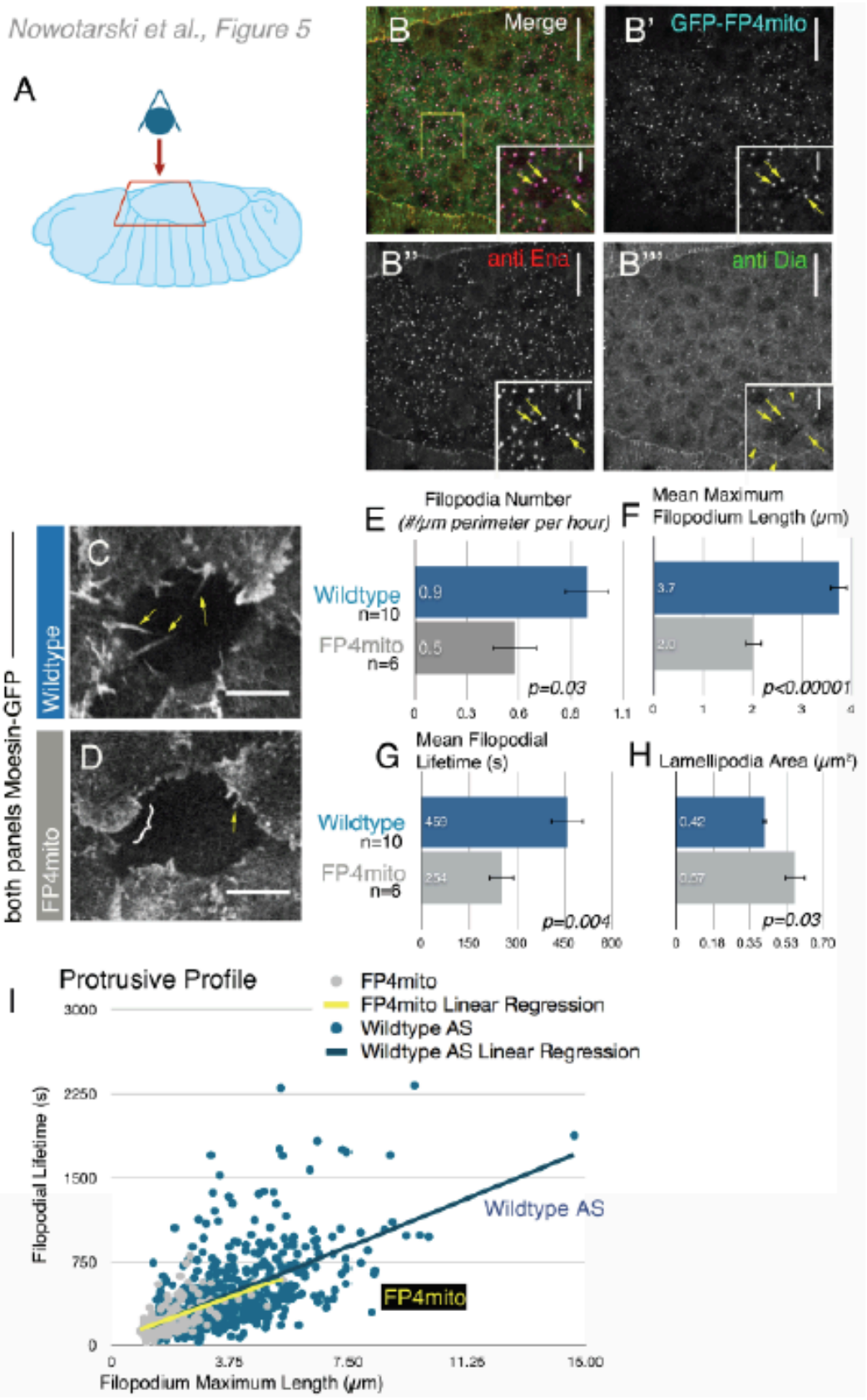
Nowotarski et al., Figure 5
A
B
Merge
B'
GFP-FP4mito
B''
anti Ena
B'''
anti Dia
both panels Moesin-GFP
Wildtype
FP4mito
C
D
E
Filopodia Number
(#/μm perimeter per hour)
Wildtype
n=10
FP4mito
n=6
0.9
0.5
p=0.03
F
Mean Maximum
Filopodium Length (μm)
3.7
2.0
p<0.00001
G
Mean Filopodial
Lifetime (s)
459
254
p=0.004
H
Lamellipodia Area (μm²)
0.42
0.27
p=0.03
I
Protrusive Profile
FP4mito
FP4mito Linear Regression
Wildtype AS
Wildtype AS Linear Regression
Filopodial Lifetime (s)
Filopodium Maximum Length (μm)
Wildtype AS
FP4mito

Figure 4.5. Expressing FP4mito in the AS attenuates filopodia initiation, length, and lifetime. (A-D). Stage 13-14 embryos. (A) Schematic illustrating view in B-D. (B-B’’’) FP4mito expression in the AS using c381 GAL4 recruits both Ena and some Dia to mitochondria. Arrows in inset = FP4mito punctae. Arrowheads = residual cortical Dia. Scale bars=20μm in B or 10μm in B insets, C and D. (C) Movie still, wild-type AS cell expressing Moe-GFP. Arrows=filopodia. (D) Representative movie still, FP4mito expression in the AS. Arrow=short filopodium, bracket=lamellipodium. (E) Mean filopodia number per um perimeter per hour (F) Mean filopodium maximum length (μm) (G) Mean filopodial lifetime (s) (H) Mean lamellipodial area. (I) FP4mito filopodia, while substantially shorter, have an unchanged protrusive profile.

Figure 4.6

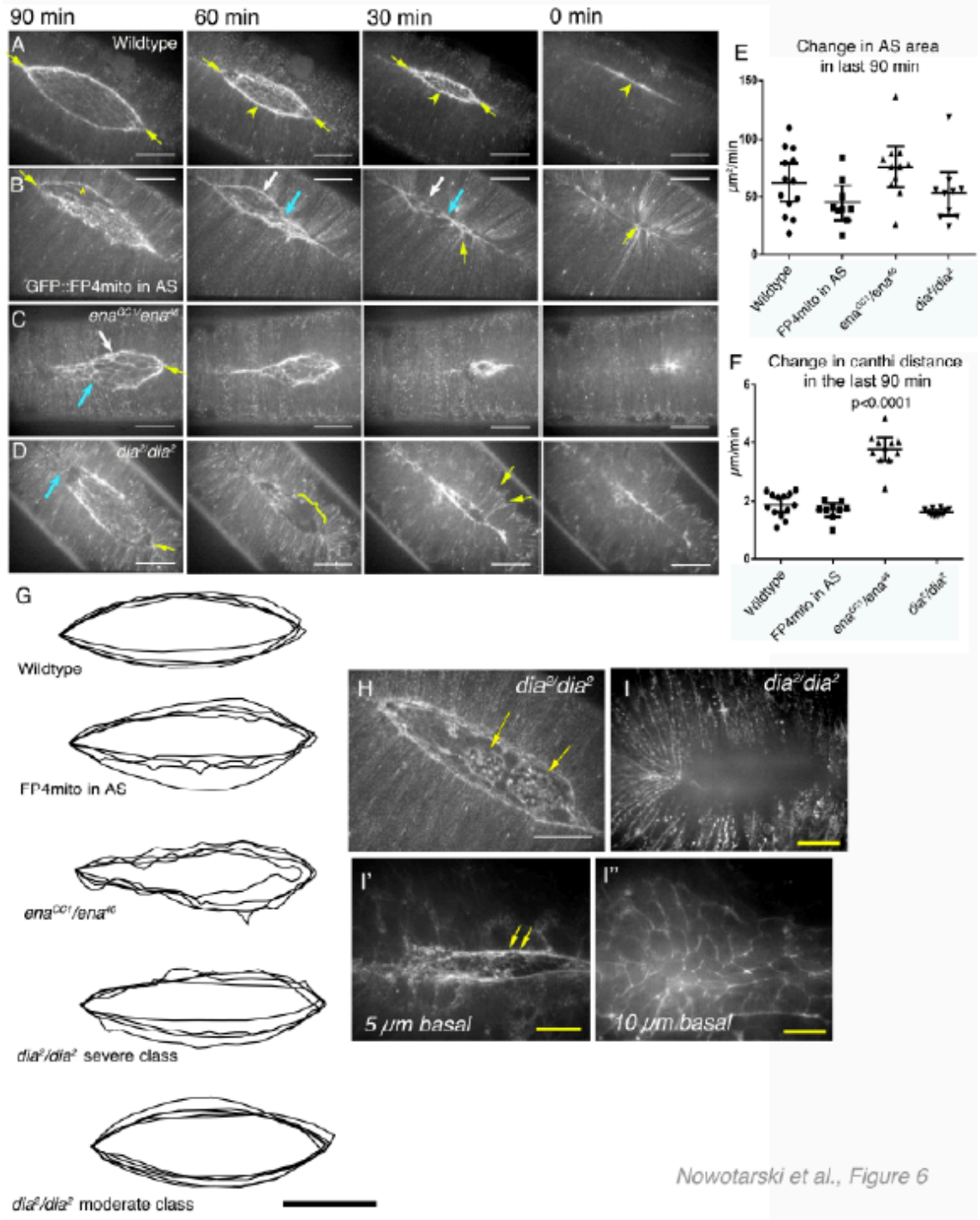
90 min
60 min
30 min
0 min
A
Wildtype
B
GFP::FP4mito in AS
C
ena^CC1/ena^46
D
dia^2/dia^2
E
Change in AS area
in last 90 min
μm²/min
Wildtype
FP4mito in AS
ena^CC1/ena^46
dia^2/dia^2
F
Change in canthi distance
in the last 90 min
p<0.0001
μm/min
Wildtype
FP4mito in AS
ena^CC1/ena^46
dia^2/dia^2
G
Wildtype
FP4mito in AS
ena^CC1/ena^46
dia^2/dia^2 severe class
dia^2/dia^2 moderate class
H
dia^2/dia^2
I
dia^2/dia^2
I'
5 μm basal
I''
10 μm basal
Nowotarski et al., Figure 6

Figure 4.6. Zygotic *ena* or *dia* mutants have substantial alteration in the process of dorsal closure but still complete closure in a timely fashion. (A-D,H,I) Movie stills, embryos expressing *sqh*-driven Moe-GFP in genotypes indicated. (A-D) Filmed from 90 min before closure. Scale bars=50μm. (A) Wildtype. Note eye shaped opening with zippering at canthi (arrows) and straight LE (arrowhead). (B) FP4 mito expressed in AS. Note alteration in shape of opening, rip between AS and LE (asterisk), differential progress of different LE cells (white and blue arrows) and puckering of epidermis (yellow arrow). (C) *ena* zygotic mutant. Note alteration in shape of opening, slowed zippering (yellow arrow), and differential progress of different LE cells (white and blue arrows). (D) *dia* zygotic mutant. Note alteration in shape of opening, rip between AS and LE (blue arrow), difference in z-plane of LE and AS (bracket) and severe puckering of the epidermis (yellow arrows). (E,F) Horizontal lines indicate mean and vertical bracket 95% CI. Statistical test = ANOVA. (E) Rates of area change in the last 90 min of closure μm2/min are unaltered. (F) Rate of canthi distance change in the last 90 min of closure differs only in *ena* mutants. (G) Representative scale matched outlines of LE actin cable aligned by anterior canthi for genotypes indicated, captured when canthi were ~160μm apart. (H) *dia* mutant displaying ripping of the AS (arrows). (I) The relationship between the epidermis and AS cells was often altered in *dia* mutants—the LE cable and AS were both several microns lower in focal plane than the lateral epidermis, unlike what we observed in wildtype.

Figure 4.7

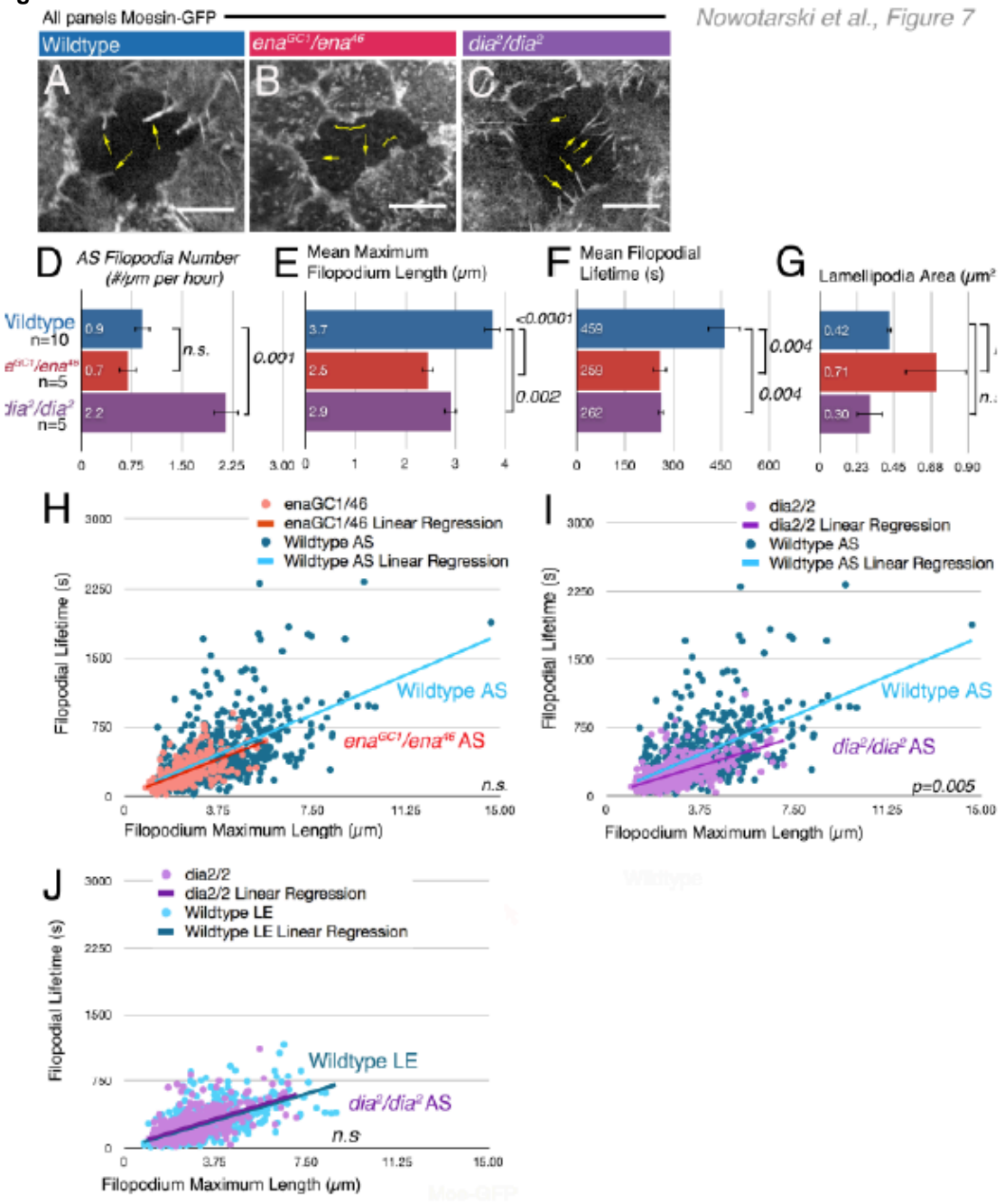
All panels Moesin-GFP
Nowotarski et al., Figure 7
Wildtype
ena^GC1/ena^46
dia^2/dia^2
A
B
C
D
AS Filopodia Number (#/µm per hour)
E
Mean Maximum Filopodium Length (µm)
F
Mean Filopodial Lifetime (s)
G
Lamellipodia Area (µm²
Wildtype n=10
n=5
n=5
n.s.
0.001
<0.0001
0.002
0.004
0.004
H
enaGC1/46
enaGC1/46 Linear Regression
Wildtype AS
Wildtype AS Linear Regression
Filopodial Lifetime (s)
Wildtype AS
ena^GC1/ena^46 AS
n.s.
Filopodium Maximum Length (µm)
I
dia2/2
dia2/2 Linear Regression
Wildtype AS
Wildtype AS Linear Regression
Filopodial Lifetime (s)
Wildtype AS
dia^2/dia^2 AS
p=0.005
Filopodium Maximum Length (µm)
J
dia2/2
dia2/2 Linear Regression
Wildtype LE
Wildtype LE Linear Regression
Filopodial Lifetime (s)
Wildtype LE
dia^2/dia^2 AS
n.s
Filopodium Maximum Length (µm)

Figure 4.7. Reducing Dia or Ena each affect AS protrusive behavior but only Dia reduction alters the protrusive profile. (A-C) Representative movie stills, AS cells, stage 13-14 embryos expressing Moe-GFP. Scale bars=10μm. (A) Wild-type AS cell. Arrows=filopodia. (B) *enaGC1/ena46* zygotic mutant. Arrows=short filopodia, bracket=lamellipodia. (C) *dia2* zygotic mutant. Arrows = filopodia. (D) Reducing Dia increases mean filopodia number while reducing Ena does not alter it. (E) Both Ena and Dia are important for mean maximum filopodium length (μm). (F) Both Ena and Dia help maintain mean filopodial lifetime of filopodia(s). (G) Lamellipodia area is statistically similar in all three genotypes. (H) In *ena* mutants length and lifetime are reduced in proportion, and thus protrusive profile is unchanged. (I) Reducing Dia alters the protrusive profile of filopodia towards shorter lifetimes at a given length. (J) Reducing Dia in the AS yields filopodia protrusive profiles more like that of WT LE filopodia.

REFERENCES

Abreu-Blanco, M. T., Verboon, J. M., and Parkhurst, S. M. (2014). Coordination of Rho family GTPase activities to orchestrate cytoskeleton responses during cell wound repair. Curr Biol *24*, 144–155.

Afshar, K., Stuart, B., and Wasserman, S. A. (2000). Functional analysis of the Drosophila diaphanous FH protein in early embryonic development. Development *127*, 1887–1897.

Antunes, M., Pereira, T., Cordeiro, J. V., Almeida, L., and Jacinto, A. (2013). Coordinated waves of actomyosin flow and apical cell constriction immediately after wounding. J Cell Biol *202*, 365–379.

Applewhite, D. A., Barzik, M., Kojima, S.-I., Svitkina, T. M., Gertler, F. B., and Borisy, G. G. (2007). Ena/VASP proteins have an anti-capping independent function in filopodia formation. Mol Biol Cell *18*, 2579–2591.

Bachmann, C., Fischer, L., Walter, U., and Reinhard, M. (1999). The EVH2 domain of the vasodilator-stimulated phosphoprotein mediates tetramerization, F-actin binding, and actinbundle formation. J Biol Chem *274*, 23549–23557.

Barzik, M., Kotova, T. I., Higgs, H. N., Hazelwood, L., Hanein, D., Gertler, F. B., and Schafer, D. A. (2005). Ena/VASP proteins enhance actin polymerization in the presence of barbed end capping proteins. J Biol Chem *280*, 28653–28662.

Bear, J. E. *et al.* (2002). Antagonism between Ena/VASP proteins and actin filament capping regulates fibroblast motility. Cell *109*, 509–521.

Bear, J. E., Loureiro, J. J., Libova, I., Fässler, R., Wehland, J., and Gertler, F. B. (2000). Negative regulation of fibroblast motility by Ena/VASP proteins. Cell *101*, 717–728.

Bilancia, C. G. *et al.* (2014). Enabled negatively regulates diaphanous-driven actin dynamics in vitro and in vivo. Dev Cell *28*, 394–408.

Block, J., Stradal, T. E. B., Hänisch, J., Geffers, R., Köstler, S. A., Urban, E., Small, J. V., Rottner, K., and Faix, J. (2008). Filopodia formation induced by active mDia2/Drf3. J Microsc *231*, 506–517.

Castrillon, D. H., and Wasserman, S. A. (1994). Diaphanous is required for cytokinesis in Drosophila and shares domains of similarity with the products of the limb deformity gene. Development *120*, 3367–3377.

Chang, F., Drubin, D., and Nurse, P. (1997). cdc12p, a protein required for cytokinesis in fission yeast, is a component of the cell division ring and interacts with profilin. J Cell Biol *137*, 169–182.

Chesarone, M. A., and Goode, B. L. (2009). Actin nucleation and elongation factors:mechanisms and interplay. Curr Opin Cell Biol *21*, 28–37.

Daou, P., Hasan, S., Breitsprecher, D., Baudelet, E., Camoin, L., Audebert, S., Goode, B. L., and Badache, A. (2014). Essential and nonredundant roles for Diaphanous formins in cortical microtubule capture and directed cell migration. Mol Biol Cell *25*, 658–668.

David, D. J. V., Tishkina, A., and Harris, T. J. C. (2010). The PAR complex regulates pulsed actomyosin contractions during amnioserosa apical constriction in Drosophila.

Development *137*, 1645–1655.

Drees.B., Friederich,E., Fradelizi,J., Louvard,D., Beckerle,M.C., and Golsteyn, R.M. (2002). Characterization of the interaction between zyxin and Ena/VASp family of proteins: implications for actin cytoskeleton organization. J.Biol.Chem. *275,* 22503-22511.

Dong, B. *et al.* (2013). Mammalian diaphanous-related formin 1 regulates GSK3β-dependent microtubule dynamics required for T cell migratory polarization. PLoS ONE *8*, e80500.

Drees, B., Friederich, E., Fradelizi, J., Louvard, D., Beckerle, M. C., and Golsteyn, R. M. Dwivedy, A., Gertler, F. B., Miller, J., Holt, C. E., and Lebrand, C. (2007). Ena/VASP function in retinal axons is required for terminal arborization but not pathway navigation. Development *134*, 2137–2146.

Echard, A., Hickson, G. R. X., Foley, E., and O'Farrell, P. H. (2004). Terminal cytokinesis events uncovered after an RNAi screen. Curr Biol *14*, 1685–1693.

Faix, J., and Grosse, R. (2006). Staying in shape with formins. Dev Cell *10*, 693–706. Fernández, B. G., Arias, A. M., and Jacinto, A. (2007). Dpp signalling orchestrates dorsal closure by regulating cell shape changes both in the amnioserosa and in the epidermis. Mech Dev *124*, 884–897.

Frank, L. H., and Rushlow, C. (1996). A group of genes required for maintenance of the amnioserosa tissue in Drosophila. Development *122*, 1343–1352.

Franke, J. D., Montague, R. A., and Kiehart, D. P. (2005). Nonmuscle myosin II generates forces that transmit tension and drive contraction in multiple tissues during dorsal closure. Curr Biol *15*, 2208–2221.

Gates, J., Mahaffey, J. P., Rogers, S. L., Emerson, M., Rogers, E. M., Sottile, S. L., Van Vactor, D., Gertler, F. B., and Peifer, M. (2007). Enabled plays key roles in embryonic epithelial morphogenesis in Drosophila. Development *134*, 2027–2039.

Gertler, F. B., Comer, A. R., Juang, J. L., Ahern, S. M., Clark, M. J., Liebl, E. C., and Hoffmann, F. M. (1995). enabled, a dosage-sensitive suppressor of mutations in the Drosophila Abl tyrosine kinase, encodes an Abl substrate with SH3 domain-binding properties. Genes Dev *9*, 521–533.

Goh, W. I., and Ahmed, S. (2012). mDia1-3 in mammalian filopodia. Commun Integr Biol *5*, 340–344.

Goh, W. I., Sudhaharan, T., Lim, K. B., Sem, K. P., Lau, C. L., and Ahmed, S. (2011). RifmDia1 interaction is involved in filopodium formation independent of Cdc42 and Rac effectors. J Biol Chem *286*, 13681–13694.

Gonçalves-Pimentel, C., Gombos, R., Mihály, J., Sánchez-Soriano, N., and Prokop, A. (2011). Dissecting regulatory networks of filopodia formation in a Drosophila growth cone model. PLoS ONE *6*, e18340.

Gorfinkiel, N., Blanchard, G. B., Adams, R. J., and Martinez-Arias, A. (2009). Mechanical control of global cell behaviour during dorsal closure in Drosophila. Development *136*, 1889–1898.

Grosshans, J., Wenzl, C., Herz, H.-M., Bartoszewski, S., Schnorrer, F., Vogt, N., Schwarz, H., and Muller, H.-A. (2005). RhoGEF2 and the formin Dia control the formation of the furrow canal by directed actin assembly during Drosophila cellularisation. Development

132, 1009–1020.

Gupton, S. L., and Gertler, F. B. (2007). Filopodia: the fingers that do the walking. Sci STKE *2007*, re5.

Gupton, S. L., Eisenmann, K., Alberts, A. S., and Waterman-Storer, C. M. (2007). mDia2 regulates actin and focal adhesion dynamics and organization in the lamella for efficient epithelial cell migration. J Cell Sci *120*, 3475–3487.

Hansen, S. D., and Mullins, R. D. (2010). VASP is a processive actin polymerase that requires monomeric actin for barbed end association. J Cell Biol *191*, 571–584.

Heisenberg, C.-P. (2009). Dorsal closure in Drosophila: cells cannot get out of the tight spot. Bioessays *31*, 1284–1287.

Hoelzle, M. K., and Svitkina, T. (2012). The cytoskeletal mechanisms of cell-cell junction formation in endothelial cells. Mol Biol Cell *23*, 310–323.

Homem, C. C. F., and Peifer, M. (2009). Exploring the roles of diaphanous and enabled activity in shaping the balance between filopodia and lamellipodia. Mol Biol Cell *20*, 5138–5155.

Hutson, M. S., Tokutake, Y., Chang, M.-S., Bloor, J. W., Venakides, S., Kiehart, D. P., and Edwards, G. S. (2003). Forces for morphogenesis investigated with laser microsurgery and quantitative modeling. Science *300*, 145–149.

Imamura, H., Tanaka, K., Hihara, T., Umikawa, M., Kamei, T., Takahashi, K., Sasaki, T., and Takai, Y. (1997). Bni1p and Bnr1p: downstream targets of the Rho family small Gproteins which interact with profilin and regulate actin cytoskeleton in Saccharomyces cerevisiae. Embo J *16*, 2745–2755.

Ingouff, M., Fitz Gerald, J. N., Guerin, C., Robert, H., Sorensen, M. B., Van Damme, D., Geelen, D., Blanchoin, L., and Berger, F. (2005). Plant formin AtFH5 is an evolutionarily conserved actin nucleator involved in cytokinesis. Nat Cell Biol *7*, 374–380.

Jacinto, A., Wood, W., Balayo, T., Turmaine, M., Martinez-Arias, A., and Martin, P. (2000). Dynamic actin-based epithelial adhesion and cell matching during Drosophila dorsal closure. Curr Biol *10*, 1420–1426.

Jacinto, A., Wood, W., Woolner, S., Hiley, C., Turner, L., Wilson, C., Martinez-Arias, A., and Martin, P. (2002a). Dynamic analysis of actin cable function during Drosophila dorsal closure. Curr Biol *12*, 1245–1250.

Jacinto, A., Woolner, S., and Martin, P. (2002b). Dynamic analysis of dorsal closure in Drosophila: from genetics to cell biology. Dev Cell *3*, 9–19.

Kiehart, D. P., Galbraith, C. G., Edwards, K. A., Rickoll, W. L., and Montague, R. A. (2000). Multiple forces contribute to cell sheet morphogenesis for dorsal closure in Drosophila. J Cell Biol *149*, 471–490.

Krause, M. *et al.* (2004). Lamellipodin, an Ena/VASP ligand, is implicated in the regulation of lamellipodial dynamics. Dev Cell *7*, 571–583.

Lai, S.-L., Chan, T.-H., Lin, M.-J., Huang, W.-P., Lou, S.-W., and Lee, S.-J. (2008). Diaphanous-related formin 2 and profilin I are required for gastrulation cell movements. PLoS ONE *3*, e3439.

Lanier, L. M., Gates, M. A., Witke, W., Menzies, A. S., Wehman, A. M., Macklis, J. D., Kwiatkowski, D., Soriano, P., and Gertler, F. B. (1999). Mena is required for neurulation and commissure formation. Neuron *22*, 313–325.

Laplante, C., and Nilson, L. A. (2006). Differential expression of the adhesion molecule Echinoid drives epithelial morphogenesis in Drosophila. Development *133*, 3255–3264.

Lebrand, C., Dent, E. W., Strasser, G. A., Lanier, L. M., Krause, M., Svitkina, T. M., Borisy, G. G., and Gertler, F. B. (2004). Critical role of Ena/VASP proteins for filopodia formation in neurons and in function downstream of netrin-1. Neuron *42*, 37–49.

Li, W., Li, Y., and Gao, F.-B. (2005). Abelson, enabled, and p120 catenin exert distinct effects on dendritic morphogenesis in Drosophila. Dev Dyn *234*, 512–522.

Loureiro, J. J., Rubinson, D. A., Bear, J. E., Baltus, G. A., Kwiatkowski, A. V., and Gertler, F. B. (2002). Critical roles of phosphorylation and actin binding motifs, but not the central proline-rich region, for Ena/vasodilator-stimulated phosphoprotein (VASP) function during cell migration. Mol Biol Cell *13*, 2533–2546.

Massarwa, R., Schejter, E. D., and Shilo, B.-Z. (2009). Apical secretion in epithelial tubes of the Drosophila embryo is directed by the Formin-family protein Diaphanous. Dev Cell *16*, 877–888.

Michelot, A., and Drubin, D. G. (2011). Building distinct actin filament networks in a common cytoplasm. Curr Biol *21*, R560–R569.

Millard, T. H., and Martin, P. (2008). Dynamic analysis of filopodial interactions during the zippering phase of Drosophila dorsal closure. Development *135*, 621–626.

Mulinari, S., Barmchi, M. P., and Hacker, U. (2008). DRhoGEF2 and diaphanous regulate contractile force during segmental groove morphogenesis in the Drosophila embryo. Mol Biol Cell *19*, 1883–1892.

Müller, H. A., and Wieschaus, E. (1996). armadillo, bazooka, and stardust are critical for early stages in formation of the zonula adherens and maintenance of the polarized blastoderm epithelium in Drosophila. J Cell Biol *134*, 149–163.

Narasimha, M., and Brown, N. H. (2004). Novel functions for integrins in epithelial morphogenesis. Curr Biol *14*, 381–385.

Pasic, L., Kotova, T., and Schafer, D. A. (2008). Ena/VASP proteins capture actin filament barbed ends. J Biol Chem *283*, 9814–9819.

Pawson, C., Eaton, B. A., and Davis, G. W. (2008). Formin-dependent synaptic growth: evidence that Dlar signals via Diaphanous to modulate synaptic actin and dynamic pioneer microtubules. J Neurosci *28*, 11111–11123.

Peng, J., Wallar, B. J., Flanders, A., Swiatek, P. J., and Alberts, A. S. (2003). Disruption of the Diaphanous-related formin Drf1 gene encoding mDia1 reveals a role for Drf3 as an effector for Cdc42. Curr Biol *13*, 534–545.

Peng, Y., Han, C., and Axelrod, J. D. (2012). Planar polarized protrusions break the symmetry of EGFR signaling during Drosophila bract cell fate induction. Dev Cell *23*, 507–518.

Pollard, T. D., and Borisy, G. G. (2003). Cellular motility driven by assembly and disassembly of actin filaments. Cell *112*, 453–465.

Raich, W. B., Agbunag, C., and Hardin, J. (1999). Rapid epithelial-sheet sealing in the Caenorhabditis elegans embryo requires cadherin-dependent filopodial priming. Curr Biol *9*,1139–1146.

Reed, B. H., Wilk, R., and Lipshitz, H. D. (2001). Downregulation of Jun kinase signaling in the amnioserosa is essential for dorsal closure of the Drosophila embryo. Curr Biol *11*, 1098–1108.

Reim, I., Lee, H.-H., and Frasch, M. (2003). The T-box-encoding Dorsocross genes function in amnioserosa development and the patterning of the dorsolateral germ band downstream of Dpp. Development *130*, 3187–3204.

Rottner, K., Behrendt, B., Small, J. V., and Wehland, J. (1999). VASP dynamics during lamellipodia protrusion. Nat Cell Biol *1*, 321–322.

Roy, S., Huang, H., Liu, S., and Kornberg, T. B. (2014). Cytoneme-mediated contactdependent transport of the Drosophila decapentaplegic signaling protein. Science *343*, 1244624.

Rørth, P. (2009). Collective cell migration. Annu. Rev. Cell Dev. Biol. *25*, 407–429.
Sanders, T. A., Llagostera, E., and Barna, M. (2013). Specialized filopodia direct long-range transport of SHH during vertebrate tissue patterning. Nature *497*, 628–632.

Schirenbeck, A., Arasada, R., Bretschneider, T., Stradal, T. E. B., Schleicher, M., and Faix, J. (2006). The bundling activity of vasodilator-stimulated phosphoprotein is required for filopodium formation. Proceedings of the National Academy of Sciences of the United States of America *103*, 7694–7699.

Schirenbeck, A., Bretschneider, T., Arasada, R., Schleicher, M., and Faix, J. (2005). The Diaphanous-related formin dDia2 is required for the formation and maintenance of filopodia. Nat Cell Biol *7*, 619–625.

Shi, Y., Zhang, J., Mullin, M., Dong, B., Alberts, A. S., and Siminovitch, K. A. (2009). The mDial formin is required for neutrophil polarization, migration, and activation of the LARG/RhoA/ROCK signaling axis during chemotaxis. J. Immunol. *182*, 3837–3845.

Solon, J., Kaya-Copur, A., Colombelli, J., and Brunner, D. (2009). Pulsed forces timed by a ratchet-like mechanism drive directed tissue movement during dorsal closure. Cell *137*, 1331–1342.

Svitkina, T. M., Bulanova, E. A., Chaga, O. Y., Vignjevic, D. M., Kojima, S.-I., Vasiliev, J. M., and Borisy, G. G. (2003). Mechanism of filopodia initiation by reorganization of a dendritic network. J Cell Biol *160*, 409–421.

Swan, K. A., Severson, A. F., Carter, J. C., Martin, P. R., Schnabel, H., Schnabel, R., and Bowerman, B. (1998). cyk-1: a C. elegans FH gene required for a late step in embryonic cytokinesis. J Cell Sci *111 (Pt 14)*, 2017–2027.

Tanizaki, H. *et al.* (2010). Rho-mDia1 pathway is required for adhesion, migration, and Tcell stimulation in dendritic cells. Blood *116*, 5875–5884.

Thumkeo, D., Shinohara, R., Watanabe, K., Takebayashi, H., Toyoda, Y., Tohyama, K., Ishizaki, T., Furuyashiki, T., and Narumiya, S. (2011). Deficiency of mDia, an actin nucleator, disrupts integrity of neuroepithelium and causes periventricular dysplasia. PLoS ONE *6*, e25465.

Tolliday, N., VerPlank, L., and Li, R. (2002). Rho1 directs formin-mediated actin ring assembly during budding yeast cytokinesis. Curr Biol *12*, 1864–1870.

Tominaga, T., Sahai, E., Chardin, P., McCormick, F., Courtneidge, S. A., and Alberts, A. S. (2000). Diaphanous-related formins bridge Rho GTPase and Src tyrosine kinase signaling. Mol Cell *5*, 13–25.

Tucker, P. K., Evans, I. R., and Wood, W. (2011). Ena drives invasive macrophage migration in Drosophila embryos. Dis Model Mech *4*, 126–134.

Vasioukhin, V., Bauer, C., Yin, M., and Fuchs, E. (2000). Directed actin polymerization is the driving force for epithelial cell-cell adhesion. Cell *100*, 209–219.

Watanabe, S. *et al.* (2013). Loss of a Rho-regulated actin nucleator, mDia2, impairs cytokinesis during mouse fetal erythropoiesis. Cell Rep *5*, 926–932.

Winkelman, J. D., Bilancia, C. G., Peifer, M., and Kovar, D. R. (2014). Ena/VASP Enabled is a highly processive actin polymerase tailored to self-assemble parallel-bundled F-actin networks with Fascin. Proceedings of the National Academy of Sciences of the United States of America *111*, 4121–4126.

Wood, W., and Martin, P. (2002). Structures in focus--filopodia. Int J Biochem Cell Biol *34*, 726–730.

Woolner, S., Jacinto, A., and Martin, P. (2005). The small GTPase Rac plays multiple roles in epithelial sheet fusion--dynamic studies of Drosophila dorsal closure. Dev Biol *282*, 163–173.

Yamana, N. *et al.* (2006). The Rho-mDia1 pathway regulates cell polarity and focal adhesion turnover in migrating cells through mobilizing Apc and c-Src. Mol Cell Biol *26*, 6844–6858.

Yang, C., Czech, L., Gerboth, S., Kojima, S.-I., Scita, G., and Svitkina, T. (2007). Novel roles of formin mDia2 in lamellipodia and filopodia formation in motile cells. PLoS Biol *5*, e317.

Young, P. E., Pesacreta, T. C., and Kiehart, D. P. (1991). Dynamic changes in the distribution of cytoplasmic myosin during Drosophila embryogenesis. Development *111*, 1–14.

CHAPTER 5: DISCUSSION

Proper regulation of the actin cytoskeleton is integral for tissue homeostasis, wound healing and, as this work highlights, proper development. Regulation of the actin cytoskeleton is directly mediated by actin binding proteins, which influence the geometry of the actin network. In my thesis work I have explored the roles of three actin-binding proteins, Ena, Dia and CP, in dynamic morphogenetic processes in *Drosophila* oogenesis and embryonic development. We first found that the antagonistic relationship between Ena and CP is important for several events in oogenesis. Second, we documented that Ena binds and inhibits Dia and provided evidence of this relationship *in vivo* in the epidermis of embryos during the morphogenetic process of dorsal closure. Finally, we built on our *in vitro* knowledge of the distinct biochemical properties of Ena and Dia on barbed ends to explore how these are used *in vivo*, revealing that in the two tissues contributing to dorsal closure, each regulator contributes differently to protrusive behavior. This new knowledge, combined with other work in the field and past work in our lab, raises many questions that remain to be explored.

Understanding Ena and Dia as machines

Recent advances in our knowledge have clarified the mechanisms of action of individual actin regulators and are beginning to offer insights into how they work together. However, these advances have left many questions to address. While we know much more about how Ena and Dia interact as machines, there are still outstanding questions surrounding the details of the exact mechanism by which they interact.

Chapter 3 details work relating to how Ena and Dia work together, addressing the large scale question of why there are two actin polymerizers in the first place, rather than one that

is heavily regulated. We find that *in vitro*, Ena's EVH1 domain binds Dia's FH1 domain and that this interaction negatively regulates Dia's action on actin in cell culture and *in vivo*, presumably at the nucleation step. This data, combined with the fact that Dia is a 7x more processive and 2x faster elongator than Ena, led to a model where perhaps Ena's regulation of Dia allows for a more rapid release mechanism for Dia in areas needing a fast actin response, rather than Dia having to go through multiple rounds of autoinhibition and membrane targeting.

Exactly how the interaction between the FH1 and EVH1 domain abrogates Dia's actin nucleation remains unclear. One attractive mechanism is that the EVH1-FH1 binding induces a conformational change in Dia's adjacent FH2 actin binding domain. Before we can speculate further, visualization of Actin, EnaEVH1 and DiaFH1FH2 in *in vitro* TIRF actin assembly assays will need to be completed, facilitating further data- driven hypotheses. In addition, further dissection of this interaction in cell culture and *in vivo* requires a direct perturbation of the Ena-Dia interaction. Devising a direct perturbation is problematic, as both Ena's EVH1 domain and Dia's FH1 domain are utilized for interactions with other proteins (multiple partners like zyxin for the EVH1 via the FPPPP consensus sequence and profilin for the FH1). Further complicating matters, the full FH1 domain is required for EVH1 binding and the FH1 appears to require canonical EVH1 binding, as mutation of the integral phenylalanine abolishes FH1 binding. It may be that upon reexamination of the EVH1 crystal structure, we may be able to try another series of mutations looking for those that weaken Dia binding without affecting other partners, but this may be unlikely. Differential binding could be assessed by IP of Dia and other known partners.

Understanding regulation of Ena and Dia during dorsal closure

The work in Chapters 3&4 documents and suggests different roles for Ena and Dia *in vivo* during dorsal closure. We found that Ena and Dia govern protrusive activity in different tissues and that in each tissue their function is likely different. Chapter 4 describes detailed quantification of protrusive behavior in the two tissues that contribute to dorsal closure — the LE cells of the lateral epidermis and the central AS cells — and reports that Ena directs

protrusive behavior along the LE and that Dia plays a greater role than Ena in filopodial lifetime in the AS. One immediate concern regarding these protrusive differences is that the differential role may be largely due to differences in relative protein levels in each tissue. Thus, it will be important to try cell dissociation and tissue specific FACs sorting, to obtain pure populations of leading edge or amnioserosa cells, allowing western blotting to parse this out.

Another possible reason for tissue specific roles in regulating protrusive activity may be due to another potentially different biochemical property between Ena and Dia: affinity and preference for profilin-actin. Around 50% of monomeric actin in the cells is postulated to be bound to profilin (Pollard & Cooper, 2009), thus placing profilin in a position of power with regard to where monomers go. It is well documented that the elongation rate of formins are increased in the presence of profilin-actin (Breitsprecher & Goode, 2013). We found this increase in rate is also true for *Drosophila* Dia (11.9 subunits/sec vs. 72.6 subunits/sec; Chapter 3). However, unlike other formins, *Drosopshila* Dia can also increase elongation rate with just actin alone, but only two-fold — compared to the seven-fold increase in presence of profilin-actin (Chapter 3). Thus, profilin appears to play a role in polymerization rates in *Drosophila*. What about Ena's preference for profilin-actin? While human VASP can increase elongation rate in the presence of profilin-actin (Hansen & Mullins, 2010), *Drosophila* Ena-based polymerization is indifferent to profilin presence in assays (Chapter3; Winkelman, Bilancia, Peifer, & Kovar, 2014). One could then imagine that Dia's affinity and ability to recruit profilin-actin would shift polymerization power away from Ena. It will be important to assess levels of profilin in each tissue to start to address if Dia's dominant role in the AS is directly related to its biochemical affinity for profilin.

This body of research also addressed how Ena and Dia work together and revealed interesting information about their relationship within and between two tissue types. In the lateral epidermis, Ena directs protrusive activity at places where it endogenously localizes in the lateral epidermis—to polarized spots at tricellular junctions and along the LE. Dia is competent to be active all over the cortex in the epidermis but is: (1) not normally active here

and (2) negatively regulated by Ena at places where Ena levels are high. In the AS, neither Ena nor Dia reveal a polarized localization, but are both isotropically distributed along the cortex. Both the differences in localization as well as spatial differences in activity within the lateral epidermis raise further questions.

First, how is Ena localized differentially in the two tissues during dorsal closure? This is likely to be partially explained by differences in localization and recruitment by different known EVH1 binding partners. Thus, analysis of Ena localization in EVH1 binding partner mutants or RNAi lines needs to be carried out – Vinculin and Pico (Lamellipodin) are good candidates for differential localization. Lamellipodin has been shown to be responsible for recruitment of Ena/VASP to the cell membrane in mammalian cells (Krause et al., 2004), while the *Drosophila* homolog Pico has been reported to localize to the cortex of nurse cells in oogenesis prior to dumping (Huelsmann, Ylänne, & Brown, 2013), where we see Ena at the tips of cytoplasmic actin filaments (Gates et al., 2009; Huelsmann et al., 2013).Vinculin also binds Ena and plays roles in force-sensing at focal adhesions and cell-cell junctions (see below and addendum; Carisey et al., 2013; Grashoff et al., 2010; Renfranz & Beckerle, 2002).

Secondly, if Dia is competent to be active all over the cortex but normally isn't, where is active Dia? Dia is normally held in an autoinhibited state, facilitated by an interaction between it's DAD and DID domains, and this inhibition is relieved by Rho binding which exposes Dia's FH1 and FH2 domains (Alberts, 2001; Gorelik, Yang, Kameswaran, Dominguez, & Svitkina, 2011; Li & Higgs, 2003; T. Otomo, Otomo, Tomchick, Machius, & Rosen, 2005; Rose et al., 2005). Our current Dia antibody (generated by the Wasserman lab at UCSD) recognizes both conformations, and because full length tagged protein is highly cytoplasmic, thus likely largely revealing the auto-inhibited form, these tools are largely unhelpful in addressing this question. However, a constitutively active altered form of Dia, lacking its autoinhibitory DAD domain, can and has yielded information about Dia's activity and regulation. Expression of this construct in the wildtype background has allowed us to hypothesize where Dia is normally autoinhibited based on actin phenotypes.

However, overexpression of an altered form of Dia may produce dominant negative effects as Dia dimerizes in its active form on actin barbed ends and can participate in transinhibition via the DID-DAD interaction. Further, as was mentioned in the discussion of Chapter 3, both actin and nucleation promoting factors can bind the DAD domain of formins to enhance actin assembly (Breitsprecher et al., 2012; Gould et al., 2011; Graziano, Jonasson, Pullen, Gould, & Goode, 2013; Heimsath & Higgs, 2012; Jaiswal et al., 2013; Moseley et al., 2004; Okada et al., 2010). Thus, overexpression of DiaΔDAD is not an ideal tool. It would be useful to have a less disruptive sensor to reveal the spatiotemporal and tissue specificity of the active form of Dia. A readily accessible idea would be to produce an antibody that can only bind the open conformation of Dia, much like the tension sensing α-catenin antibody, a18 (Yonemura, Wada, Watanabe, Nagafuchi, & Shibata, 2010). Three regions of Dia would be candidates for this antibody production, both the DID or DAD (available only when not bound to each other) and perhaps the FH1 domain, as the FH1 and FH2 domains are potentially uncovered under autoinhibition relief. It is tempting to further speculate that with this reagent in hand, we *may* be able identify tissues — and perhaps even subcellular localizations that would co-label for both Ena antibody staining and this new, open, and presumably active Dia antibody — to reveal a spatiotemporal catalog of places and times where Ena and Dia interaction is potentially important.

Finally, how are both Ena and Dia regulated in each tissue during dorsal closure? Members of the Rho family of GTPases are known to regulate the cytoskeleton. In the case of Dia, this link is direct, with Rho binding the GBD domain alleviating autoinhibition and allowing cortical recruitment of the active form of the protein (Alberts, 2001; Gorelik et al., 2011; Li & Higgs, 2003; T. Otomo et al., 2005; Rose et al., 2005). In mammalian cell culture, Ena/VASP is linked indirectly to both Cdc42 activity and Rap1 activity by the membrane deforming and curvature sensing protein IRSp53 (Disanza et al., 2013) and the MRL family of proteins— RIAM and Lamellipodin (Pico; reviewed in Legg & Machesky, 2004), respectively. Use of tissue-specific driven, dominant negative, and constitutively active proteins has revealed that the Rho family GTPases play partially redundant roles

during dorsal closure (Harden, Loh, Chia, & Lim, 1995; Harden, Ricos, Ong, Chia, & Lim, 1999). Rac is required for proper LE actin cable formation as well as protrusive activity from the LE cells though dorsal closure still proceeds to completion as AS cells can still constrict properly and draw the LE cells together (Woolner, Jacinto, & Martin, 2005). Cdc42 is important for establishment and maintenance of the LE cytoskeleton and influences DPAK levels (Harden et al., 1999). Rho regulates the LE cytoskeleton in segment border cells (Harden et al., 1999), most likely via Dia (Homem & Peifer, 2008). These overlapping roles, combined with potential indirect effects of multiple GTPases on Ena, make understanding how they regulate Ena and Dia challenging to parse out. It would be best to work up the pathway starting with direct binding partners. However, in the long run it would be helpful to gain a better spatiotemporal resolution of GTPase activity by moving currently used activity sensor probes (modified for *Drosophila* expression) into the dorsal closure model through tissue specific expression. The GTPase switch is flipped by GAPs and GEFs and it will also be useful to look at which of these yield dorsal closure defects.

Moving closer to direct regulation of Ena and Dia, the aforementioned multiple EVH1 domain-binding partners provide an easily testable approach for requirement for Ena localization. While localization is important, we also need to think about activity. In regards to potential active vs. inactive pools of Ena, it is important to think about another binding partner, Abelson Kinase (Abl). Ena was originally identified in a screen for proteins that rescue *abl* phenotypes (Gertler, Doctor, & Hoffmann, 1990) and subsequent work from our lab has shown that *abl* maternal and zygotic mutants have dorsal closure defects: dorsal closure is slowed, LE cells have obvious defects in actin cable formation and Ena is no longer uniformly distributed along the LE dots (Grevengoed, Loureiro, Jesse, & Peifer, 2001). Further work from our lab in which I was involved also revealed that flies expressing a constitutively active form of Abl, while largely able to complete dorsal closure, have defects—including a reduction of filopodia produced by the LE cells. Ena is a key target of activated Abl here, as the active Abl defects are enhanced by reducing Ena on top of its negative regulation and are also alleviated by Ena overexpression (Stevens et al., 2008). The

data above combined with the observation that punctae of Ena can be followed traveling from LE dots to filopodial tips with live confocal microscopy (Homem & Peifer, 2009) has led to the hypothesis that the LE dots are storage places for Ena and that Ena is held there by Abl, poised for deployment to protrusions. This hypothesis still remains to be tested, and it will be of interest to look at Ena turnover rates at this location while modulating Abl activity. Answering this question, in tandem with understanding how other binding partners interact with Ena, will start to address this larger question: How is protrusive activity restricted in a polarized manner to the dorsal edge of the LE cells?

The fact that Ena overexpression produces ectopic protrusive behavior at places where Ena normally localizes, like the LE and even more interestingly, at the tricellular junctions, raises questions as to how Ena's localization is polarized in the lateral epidermis at these locations. Negative regulation by Abl may provide a partial explanation for this along the LE dots, and it appears at the tricellular junctions that Abl is part, but not all of the equation. While Ena overexpression produces ectopic actin structures in the shape of filopodia on the cell exterior, loss of Abl induces internal actin flares at this location (Rogers et al., unpublished data), suggesting both that Abl does more at this location than just sequester Ena and that either something about loss of Abl changes the underlying actin so that Ena cannot induce ectopic protrusions, and/or that loss of Abl changes location/activity of another Ena binding partner needed at the membrane to induce actin polymerization outward into filopodial protrusions.

Both of these locations — the LE dots (where the actin cable is anchored) and the lateral epidermal tricellular junctions — are areas experiencing tension. Work in epithelial sheets is beginning to point at tricellular junctions as places experiencing tension (Ebrahim et al., 2013; Trichas et al., 2012). Laser ablation experiments from the Kiehart lab have shown that the LE actin cable where LE dots are located, as well as the more ventral lateral epidermis, are both under tension (Kiehart, Galbraith, Edwards, Rickoll, & Montague, 2000). Further, work from several labs shows the LE dots accumulate both junctional proteins, as well as proteins associated with focal adhesions and stress fibers (Tulu and Kiehart, personal

communication; Grevengoed et al., 2001; Narasimha & Brown, 2004), and are in very close proximity to integrin localization (Narasimha & Brown, 2004). We consider tension as a recruitment mechanism below.

Thus, binding partners and tension likely regulate Ena's polarized localization at tricellular junctions and LE dots, and Dia's activity at the cell cortex is likely to be regulated by Rho, also connected to tension. Previous work in the lab has shown that expression of a constitutively active form of Dia lacking both the GBD and DAD domain induces premature contractility in AS cells and segmental groove cells in the lateral epidermis (Homem & Peifer, 2008). The model for this activity holds that Dia activation stabilizes both actin and active myosin at adherens junctions. We explore this relationship between actin, myosin and junctions further below.

Forcing a move towards a junction

During development cells must maintain a balance between being able to change shape and move (using the actomyosin cytoskeleton to generate force), with maintaining tissue integrity, via cell – cell adhesive junctions. Actin is at the center of this, playing integral roles at cell – cell junctions (junctional actin), in cell motility and shape change, as well as in actomyosin-based contractility. Just as the actin cytoskeleton is locally plastic, with local changes in regulators affecting geometry, the shared finite cellular pool of actin monomers makes junctional actin, actomyosin, and cortex actin all a part of a single network where presumably large changes in one can affect another.

Actin itself is a platform for force; F-actin is an inherently stiff rod when shorter than it's persistent length of 10μm (Harasim, Wunderlich, Peleg, Kröger, & Bausch, 2013) and filaments in this range can be bent by the buckling force put on them by both motors and polymerizers (reviewed in Blanchoin, Boujemaa-Paterski, Sykes, & Plastino, 2014). F-actin can be used as a platform for force in the cell as processive assemblies of myosin motor protein bind to stiff, anti-parallel bundled actin filaments and then pull to generate contractile force capable of driving deformation of cell shape. Two well-characterized places where actomyosin plays a role are at medial actomyosin networks at the cortex and at the Adherens

junctions (AJs) in junctional actomyosin (Engl, Arasi, Yap, Thiery, & Viasnoff, 2014; K. C. Liu & Cheney, 2012; Simões, Mainieri, & Zallen, 2014). Importantly, the medial myosin network is connected to junctional actomyosin and this connection is integral to couple contraction of the medial network to deformation of the junctions, resulting in cell shape change.

One of the best examples of this net cell shape change mediated by actomyosin is during *Drosophila* gastrulation. Here, the actomyosin network induces apical constriction in ventral furrow cells, which facilitates internalization of the mesoderm (Dawes-Hoang et al., 2005; A. C. Martin, Kaschube, & Wieschaus, 2009). In this model tissue, coupling of the medial actomyosin network to junctional actomyosin is integral for shape change and maintenance of the shrinking apical domain via a ratchet, which is provided by the transcriptional regulator Twist (A. C. Martin et al., 2009). During dorsal closure AS cells undergo much the same process, but here the ratchet mechanism is provided by the LE actin cable (Solon, Kaya-Copur, Colombelli, & Brunner, 2009).

Could contractility in the AS cells be connected to the filopodia observed in the AS? When cells apically constrict, the junctional domain is shortened, as is the apical membrane. Perhaps the filopodia produced by the AS cells are a storage place for membrane while cell area is shrinking? While this may be a conserved event in apical constriction, other *Drosophila* cells that apically constrict, such as ventral furrow cells, are much smaller apically and actin-based protrusions may be harder to document. The increasing ability to challenge and bypass the resolution limits of light microscopy may reveal these in time. Another potential and not mutually exclusive explanation for these filopodia in the AS is a shift in the pan-cellular actin network. During the AS cell shape change, the shrinking cortex and junctions may make a large pool of g-actin available. Assessment of the ratio between F and G actin levels during closure would start to address this.

At least in the case of apical constriction in the ventral furrow cells, the actomyosin ratchet mechanism requires proper adhesion as tears arise in *arm* RNAi embryos (A. C. Martin, Gelbart, Fernandez-Gonzalez, Kaschube, & Wieschaus, 2010). This combined with

the idea that the leading edge actin cable during dorsal closure would likely not form a proper ratchet without being able to adhere to the underlying AS cells (Narasimha & Brown, 2004; Solon et al., 2009) makes the coupling of adhesion to cell shape change interesting. Recent work in press from the Yap lab has shown a positive feedback loop between actin polymerization at junctions and contractility mediates force strengthening at junctions (see addendum; Leerberg et al., in press). While Arp2/3 has been linked to AJ formation in *Drosophila* (see below), in the Yap lab's cell culture model, actin polymerization increases in response to applied force and this is mediated through vinculin-recruited Mena/VASP (see addendum). While *ena* maternal and zygotic mutants do not appear to have strong defects in overall junctional integrity (Gates et al., 2007), it may be playing a strengthening role, especially in cells experiencing tension, like the leading edge cells. Leading edge cell actin cable integrity or its connection to cell – cell junctions may thus depend on Ena (Choi et al., 2011). In the AS, Ena localizes robustly to the AS cell cortex, more so than to filopodia tips (Chapter 4). Due to this, it is interesting to speculate that perhaps Ena's role here is to help strengthen junctions in response to force generated by myosin. This could be tested using a weak mutation of DE-cadherin in tandem with Ena loss, or by laser cutting of AS cell junctions in an *ena* mutant. Further, pairing an *ena* zygotic mutant with an endogenous DE-Cadherin fluorescent reporter may yield additional information, allowing us to measure the amplitude and period of myosin-based amnioserosal cell contraction. Since in the colon cell model above, E-cadherin organization is dependent on Mena/VASP, it will also allow us to explore levels of cadherin at junctions.

To take this even further, if Ena plays roles responding to force and reinforcing junctions in response to tension *in vivo,* it will be important to determine if this is a tissue/time specific role of Ena at junctions in dorsal closure or a conserved function across embryonic development. Luckily, there are other well-documented places and times in *Drosophila* embryonic development where actomyosin contractility generates tension. One such place is the previously discussed ventral furrow formation. A second is during germband extension, where the DV borders of epithelial cells accumulate supracellular myosin cables, which

generate highest tension at their termini (Fernandez-Gonzalez, Simões, Röper, Eaton, & Zallen, 2009). It will be interesting to see if Ena localization at these times and places is elevated.

Further, albeit anecdotal, evidence for a role for Ena in tissues experiencing tension comes in from pharynx formation. The cells of the pharynx are smaller than their neighbors, square shaped and aligned in column form with very straight borders — indicative of cells exerting tension via contractile force (see addendum Figure A.1). Interestingly Ena localizes strongly to the cortex and tricellular junctions of these cells (my unpublished data). Addressing potentially enriched myosin localization via antibody staining and laser cutting experiments would address if this location is experiencing tension. If this were the case, detailed quantification of Ena localization, Ena turnover rates and further experiments modulating adhesion at this location would be carried out.

Is Ena solely responsible for tension reinforcement of junctions? This may be true in some tissues, but this is highly unlikely to be universally true or even necessarily true for both tissues in dorsal closure. Previous work in the lab has revealed that Dia plays an important role in junctional maintenance as determined by DE-Cadherin staining during early dorsal closure (Homem & Peifer, 2008). In fact, as previously mentioned, expression of active Dia promotes stabilization of AJs and recruitment of junctional myosin (Homem & Peifer, 2008). Given the major forces that are at play during this developmental process, it would not be surprising if Ena and Dia would both play redundant roles in force strengthening junctions.

Signaling through filopodia

Filopodia have historically been thought of as sensory structures that mediate cell migration and directionality (reviewed in Gupton & Gertler, 2007). However, despite a good deal of work with regard to filopodia in growth cones in neurons and their correlation with guidance and migration (Chien, Rosenthal, Harris, & Holt, 1993; Davenport, Dou, Mills, & Kater, 1996; Davenport, Dou, Rehder, & Kater, 1993; Gomez & Letourneau, 1994; Koleske, 2003; Ono et al., 1997; Rösner, Möller, Wassermann, Mihatsch, & Blum, 2007), there is still a surprising lack of data to confirm the function of filopodia in this capacity. Dorsal closure

not only provides an excellent place for assessment of interplay between junctional actin, actomyosin contractility and protrusive behavior, but also provides a place and time when developmental signaling is robust. The AS cells have active JNK signaling prior to dorsal closure, which is then down-regulated, and this down-regulation is required for proper specification of the LE (reviewed in Harden, 2002). JNK-dependent, Wg pathway-driven expression of decapentaplegic (dpp) is present in the LE cells (Harden, 2002; McEwen, Cox, & Peifer, 2000). Transmission of the early JNK signal in the AS to the LE cells is thought to rely on diffusion of paracrine signals. JNK and Dpp signaling also play a similar role in another closely related tissue rearrangement during pupal development known as thorax closure, where two opposing tissue sheets migrate and meet at the dorsal midline (Martin-Blanco, Pastor-Pareja, & Garcia-Bellido, 2000), which suggests a common role in this type of sheet migration.

The recent discovery and documentation of signaling filopodia, cytonemes, and their integral role in Dpp signaling in the *Drosophila* wing disc provides another possible explanation for the purpose of filopodia in the non-motile cells of the AS. Work by the Kornberg lab has shown that Dia plays a role in cytoneme formation/maintenance in the wing disc (Roy, Huang, Liu, & Kornberg, 2014). This, along with our data that Dia governs AS filopodia, makes exploring these filopodia as cytonemes an attractive idea.

Probing an integrated network

The actin network is plastic. As the actin field moves forward it's becoming clearer that absence of a given actin regulator shifts activity to other members of the network. One specific, relevant example comes from our own work: loss of capping protein promotes filopodia formation via Enabled (Gates et al., 2007; S. L. Rogers & Rogers, 2008). We've explored this capping/anti-capping antagonistic relationship during oogenesis in Chapter 2, and past work in the lab has explored shifts in protrusive activity controlled by relative levels of Ena and Dia along the leading edge of dorsal closure (Bilancia et al., 2014; Homem & Peifer, 2009). However, the actin network consists of many more players, and our 202 interpretations need to be viewed in that light. Other players must be considered moving

forward, which raises the question: How do other actin regulators contribute to the specialized actin structures in development on which we focus?

To move forward with integrating other members of the actin regulatory network, we need to make further use of the multidisciplinary micro-to-macro workflow that we have utilized in Chapters 3 and 4. As all proteins are machines, it's important to understand how they work in simple settings before studying them in more complex situations. This is further underscored in the case of the actin cytoskeleton, since the network is both locally plastic, and in cells and animals, each actin network interacts with and is influenced by other nonlocal pools of subcellular actin and other force mechanisms in the cell (see above and addendum). Given this complexity, understanding what happens with defined concentrations of players in the simpler in vitro assays is integral to understanding (1) what's happening locally at a specific place and time within a cell, which will allow (2) a more complete picture of how the pan-cellular actin pool is working together in the cell under different conditions (such as spreading, protrusive activity, migration), which can then further help us understand (3) how this is coupled even more globally, in tissues *in vivo*.

Luckily, current technology allows for total internal reflection microscopy with spectral unmixing, and thus imaging more than 3 labeled purified proteins simultaneously in in vitro actin assembly assays *is at least theoretically possible*. The ability to label multiple players in these assays will help create a clear picture of how these proteins are interacting and how that correlates with actin dynamics in the simplest setting. Moving the information we gain from these integrated, in-vitro reconstitution assays into cell culture is aided by current protrusion tracking software like Cell Geo (Chapter3; (Tsygankov et al., 2014). One challenge in doing so is that *in vivo* background autofluoresence currently complicates use of software like CellGeo requiring a more binary readout. Creating single clones in tissues using a high signal-to-noise reporter would be best; however, there are only four chromosomes to manipulate and combining overexpression constructs with mutants could prove to be difficult. As we begin integrating multiple actin players into cell culture assays, it will be interesting to explore whether the use of the protrusive profile as a fingerprint for regulators

influencing filopodia, as described in Chapter 4, can be further refined. Further validation and use of the protrusive profile metric will be helpful moving forward as we manipulate and dissect the roles of multiple players in actin regulation *in* vivo. The advent of CRISPr technology is poised to make genetics more straightforward in the future, enabling dissection of a complex network *in vivo*.

With which actin regulators should we begin? Recent work *in vitro* has shown that the frequency and length of Ena's processive runs on the ends of an actin filament are dramatically increased on filaments bundled by fascin, allowing for a feedback cycle to create more thick-bundled filaments (Winkelman et al., 2014). Whether or not this relationship holds true *in vivo* remains to be tested. We already know that both Fascin and Ena play roles in hemocyte migration (Tucker, Evans, & Wood, 2011; Zanet et al., 2009b), and further exploration in other tissues will need to be carried out. The filopodia-like cytoplasmic actin filaments in oogenesis and the filopodia along the LE in dorsal closure are both excellent places to test this as both Fascin and Ena localize to these structures (my unpublished observations; Cant & Cooley, 1996; Zanet, Payre, & Plaza, 2009a).

The Arp2/3 complex is another factor that must be integrated into how the actin network functions *in vivo*. Much work has been done *in vitro* describing Arp2/3 activation by WASP and WAVE (reviewed in Takenawa & Suetsugu, 2007) and mechanism of nucleation (reviewed in Cooper, Wear, & Weaver, 2001; Mullins & Pollard, 1999). Further work describing the interplay of Arp2/3 with CP has also been carried out in cell culture (Akin & Mullins, 2008). In cell culture and in development we know that components of Arp2/3 are necessary for almost as wide a variety of processes as actin itself, such as cell spreading and lamellipodia formation (D'Ambrosio & Vale, 2010; Ingerman, Hsiao, & Mullins, 2013; S. L. Rogers & Rogers, 2008), polarity and ring canal formation in oogenesis (Hudson & Cooley, 2002; Leibfried, Müller, & Ephrussi, 2013), pseudocleavage furrow formation (Stevenson, Hudson, Cooley, & Theurkauf, 2002), AJ formation (Herszterg, Leibfried, Bosveld, Martin, & Bellaiche, 2013; Sarpal et al., 2012), filopodia formation in growth cones (Gonçalves-Pimentel, Gombos, Mihály, Sánchez-Soriano, & Prokop, 2011), microvilli formation and

endocytosis (Georgiou, Marinari, Burden, & Baum, 2008; Rajan, Tien, Haueter, Schulze, & Bellen, 2009), myoblast fusion (Richardson, Beckett, Nowak, & Baylies, 2007), bristle development (Frank, Hopmann, Lenartowska, & Miller, 2006), and maintenance of the blood brain barrier (Hatan, Shinder, Israeli, Schnorrer, & Volk, 2011).

The myriad of roles played by Arp2/3 *in vivo* are sure to complicate assessment of its function during some developmental processes, but the ability to use RNAi in a tissue specific manner offers a method to bypass early mutant and tissue specific phenotypes. Specifically, our AS cell model offers an excellent place to start to assess the cell and tissue biological implications of Arp2/3. Early phenotypes in the AS that may arise from RNAi expression (i.e. germbarnd extension/retraction) may be navigated using temperature shifts to alter GAL4 activity and thus expression levels. We can then start to probe interplay between actin nucleators/polymerizers in this tissue as both *ena* and *dia* zygotic mutants are viable through dorsal closure (Chapter 4). Once we detail tissues and subcellular localizations where Arp2/3 plays a role, we can then expand on this assessment by exploring upstream activation of the Arp2/3 complex. It will be important to parse out the pathway of activation by via Wave and/or WASP.

Integrating Arp2/3 into our understanding of the network also allows us to start to address another specific question regarding another actin binding protein, profilin: Do different nucleators/polymerizers preferentially use profilin-actin monomers? As previously mentioned we know that there is a difference between Ena and Dia's preference for profilinactin, but how well the Arp2/3 nucleation machinery uses profilin-actin is currently unknown, with recent work suggesting it is not efficient (James Bear, personal communication). As we integrate Arp2/3 into our network with Ena and Dia, it will be important to understand the affinity for profilin-actin for all players.

In summary, moving forward with Ena and Dia's roles in morphogenesis requires direct assessment of the details of their interaction on a biochemical level, further work regarding the spatiotemporal characterization of binding partners, and regulation by both Abl and upstream GTPases. Moreover, as force and tension are important driving factors in

morphogenesis, it will be interesting to start looking at Ena and Dia behavior at places under tension, perhaps revealing more about their roles at junctions and in actomyosin contractility. Finally, the integrated nature of the actin cytoskeleton requires that we start an integrated analysis of other actin binding and regulatory proteins to understand local actin network behavior that can then be applied to a more global network *in vivo.* There are still a lot of exciting experiments to be done.

REFERENCES

Akin, O., & Mullins, R. D. (2008). Capping protein increases the rate of actin-based motility by promoting filament nucleation by the Arp2/3 complex. *Cell*, *133*(5), 841–851. doi:10.1016/j.cell.2008.04.011

Alberts, A. S. (2001). Identification of a carboxyl-terminal diaphanous-related formin homology protein autoregulatory domain. *The Journal of biological chemistry*, *276*(4), 2824–2830.

Bilancia, C. G., Winkelman, J. D., Tsygankov, D., Nowotarski, S. H., Sees, J. A., Comber, K., et al. (2014). Enabled negatively regulates diaphanous-driven actin dynamics in vitro and in vivo. *Developmental cell*, *28*(4), 394–408. doi:10.1016/j.devcel.2014.01.015

Blanchoin, L., Boujemaa-Paterski, R., Sykes, C., & Plastino, J. (2014). Actin dynamics, architecture, and mechanics in cell motility. *Physiological reviews*, *94*(1), 235–263. doi:10.1152/physrev.00018.2013

Breitsprecher, D., & Goode, B. L. (2013). Formins at a glance. *Journal of cell science*, *126*(Pt 1), 1–7. doi:10.1242/jcs.107250

Breitsprecher, D., Jaiswal, R., Bombardier, J. P., Gould, C. J., Gelles, J., & Goode, B. L. (2012). Rocket launcher mechanism of collaborative actin assembly defined by single molecule imaging. *Science (New York, NY)*, *336*(6085), 1164–1168. doi:10.1126/science.1218062

Cant, K., & Cooley, L. (1996). Single amino acid mutations in Drosophila fascin disrupt actin bundling function in vivo. *Genetics*, *143*(1), 249–258.

Carisey, A., Tsang, R., Greiner, A. M., Nijenhuis, N., Heath, N., Nazgiewicz, A., et al. (2013). Vinculin regulates the recruitment and release of core focal adhesion proteins in a force-dependent manner. *Current biology : CB*, *23*(4), 271–281. doi:10.1016/j.cub.2013.01.009

Chien, C. B., Rosenthal, D. E., Harris, W. A., & Holt, C. E. (1993). Navigational errors made by growth cones without filopodia in the embryonic Xenopus brain. *Neuron*, *11*(2), 237–251.

Choi, W., Jung, K.-C., Nelson, K. S., Bhat, M. A., Beitel, G. J., Peifer, M., & Fanning, A. S. (2011). The single Drosophila ZO-1 protein Polychaetoid regulates embryonic morphogenesis in coordination with Canoe/afadin and Enabled. *Molecular biology of the cell*, *22*(12), 2010–2030. doi:10.1091/mbc.E10-12-1014

Cooper, J. A., Wear, M. A., & Weaver, A. M. (2001). Arp2/3 complex: advances on the inner workings of a molecular machine. *Cell*, *107*(6), 703–705.

D'Ambrosio, M. V., & Vale, R. D. (2010). A whole genome RNAi screen of Drosophila S2 cell spreading performed using automated computational image analysis. *The Journal of cell biology*, *191*(3), 471–478. doi:10.1083/jcb.201003135

Davenport, R. W., Dou, P., Mills, L. R., & Kater, S. B. (1996). Distinct calcium signaling within neuronal growth cones and filopodia. *Journal of neurobiology*, *31*(1), 1–15. doi:10.1002/(SICI)1097-4695(199609)31:1<1::AID-NEU1>3.0.CO;2-6

Davenport, R. W., Dou, P., Rehder, V., & Kater, S. B. (1993). A sensory role for neuronal

growth cone filopodia. *Nature*, *361*(6414), 721–724. doi:10.1038/361721a0

Dawes-Hoang, R. E., Parmar, K. M., Christiansen, A. E., Phelps, C. B., Brand, A. H., & Wieschaus, E. F. (2005). folded gastrulation, cell shape change and the control of myosin localization. *Development (Cambridge, England)*, *132*(18), 4165–4178. doi:10.1242/dev.01938

Disanza, A., Bisi, S., Winterhoff, M., Milanesi, F., Ushakov, D. S., Kast, D., et al. (2013). CDC42 switches IRSp53 from inhibition of actin growth to elongation by clustering of VASP. *The EMBO journal*, *32*(20), 2735–2750. doi:10.1038/emboj.2013.208

Ebrahim, S., Fujita, T., Millis, B. A., Kozin, E., Ma, X., Kawamoto, S., et al. (2013). NMII forms a contractile transcellular sarcomeric network to regulate apical cell junctions and tissue geometry. *Current biology : CB*, *23*(8), 731–736. doi:10.1016/j.cub.2013.03.039

Engl, W., Arasi, B., Yap, L. L., Thiery, J. P., & Viasnoff, V. (2014). Actin dynamics modulate mechanosensitive immobilization of E-cadherin at adherens junctions. *Nature cell biology*, *16*(6), 587–594. doi:10.1038/ncb2973

Fernandez-Gonzalez, R., Simões, S. de M., Röper, J.-C., Eaton, S., & Zallen, J. A. (2009). Myosin II dynamics are regulated by tension in intercalating cells. *Developmental cell*, *17*(5), 736–743. doi:10.1016/j.devcel.2009.09.003

Frank, D. J., Hopmann, R., Lenartowska, M., & Miller, K. G. (2006). Capping protein and the Arp2/3 complex regulate nonbundle actin filament assembly to indirectly control actin bundle positioning during Drosophila melanogaster bristle development. *Molecular biology of the cell*, *17*(9), 3930–3939. doi:10.1091/mbc.E06-06-0500

Gates, J., Mahaffey, J. P., Rogers, S. L., Emerson, M., Rogers, E. M., Sottile, S. L., et al. (2007). Enabled plays key roles in embryonic epithelial morphogenesis in Drosophila. *Development (Cambridge, England)*, *134*(11), 2027–2039. doi:10.1242/dev.02849

Gates, J., Nowotarski, S. H., Yin, H., Mahaffey, J. P., Bridges, T., Herrera, C., et al. (2009). Enabled and Capping protein play important roles in shaping cell behavior during Drosophila oogenesis. *Developmental biology*, *333*(1), 90–107. doi:10.1016/j.ydbio.2009.06.030

Georgiou, M., Marinari, E., Burden, J., & Baum, B. (2008). Cdc42, Par6, and aPKC regulate Arp2/3-mediated endocytosis to control local adherens junction stability. *Current biology : CB*, *18*(21), 1631–1638. doi:10.1016/j.cub.2008.09.029

Gertler, F. B., Doctor, J. S., & Hoffmann, F. M. (1990). Genetic suppression of mutations in the Drosophila abl proto-oncogene homolog. *Science (New York, NY)*, *248*(4957), 857–860.

Gomez, T. M., & Letourneau, P. C. (1994). Filopodia initiate choices made by sensory neuron growth cones at laminin/fibronectin borders in vitro. *The Journal of neuroscience : the official journal of the Society for Neuroscience*, *14*(10), 5959–5972.

Gonçalves-Pimentel, C., Gombos, R., Mihály, J., Sánchez-Soriano, N., & Prokop, A. (2011). Dissecting regulatory networks of filopodia formation in a Drosophila growth cone model. *PloS one*, *6*(3), e18340. doi:10.1371/journal.pone.0018340

Gorelik, R., Yang, C., Kameswaran, V., Dominguez, R., & Svitkina, T. (2011). Mechanisms of plasma membrane targeting of formin mDia2 through its amino terminal domains. *Molecular biology of the cell*, *22*(2), 189–201. doi:10.1091/mbc.E10-03-0256

Gould, C. J., Maiti, S., Michelot, A., Graziano, B. R., Blanchoin, L., & Goode, B. L. (2011). The formin DAD domain plays dual roles in autoinhibition and actin nucleation. *Current biology : CB*, *21*(5), 384–390. doi:10.1016/j.cub.2011.01.047

Grashoff, C., Hoffman, B. D., Brenner, M. D., Zhou, R., Parsons, M., Yang, M. T., et al. (2010). Measuring mechanical tension across vinculin reveals regulation of focal adhesion dynamics. *Nature*, *466*(7303), 263–266. doi:10.1038/nature09198

Graziano, B. R., Jonasson, E. M., Pullen, J. G., Gould, C. J., & Goode, B. L. (2013). Ligand induced activation of a formin-NPF pair leads to collaborative actin nucleation. *The Journal of cell biology*, *201*(4), 595–611. doi:10.1083/jcb.201212059

Grevengoed, E. E., Loureiro, J. J., Jesse, T. L., & Peifer, M. (2001). Abelson kinase regulates epithelial morphogenesis in Drosophila. *The Journal of cell biology*, *155*(7), 1185–1198. doi:10.1083/jcb.200105102

Gupton, S. L., & Gertler, F. B. (2007). Filopodia: the fingers that do the walking. *Science's STKE : signal transduction knowledge environment*, *2007*(400), re5. doi:10.1126/stke.4002007re5

Hansen, S. D., & Mullins, R. D. (2010). VASP is a processive actin polymerase that requires monomeric actin for barbed end association. *The Journal of cell biology*, *191*(3), 571–584. doi:10.1083/jcb.201003014

Harasim, M., Wunderlich, B., Peleg, O., Kröger, M., & Bausch, A. R. (2013). Direct observation of the dynamics of semiflexible polymers in shear flow. *Physical review letters*, *110*(10), 108302.

Harden, N. (2002). Signaling pathways directing the movement and fusion of epithelial sheets: lessons from dorsal closure in Drosophila. *Differentiation; research in biological diversity*, *70*(4-5), 181–203. doi:10.1046/j.1432-0436.2002.700408.x

Harden, N., Loh, H. Y., Chia, W., & Lim, L. (1995). A dominant inhibitory version of the small GTP-binding protein Rac disrupts cytoskeletal structures and inhibits developmental cell shape changes in Drosophila. *Development (Cambridge, England)*, *121*(3), 903–914.

Harden, N., Ricos, M., Ong, Y. M., Chia, W., & Lim, L. (1999). Participation of small GTPases in dorsal closure of the Drosophila embryo: distinct roles for Rho subfamily proteins in epithelial morphogenesis. *Journal of cell science*, *112 (Pt 3)*, 273–284.

Hatan, M., Shinder, V., Israeli, D., Schnorrer, F., & Volk, T. (2011). The Drosophila blood brain barrier is maintained by GPCR-dependent dynamic actin structures. *The Journal of cell biology*, *192*(2), 307–319. doi:10.1083/jcb.201007095

Heimsath, E. G., & Higgs, H. N. (2012). The C terminus of formin FMNL3 accelerates actin polymerization and contains a WH2 domain-like sequence that binds both monomers and filament barbed ends. *The Journal of biological chemistry*, *287*(5), 3087–3098. doi:10.1074/jbc.M111.312207

Herszterg, S., Leibfried, A., Bosveld, F., Martin, C., & Bellaiche, Y. (2013). Interplay between the dividing cell and its neighbors regulates adherens junction formation during cytokinesis in epithelial tissue. *Developmental cell*, *24*(3), 256–270. doi:10.1016/j.devcel.2012.11.019

Homem, C. C. F., & Peifer, M. (2008). Diaphanous regulates myosin and adherens junctions to control cell contractility and protrusive behavior during morphogenesis. *Development (Cambridge, England)*, *135*(6), 1005–1018. doi:10.1242/dev.016337

Homem, C. C. F., & Peifer, M. (2009). Exploring the roles of diaphanous and enabled activity in shaping the balance between filopodia and lamellipodia. *Molecular biology of the cell*, *20*(24), 5138–5155. doi:10.1091/mbc.E09-02-0144

Hudson, A. M., & Cooley, L. (2002). A subset of dynamic actin rearrangements in Drosophila requires the Arp2/3 complex. *The Journal of cell biology*, *156*(4), 677–687. doi:10.1083/jcb.200109065

Huelsmann, S., Ylänne, J., & Brown, N. H. (2013). Filopodia-like actin cables position nuclei in association with perinuclear actin in Drosophila nurse cells. *Developmental cell*, *26*(6), 604–615. doi:10.1016/j.devcel.2013.08.014

Ingerman, E., Hsiao, J. Y., & Mullins, R. D. (2013). Arp2/3 complex ATP hydrolysis promotes lamellipodial actin network disassembly but is dispensable for assembly. *The Journal of cell biology*, *200*(5), 619–633. doi:10.1083/jcb.201211069

Jaiswal, R., Stepanik, V., Rankova, A., Molinar, O., Goode, B. L., & McCartney, B. M. (2013). Drosophila homologues of adenomatous polyposis coli (APC) and the formin diaphanous collaborate by a conserved mechanism to stimulate actin filament assembly. *The Journal of biological chemistry*, *288*(19), 13897–13905. doi:10.1074/jbc.M113.462051

Kiehart, D. P., Galbraith, C. G., Edwards, K. A., Rickoll, W. L., & Montague, R. A. (2000). Multiple forces contribute to cell sheet morphogenesis for dorsal closure in Drosophila. *The Journal of cell biology*, *149*(2), 471–490.

Koleske, A. J. (2003). Do filopodia enable the growth cone to find its way? *Science's STKE : signal transduction knowledge environment*, *2003*(183), pe20. doi:10.1126/stke.2003.183.pe20

Krause, M., Leslie, J. D., Stewart, M., Lafuente, E. M., Valderrama, F., Jagannathan, R., et al. (2004). Lamellipodin, an Ena/VASP ligand, is implicated in the regulation of lamellipodial dynamics. *Developmental cell*, *7*(4), 571–583. doi:10.1016/j.devcel.2004.07.024

Legg, J. A., & Machesky, L. M. (2004, November). MRL proteins: leading Ena/VASP to Ras GTPases. *Nature cell biology*, pp. 1015–1017. doi:10.1038/ncb1104-1015

Leibfried, A., Müller, S., & Ephrussi, A. (2013). A Cdc42-regulated actin cytoskeleton mediates Drosophila oocyte polarization. *Development (Cambridge, England)*, *140*(2), 362–371. doi:10.1242/dev.089250

Li, F., & Higgs, H. N. (2003). The mouse Formin mDia1 is a potent actin nucleation factor regulated by autoinhibition. *Current biology : CB*, *13*(15), 1335–1340.

Liu, K. C., & Cheney, R. E. (2012). Myosins in cell junctions. *Bioarchitecture*, *2*(5), 158–170. doi:10.4161/bioa.21791

Martin, A. C., Gelbart, M., Fernandez-Gonzalez, R., Kaschube, M., & Wieschaus, E. F. (2010). Integration of contractile forces during tissue invagination. *The Journal of cell biology*, *188*(5), 735–749. doi:10.1083/jcb.200910099

Martin, A. C., Kaschube, M., & Wieschaus, E. F. (2009). Pulsed contractions of an actinmyosin network drive apical constriction. *Nature*, *457*(7228), 495–499. doi:10.1038/nature07522

Martin-Blanco, E., Pastor-Pareja, J. C., & Garcia-Bellido, A. (2000). JNK and decapentaplegic signaling control adhesiveness and cytoskeleton dynamics during thorax closure in Drosophila. *Proceedings of the National Academy of Sciences of the United States of America*, *97*(14), 7888–7893.

McEwen, D. G., Cox, R. T., & Peifer, M. (2000). The canonical Wg and JNK signaling cascades collaborate to promote both dorsal closure and ventral patterning. *Development (Cambridge, England)*, *127*(16), 3607–3617.

Moseley, J. B., Sagot, I., Manning, A. L., Xu, Y., Eck, M. J., Pellman, D., & Goode, B. L. (2004). A conserved mechanism for Bni1- and mDia1-induced actin assembly and dual regulation of Bni1 by Bud6 and profilin. *Molecular biology of the cell*, *15*(2), 896–907. doi:10.1091/mbc.E03-08-0621

Mullins, R. D., & Pollard, T. D. (1999). Structure and function of the Arp2/3 complex. *Current opinion in structural biology*, *9*(2), 244–249.

Narasimha, M., & Brown, N. H. (2004). Novel functions for integrins in epithelial morphogenesis. *Current biology : CB*, *14*(5), 381–385. doi:10.1016/j.cub.2004.02.033

Okada, K., Bartolini, F., Deaconescu, A. M., Moseley, J. B., Dogic, Z., Grigorieff, N., et al. (2010). Adenomatous polyposis coli protein nucleates actin assembly and synergizes with the formin mDia1. *The Journal of cell biology*, *189*(7), 1087–1096. doi:10.1083/jcb.201001016

Ono, K., Shokunbi, T., Nagata, I., Tokunaga, A., Yasui, Y., & Nakatsuji, N. (1997). Filopodia and growth cones in the vertically migrating granule cells of the postnatal mouse cerebellum. *Experimental brain research*, *117*(1), 17–29.

Otomo, T., Otomo, C., Tomchick, D. R., Machius, M., & Rosen, M. K. (2005). Structural basis of Rho GTPase-mediated activation of the formin mDia1. *Molecular cell*, *18*(3), 273–281. doi:10.1016/j.molcel.2005.04.002

Pollard, T. D., & Cooper, J. A. (2009). Actin, a central player in cell shape and movement. *Science (New York, NY)*, *326*(5957), 1208–1212. doi:10.1126/science.1175862

Rajan, A., Tien, A.-C., Haueter, C. M., Schulze, K. L., & Bellen, H. J. (2009). The Arp2/3 complex and WASp are required for apical trafficking of Delta into microvilli during cell fate specification of sensory organ precursors. *Nature cell biology*, *11*(7), 815–824. doi:10.1038/ncb1888

Renfranz, P. J., & Beckerle, M. C. (2002). Doing (F/L)PPPPs: EVH1 domains and their proline-rich partners in cell polarity and migration. *Current opinion in cell biology*, *14*(1), 88–103.

Richardson, B. E., Beckett, K., Nowak, S. J., & Baylies, M. K. (2007). SCAR/WAVE and Arp2/3 are crucial for cytoskeletal remodeling at the site of myoblast fusion. *Development (Cambridge, England)*, *134*(24), 4357–4367. doi:10.1242/dev.010678

Rogers, S. L., & Rogers, G. C. (2008). Culture of Drosophila S2 cells and their use for RNAi-mediated loss-of-function studies and immunofluorescence microscopy. *Nature*

protocols, *3*(4), 606–611. doi:10.1038/nprot.2008.18

Rose, R., Weyand, M., Lammers, M., Ishizaki, T., Ahmadian, M. R., & Wittinghofer, A. (2005). Structural and mechanistic insights into the interaction between Rho and mammalian Dia. *Nature*, *435*(7041), 513–518. doi:10.1038/nature03604

Roy, S., Huang, H., Liu, S., & Kornberg, T. B. (2014). Cytoneme-mediated contactdependent transport of the Drosophila decapentaplegic signaling protein. *Science (New York, NY)*, *343*(6173), 1244624. doi:10.1126/science.1244624

Rösner, H., Möller, W., Wassermann, T., Mihatsch, J., & Blum, M. (2007). Attenuation of actinomyosinII contractile activity in growth cones accelerates filopodia-guided and microtubule-based neurite elongation. *Brain research*, *1176*, 1–10. doi:10.1016/j.brainres.2007.07.081

Sarpal, R., Pellikka, M., Patel, R. R., Hui, F. Y. W., Godt, D., & Tepass, U. (2012). Mutational analysis supports a core role for Drosophila α-catenin in adherens junction function. *Journal of cell science*, *125*(Pt 1), 233–245. doi:10.1242/jcs.096644

Simões, S. de M., Mainieri, A., & Zallen, J. A. (2014). Rho GTPase and Shroom direct planar polarized actomyosin contractility during convergent extension. *The Journal of cell biology*, *204*(4), 575–589. doi:10.1083/jcb.201307070

Solon, J., Kaya-Copur, A., Colombelli, J., & Brunner, D. (2009). Pulsed forces timed by a ratchet-like mechanism drive directed tissue movement during dorsal closure. *Cell*, *137*(7), 1331–1342. doi:10.1016/j.cell.2009.03.050

Stevens, T. L., Rogers, E. M., Koontz, L. M., Fox, D. T., Homem, C. C. F., Nowotarski, S. H., et al. (2008). Using Bcr-Abl to examine mechanisms by which abl kinase regulates morphogenesis in Drosophila. *Molecular biology of the cell*, *19*(1), 378–393. doi:10.1091/mbc.E07-01-0008

Stevenson, V., Hudson, A., Cooley, L., & Theurkauf, W. E. (2002). Arp2/3-dependent pseudocleavage [correction of psuedocleavage] furrow assembly in syncytial Drosophila embryos. *Current biology : CB*, *12*(9), 705–711.

Takenawa, T., & Suetsugu, S. (2007). The WASP-WAVE protein network: connecting the membrane to the cytoskeleton. *Nature reviews. Molecular cell biology*, *8*(1), 37–48. doi:10.1038/nrm2069

Trichas, G., Smith, A. M., White, N., Wilkins, V., Watanabe, T., Moore, A., et al. (2012). Multi-cellular rosettes in the mouse visceral endoderm facilitate the ordered migration of anterior visceral endoderm cells. *PLoS biology*, *10*(2), e1001256. doi:10.1371/journal.pbio.1001256

Tsygankov, D., Bilancia, C. G., Vitriol, E. A., Hahn, K. M., Peifer, M., & Elston, T. C. (2014). CellGeo: a computational platform for the analysis of shape changes in cells with complex geometries. *The Journal of cell biology*, *204*(3), 443–460. doi:10.1083/jcb.201306067

Tucker, P. K., Evans, I. R., & Wood, W. (2011). Ena drives invasive macrophage migration in Drosophila embryos. *Disease models & mechanisms*, *4*(1), 126–134. doi:10.1242/dmm.005694

Winkelman, J. D., Bilancia, C. G., Peifer, M., & Kovar, D. R. (2014). Ena/VASP Enabled is a highly processive actin polymerase tailored to self-assemble parallel-bundled F-actin networks with Fascin. *Proceedings of the National Academy of Sciences of the United States of America*, *111*(11), 4121–4126. doi:10.1073/pnas.1322093111

Woolner, S., Jacinto, A., & Martin, P. (2005). The small GTPase Rac plays multiple roles in epithelial sheet fusion--dynamic studies of Drosophila dorsal closure. *Developmental biology*, *282*(1), 163–173. doi:10.1016/j.ydbio.2005.03.005

Yonemura, S., Wada, Y., Watanabe, T., Nagafuchi, A., & Shibata, M. (2010). alpha-Catenin as a tension transducer that induces adherens junction development. *Nature cell biology*, *12*(6), 533–542. doi:10.1038/ncb2055

Zanet, J., Payre, F., & Plaza, S. (2009a). Fascin for cell migration in Drosophila. *Fly*, *3*(4), 281–282.

Zanet, J., Stramer, B., Millard, T., Martin, P., Payre, F., & Plaza, S. (2009b). Fascin is required for blood cell migration during Drosophila embryogenesis. *Development (Cambridge, England)*, *136*(15), 2557–2565. doi:10.1242/dev.036517

ADDENDUM: CELL BIOLOGY: A TENSE BUT GOOD DAY FOR ACTIN AT CELL-CELL JUNCTIONS

Stephanie Nowotarski1 and Mark Peifer1,2*

1 Department of Biology, University of North Carolina at Chapel Hill, Chapel Hill, NC 27599-3280, USA

2 Lineberger Comprehensive Cancer Center, University of North Carolina at Chapel Hill, Chapel Hill, NC 27599, USA

Preface

As an addendum pertaining heavily to the previous discussion chapter, I have included a dispatch written with Mark Peifer published in *Current Biology* highlighting the work from Leerberg et al., from Alpha Yap's laboratory.

Cells have evolved an elegant tuning mechanism to maintain tissue integrity, in which increasing mechanical tension stimulates actin assembly at cell-cell junctions. The mechanosensitive junctional protein alpha-catenin acts through vinculin and Ena/VASP proteins to reinforce the cell against mechanical stress.

During embryonic development and tissue homeostasis, cells must balance the need to maintain tissue integrity, via cell-cell adhesive junctions, with the need to change shape and move, using the actomyosin cytoskeleton to generate force. In the good old days, the relationship between cell-cell adherens junctions (AJs) and the cytoskeleton was simple—the cadherin-catenin complex directly linked to actin

filaments via a-catenin (Fig. A.1A). This provided a great way to build a stuffed animal, with cells glued together and made stiff. However, the last decade shook up this paradigm, revealing diverse ways of linking AJs and the cytoskeleton during the dynamic events of morphogenesis. Now a study by Leerberg et al. reveals new complexity in this linkage process, providing evidence for a feedback loop that ensures the junctional-cytoskeletal linkage is maintained in the face of mechanical force.

Classic cadherin extracellular domains provide the adhesive interface joining cells to one another (Meng & Takeichi, 2009), but the adhesive force provided by single cadherin-cadherin interactions is quite small. To maintain effective adhesion, cadherins must be organized into multiprotein arrays. This is achieved in part by trans-interactions among cadherins, but is primarily maintained by interactions between cytoplasmic proteins that bind cadherin tails and the underlying actin cytoskeleton. In most epithelial cells, cadherins form an adhesive interface all along the lateral domain, but are organized into special adhesive complexes at the apical end, forming the AJ (or zonula adherens or ZA; (Meng & Takeichi, 2009). The cadherin:actin cytoskeleton relationship is a two way street, with cadherin-based adhesion essential for polarized apical assembly of a specialized actin array (Gumbiner, Stevenson, & Grimaldi, 1988) and this actin array is essential to stabilize cadherin-based junctions(Quinlan & Hyatt, 1999). The link connecting cadherins and actin was thought to be direct, mediated by ß-catenin and a-catenin (Fig. A.1A). However, work in 2005 cast doubt on this textbook view (Yamada, Pokutta, Drees, Weis, & Nelson, 2005), stimulating a series of experiments revealing that there are multiple connectors e.g., (Abe & Takeichi, 2008; J. K. Sawyer, Harris, Slep, Gaul, & Peifer, 2009)employed at different times and places, and importantly for this discussion, under different force regimes.

These connections stabilize cell adhesion in a static epithelial sheet but are even more critical as cells change shape and move(T. J. C. Harris & Tepass, 2010).

Nowhere is this more apparent than during the dramatic events of embryonic morphogenesis, during which actomyosin powers tissue rearrangements via the coordinated action of many individual cells. For example, apical constriction, in which an apical actomyosin network changes a columnar cell into a pyramid, drives critical events from mammalian neural tube closure to *Drosophila* mesoderm invagination (J. M. Sawyer et al., 2010). More complex, planar polarized actomyosin driven events drive another common developmental process, convergent elongation, which elongates the anterior-posterior body axis of many animals. Linking actin to AJs also plays an important role at the adhesive front during collective cell migration and embryonic wound healing. Even seemingly simple events, like responding to cell division, require remodeling of AJs and their cytoskeletal partners. In each event, force is exerted on AJs, and thus the connection must be mechanically secure. Eliminating the function of potential AJ-actomyosin cross-linkers like Canoe/Afadin disrupts completion of these morphogenetic events, disrupting development e.g., (Kwiatkowski et al., 2010; J. K. Sawyer et al., 2009).

To assemble secure connections between AJs and actin, cells must first assemble actin at AJs. Like cadherins, F-actin localizes in apical circumferential rings along the AJ in cell culture and *in vivo*. This junctional actin is highly dynamic, with~80% turning over with a t1/2=10-50s. There are three well-characterized classes of actin assembly machines that are candidates for assembling junctional actin (Chesarone & Goode, 2009). The Arp2/3 complex is activated by WASP family proteins and nucleates daughter filaments on the sides of existing filaments, thus promoting branched actin networks. Formins associate with F-actin barbed ends and facilitate rapid addition of profilin-actin, promoting linear actin networks. Lastly, Ena/VASP proteins (Ena/Mena/VASP/Evl) also aid barbed end polymerization and facilitate actin bundling through their ability to tetramerize. Despite the fact that the junctional actin array is largely composed of linear actin filaments, previous work suggests that actin nucleation at AJs occurs through Rac-WAVE-Arp2/3 pathway

(Tang & Brieher, 2012; Verma et al., 2012), while the WIRE, N-WASP pathway appears to play a role in reorganization. However, data suggested possible roles for formins and Ena/VASP proteins in other cell types (Michael & Yap, 2013).

The dynamic nature of junctional-actin connections opens the possibility that feedback loops may exist that allow cells to respond to dynamic changes in force generation both within cells and among neighbors. FRET-based biosensors confirm that cadherins are under tension in epithelia and that connection to actomyosin is essential for this. However, for cells to respond to force, they must be able to sense tension. Studies of integrin-based focal adhesions (FAs) provided paradigms —in FAs proteins like talin change conformation in response to tension, leading to increased recruitment of the actin-binding protein vinculin (Maruthamuthu, Aratyn-Schaus, & Gardel, 2010). Similarly, recent work suggests both a-catenin and vinculin can act as force sensors at AJs. In the case of a-catenin, the a18-antibody recognizes an a-catenin epitope exposed only when AJs are under tension(Yonemura, Wada, Watanabe, Nagafuchi, & Shibata, 2010). This led to the suggestion that tension induces a conformational change in a-catenin, exposing the epitope and the overlapping vinculin binding site, increasing vinculin recruitment (Fig. A.1B).

Cells thus have a mechanism built into AJs to sense tension. How do they respond? One danger faced by cells is that the dynamic forces involved in morphogenesis will exceed the resistance of junctional-actin connections and thus disrupt connections. This is exactly what one observes in situations when levels of putative actin cross-linkers like a-catenin or Afadin/Canoe are reduced. How then do cells react to tension to prevent junctional disruption? Leerberg et al. find that contractility supports and tunes actin assembly at AJs (Fig. A.1B,C; Leerberg et al., 2014). In their polarized colon cell model, there is a rich perijunctional F-actin pool at AJs, and they find that both steady- state F-actin and actin assembly at the AJ is stimulated by myosin-based contractility. They thus hypothesized integral roles for both actin binding proteins and proteins promoting actin polymerization. Based on its

tension-dependent localization to AJs, they considered vinculin as a candidate modulator. Strikingly, they found that vinculin accumulated at AJs in a tensiondependent way, via it's binding with a-catenin (Fig. A.1A). More importantly, vinculin was required for the increase in steady state F-actin and new actin polymerization in response to myosin-based tension. They confirmed this by demonstrating that an a-catenin mutant unable to bind vinculin cannot support tension-dependent increases in actin assembly.

The tension-dependent increase in F-actin suggested actin nucleating/polymerizing proteins might be recruited by vinculin. The authors quickly ruled out Arp2/3 as the direct actin modulator and thus turned to Ena/VASP proteins (Leerberg et al., 2014). They found both Mena and VASP co-localized with vinculin at AJs and that vinculin was the dominant mechanism for their AJ recruitment (Fig. A.1A). They went on to reveal that Mena/VASP are necessary for vinculin's ability to regulate junctional actin (Mena and VASP were simultaneously inactivated by recruitment to mitochondria). Further, when they engineered vinculin-independent Mena/VASP recruitment to AJs, this was sufficient to render junctional actin assembly resistant to myosin inhibition, and thus making it independent of tension. Thus Ena/VASP proteins appear to be the dominant players in tension-dependent actin regulation.

To cap off this work, they asked what role tension-dependent actin assembly plays in epithelial integrity, tying it back to potential roles in morphogenesis (Leerberg et al., 2014). They found that Mena/VASP dependent actin assembly is necessary for AJ stabilization of E-Cadherin, reflecting the two-way feedback noted above between cadherin-catenins and the underlying actin. Finally, they used elegant laser-surgery to cut AJs and directly measure junctional tension. Recruitment of Mena/VASP to AJs is both necessary and sufficient to support junctional contractile tension. Together these data reveal a highly novel feedback mechanism, supporting a model in which a-catenin, when under tension, undergoes a conformational change and recruits vinculin (and perhaps actin directly; Leerberg et al., 2014). Vinculin, in

turn, can both bind F-actin and recruit Mena/VASP to barbed ends. The resulting linear actin array at AJs provides a parallel actin network favorable for myosin, thus creating more tension and promoting more actin assembly (Fig. A.1A).

These novel insights into a tension-generated feedback loop help us understand how cells resist force during the dynamic events of morphogenesis, and also open many new questions. At the mechanistic level, it will be important to further probe events in the model, including the hypothesized conformational change in a-catenin, the Mena/VASP independent role of vinculin in actin filament alignment at AJs (Leerberg et al., 2014), and the effects actin stabilization has on the supramolecular organization of cadherin-catenin complexes. Pushing outward, it will be interesting to determine if different cell types use different mechanisms to achieve the same end, while exploring levels of baseline tension on AJs and differing actin architectures in cells in different tissues and in different cultured cell lines (Fig. A.1B). The role of tricellular junctions is also a topic for further exploration. Further, cells in tissue also need to contend with force generated at basal FAs, and the balance between this and the AJ forces will be important to consider. Finally, it will be exciting to take these new insights *in vivo*, exploring the roles of vinculin in morphogenesis and examining events where Ena/VASP proteins are already known to influence morphogenesis, such as *Drosophila* dorsal closure (Gates et al., 2007), and exploring how cells accommodate differences in tension across tissues (Fig. A.1C ; Martin, Gelbart, Fernandez-Gonzalez, Kaschube, & Wieschaus, 2010) or, in a planar-polarized way, within individual cells (e.g. Simões, Mainieri, & Zallen, 2014).

Figure A.1

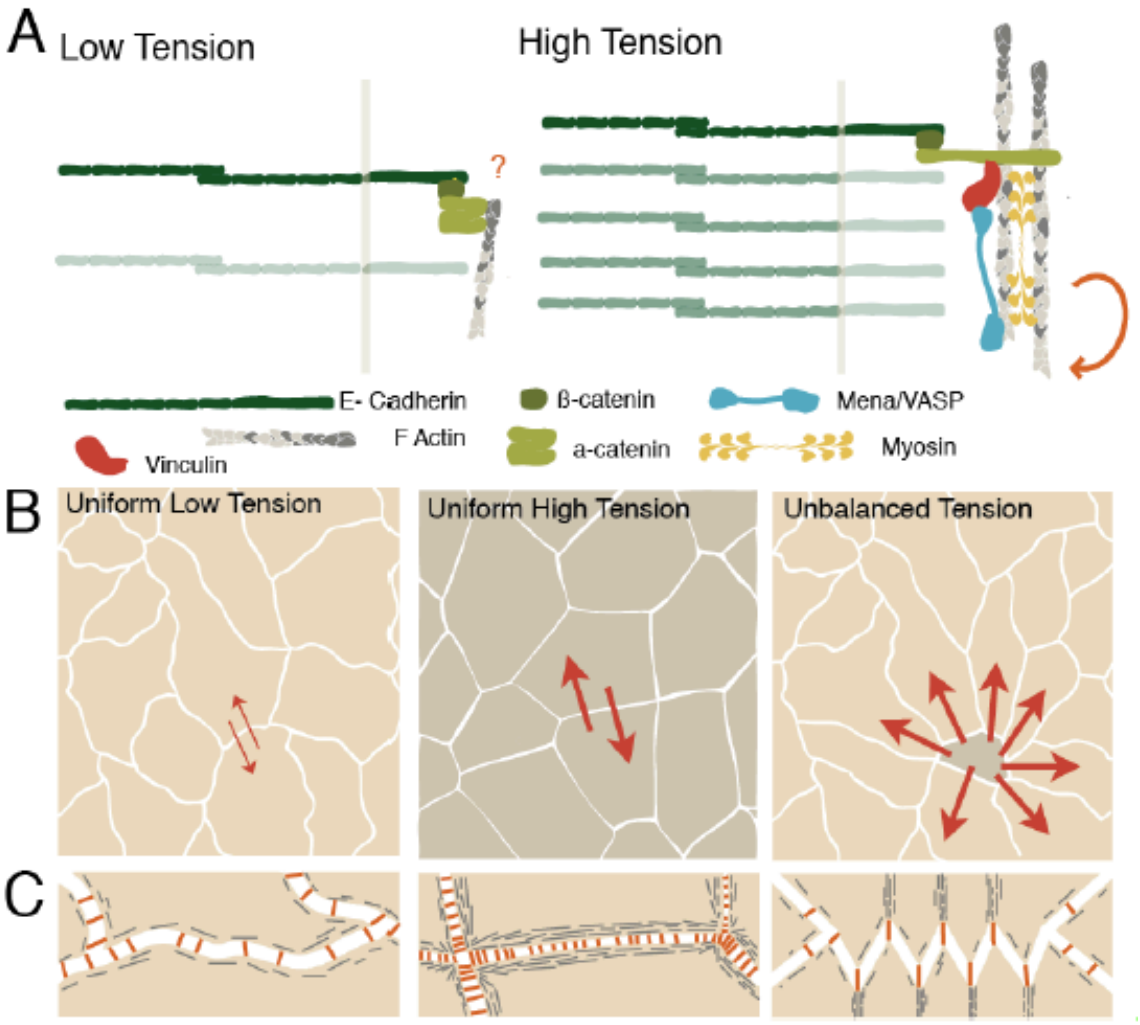

Figure A.1. Model for tension feedback loop at adherens junctions
(A) Under low tension, a-catenin is associated with B-catenin and E-cadherin in a closed conformation. In this state, the ability of a-catenin to bind actin is unclear. Under high tension, a conformational change allows a-catenin to recruit vinculin, which in turn binds Mena and VASP, promoting actin polymerization at barbed ends. This increased unbranched actin is favorable for myosin recruitment and action, this generating more force, inciting a positive feedback loop between tension and actin polymerization. (B) Cell sheets experiencing uniform low, uniform high or unbalanced tension. Increased tension straightens cell borders. Red arrows indicate force exerted on neighbors. (C) Close-up diagram of cell borders under low, high or orthogonal F-actin-mediated tension (F-actin, gray lines). Ecadherin (red lines) accumulates at junctions under high tension and is enriched at tricellular junctions.

REFERENCES

Abe, K., & Takeichi, M. (2008). EPLIN mediates linkage of the cadherin catenin complex to F-actin and stabilizes the circumferential actin belt. *Proceedings of the National Academy of Sciences of the United States of America*, *105*(1), 13–19. doi:10.1073/pnas.0710504105

Chesarone, M. A., & Goode, B. L. (2009). Actin nucleation and elongation factors: mechanisms and interplay. *Current opinion in cell biology*, *21*(1), 28–37. doi:10.1016/j.ceb.2008.12.001

Gates, J., Mahaffey, J. P., Rogers, S. L., Emerson, M., Rogers, E. M., Sottile, S. L., et al. (2007). Enabled plays key roles in embryonic epithelial morphogenesis in Drosophila. *Development (Cambridge, England)*, *134*(11), 2027–2039. doi:10.1242/dev.02849

Gumbiner, B., Stevenson, B., & Grimaldi, A. (1988). The role of the cell adhesion molecule uvomorulin in the formation and maintenance of the epithelial junctional complex. *The Journal of cell biology*, *107*(4), 1575–1587.

Harris, T. J. C., & Tepass, U. (2010). Adherens junctions: from molecules to morphogenesis. *Nature reviews. Molecular cell biology*, *11*(7), 502–514. doi:10.1038/nrm2927

Kwiatkowski, A. V., Maiden, S. L., Pokutta, S., Choi, H.-J., Benjamin, J. M., Lynch, A. M., et al. (2010). From the Cover: In vitro and in vivo reconstitution of the cadherin-cateninactin complex from Caenorhabditis elegans. *Proceedings of the National Academy of Sciences of the United States of America*, *107*(33), 14591–14596. doi:10.1073/pnas.1007349107

Leerberg, J.M., Gomez, G.A., Verma, S., Moussa, E.J., Wu, S.K., Priya, R., Hoffman, B.D., Grashoff, C., Schwartz, M.A., and Yap, A.S. (2014). Tension-sensitive actin assembly supports contractility at the epithelial zonula adherens. Curr Biol *in press*.

Martin, A. C., Gelbart, M., Fernandez-Gonzalez, R., Kaschube, M., & Wieschaus, E. F. (2010). Integration of contractile forces during tissue invagination. *The Journal of cell biology*, *188*(5), 735–749. doi:10.1083/jcb.200910099

Maruthamuthu, V., Aratyn-Schaus, Y., & Gardel, M. L. (2010). Conserved F-actin dynamics and force transmission at cell adhesions. *Current opinion in cell biology*, *22*(5), 583–588. doi:10.1016/j.ceb.2010.07.010

Meng, W., & Takeichi, M. (2009). Adherens junction: molecular architecture and regulation. *Cold Spring Harbor perspectives in biology*, *1*(6), a002899. doi:10.1101/cshperspect.a002899

Michael, M., & Yap, A. S. (2013). The regulation and functional impact of actin assembly at cadherin cell-cell adhesions. *Seminars in cell & developmental biology*, *24*(4), 298–307. doi:10.1016/j.semcdb.2012.12.004

Quinlan, M. P., & Hyatt, J. L. (1999). Establishment of the circumferential actin filament network is a prerequisite for localization of the cadherin-catenin complex in epithelial cells. *Cell growth & differentiation : the molecular biology journal of the American Association for Cancer Research*, *10*(12), 839–854.

Sawyer, J. K., Harris, N. J., Slep, K. C., Gaul, U., & Peifer, M. (2009). The Drosophila afadin homologue Canoe regulates linkage of the actin cytoskeleton to adherens junctions during apical constriction. *The Journal of cell biology*, *186*(1), 57–73.

doi:10.1083/jcb.200904001

Sawyer, J. M., Harrell, J. R., Shemer, G., Sullivan-Brown, J., Roh-Johnson, M., & Goldstein, B. (2010). Apical constriction: a cell shape change that can drive morphogenesis. *Developmental biology*, *341*(1), 5–19. doi:10.1016/j.ydbio.2009.09.009

Simões, S. de M., Mainieri, A., & Zallen, J. A. (2014). Rho GTPase and Shroom direct planar polarized actomyosin contractility during convergent extension. *The Journal of cell biology*, *204*(4), 575–589. doi:10.1083/jcb.201307070

Tang, V. W., & Brieher, W. M. (2012). α-Actinin-4/FSGS1 is required for Arp2/3-dependent actin assembly at the adherens junction. *The Journal of cell biology*, *196*(1), 115–130. doi:10.1083/jcb.201103116

Verma, S., Han, S. P., Michael, M., Gomez, G. A., Yang, Z., Teasdale, R. D., et al. (2012). A WAVE2-Arp2/3 actin nucleator apparatus supports junctional tension at the epithelial zonula adherens. *Molecular biology of the cell*, *23*(23), 4601–4610. doi:10.1091/mbc.E12-08-0574

Yamada, S., Pokutta, S., Drees, F., Weis, W. I., & Nelson, W. J. (2005). Deconstructing the cadherin-catenin-actin complex. *Cell*, *123*(5), 889–901. doi:10.1016/j.cell.2005.09.020

Yonemura, S., Wada, Y., Watanabe, T., Nagafuchi, A., & Shibata, M. (2010). alpha-Catenin as a tension transducer that induces adherens junction development. *Nature cell biology*, *12*(6), 533–542. doi:10.1038/ncb2055